US Army Corps
of Engineers
Waterways Experiment
Station

Technical Report REMR-HY-11
September 1993

2

Repair, Evaluation, Maintenance, and Rehabilitation Research Program

STREMR: Numerical Model for Depth-Averaged Incompressible Flow

by *Robert S. Bernard*
Hydraulics Laboratory

Prepared for Headquarters, U.S. Army Corps of Engineers

The following two letters used as part of the number designating technical reports of research published under the Repair, Evaluation, Maintenance, and Rehabilitation (REMR) Research Program identify the problem area under which the report was prepared:

	Problem Area		Problem Area
CS	Concrete and Steel Structures	EM	Electrical and Mechanical
GT	Geotechnical	EI	Environmental Impacts
HY	Hydraulics	OM	Operations Management
CO	Coastal		

The contents of this report are not to be used for advertising, publication, or promotional purposes. Citation of trade names does not constitute an official endorsement or approval of the use of such commercial products.

♻ PRINTED ON RECYCLED PAPER

Repair, Evaluation, Maintenance, and
Rehabilitation Research Program

Technical Report REMR-HY-11
September 1993

STREMR: Numerical Model for Depth-Averaged Incompressible Flow

by Robert S. Bernard
Hydraulics Laboratory

U.S. Army Corps of Engineers
Waterways Experiment Station
3909 Halls Ferry Road
Vicksburg, MS 39180-6199

Final report

Approved for public release; distribution is unlimited

Prepared for U.S. Army Corps of Engineers
Washington, DC 20314-1000
Under Civil Works Research Work Units 32319 and 32656

US Army Corps of Engineers
Waterways Experiment Station

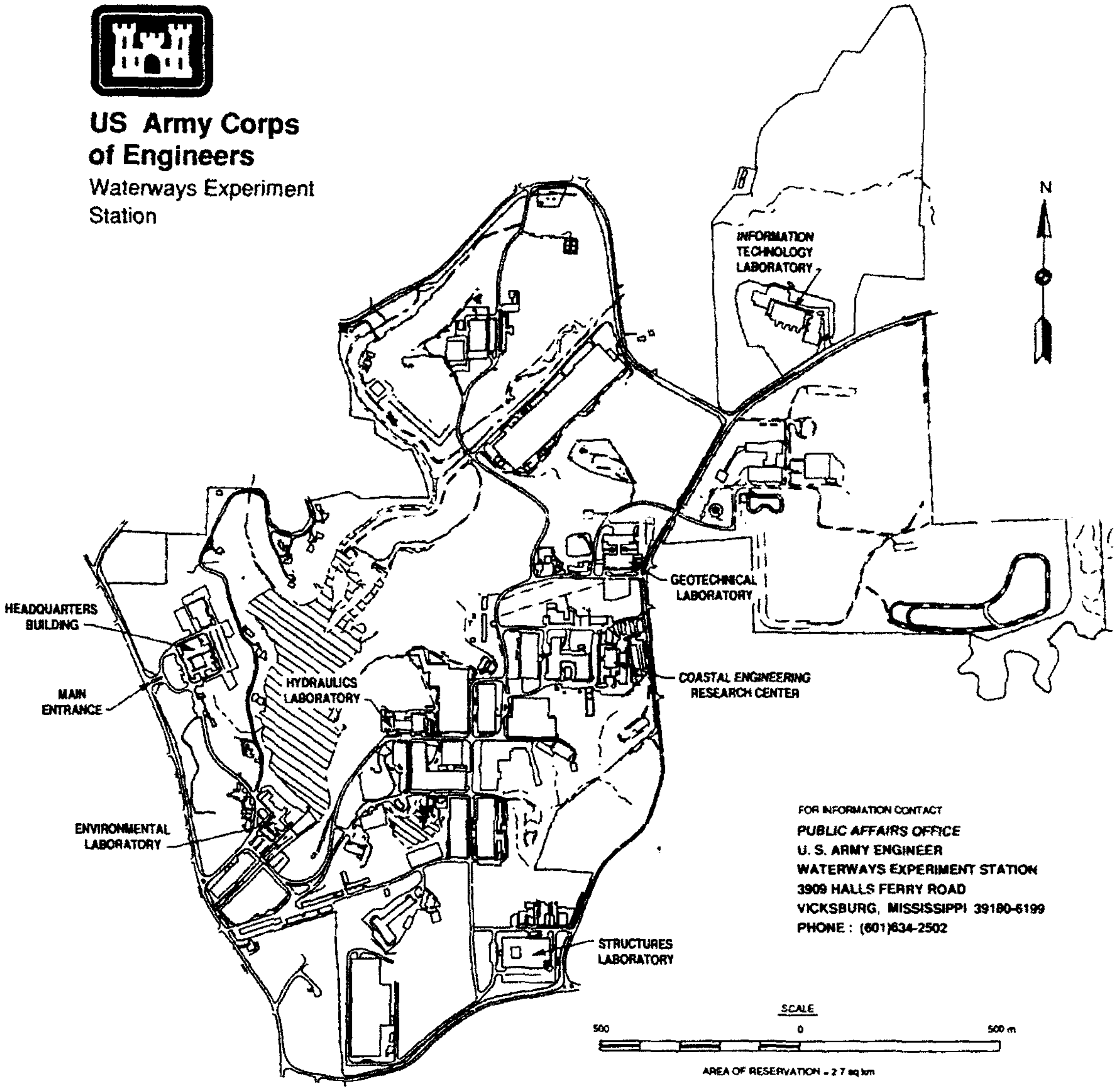

FOR INFORMATION CONTACT
PUBLIC AFFAIRS OFFICE
U. S. ARMY ENGINEER
WATERWAYS EXPERIMENT STATION
3909 HALLS FERRY ROAD
VICKSBURG, MISSISSIPPI 39180-6199
PHONE : (601)634-2502

Waterways Experiment Station Cataloging-in-Publication Data

Bernard, Robert S.
STREMR : numerical model for depth-averaged incompressible flow / by Robert S. Bernard ; prepared for U.S. Army Corps of Engineers.
181 p. : ill. ; 28 cm. — (Technical report ; REMR-HY-11)
Includes bibliographical references.
1. Channels (Hydraulic engineering) — Computer programs. 2. STREMR (Computer program) 3. Hydraulics — Computer programs. 4. Turbulence — Computer programs. I. United States. Army. Corps of Engineers. II. U.S. Army Engineer Waterways Experiment Station. III. Repair, Evaluation, Maintenance, and Rehabilitation Research Program. IV. Title: STREMR: numerical model for depth-averaged incompressible flow. V. Title. VI. Series: Technical report (U.S. Army Engineer Waterways Experiment Station) ; REMR-HY-11.
TA7 W34 no.REMR-HY-11

Contents

Preface

This report concerns research and development conducted from October 1988 through March 1992 by personnel of the Reservoir Water Quality Branch (RWQB), Hydraulic Structures Division (HSD), Hydraulics Laboratory (HL), US Army Engineer Waterways Experiment Station (WES), under the Repair, Evaluation, Maintenance, and Rehabilitation (REMR) research program authorized by the Headquarters, US Army Corps of Engineers (HQUSACE). Major funding was provided under REMR Work Unit 32319, "Predictive Techniques for Approach Flow to Spillways and Other Structures," and REMR Work Unit 32656, "Dissemination and Improvement of STREMR Model." Additional funding was provided by the research program for Flood Control Structures, Work Unit 32542, "River Bend System Hydraulics - Imposed Force Component"; by the research program for Improvement of Operations and Maintenance Techniques, Work Unit 32350, "Estuarine Channel Maintenance by Training Structures"; by the Numerical Model Maintenance Program, which is supported by USACE field offices and administered by the Directorate for Research and Development; and by the US Bureau of Reclamation through an interagency agreement for development of a k-ϵ turbulence model.

Dr. Robert S. Bernard, RWQB, prepared this report under the general supervision of Messrs. Frank A. Herrmann, Jr., Director, HL; Richard A. Sager, Assistant Director, HL; Glenn A. Pickering, Chief, HSD; and Dr. Jeffery P. Holland, Chief, RWQB. Technical counsel was provided by Messrs. Michael L. Schneider and Stacy E. Howington, RWQB; by Dr. Raymond S. Chapman, private consultant to WES; by Dr. Hartmut Kapitza, GKSS Research Center, Geesthacht, Germany; and by Drs. Gary Parker and Helgi Johannesson, University of Minnesota. The STREMR subroutines for solving the discrete Poisson equation were written by Dr. Kapitza.

The coordinator for the REMR Program was Mr. William N. Rushing, Directorate of Research and Development, HQUSACE. Members of the REMR Overview Committee were Mr. James E. Crews, Chairman, and Dr. Tony C. Liu, HQUSACE. The REMR Technical Monitor for Hydraulics was Mr. Glen Drummond, HQUSACE; and the REMR Program Manager at WES was Mr. William F. McCleese, Structures Laboratory. The Hydraulics Problem Area Leader was Mr. Pickering.

At the time of publication of this report, Dr. Robert W. Whalin was Director of WES and COL Bruce K. Howard, EN, was Commander.

Conversion Factors, Non-SI to SI Units of Measurement

Non-SI units of measurement used in this report can be converted to SI units as follows:

Multiply	By	To Obtain
cubic feet	0.02832	cubic meters
degrees	0.01745	radians
feet	0.3048	meters
inches	2.540	centimeters
square feet	0.09290	square meters

1 Introduction

Background

STREMR is a computer code (numerical model) that generates discrete solutions of the incompressible Navier-Stokes equations for depth-averaged (or width-averaged) two-dimensional (2-D) flow. The present version runs on machines ranging from personal computers to supercomputers. It is suitable for routine use by field engineers and others with an interest in depth-averaged flow modeling. Previous experience with numerical models is helpful but not mandatory for first-time users. STREMR can be used as a training aid for prospective modelers, as a handy means of qualitative flow visualization, and as a practical device for quantitative flow prediction. If its empirical coefficients are fine-tuned for agreement with a particular physical model, the code can also be used to extrapolate test data from laboratory scale to full scale. Without site-specific tuning or adjustment of any kind, however, STREMR predictions are still accurate enough to expedite the design of a new hydraulic structure or the rehabilitation of an old one. Earlier versions of the model have proven useful in studies concerning bendways, diversion tunnels, pump stations, training structures, and bank protection.

The STREMR code computes the mutual interactions between sidewalls, obstacles, and bathymetry to predict the resulting depth-averaged flow in channels of arbitrary shape. The primary input consists of a computational grid (created by a separate grid-generation code), optional velocity distributions along user-specified inflow and outflow boundaries, and sufficient data for depth (or bottom and surface elevation) to reconstruct the bathymetry by interpolation.

STREMR eliminates a great deal of user guesswork by incorporating a k-ε turbulence model and a three-dimensional (3-D) secondary flow correction. The turbulence model generates an eddy viscosity from the computed primary flow; and the secondary flow correction accounts for the interaction between lateral curvature and vertical nonuniformity, which causes high velocities to migrate toward the outsides of channel bends. Manning's coefficient for bottom friction is the only empirical parameter required in the code input.

STREMR uses a finite-volume discretization scheme with curvilinear grids to accommodate irregular 2-D flow boundaries, and it accounts for nonuniform bathymetry by assigning a different depth to each grid cell. This stair-stepped discretization of depth is admissible to the extent that depth-averaging itself is admissible. If the depth-induced forces vary gently enough with position, the resulting 3-D effects will be weak enough to be approximated with depth-averaged corrections for bottom friction and secondary flow. If they vary too strongly with position, however, the flow will have 3-D components large enough to invalidate the use of a 2-D model altogether.

STREMR imposes a rigid-lid approximation instead of a free surface, but it can be used for free-surface flow wherever the local Froude number is 0.5 or less. If variations in the width and depth of flow are sufficiently gentle, and if there are no obstacles present (piers, dikes, islands, etc.), then the code may be applicable at Froude numbers as high as 0.7. In any case, the computed pressure is equivalent to the displacement of a free surface, and it can be used as an approximation thereof. The lower the Froude number, the more accurate the approximation becomes. The absence of a true free surface makes STREMR unsuitable for calculations involving hydraulic jumps and moving surface waves.

Purpose and Scope

This report serves as three documents in one: an instruction manual for STREMR users; a compendium of examples for code execution and model verification; and a review of the governing equations, the discrete mathematics, and the computational algorithms. Part II is an overview of model capabilities and operation; Part III gives detailed instructions for input and execution; and Part IV explains the form and content of STREMR output. Part V presents examples of STREMR input along with computed results and test data, and Part VI offers conclusions. Appendix A enumerates the governing equations for the primary flow; Appendix B describes the turbulence model; and Appendix C discusses the secondary flow correction. Appendix D explains the transformation from Cartesian to curvilinear coordinates; Appendix E derives the finite-volume discretization; and Appendix F reviews the algorithms used to solve the discrete equations.

2 STREMR Overview

Input

User input for STREMR is read from an external file in namelist format. This input consists mainly of designations for grid cell types, initial velocity distributions for inflow and outflow, and specifications for bathymetry and bottom friction. Additional input parameters allow the user to select or reject options such as the turbulence model and the secondary flow correction. Grid coordinates are read from a second external file created by a separate grid-generation code.

Computational Procedures

After reading input for a cold start (no previously computed flow), STREMR uses the input velocities to compute a mass-conserving initial flow, which it imposes as a starting condition. The code then marches forward in time, using a MacCormack predictor-corrector scheme (MacCormack 1969) for the momentum equation and an Euler upwind scheme (Anderson, Tannehill, and Pletcher 1984) for the turbulence and secondary flow equations. The MacCormack scheme is a modified version (Bernard 1986, 1989) with pressure computed from a Poisson equation. The solution technique for the Poisson equation is a preconditioned conjugate-gradient method reported by Kapitza and Eppel (1987), and the conjugate-gradient subroutines in STREMR were written by Kapitza (1987). See Appendices A-F for a complete description of the governing equations and the computational algorithms.

Computational Grids

STREMR uses a finite-volume discretization scheme with curvilinear boundary-fitted grids for irregular 2-D regions (Figure 1). The depth-averaged flow equations are transformed from Cartesian (x,y) coordinates, with arbitrary spacing $(\Delta x, \Delta y)$, to curvilinear (i,j) coordinates with unit spacing $(\Delta i, \Delta j)$ so that $\Delta i = \Delta j = 1$ between the grid lines. Every grid cell is square in the computational (i,j) plane regardless of its appearance in the Cartesian (x,y)

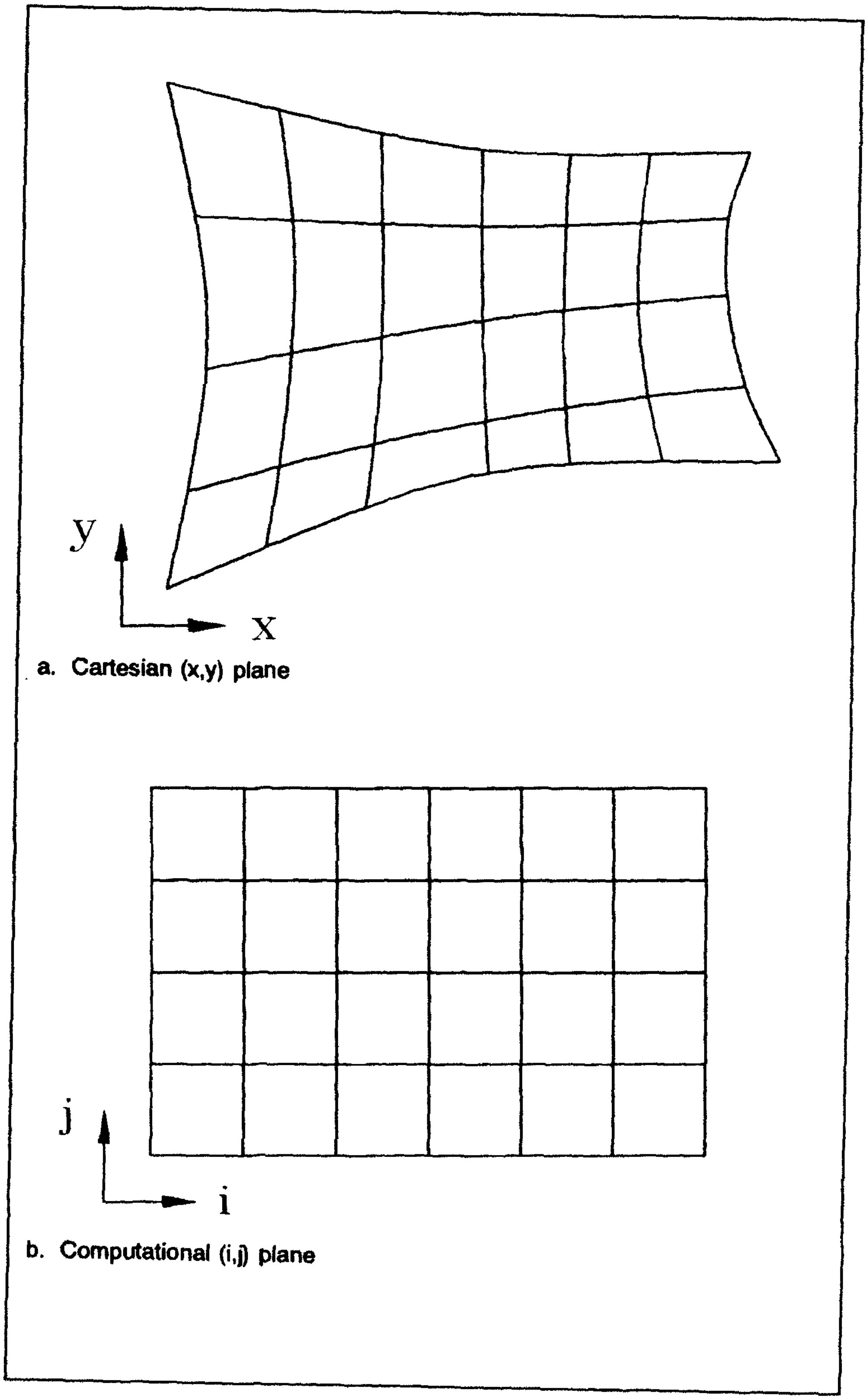

a. Cartesian (x,y) plane

b. Computational (i,j) plane

Figure 1. Grid appearance in Cartesian and computational planes

plane, and all information concerning cell size and shape (in the Cartesian plane) is absorbed into the coefficients of the transformation. The transformed equations are more complicated than their Cartesian counterparts, but the computational logic is the same as that for a uniformly spaced rectangular grid. See Appendices D and E for details concerning the transformation and discretization.

A grid cell is a miniature control volume, for which STREMR calculates face-centered fluxes (U,V), cell-centered velocities (u,v), and a cell-centered pressure p. Figure 2 shows the discrete locations at which the cell-centered and face-centered quantities are computed. The fluxes U and V are volumetric flux components normal to cell faces of constant i and constant j, respectively. Volumetric flux is the product of depth at the cell face, length of the cell face, and velocity normal to the cell face.

As the computed flow evolves in time, only U, V, and p are carried from one time-step to the next. The Cartesian velocity components u and v are computed from U and V only when they are needed. The staggered placement of discrete variables (cell-centered pressure and face-centered flux) is called a marker-and-cell (MAC) grid. Curvilinear MAC grids can be produced by numerical grid-generation codes such as WESCOR (Thompson 1983), which fits the grid to the boundaries of the flow; or they can be fabricated by any other boundary-conforming procedure that arranges the grid cells in rows and columns according to i and j. Once the grid has been generated, attention can be focused primarily on the computational (i,j) plane (Figure 3).

Cell Indices and Computational Coordinates

The computational coordinates (i,j) run from $i = 0$ to $i = IMAX$ and from $j = 0$ to $j = JMAX$ for a grid that covers IMAX spaces in the i-direction and JMAX spaces in the j-direction. These integer coordinates (i,j) serve two purposes (Figure 2). First, they define the location of each node; and second, they serve as indices (labels) for each cell. Thus, in the computational plane, *cell* (i,j) is the grid cell whose upper right-hand corner lies at *node* (i,j). Since there is sometimes no physical difference between plan view and elevation view for 2-D flow, it is generally expedient to use the generic term "east" for the positive i-direction, and "north" for the positive j-direction.

Consider the hypothetical 12 X 8 grid shown in Figure 3, for which $IMAX = 12$ and $JMAX = 8$. Cells *in* the grid are indicated by solid lines, and phantom cells *outside* the grid are indicated by dashed lines. Node (0,0) lies at the origin (intersection) of the i- and j-axes, which is the southwest corner of the entire grid. This node is also the southwest corner of grid cell (1,1), and the northeast corner of phantom cell (0,0). The northeast corner of the entire grid is node (12,8), which is also the northeast corner of grid cell (12,8), and the southwest corner of phantom cell (13,9). Note that the phantom cells are not part of the grid itself, and they are *not* generated with the grid. Phantom

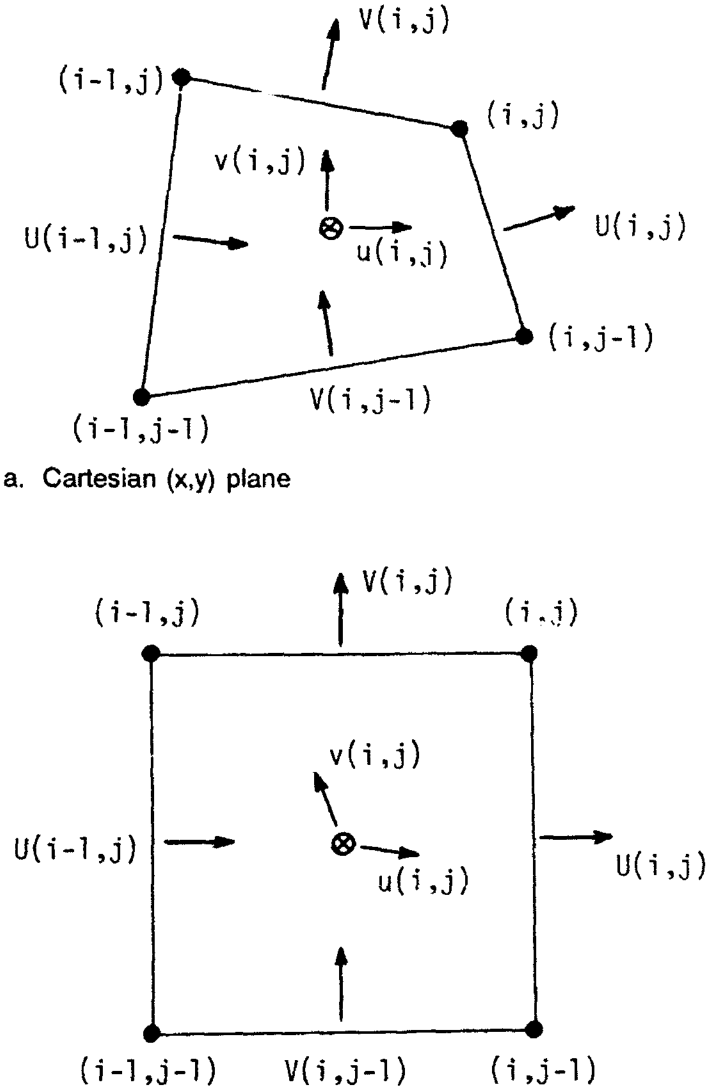

a. Cartesian (x,y) plane

b. Computational (i,j) plane

Figure 2. Discrete placement of cell-centered velocities (u,v), face-centered fluxes (U,V), and grid nodes (•) for cell (i,j)

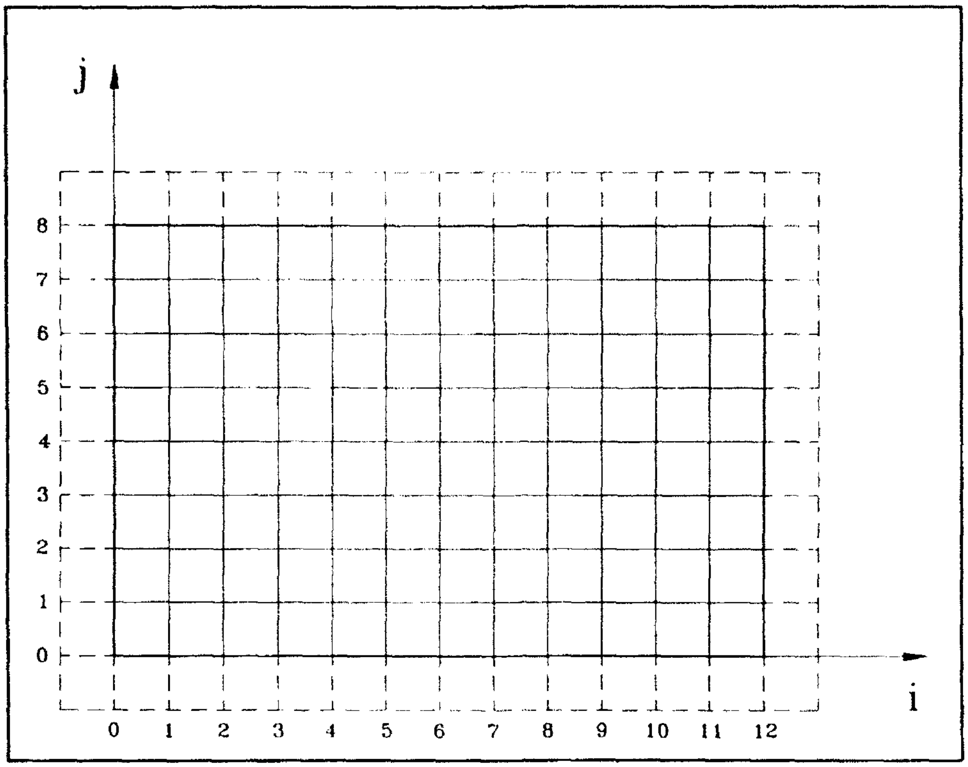

Figure 3. Computational (i,j) plane with hypothetical 12 × 8 grid (solid lines) surrounded by phantom cells (dashed lines)

cells are merely dummy locations required by STREMR logic in the computational plane.

Grid Cell Types

STREMR classifies cells into six types: FIELD, NOSLIP, SLIP, FLUX, OPEN, and OUT. Grid cells that lie in the flow and touch no boundaries are FIELD cells. Grid cells that lie in the flow *and* touch boundaries may be either NOSLIP, SLIP, FLUX, or OPEN cells. OUT cells are phantom cells outside the grid, or inactive (no-flow) cells inside an obstacle (Figure 4).

Flow enters or leaves the grid through FLUX and OPEN cells, and these must have at least one entire *face* on a boundary. The volumetric flux through a FLUX boundary face is constant, but the volumetric flux through an OPEN boundary face changes as the flow evolves. It is best to designate inflow cells as FLUX cells and outflow cells as either FLUX or OPEN cells.

SLIP cells touch boundaries that impose no tangential force (sidewall friction) on the flow, and NOSLIP cells touch boundaries that do impose a tangential force. SLIP and NOSLIP cells must have at least one *corner* on a boundary.

FIELD cells touch *no* boundaries at all, and these are designated automatically by STREMR. OUT cells touch only the boundaries or each other. Phantom cells and no-flow cells inside obstacles (generated with the grid) are automatically designated as OUT cells by STREMR. Note that solid obstacles (piers, dikes, islands, etc.) are always filled with OUT cells and surrounded by SLIP or NOSLIP cells (Figure 4).

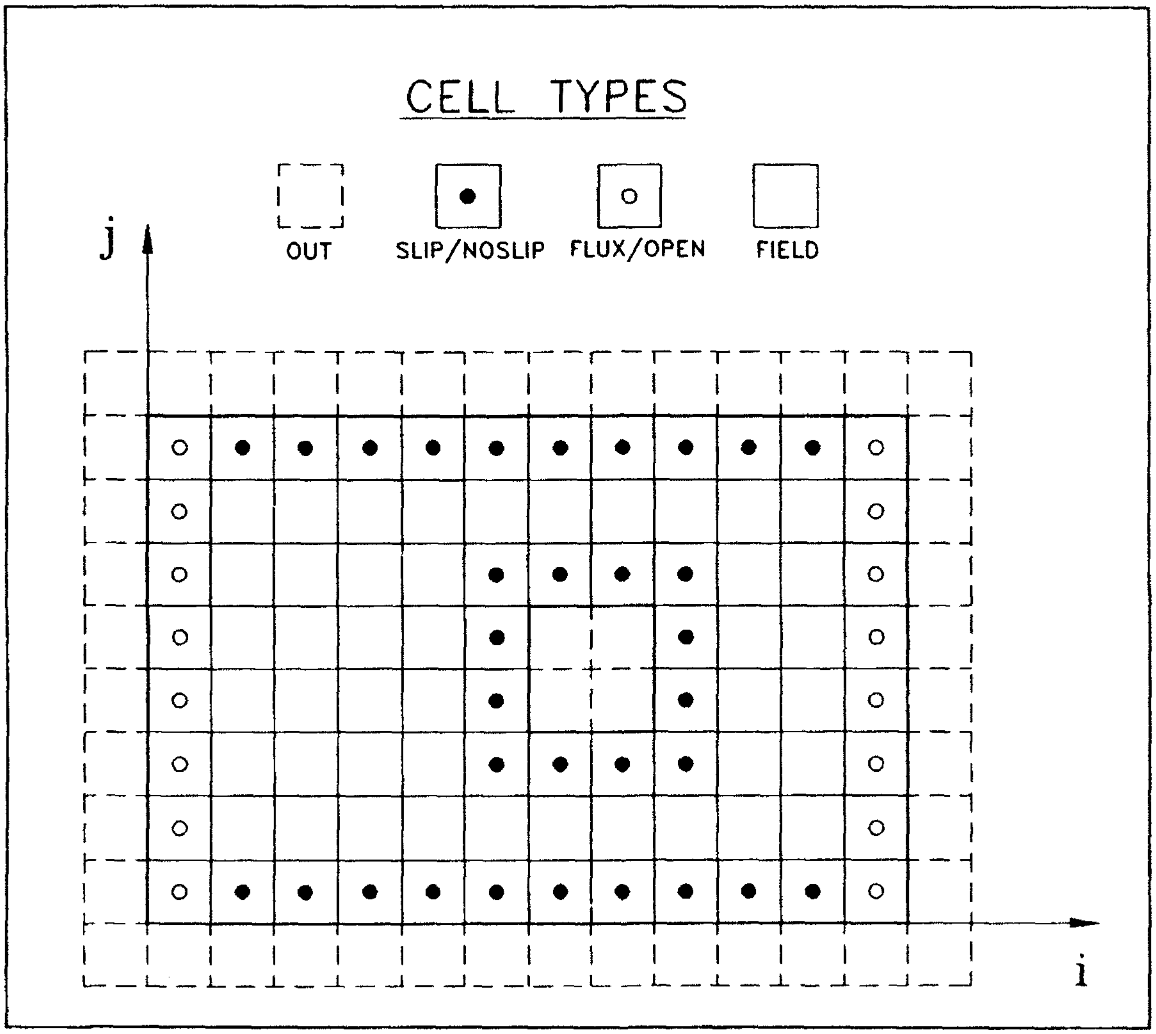

Figure 4. Computational (i,j) plane with 12 × 8 grid and 2 × 2 obstacle

STREMR makes all boundary-adjacent grid cells NOSLIP by default, and the user must specify other cell types (SLIP, FLUX, or OPEN) wherever they are needed along the boundaries. NOSLIP cells can be converted to SLIP cells with a single input entry for the entire grid. Any previously specified type except OPEN can be changed (by subsequent input) to any other type except FIELD. A cell can be designated OPEN only once, as part of a single row or column of OPEN cells; its type *cannot* be changed by subsequent input.

Flowrate

The total flowrate is constant for the grid as a whole, and the fluxes *U* and *V* through the boundary faces of each FLUX cell are constant. The total flowrate is either specified by the user (default) or computed from the input velocities.

For OPEN cells, the net flow through a continuous boundary segment of OPEN faces is constant, but the flow distribution along that segment may change with time. For this reason, groups of OPEN cells have to be specified as distinct rows or columns in the computational (i,j) plane. STREMR assigns a particular flowrate to each user-defined row or column of OPEN cells, and these rows and columns must *not* overlap.

Grid Quality

Grids need not be orthogonal nor uniformly spaced in the Cartesian (x,y) plane, but it is best to avoid sharply skewed gridlines and abrupt changes in grid spacing (Figure 5). Excessive skewness and disparate spacing may degrade accuracy and promote numerical instability. As a rule of thumb, the angles between intersecting gridlines should be kept between 45 deg[1] and 135 deg; and the local change in grid spacing should be no more than 30 percent from one cell to the next. It is also wise to avoid cell aspect ratios (length/width) greater than 10 wherever sharp flow gradients may occur in the *lengthwise* direction. If possible, grid cells should be oriented so that the grid spacing is finest in the direction of the strongest depth or velocity gradient.

At least two grid spaces are needed to represent an obstacle normal to the general direction of flow (Figure 4); but this is sufficient only for the crudest possible representation. Five to ten spaces will produce much better results, but may still leave grid-associated errors of 20 percent or more in computed details such as the reattachment length for a separated flow. Twenty spaces may reduce these errors to 3 percent or less. See Part V, Examples 2A, 2B, 3A, and 3B for supporting evidence.

There is an important point to remember concerning the magnitudes of the Cartesian coordinates (x,y). In the process of discretization, STREMR computes the difference between the Cartesian coordinates of neighboring grid cells. If these coordinates are very large, and their differences very small, accuracy may be needlessly lost. To avoid this, make sure that the magnitudes of the Cartesian coordinates (x,y) are commensurate with the size of the grid in the Cartesian (x,y) plane. For example, if the grid covers only 100 metres in the x-direction and 300 metres in the y-direction, then neither x nor y should

[1] A table of factors for converting non-SI units of measurement to SI (metric) units is presented on page ix).

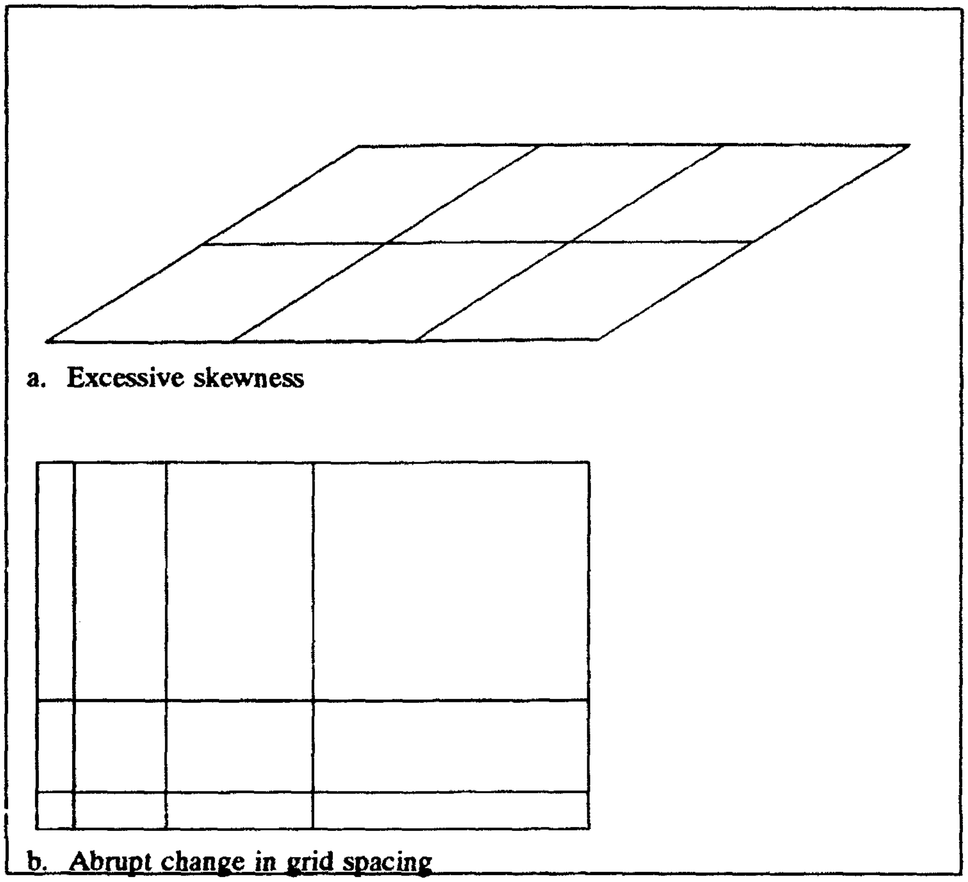

a. Excessive skewness

b. Abrupt change in grid spacing

Figure 5. Undesirable features for computational grid in Cartesian (x,y) plane

exceed 1000 metres. If the original value for the maximum x-coordinate is 1,000,000 metres in this case, the (x,y) origin needs to be moved so that the maximum x-coordinate becomes 1000 metres or less. Otherwise, four significant figures will be lost in each differencing operation.

Nonuniform Bathymetry

STREMR employs depth-averaged approximations for bottom friction and 3-D secondary flow, but these are valid only for *gentle* variations in depth (Figure 6). This means that the bottom slope should be less than 45 deg (measured from the horizontal) when it involves a change in depth of 50 percent or more over the entire slope. Submerged features may cause numerical instability if they impose dramatic depth changes with bottom slopes greater than 45 deg; but even when they do run successfully, the computed results should be viewed with considerable skepticism. Side slopes greater than 45 deg should be replaced with vertical sidewalls.

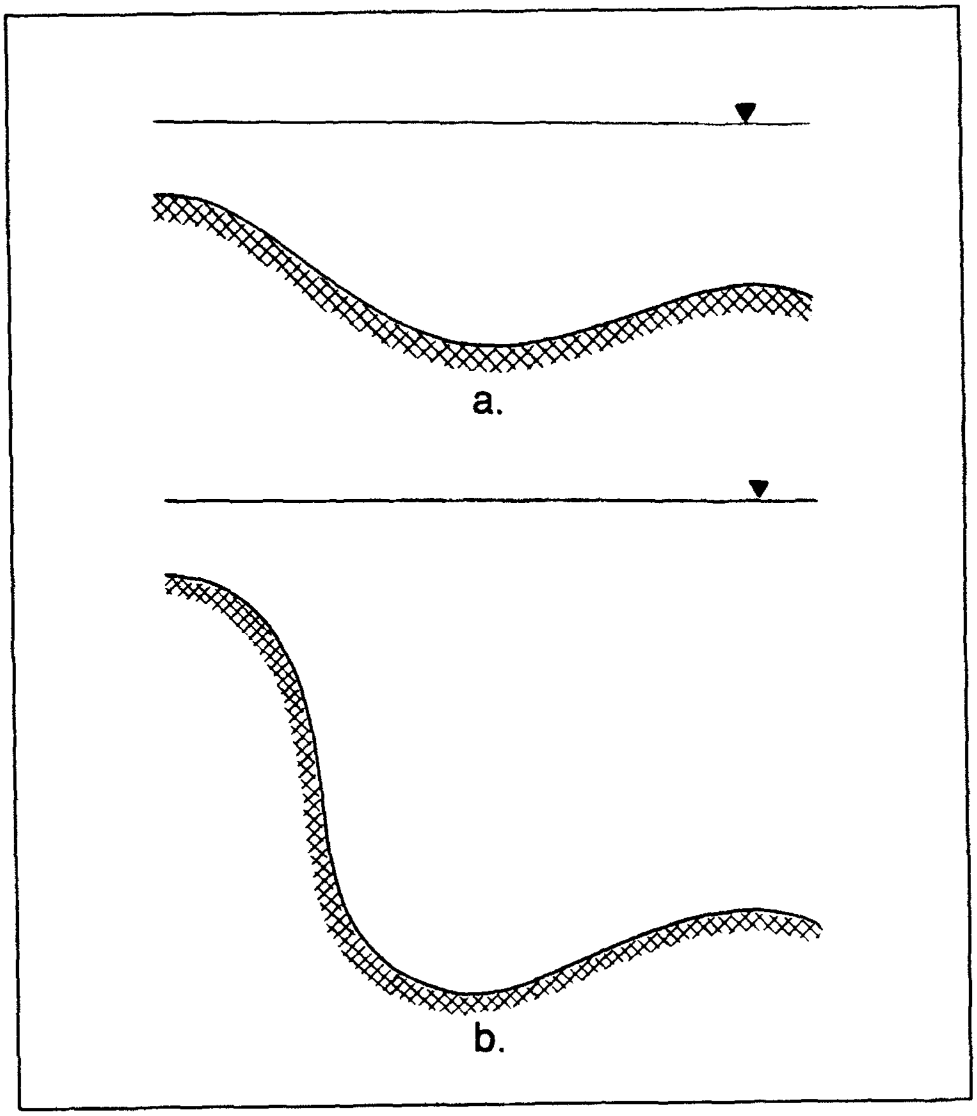

Figure 6. Elevation view of gentle (a) and abrupt (b) variations in depth

STREMR accommodates nonuniform bathymetry by allowing a different depth in every grid cell, which produces a stair-stepped depth discretization in the computational space (Figure 7). Note, however, that the same depth is assigned to every grid cell by default, and this has to be changed for individual cells and groups of cells by user input.

STREMR accepts input for either the flow depth or the bottom and surface elevations, but not for depth and elevations together. If elevations are specified, STREMR obtains the depth by subtracting the elevation of the bottom from the elevation of the surface. Depth (or elevation) input is accepted for sections, line segments, individual cells (or points), and also for the grid as a whole. Input for sections must be specified with computational (*i,j*) coordinates, but input for line segments and points can be specified with either (*i,j*) or (*x,y*) coordinates.

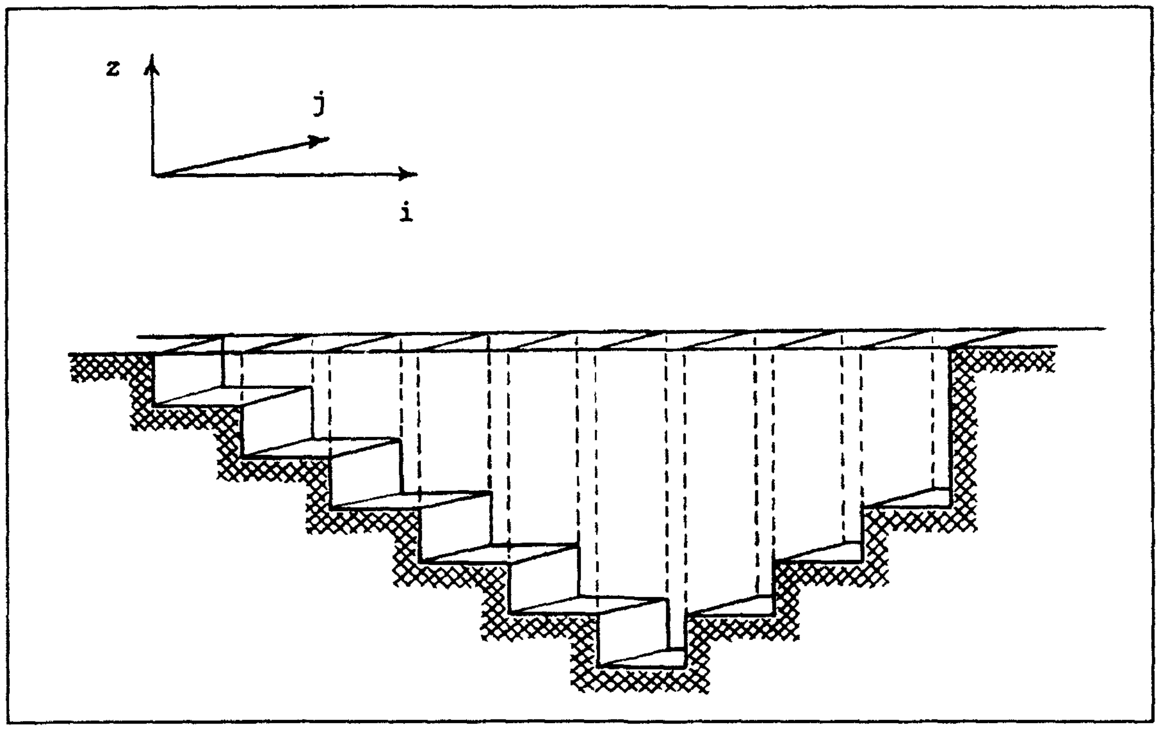

Figure 7. Discrete representation of flow depth (negative z-direction) for a row of grid cells in the computational (i,j) plane

Bottom Friction

STREMR accounts for bottom resistance with Manning's equation, which gives the (nondimensional) bottom friction factor (Appendix A) as a function of the depth and the Manning coefficient *n*. Values for *n* are specified in the same manner as the depth, with input accepted for sections, line segments, individual cells (or points), and also for the grid as a whole. Note that the default condition in STREMR is *no* bottom friction ($n = 0$), and it is up to the user to input nonzero values.

Automatic Interpolation of Input

STREMR offers an optional interpolation scheme that fills in the values of Manning's coefficient and depth (or elevation) at all locations not specified in the user input. In this scheme, STREMR treats the values at the specified locations as though they were fixed boundary conditions, and then solves a Laplace equation for the values at the remaining (unspecified) locations. This allows the creation of a smooth distribution from sparse user input. The interpolation is activated by default, but it can be rejected by user input.

Eddy Viscosity

STREMR accounts for turbulence by including an eddy viscosity in the depth-averaged governing equations for the primary and secondary flow. This is obtained from a k-ε turbulence model (Launder and Spalding 1974), which consists of empirical transport equations for the turbulence energy k and the turbulence dissipation rate ε. STREMR solves these equations and computes the local eddy viscosity ν from the results.

Included with the k-ε model is an empirical procedure for calculating turbulence energy, dissipation rate, and shear stress near sidewalls and obstacles. This procedure is not suitable for modeling turbulent boundary layers, but it does a fair job of predicting flow separation on curved sidewalls. See Part IV, Example 4, for supporting evidence.

The turbulence model is activated in STREMR by default; but it is optional, and users can reject it via the input. If the turbulence model is rejected, then STREMR uses a kinematic viscosity specified by the user. In the latter case, the code accepts only one viscosity for the entire flow, and the sidewall shear stress is then calculated from a viscous no-slip condition (Appendix B). Ordinarily one *should* keep the turbulence model activated in STREMR calculations, because it offers a better approximation for the eddy viscosity than can be obtained by guesswork alone. Only for laminar flow calculations (at low Reynolds number) should the turbulence model be omitted.

Secondary Flow Correction

Curved channels often develop a 3-D secondary flow (spiral motion) that causes the highest velocities to migrate toward the outsides of the bends. STREMR accounts for this by solving an empirical transport equation for streamwise vorticity (Appendix C), which creates a secondary shear stress in the depth-averaged momentum equation (Appendix A). The secondary flow correction is activated by default, but no secondary flow is produced unless Manning's coefficient is greater than zero. Users can reject it altogether via the input (regardless of the value of Manning's coefficient).

Dimensional Units

Internally STREMR uses only SI units of length (meters), but input may be specified in SI units (meters, square meters, cubic meters, and seconds) *or* English units (feet, square feet, cubic feet, and seconds). Printed output is available in SI or English units, with time expressed in seconds. A table for converting English units to SI units is given on page ix.

Variable Time-Step

Users may either specify a fixed time-step or let STREMR set its own variable time-step automatically from numerical stability considerations. The variable time-step eliminates much guesswork from the input, and it allows the code to approach a steady state as quickly as possible. Users may specify the interval at which the time-step is to be reset.

Output

STREMR stores information for printing, plotting, and future hot starts (restarts from a previously computed flow) in separate output files. Condensed flow information is available at user-specified print intervals, and a cell-by-cell printout is available at user-specified storage intervals. Output to be used for future hot starts is overwritten after each storage interval. At the beginning of a hot start, STREMR reads a previously computed hot-start file before reading the namelist input. Printed maps of the relative values of selected variables are available at the end of each STREMR run.

3 STREMR Input and Execution

Array Dimensions

The 2-D arrays in STREMR have dimensions IDIM and JDIM in the *i*- and *j*-directions, respectively. These dimensions are specified by parameter statements in *each* of the five subroutines of the source code; e.g.,

PARAMETER (*IDIM* = 52 , *JDIM* = 19)

Inside the grid, the *cell* indices run from $i = 1$ to $i = IMAX$ and from $j = 1$ to $j = JMAX$; but STREMR also uses a perimeter of phantom OUT cells around the outside of the grid (Figure 4). The indices for the STREMR *arrays* must then run from $i = 0$ to $i = IMAX + 1$ and from $j = 0$ to $j = JMAX + 1$ at the very least.

In general, IDIM *must* equal or exceed $IMAX + 1$ and JDIM *must* equal or exceed $JMAX + 1$; but the code runs faster with $IDIM = IMAX + 1$ and $JDIM = JMAX + 1$. For grids with 500 cells or more, it is usually worthwhile to recompile STREMR to these dimensions with each change of IMAX and JMAX (i.e., with each change of grid dimensions). In any case, the source code has to be *recompiled* whenever IDIM and JDIM are changed for any reason.

Before changing IDIM, note that IDIM must have the *same* value in each of the *five* STREMR subroutines. That also goes for JDIM; but note that IDIM and JDIM need not be equal to each other.

Namelists and Variable Types

The namelist input format is an extension of FORTRAN 77 that is supported by many FORTRAN compilers. It is especially convenient for codes that accept numerous input parameters, as STREMR does. Namelist format differs from standard input format in that it recognizes input quantities by their FORTRAN names instead of by their locations in an input file.

STREMR employs namelist format for all user-specified input. *Variables* may be specified in *any* order within a given namelist, but the *namelists* themselves must appear in a *specific* order. Individual variables can be omitted from a given namelist, in which case the code will assign default values (for a cold start) or previously stored values (for a hot start) to the omitted variables. Certain *required* namelists must never be omitted from the input. Missing namelists and namelists out of order will cause STREMR to stop or abort.

A cold start requires *three* different namelists (in order) called BEGIN, PARAM, and INPUT. A hot start requires BEGIN and PARAM, but *not* INPUT. In either case, BEGIN and PARAM appear only *once* each; but INPUT appears repeatedly (at least *ten* times) in the input for a cold start. Each of these namelists accepts three types of variables: CHARACTER, INTEGER, and REAL (floating-point).

Namelist BEGIN

The first input namelist for hot starts *and* cold starts is BEGIN, which accepts the input variables explained in Tables 1-3. When specifying input values, it is helpful to organize the variables in columns according to their type. Consider the following hypothetical example:

```
&BEGIN  START='COLD'       ,    IREF=1,    TURBIN=0.003,
         FLOW='FLOWRATE'   ,    JREF=5,    PECLET=50.   ,
       IUNITS='METRIC'     ,
        TITLE='HYPOTHETICAL INPUT' &END
```

Note that an ampersand & in column 2 must *always* precede the first letter of the namelist name in column 3. This signals the beginning of the input for a given namelist, and the delimiter &END signals the end. A comma must follow each value assigned, except for the last entry in the namelist, which is followed by &END.

START activates cold starts and hot starts. The only variable that *must* be specified for hot starts is *START = 'HOT'*, but STREMR also reads and uses new values (if any) specified for IREF, JREF, and TITLE. It is usually better *not* to change IREF and JREF from their cold-start values, but TITLE may change with each new hot start. The other variables in namelist BEGIN have no influence on hot starts.

If *VGUESS = 'YES'*, STREMR uses *all* velocities input by the user to calculate an initial flow field. These velocities are adjusted automatically to achieve conservation of mass, but the resulting vorticity is the same as that imposed by the input velocities. Otherwise, when *VGUESS = 'NO'*,

Table 1
CHARACTER Variables Used in Namelist BEGIN

Variable	Value	Explanation
START =	'COLD'	Cold start (default).
START =	'HOT'	Hot start.
VGUESS =	'YES'	All user-specified velocities will be used for the initial flow.
VGUESS =	'NO'	Only user-specified velocities in FLUX and OPEN cells will be used for the initial flow (default).
FLOW =	'FLOWRATE'	Flowrate will be specified by user (default).
FLOW =	'INFLOW'	Flowrate will be computed from user-specified inflow velocities.
FLOW =	'OUTFLOW'	Flowrate will be computed from user-specified outflow velocities.
IUNITS =	'METRIC'	Input units will be SI (metric) units: meters, square meters, cubic meters, and seconds (default).
IUNITS =	'ENGLISH'	Input units will be non-SI (English) units: feet, square feet, cubic feet, and seconds.
ELEVAT =	'YES'	Depth values will be computed from surface and bottom elevations specified by user.
ELEVAT =	'NO'	Depth values will be input directly by user (default).
INTERP =	'YES'	Unspecified values for depth, etc., will be computed by interpolation (default).
INTERP =	'NO'	Unspecified values for depth, etc., will be assigned the default value or the user-specified general value for that quantity.
TITLE =	' --'	User-specified title for plots and printed output. Maximum length is 80 characters and spaces.

Table 2
INTEGER Variables Used in Namelist BEGIN

Variable	Explanation
IREF	I-index of reference cell which will be assigned a zero value of pressure. Default value is that for the first FLUX or OPEN cell to be found in a left-to-right, bottom-to-top search of the computational (i,j) plane.
JREF	J-index of reference cell. Default value is assigned in same manner as that for IREF.

Table 3
REAL Variables Used in Namelist BEGIN

Variable	Explanation
TURBIN	Inflow value for ratio of turbulence energy to velocity squared. (Default = 0.003)
PECLET	Initial Peclet number in reference cell. Used only with turbulence model. (Default = 50.)
REDUCE	Scale-reduction factor by which all input for depth, elevation, velocity, and grid spacing will be divided. (Default = 1.)

STREMR uses *only* the normal components of the input velocities along FLUX and OPEN boundaries. In this case, the resulting initial flow inside the grid is irrotational (no vorticity). The default (*VGUESS = 'NO'*) should ordinarily be used, but the alternative (*VGUESS = 'YES'*) is sometimes needed so that small initial velocities can be specified in troublesome areas to avoid numerical instability.

When *FLOW = 'FLOWRATE'* (default), STREMR adjusts the inflow and outflow velocities so that they match a user-specified flow rate before computing the internal initial flow. When *FLOW = 'INFLOW'*, the outflow velocities are adjusted to match the flow rate produced by the user-specified inflow velocities. The opposite is true when *FLOW = 'OUTFLOW'*. Regardless of the option chosen, however, the adjusted velocities have the same *relative* distributions (along FLUX and OPEN boundaries) as the input velocities.

IUNITS determines the units for all input flow variables except Manning's coefficient (for which no units have to be specified). This eliminates the need to specify units for *any* input variable unless they are *different* from IUNITS. ELEVAT determines whether the code will accept input for depth or for bottom and surface elevations. STREMR accepts depth *or* elevation, but *not* both. INTERP controls the automatic interpolation of input for depth (or elevation) and Manning's coefficient.

The reference cell (IREF,JREF) is used for setting reference values for pressure, turbulence energy, and turbulence dissipation rate. In principle it can be any cell *except* an OUT cell. Nevertheless, since the rigid-lid pressure is the same as free-surface displacement at low Froude number, it is best to place the reference cell next to the midpoint of an inflow boundary. This is the equivalent to setting a reference elevation for the water surface at a single upstream location. The computed pressure then gives the decline in water-surface elevation necessary to maintain the input flowrate, regardless of any other user-specified depths or elevations.

The scale-reduction factor REDUCE is a convenient parameter for changing the model scale *without* changing the input for the grid or the bathymetry. It is especially useful when comparing STREMR predictions (for a given geometry) with small-scale data from physical models *and* with full-scale data from field tests. *All* x- and y-coordinates for the grid and *all* input values for velocity and depth (or elevation) are *divided* by REDUCE. Thus, REDUCE must be *less* than unity to *increase* the scale and *greater* than unity to *decrease* the scale. Note that if FLOW = 'FLOWRATE', however, the user-specified flow rate is *not* changed by REDUCE.

The variables TURBIN and PECLET are used by STREMR only when the turbulence model is activated (default). TURBIN is the ratio of turbulence energy to initial velocity squared in the reference cell (IREF,JREF), and this reference energy is the inflow turbulence energy for all FLUX cells. PECLET is the initial Peclet number (cell Reynolds number) in the reference cell, based on the local grid spacing and the initial velocity (Appendix B). This determines the inflow dissipation rate for all FLUX cells. The default values (TURBIN = 0.003 and PECLET = 50.) should ordinarily suffice for most STREMR applications, but they can be changed at the user's discretion.

Namelist PARAM

The second input namelist for hot starts *and* cold starts is PARAM, which accepts the input variables explained in Tables 4-6. These variables may be assigned one set of values for a cold start and a different set of values for subsequent hot starts. As with BEGIN, it is helpful to arrange the input for PARAM in columns according to type. Consider the following hypothetical example:

```
&PARAM  PUNITS='METRIC', NSTEPS=300,  DTIME=0.1,
        ALLOUT='YES'   , NSTORE=200,  RECAP=2.5,
          MAPS='YES'   , NSTOMO=100,   DRAG=1.0,
         TIMER='NO'    , INFORM=10 ,   AVIS=1.0,
                          ITERS=3  &END
```

The CHARACTER variables in PARAM serve as on/off switches for options that can be activated or deactivated for cold starts and subsequent hot starts. For example, one might run a cold start with a variable time-step (TIMER = 'YES') and a hot start with a fixed time-step (TIMER = 'NO') whose value is given by DTIME in the input.

PUNITS determines the units in which all output will be printed, regardless of the input units set by IUNITS (in namelist BEGIN). This does *not* affect the units for *stored* output, however, which are always metric (SI) units.

NSTEPS is the total number of time-steps executed in a given run. If NSTEPS = 0 (cold starts *only*), STREMR will compute and store the initial flow without marching forward in time. This option is convenient when trying

Table 4
CHARACTER Variables Used in Namelist PARAM

Variable	Value	Explanation
PUNITS =	'METRIC'	Printed information will be in SI (metric) units: meters, square meters, cubic meters, and seconds (default).
PUNITS =	'ENGLISH'	Printed information will be in English units: feet, square feet, cubic feet, and seconds.
ALLOUT =	'YES'	Complete listing of flow variables will be printed each time output is stored for plotting and hot starts (default).
ALLOUT =	'NO'	Complete listing of flow variables will not be printed, but partial listing may be printed, depending on input values for the print indices (IPMIN, IPMAX, JPMIN, JPMAX, ISKIP, and JSKIP).
MAPS =	'YES'	Maps of cell types and flow variables will be printed at end of STREMR run (default).
MAPS =	'NO'	Maps will not be printed.
TIMER =	'YES'	Variable time-step will be activated (default).
TIMER =	'NO'	Variable time-step will not be activated.
KETURB =	'YES'	Turbulence model will be activated (default).
KETURB =	'NO'	Turbulence model will not be activated.
BENDER =	'YES'	Secondary flow will be activated (default).
BENDER =	'NO'	Secondary flow will not be activated.

Table 5
INTEGER Variables Used in Namelist PARAM

Variable	Explanation
NSTEPS	Total number of time-steps to be executed in a given run. (Default = 1)
NSTORE	First time-step for which output is to be stored. (Default = 1)
NSTOMO	Subsequent interval beyond NSTORE (in time-steps) at which output is to be stored. (Default = 1)
INFORM	Interval (in time-steps) at which variable time-step will be reset, and at which condensed flow information will be printed. (Default = 10)
ITERS	Number of iterations used in solution of Poisson equation for pressure. (Default = 3)
IMAP	Maximum width of printed maps in the computational (i,j) plane (measured in grid spaces). Maps with width greater than IMAP will be broken into horizontal sections and stacked with the leftmost section on top. (Default = 130)

(Continued)

Table 5 (Concluded)

Variable	Explanation
IPMIN	Smallest I-index for partial cell-by-cell listing of flow variables. (Default = 0)
IPMAX	Largest I-index for partial listing. (Default = 0)
JPMIN	Smallest J-index for partial listing. (Default = 0)
JPMAX	Largest J-index for partial listing. (Default = 0)
ISKIP	Skip interval for I-index in partial listing. (Default = 1)
JSKIP	Skip interval for J-index in partial listing. (Default = 1)

Table 6
REAL Variables used in Namelist PARAM

Variable	Explanation
DTIME	Time-step in seconds if TIMER = 'NO'. (Default = 1.0)
SAFE	Safety factor for automatic calculation of variable time-step if TIMER = 'YES'. (Default = 0.9)
DRAG	Coefficient for increasing or decreasing sidewall shear stress. Used only with turbulence model. (Default = 1.0)
AVIS	Coefficient for increasing or decreasing all viscosity, whether input by user or computed by turbulence model. (Default = 1.0)
RECAP	Turbulence adjustment parameter R_C *for eddy viscosity.* (Default = 2.5) Set RECAP = 1.0 for standard k-ε model.
ASEC	Production coefficient A_S for secondary flow. Do not change default value without reading Appendix C! (Default = 5.0)
DSEC	Decay coefficient D_S for secondary flow. Do not change default value without reading Appendix C! (Default = 0.5)

new grids or new sets of input, because it allows users to find and correct many kinds of input errors without wasting much computer time on erroneous calculations. If no input errors are found, the stored initial flow can be used as input for a hot start. Note that for hot starts, however, NSTEPS *must* be greater than zero.

NSTORE is the first interval (number of time-steps) after which data will be stored for plots and future hot starts, and NSTOMO is the subsequent interval for storage. Thus, the first set of data will be stored when NSTORE time-steps have been computed; and the second set will be stored when NSTORE + NSTOMO time-steps have been computed since the beginning of the run. Storage is repeated at intervals of NSTOMO time-steps until the total number reaches NSTEPS for that run.

ALLOUT determines whether a cell-by-cell listing of flow variables will be printed at the end of each storage interval. If ALLOUT = 'YES' (default), STREMR prints a complete listing of flow variables. Otherwise, if ALLOUT = 'NO', STREMR prints a partial listing *unless* IPMIN = 0. Thus, one may obtain a full listing, a partial listing, or no listing at all. MAPS determines whether maps of cell types and relative values of flow variables (1 to 9) will be printed at the *end* of the run. These maps are also printed when a calculation becomes unstable (regardless of the input value for MAPS) *if* STREMR can detect the instability before blowing up.

KETURB and BENDER, respectively, control the turbulence model and the secondary flow correction. When KETURB = 'YES' (default), the computed flow is turbulent, with eddy viscosity generated automatically by the turbulence model. When KETURB = 'NO', the computed flow is laminar, with constant viscosity (user-specified). Likewise, when BENDER = 'YES' (default), the influence of secondary flow is included with bottom friction. Otherwise, when BENDER = 'NO', the secondary flow is omitted altogether.

With the variable time-step activated (default), the time-step is computed automatically by STREMR, and no input value is needed for DTIME. At designated intervals (INFORM), and at the end of each storage interval, STREMR resets the variable time-step and prints condensed information about the current state of the computed flow.

The condensed information includes a quantity called EMAX, which is an index for convergence of the iterative pressure calculation. As a rule of thumb, EMAX should be less than 0.02, but larger values may be acceptable for transient flow conditions. Anomalies are often quite noticeable in the computed flow when EMAX approaches or exceeds 0.1. Increasing ITERS (the number of pressure iterations) usually reduces EMAX, and vice versa.

Whenever the variable time-step is activated (TIMER = 'YES'), default values should ordinarily be used for the REAL variables in namelist PARAM. Note that SAFE is the fraction of the maximum allowable time-step that STREMR will use in setting the variable time-step. If stability problems arise, they can sometimes be overcome by making SAFE less than its default value (0.9). If the variable time-step is *not* activated (TIMER = 'NO'), a fixed value must be specified for the time-step DTIME in seconds. In the latter case, stability problems can sometimes be overcome by reducing DTIME.

Whenever the turbulence model is activated (KETURB = 'YES'), sidewall resistance can be increased (or decreased) by making DRAG greater (or less) than unity. The eddy viscosity can be reduced (or increased) in regions of low velocity and strong turbulence by increasing (or reducing) RECAP, which is the STREMR name for the turbulence adjustment parameter R_C in Appendix B.

The default value RECAP = 2.5 is used for the modified k-ε model in STREMR, and it is set slightly high to compensate for anticipated grid error on coarse grids. Note that the *standard* k-ε model can be imposed by setting RECAP = 1.0. With or without the turbulence model activated, however, the viscosity can be uniformly increased (or decreased) everywhere by making AVIS greater (or less) than unity. As for the secondary-flow coefficients A_S and D_S in Appendix C, only the default values (ASEC = 5.0 and DSEC = 0.5) should be used for the corresponding STREMR parameters.

Namelist INPUT

For cold starts *only*, the third namelist is INPUT. This namelist is used *repeatedly* for the input of cell types and for the input of general (global) values, section values, line values, and random (single-cell) values of the initial flow variables. Even if no cell types or flow variables are specified for a cold start, INPUT *must* appear *at least ten times*:

```
&INPUT ITEM='CELL TYPES'   &END
&INPUT ITEM='END'          &END
&INPUT ITEM='GENERAL'  &END
&INPUT ITEM='END'      &END
&INPUT ITEM='SECTION'  &END
&INPUT ITEM='END'      &END
&INPUT ITEM='LINE'   &END
&INPUT ITEM='END'    &END
&INPUT ITEM='RANDOM' &END
&INPUT ITEM='END'      &END
```

If any one of these ten INPUT namelists is missing or out of order, STREMR will stop or abort.

The *ten* required occurrences of INPUT come in *five* pairs, which open and close *five* different categories of input. In each pair, the character variable ITEM opens the input category (e.g., ITEM = 'CELL TYPES'), and it also closes the input category (ITEM = 'END'). Additional INPUT namelists can be inserted between the opening/closing pair for each category, with ITEM used to indicate the input quantities to be specified in each case.

Input for Cell Types

In the *first* input category, the namelist INPUT is used to specify cell types. The integer pairs (*I1*,*J1*) and (*I2*,*J2*) indicate rows (*J1* = *J2*), columns (*I1* = *I2*), and rectangular sections (*I1* ≠ *I2* and *J1* ≠ *J2*) in the computational (*i*,*j*) plane. The INPUT namelist instructions for cell types are given in Table 7.

Each row or column of OPEN cells has a separate identity and must *not* overlap any other row or column of OPEN cells. Note also that OPEN cells

Table 7
Instructions for INPUT Namelist Sequence to Specify Cell Types

1. The opening INPUT namelist for cell types contains only the CHARACTER variable
ITEM = 'CELL TYPES'

2. Intermediate INPUT namelists (if any) must contain ITEM and the INTEGER indices I1, I2, J1, and J2. ITEM indicates the cell type to be specified. The indices dictate cell locations in the (i,j) plane.

Variable	Value	Explanation
ITEM =	'FLUX'	FLUX cells (*fixed inflow or outflow*)
ITEM =	'OPEN'	OPEN cells (*variable inflow or outflow*)
ITEM =	'SLIP'	SLIP cells (*no sidewall friction*)
ITEM =	'NOSLIP'	NOSLIP cells (*default along boundaries*)
ITEM =	'OUT'	OUT cells (phantom cells outside grid and inactive cells inside obstacles)
ITEM =	'ALL SLIP'	Converts all existing NOSLIP cells to SLIP cells
I1 =	...	Smallest INTEGER i-index for row, column, or section (1 to IMAX)
J1 =	...	Smallest INTEGER j-index for row, column, or section (1 to JMAX)
I2 =	...	Largest INTEGER i-index for row, column, or section (1 to IMAX)
J2 =	...	Largest INTEGER j-index for row, column, or section (1 to JMAX)

3. Item 2 must be repeated for each separate row, column, or section of cell types to be specified.

4. The closing INPUT namelist for cell types contains only the CHARACTER variable
ITEM = 'END'

cannot be changed by subsequent input. STREMR will stop if the cell type is specified more than once for an OPEN cell at a single location in the computational (*i,j*) plane. See Appendix E for an explanation of the radiation boundary condition for OPEN cells.

Input for SLIP, NOSLIP, and OUT cells can be specified in rectangular sections, as long as the final configuration leaves only rows and columns of SLIP and NOSLIP cells. In this case, the indices (*I1,J1*) indicate the lower left cell and (*I2,J2*) the upper right cell of the section. Input for FLUX, SLIP, NOSLIP, and OUT cells *can* overlap. When the cell type is specified more than once for a FLUX, SLIP, NOSLIP, or OUT cell with indices (*i,j*), the *last* designation *replaces* all *previous* designations. Remember that NOSLIP is the default cell type along all grid boundaries. Any cell that does *not* lie next to a boundary (i.e., does not touch an OUT cell) is a FIELD cell by default.

Since any cell type (except OPEN) can be changed to any other cell type (except FIELD) by subsequent input, it is possible to create internal obstacles that were not generated with the original grid. Consider the following hypothetical INPUT sequence:

```
&INPUT ITEM='CELL TYPES'                                    &END
&INPUT ITEM='NOSLIP' , I1=2 , J1=1 , I2=19, J2=1   &END
&INPUT ITEM='SLIP'   , I1=2 , J1=10, I2=19, J2=10  &END
&INPUT ITEM='NOSLIP' , I1=11, J1=3 , I2=13, J2=8   &END
&INPUT ITEM='OUT'    , I1=12, J1=4 , I2=12, J2=7   &END
&INPUT ITEM='FLUX'   , I1=1 , J1=1 , I2=1 , J2=10  &END
&INPUT ITEM='OPEN'   , I1=20, J1=1 , I2=20, J2=10  &END
&INPUT ITEM='END'                                           &END
```

In the computational (i,j) plane, this INPUT sequence creates an obstacle 1 cell thick (in the i-direction) and 4 cells wide (in the j-direction) inside a grid with 20 cells in the i-direction and 10 cells in the j-direction. The west end of the grid is a FLUX boundary, and the east end is an OPEN boundary. *Between* the ends, the north and south grid boundaries are SLIP and NOSLIP, respectively.

In its printed maps of cell types, STREMR uses the following numerals to indicate the six different types in the computational plane:

0 = OUT   1 = FIELD   2 = NOSLIP   3 = SLIP   4 = FLUX   5 = OPEN

Thus, for the hypothetical INPUT sequence above, the map of cell types printed by STREMR would be:

```
43333333333333333335
41111111111111111115
41111111112221111115
41111111112021111115
41111111112021111115
41111111112021111115
41111111112021111115
41111111112221111115
41111111111111111115
42222222222222222225
```

Placement of Cell Types

There are limitations on the placement of the various cell types. Some of these are rules that *must* be followed if STREMR is to run at all, while others are simply guidelines that improve the quality of computed results. Using the same numerals as before to indicate cell types, the rules and recommendations for cell placement are given below:

a. No FIELD cell may touch an OUT cell. Only SLIP, NOSLIP, FLUX, and OPEN cells may touch an OUT cell. For example, STREMR will stop if it encounters the following arrangement of cells:

```
11111
10001
10001
11111
```

b. SLIP, NOSLIP, FLUX, and OPEN cells are allowed only as single rows and columns. STREMR will stop if it encounters any of the following arrangements of cells:

```
22   33   44444   5     5
22   33   44444   55    55
     33   44444   555   555
```

c. SLIP and NOSLIP cells must touch at least one OUT cell. This includes the phantom OUT cells that surround the grid (Figure 4). STREMR will stop if it encounters any of the following arrangements of cells:

```
11111   111   111   1111
12221   121   131   1331
11111   121   131   1111
        111   111
```

d. FLUX and OPEN cells must have at least one entire face in common with an out cell. This includes the phantom OUT cells that surround the grid (Figure 4). STREMR will stop if it encounters any of the following arrangements of cells:

```
11111   1111111   1111111
14441   1422241   1533351
11111   1200021   1300031
        1422241   1300031
                  1533351
                  1111111
```

e. It is best not to place rows or columns of OPEN cells next to rows or columns of FLUX cells. STREMR may have trouble with the following arrangements of cells:

```
222224   555444   555555
111114   311112   111114
111114   311112   111114
111115   311112   111114
111115   311112   111114
333335   311112   222224
```

f. It is best not to place OPEN cells next to obstacles and indentations. STREMR may have trouble with the following arrangements of cells:

```
111111111111111   111111111111111
111113555531111   111111111111111
111113000031111   111112555521111
111113000031111   111112000021111
111113333331111   111112000021111
111111111111111   222222000022222
```

g. Whenever possible, it is best if OPEN cells extend all the way across the end of a channel or the end of a channel arm. For example, the following are well-placed distributions of OPEN cells:

```
22222222222225   22222222222225
11111111111115   11111111111115
11111111111115   11111111111115
11111111111115   11111111111115
11111111111115   11122222222225
11111111111115   11120000000000
11111111111115   11120000000000
11111111111115   11122222222225
11111111111115   11111111111115
11111111111115   11111111111115
22222222222225   22222222222225
```

The foregoing maps of cell types show only portions of a hypothetical grid, and they show none of the phantom OUT cells that always surround the grid (Figures 3 and 4). Remember that SLIP and NOSLIP cells can be specified in sections *if* subsequent input for OUT cells (by row, column, or section) leaves only *rows* and *columns* of SLIP and NOSLIP cells in the resulting (final) configuration. STREMR checks the final arrangement of the input cell types and prints the locations and types of fatally misplaced cells.

Input for Quantities Other than Cell Types

The INTEGER indices I1, J1, I2, and J2 are used in general to define rows, columns, lines, sections, and single cells in the *computational* (*i,j*) plane. For input quantities *other* than cell types, however, the REAL (floating-point) coordinates X1, Y1, X2, and Y2 are also used to define lines and points in the *Cartesian* (*x,y*) plane as well.

VALUES is a one-dimensional REAL array that is used to specify floating-point input quantities such as depth, elevation, velocity, and Manning's coefficient. The character variable UNITS indicates the units for individual input quantities. Note that UNITS needs to be specified only for each occurrence of INPUT in which UNITS is *different* from IUNITS.

General (Default) Values

In the *second* input category, the namelist INPUT is used to specify general values of parameters and flow variables for the grid as a whole. The INPUT namelist instructions for general values are given in Table 8. These values replace the default values that would otherwise be used by STREMR. A hypothetical INPUT sequence for general values might have the following appearance:

Table 8
Instructions for INPUT Namelist Sequence to Specify General Values

1. The opening INPUT namelist for general values contains only the CHARACTER variable
ITEM = 'GENERAL'

2. Intermediate INPUT namelists (if any) must contain ITEM and VALUES. ITEM indicates the input quantity, and VALUES gives its REAL value. The optional CHARACTER variable UNITS is for units other than IUNITS.

Variable	**Value**	**Explanation**
ITEM =	'X-VELOCITY'	X-component of velocity (Default = 0.0)
ITEM =	'Y-VELOCITY'	Y-component of velocity (Default = 0.0)
ITEM =	'I-VELOCITY'	I-component of velocity (Default = 0.0)
ITEM =	'J-VELOCITY'	J-component of velocity (Default = 0.0)
ITEM =	'FLOWRATE'	Flowrate (Default = 1.0)
ITEM =	'MANNING'	Manning's coefficient (Default = 0.0)
ITEM =	'DEPTH'	Depth (Default = 1.0)
ITEM =	'SURFACE'	Surface elevation (Default = 1.0)
ITEM =	'BOTTOM'	Bottom elevation (Default = 0.0)
ITEM =	'DEEPER'	Constant added to all STREMR flow depths (Default = 0.0)
ITEM =	'VISCOSITY'	Kinematic viscosity (Default = 0.000001)
ITEM =	'GRID'	UNITS will be specified for grid
VALUES =	...	Single REAL value for input quantity
UNITS =	'METRIC'	SI units (if different from IUNITS)
UNITS =	'ENGLISH'	Non-SI units (if different from IUNITS)

3. Item 2 must be repeated for each general value to be specified.

4. The closing INPUT namelist for general values contains only the CHARACTER variable
ITEM = 'END'

```
&INPUT ITEM='GENERAL'                        &END
&INPUT ITEM='FLOWRATE'  , VALUES=20.    &END
&INPUT ITEM='DEPTH'         , VALUES=1.      &END
&INPUT ITEM='I-VELOCITY' , VALUES=1.      &END
&INPUT ITEM='MANNING'   , VALUES=0.02 &END
&INPUT ITEM='END'                              &END
```

With automatic interpolation activated by INTERP = 'YES' in namelist BEGIN (default), general values will be imposed in all SLIP, NOSLIP, FLUX, and OPEN cells, *exept* those where other values have been specified by subsequent input (see below). Otherwise, when INTERP = 'NO', general values will be used in *all* grid cells, *exept* those where other values have been specified by subsequent input.

Remember that when VGUESS = 'NO' in namelist BEGIN (default), STREMR uses only the input velocity components *normal* to FLUX and OPEN boundaries when it computes the initial flow inside the grid. In this case, the general velocity affects only those FLUX and OPEN cells for which there is no subsequent velocity input. Otherwise, when VGUESS = 'YES', the general velocity influences *all* grid cells for which there is no subsequent velocity input.

Note also that STREMR accepts *either* x- and y-components *or* i- and j-components for input velocity (general or otherwise), depending on which is specified *last*. For example, if an x-component is specified first and a j-component is specified afterward, then STREMR uses *only* the j-component.

STREMR accepts input values for depth only when ELEVAT = 'NO' in namelist BEGIN (default). Otherwise, when ELEVAT = 'YES', it accepts input values for surface and bottom elevations instead of depth. Note that when ITEM = 'DEEPER', the value specified for VALUES is a constant that will be divided by the scale factor REDUCE and added to *all* depths otherwise resulting from the input for depth or elevation. This allows users to increase or decrease the flow depth by the same amount everywhere, without having to change the rest of the input for bathymetry.

Remember that when KETURB = 'YES' in namelist BEGIN (default), STREMR computes eddy viscosity from the turbulence model, and no general value is needed for viscosity. Otherwise, when KETURB = 'NO', be sure to specify a general value for viscosity.

Section Values

In the *third* input category, the namelist INPUT is used to specify values for parameters and flow variables in rectangular sections of the computational (*i,j*) plane. The INPUT namelist instructions for section values are given in Table 9. Values are assigned by rows (I1 to I2), beginning with the J1 row and ending with the J2 row. Be careful that the number of values specified

Table 9
Instructions for INPUT Namelist Sequence to Specify Section Values

1. The opening INPUT namelist for section values contains only the CHARACTER variable
ITEM = 'SECTION'

2. Intermediate INPUT namelists (if any) must contain ITEM, VALUES, and I1, I2, J1, and J2. ITEM indicates the input quantity. VALUES gives its REAL values. UNITS (optional) is for units other than IUNITS.

Variable	Value	Explanation
ITEM =	'X-VELOCITY'	X-component of velocity
ITEM =	'Y-VELOCITY'	Y-component of velocity
ITEM =	'I-VELOCITY'	I-component of velocity
ITEM =	'J-VELOCITY'	J-component of velocity
ITEM =	'MANNING'	Manning's coefficient
ITEM =	'DEPTH'	Depth
ITEM =	'SURFACE'	Surface elevation
ITEM =	'BOTTOM'	Bottom elevation
I1 =	...	Smallest INTEGER i-index for section
J1 =	...	Smallest INTEGER j-index for section
I2 =	...	Largest INTEGER i-index for section
J2 =	...	Largest INTEGER j-index for section
VALUES =	...	Multiple REAL values for input quantity
UNITS =	'METRIC'	SI units (if different from IUNITS)
UNITS =	'ENGLISH'	Non-SI units (if different from IUNITS)

3. Item 2 must be repeated for each different section and for each variable that is to be assigned section values.

4. The closing INPUT namelist for section values contains only the CHARACTER variable
ITEM = 'END'

fills the section exactly. A hypothetical INPUT sequence for section values might have the following appearance:

```
&INPUT ITEM='SECTION'                                               &END
&INPUT ITEM='DEPTH'     , I1=2, I2=7, J1=3, J2=5, VALUES=18*1.2
&INPUT ITEM='MANNING' , I1=4, I2=5, J1=6, J2=7,
                                    VALUES=0.021,0.022,0.022,0.021  &END
&INPUT ITEM='END'                                                   &END
```

Note that the input values for the array VALUES can be specified sequentially as REAL numbers separated by commas, *and* as INTEGER multiples of single REAL numbers, as shown above.

Line Values

In the *fourth* input category, INPUT is used to specify user-designated values for parameters and flow variables along lines in either the computational (*i,j*) plane or the Cartesian (*x,y*) plane. The INPUT namelist instructions for line values are given in Table 10. In this case, the end points must be specified for the line, along with the respective end-point values for the input quantity. End points for a single line may be specified as either (*i,j*) or (*x,y*) coordinates, but not both.

STREMR uses linear interpolation (with respect to arc length) to distribute values of the designated variable between the two end points, but the lines connecting end points are not necessarily straight. Given a pair of Cartesian (*x,y*) end points, the code finds two cells whose centers lie closest to these points. It then finds the shortest connection between the centers of the end-point cells in the computational (*i,j*) plane. That connection might be a row, a column, a diagonal, or a combination thereof. The centers of the connecting cells are the interpolation points for the input variable. A hypothetical INPUT namelist sequence for line input might have the following form:

```
&INPUT ITEM='LINE'                                                        &END
&INPUT ITEM='DEPTH'     , I1=3  , J1=2  , I2=1  , J2=7  , VALUES=1.10,0.90 &END
&INPUT ITEM='MANNING' , X1=2.1, Y1=1.3, X2=6.4, Y2=0.8, VALUES=0.01,0.02 &END
&INPUT ITEM='END'                                                         &END
```

Note that for line input, I1 can be greater than I2, and J1 greater than J2. Likewise, X1 can be greater than X2, and Y1 greater than Y2.

Values for Cells and Points at Random

In the *fifth* input category, INPUT is used to specify parameters and flow variables at random for individual cells (I1,J1) in the computational plane and for individual points (X1,Y1) in the Cartesian plane. The INPUT namelist instructions for random values are given in Table 11. A hypothetical namelist sequence for random input might have the following form:

```
&INPUT ITEM='RANDOM'                                &END
&INPUT ITEM='DEPTH'     , X1=8.6, Y1=7.9, VALUES=1.05 &END
&INPUT ITEM='MANNING'.  I1=2  , J2=9  , VALUES=0.01 &END
&INPUT ITEM='END'                                   &END
```

Table 10
Instructions for INPUT Namelist Sequence to Specify Line Values

1. The opening INPUT namelist for line values contains only the CHARACTER variable
ITEM = 'LINE'

2. Intermediate INPUT namelists (if any) must contain ITEM, VALUES, and the indices I1, I2, J1, and J2 (or the Cartesian coordinates X1, X2, Y1, and Y2). In this case, VALUES gives the input values for the two end cells (I1,J1) and (I2,J2) *or* for the two Cartesian end points (X1,Y1) and (X2,Y2).

Variable	Value	Explanation
ITEM =	'...'	Same as for section input
UNITS =	'...'	Same as for section input
VALUES =	...	REAL values for input quantity at the two end points of the line
I1 =	...	INTEGER i-index for cell containing first end point
J1 =	...	INTEGER j-index for cell containing first end point
I2 =	...	INTEGER i-index for cell containing second end point
J2 =	...	INTEGER j-index for cell containing second end point
X1 =	...	REAL x-coordinate for first end point
Y1 =	...	REAL y-coordinate for first end point
X2 =	...	REAL x-coordinate for second end point
Y2 =	...	REAL y-coordinate for second end point

3. Item 2 must be repeated for each different line and for each variable that is to be assigned line values.

4. The closing INPUT namelist for line values contains only the CHARACTER variable
ITEM = 'END'

Figure 8 shows the complete sequence of hypothetical namelists for BEGIN, PARAM, and INPUT in proper order.

Execution

Table 12 summarizes the main steps carried out by STREMR for hot starts and cold starts. With all the namelists assembled in a command file or an input file, and with the grid data assigned to a second input file, the user is ready to execute a flow calculation.

When executing a cold start (START = 'COLD') for a new grid or a new

Table 11
Instructions for INPUT Namelist Sequence to Specify Random Values

1. The opening INPUT namelist for random values contains only the CHARACTER variable
ITEM = 'RANDOM'

2. Intermediate INPUT namelists (if any) must contain ITEM, VALUES, and the indices I1 and J1 (or the Cartesian coordinates X1 and Y1). In this case, VALUES gives the value of the input quantity *in* the cell (I1,J1) or *at* the Cartesian point (X1,Y1).

Variable	Value	Explanation
ITEM =	'...'	Same as for section input
UNITS =	'...'	Same as for section input
VALUES =	...	Single REAL value for input quantity
I1 =	...	INTEGER i-index for grid cell
J1 =	...	INTEGER j-index for grid cell
X1 =	...	REAL x-coordinate for Cartesian point
Y1 =	...	REAL y-coordinate for Cartesian point

3. Item 2 must be repeated for each different cell or point and for each variable that is to be assigned *individual point values or cell values.*

4. The closing INPUT namelist for random values contains only the CHARACTER variable
ITEM = 'END'

set of flow parameters, it is wise to make the first run with NSTEPS = 0. STREMR will then calculate and store the initial flow, print all information requested by the user, and stop. This is convenient for detecting errors in the input, but it works only for cold starts. For hot starts (START = 'HOT'), NSTEPS = 1 is the fewest number of time-steps permissible.

Except when computing time-dependent flow, it is preferable to use a variable time-step (TIMER = 'YES'). Even for time-dependent flow, it is a good idea to make a short test run with a variable time-step to find out what the fixed time-step should be. A longer run can then be executed with a fixed time-step.

If the real flow has no steady state, as is often the case when obstacles are present, then STREMR should likewise reach no steady state. If the real flow does have a steady state, then STREMR should reach a condition in which the computed velocities hover about their steady-state values. In the latter case, there will be no discernible change in plotted streamlines, and hardly any change in plotted velocity vectors. For practical purposes this *is* the steady state. There is little point in further calculation when the maximum and minimum values of velocity (in the condensed flow information) have remained unchanged for several hundred time-steps.

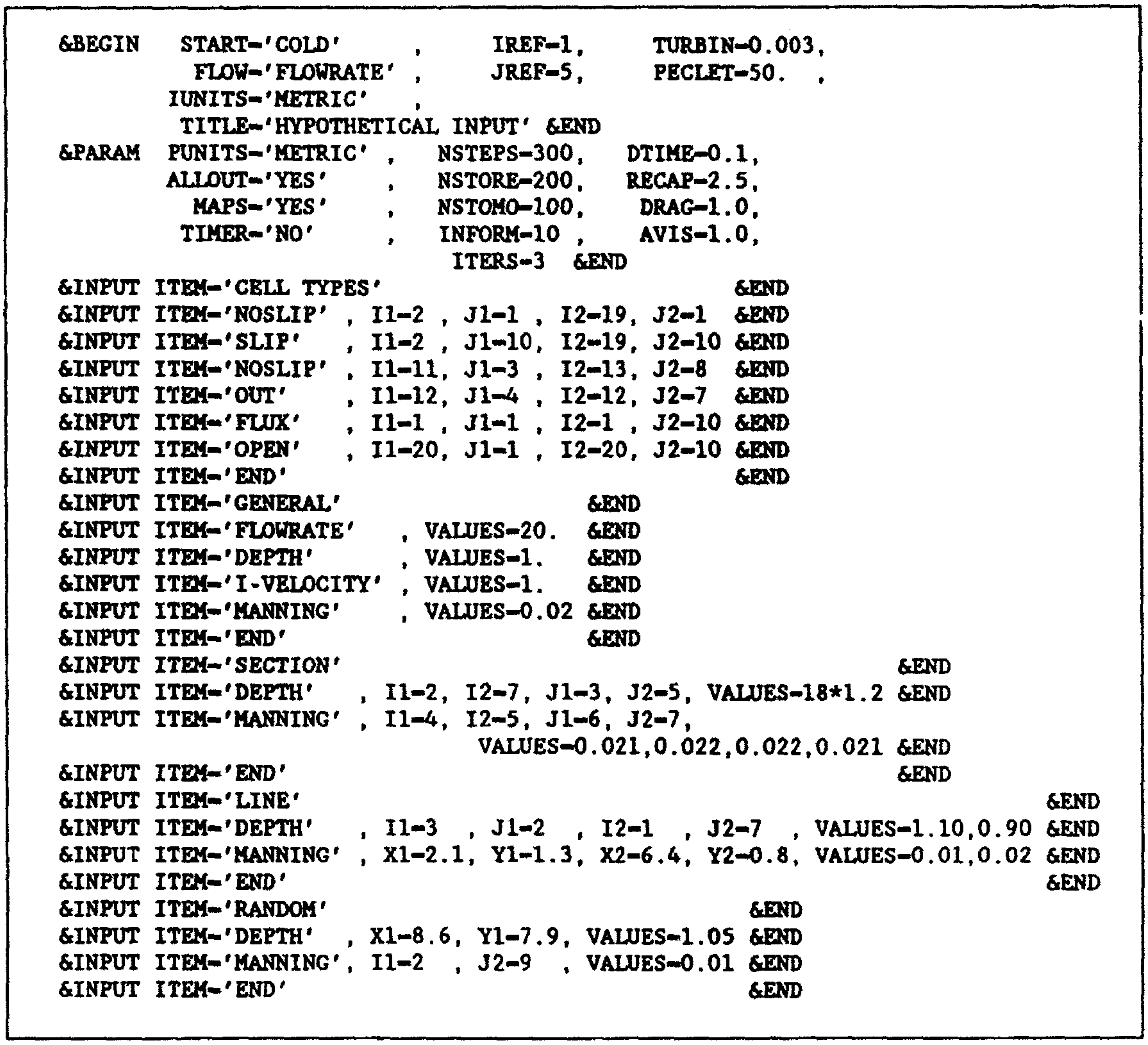

```
&BEGIN   START='COLD'      ,      IREF=1,      TURBIN=0.003,
          FLOW='FLOWRATE' ,      JREF=5,      PECLET=50.  ,
        IUNITS='METRIC'    ,
         TITLE='HYPOTHETICAL INPUT' &END
&PARAM  PUNITS='METRIC' ,   NSTEPS=300,   DTIME=0.1,
        ALLOUT='YES'    ,   NSTORE=200,   RECAP=2.5,
          MAPS='YES'    ,   NSTOMO=100,    DRAG=1.0,
         TIMER='NO'     ,   INFORM=10 ,    AVIS=1.0,
                              ITERS=3  &END
&INPUT ITEM='CELL TYPES'                          &END
&INPUT ITEM='NOSLIP' , I1=2 , J1=1 , I2=19, J2=1  &END
&INPUT ITEM='SLIP'   , I1=2 , J1=10, I2=19, J2=10 &END
&INPUT ITEM='NOSLIP' , I1=11, J1=3 , I2=13, J2=8  &END
&INPUT ITEM='OUT'    , I1=12, J1=4 , I2=12, J2=7  &END
&INPUT ITEM='FLUX'   , I1=1 , J1=1 , I2=1 , J2=10 &END
&INPUT ITEM='OPEN'   , I1=20, J1=1 , I2=20, J2=10 &END
&INPUT ITEM='END'                                 &END
&INPUT ITEM='GENERAL'                   &END
&INPUT ITEM='FLOWRATE'   , VALUES=20.  &END
&INPUT ITEM='DEPTH'      , VALUES=1.   &END
&INPUT ITEM='I-VELOCITY' , VALUES=1.   &END
&INPUT ITEM='MANNING'    , VALUES=0.02 &END
&INPUT ITEM='END'                       &END
&INPUT ITEM='SECTION'                                       &END
&INPUT ITEM='DEPTH'   , I1=2, I2=7, J1=3, J2=5, VALUES=18*1.2 &END
&INPUT ITEM='MANNING' , I1=4, I2=5, J1=6, J2=7,
                             VALUES=0.021,0.022,0.022,0.021 &END
&INPUT ITEM='END'                                           &END
&INPUT ITEM='LINE'                                                  &END
&INPUT ITEM='DEPTH'   , I1=3  , J1=2  , I2=1  , J2=7  , VALUES=1.10,0.90 &END
&INPUT ITEM='MANNING' , X1=2.1, Y1=1.3, X2=6.4, Y2=0.8, VALUES=0.01,0.02 &END
&INPUT ITEM='END'                                                   &END
&INPUT ITEM='RANDOM'                               &END
&INPUT ITEM='DEPTH'  , X1=8.6, Y1=7.9, VALUES=1.05 &END
&INPUT ITEM='MANNING', I1=2  , J2=9  , VALUES=0.01 &END
&INPUT ITEM='END'                                  &END
```

Figure 8. Complete sequence of hypothetical namelists (in proper order)

Table 12
STREMR Operations for Cold Starts and Hot Starts

Cold Start	Hot Start
Read namelist BEGIN	Read namelist BEGIN
Read grid input file	Read namelist PARAM
Read namelist PARAM	Execute flow calculation for specified number of time-steps (NSTEPS)
Read namelist INPUT for cell types	Print condensed information and calculate time-step size at specified intervals (INFORM)
Read namelist INPUT for general values	Print flow variables and write output to plot and hot-start files at specified intervals (NSTORE, NSTOMO)
Read namelist INPUT for section values	Print maps of flow variables
Read namelist INPUT for line values	
Read namelist INPUT for random values	
Execute flow calculation for specified number of time-steps (NSTEPS)	
Print condensed information and calculate time-step size at specified intervals (INFORM)	
Print flow variables and write output to plot and hot-start files at specified intervals (NSTORE, NSTOMO)	
Print maps of flow variables	

4 STREMR Output

Types of Output

The STREMR code generates separate output for printing, plotting, and subsequent hot starts. Printed output appears on the monitor screen during interactive execution, but it is diverted to a default device (log file, printer, etc.) during batch execution. Data for plotting and for subsequent hot starts are written to separate output files.

Cell-by-Cell Printout of Flow Variables

When ALLOUT = 'YES' in namelist BEGIN (default), STREMR prints a complete cell-by-cell listing of cell-centered values for the primary flow variables. When ALLOUT = 'NO', STREMR prints a partial cell-by-cell listing *if* the print indices IPMIN, IPMAX, JPMIN, and JPMAX are *all* greater than zero in namelist PARAM. These are cell indices that determine the southwest corner (IPMIN,JPMIN) and the northeast corner (IPMAX,JPMAX) for the section of the computational plane included in the partial listing. The integers ISKIP and JSKIP set the i- and j-intervals at which information is printed. In the order of their appearance, the quantities that are printed are the cell indices (i,j), cell type, x-velocity (u), y-velocity (v), resultant flow speed $(u^2+v^2)^{1/2}$, pressure (p), depth (h), viscosity (ν), bottom friction factor (C_f), turbulence energy per unit mass (k), rate of turbulence energy dissipation per unit mass (ε), and Froude number (Fr).

When PUNITS = 'METRIC' in namelist PARAM (default), the printed variables are given in SI units with velocity in meters per second, pressure in meters of water, depth in meters, viscosity in square meters per second, energy (per unit mass) in square meters per square second, and energy-dissipation rate (per unit mass) in square meters per cubic second. When PUNITS = 'ENGLISH', the printed variables are given in non-SI English units with velocity in feet per second, pressure in feet of water, depth in feet, viscosity in square feet per second, energy (per unit mass) in square feet per square second, and energy-dissipation rate (per unit mass) in square feet per cubic second.

The bottom friction factor C_f is a dimensionless function of depth h and Manning's coefficient n given in Appendix A. The Froude number Fr is the dimensionless ratio of local flow speed (resultant depth-averaged velocity) to free-surface wave speed, given by

$$Fr = \sqrt{\frac{u^2 + v^2}{gh}} \tag{1}$$

where g is gravitational acceleration. The printed viscosity is the local value of viscosity (computed from the turbulence model or input by the user), which *includes* the effect of the amplification factor AVIS.

Printout of Friction and Pressure Coefficients for Sidewalls

After the cell-by-cell printout of flow variables (if any), STREMR prints the sidewall friction coefficient C_f and the sidewall pressure coefficient C_p for all SLIP and NOSLIP boundary faces that were included in the cell-by-cell printout. The formulas for these quantities are given by

$$C_f = \frac{\tau_D}{(u_0^2 + v_0^2)} \tag{2}$$

$$C_p = \frac{2p}{\rho(u_0^2 + v_0^2)} \tag{3}$$

where p is the pressure, and τ_D is the sidewall shear stress (Appendix B) computed (for turbulent flow) from the turbulence model or (for laminar flow) from a viscous no-slip condition. The quantities u_0 and v_0 are the cell-centered velocity components in reference cell (IREF,JREF).

Although the same symbol C_f is used here for bottom *and* sidewall friction coefficients, both of which arise from turbulent shear stress, the two quantities are computed differently in STREMR. The bottom friction coefficient accounts for the vertical influence of turbulence along the bottom, and it is calculated from Manning's coefficient n. The sidewall friction coefficient accounts for the lateral influence of turbulence along the sidewalls, and it is calculated from the sidewall shear stress τ_D produced by the STREMR version of the k-ε turbulence model.

Printout of Condensed Flow Information

At user-specified print intervals (INFORM) and at the end of each storage interval (NSTORE, NSTOMO), STREMR prints out condensed information about the computed flow. The definitions for the printed symbols are:

PMAX = maximum pressure
PMIN = minimum pressure
FMAX = maximum Froude number
FMIN = minimum Froude number
UMAX = maximum x-velocity
UMIN = minimum x-velocity
VMAX = maximum y-velocity
VMIN = minimum y-velocity
VISMAX = maximum viscosity
VISMIN = minimum viscosity
PECMAX = maximum Peclet number (cell Reynolds number)
PECMIN = minimum Peclet number (cell Reynolds number)
TKEMAX = maximum turbulence energy
TKEMIN = minimum turbulence energy
EPSMAX = maximum turbulence dissipation rate
EPSMIN = minimum turbulence dissipation rate
SMAX = maximum stream function
SMIN = minimum stream function
DUAVE = average relative change in x-velocity
DVAVE = average relative change in y-velocity
DUMAX = maximum relative change in x-velocity
DVMAX = maximum relative change in y-velocity
EMAX = maximum relative flux imbalance
DTMAX = new value for maximum allowable time-step
DT = time-step previously used

The Peclet number (cell Reynolds number) is proportional to velocity and streamwise cell length and inversely proportional to viscosity. For STREMR calculations *without* the turbulence model activated, the user-specified viscosity (amplified by AVIS) needs to be large enough to keep the Peclet number smaller than 50 in flow regions with appreciable velocity gradients. Otherwise, there may not be enough viscosity to prevent numerical instability. For STREMR calulations *with* the turbulence model activated (default), the Peclet number is not so important, because eddy viscosity is created in response to the velocity gradients themselves. Nevertheless, extremely large values for PECMAX (perhaps greater than 1000) just prior to instability may indicate a need for more viscosity or a finer grid.

STREMR computes the stream function ψ only so that streamlines can be plotted, and this operation is not part of the flow calculation itself. It is done after the fact (when flow information is to be printed or stored) by numerical integration of the spatial derivatives

$$\psi_x = -hv \tag{4}$$

$$\psi_y = hu \tag{5}$$

Maximum and minimum values (SMAX and SMIN) are printed for ψ in the condensed flow information. These are intended to guide the user in choosing the range of ψ that is to be included in streamline plots.

Relative changes in the cell-centered velocity components are defined for a given ιime-step by the relations

$$\Delta u_{relative} = \frac{|\Delta u|}{\sqrt{u^2 + v^2}} \tag{6}$$

$$\Delta v_{relative} = \frac{|\Delta v|}{\sqrt{u^2 + v^2}} \tag{7}$$

The printed values DUAVE and DVAVE are spatial averages of the relative changes, and DUMAX and DVMAX are the largest values for the entire grid.

Conservation of mass demands that the net volumetric flux (outflow minus inflow) be zero for every cell of the grid. Expressed in terms of the face-centered fluxes (Figure 2) for any cell (*i,j*), this means that

$$U(i,j) + V(i,j) - U(i-1,j) - V(i,j-1) = 0 \tag{8}$$

To indicate the degree to which Equation 8 is *not* satisfied, STREMR uses the relative flux imbalance E defined by

$$E = \frac{2|U(i,j) - U(i-1,j) + V(i,j) - V(i,j-1)|}{|U(i,j)| + |U(i-1,j)| + |V(i,j)| + |V(i,j-1)|} \tag{9}$$

Thus, the relative flux imbalance for cell (*i,j*) is the absolute difference between volumetric inflow and outflow, divided by the average of the two.

The maximum relative flux imbalance EMAX is the largest value of E for the entire grid. It is an index for convergence of the pressure calculation, as well as for conservation of mass. Ordinarily EMAX should be less than 0.02, but values as high as 0.05 may be acceptable, especially for transient flow. If EMAX consistently exceeds 0.1, the computed flow is no good; but if EMAX eventually falls to 0.02 or less, then mass is adequately conserved for most STREMR applications. EMAX can usually be reduced by increasing the number of pressure iterations ITERS in namelist PARAM, and vice versa.

The significance of the other printed quantities should be self-evident, but there is one more point worth mentioning. Due to an alternating (directional) bias in the MacCormack scheme for discretizing advective terms (Appendix F), STREMR never converges to a true steady state. Instead, it *hovers* about the steady state. Thus, no matter how long the code runs, one or more grid cells may exhibit small (but noticeable) changes in velocity. For this reason, the velocity increments DUAVE, DVAVE, DUMAX, and DVMAX may be poor indicators of the steady state. Better indicators are the velocity extremes UMAX, VMAX, UMIN, and VMIN, as well as the stream-function extremes SMAX and SMIN. The steady state is at hand when these quantities cease to change, or when they change very little over several hundred time-steps.

Printed Maps of Flow Variables

At the end of each run for which MAPS = 'YES' in namelist PARAM, STREMR prints maps of the computational (i,j) plane that show the locations of the various cell types and the relative magnitudes of selected flow variables. These maps run from 1 to IMAX in the i-direction, and from 1 to JMAX in the j-direction. Internal OUT cells (inside obstacles and indentions) are always represented by the numeral 0, but phantom OUT cells that surround the grid (Figure 4) are *not* shown at all.

The first map to be printed is the map of cell types, in which the following numerals are used to indicate the different types of cells:

O = OUT   1 = FIELD   2 = NOSLIP   3 = SLIP   4 = FLUX   5 = OPEN

The integer variable IMAP in namelist PARAM determines the maximum length of all maps in the i-direction. If IMAX is greater than IMAP, then the map is terminated at $i = IMAP$ and continued below (as though it were another map) starting at $i = IMAP+1$.

The next map (after cell types) is that for relative depth, and it is printed only if the depth is nonuniform. The difference between the maximum depth and the minimum depth is divided into nine intervals, and the depth for each grid cell is indicated by map numerals ranging from 1 to 9, depending on the particular interval in which that depth falls. This same procedure is used to generate maps for the relative values of other variables.

The map for depth is followed by maps for the bottom friction factor, viscosity, pressure, turbulence energy, turbulence dissipation rate, flow speed, stream function, Froude number, flux imbalance, and Peclet number. If the bottom friction is uniform, its map will not be printed. If the k-ε turbulence model is not activated, there will be no map printed for viscosity, turbulence energy, or dissipation rate. If negative values exist for stream function and pressure, the map numeral 9 indicates the highest values in a positive sense, and the map numeral 1 indicates the lowest values in a negative sense. Otherwise, for these and the remaining flow variables, the map numerals 9 and 1 indicate the largest and smallest values, respectively, in a positive sense.

Output for Plots and Hot Starts

At user-specified storage intervals given by NSTORE and NSTOMO in namelist PARAM, STREMR writes output (for plotting) to an external file assigned by the user. The first four quantities written are TITLE, IMAX, JMAX, and NOTIME (number of elapsed time steps). These are followed by arrays for selected flow variables, which are stored in the order given below. The FORTRAN name for the array is shown on the left, and the algebraic symbol is shown in parentheses on the right.

U	x-velocity (u)
V	y-velocity (v)
STRM	stream function (ψ)
DEEP	depth (h)
EDDY	eddy viscosity (ν)
PCO	pressure (p)
TKN	turbulence energy (k)
TDN	turbulence-energy dissipation rate (ε)
TYPE	cell type

Each array is written to the plot output file by a double DO-loop that runs from 1 to IMAX (inner loop) and from 1 to JMAX (outer loop) for all quantities except the stream function (STRM). The DO-loops for STRM run from 0 to IMAX and from 0 to JMAX, because STRM is computed at the grid nodes instead of the cell centers. This output file can later be used as input for a plot code, which must read the stored information in the same order in which it was written. In the plot code, the array dimensions corresponding to IDIM and JDIM in STREMR must equal or exceed $IMAX + 1$ and $JMAX + 1$, respectively.

At the same storage intervals as those for plot output, STREMR writes information needed for hot starts to a separate hot-start output file. In this case, however, the output file is overwritten at each storage interval. At the end of each run, only the last hot-start output is available for subsequent hot starts. Note that when reading a particular hot-start file in a subsequent run, the STREMR array dimensions IDIM and JDIM must be the same as they were when the hot-start file was created.

5 STREMR Examples and Verification

Background

Examples of code input and computed results are presented in this part to offer prospective users a brief demonstration of what STREMR can do with only modest input. All the grids were generated with MESH89, [1] and all the plots were created with PLOT89.[2] These codes are not discussed in this report, however, because they are separate from STREMR, and they will be replaced as better software becomes available. In any case, it is not difficult to change the STREMR input/output format to accommodate a new grid generator or plot code.

When a grid is described as a 12 X 8 grid, this means that the bounding rectangle for the grid (Figure 3) covers 12 spaces in the i-direction and 8 spaces in the j-direction, with its origin at node (0,0) in the computational *(i,j)* plane. There are no units (other than grid spaces) for *i* and *j*, and the computational (i,j) axes can point in *any* direction in the Cartesian (x,y) plane. For straight channels, it may seem logical for the i-axis to point in the x-direction, and for the j-axis to point in the y-direction; but STREMR works either way, and the *Cartesian* orientation of the i- and j-axes is up to the user.

The code runs faster when IMAX is greater than JMAX, rather than vice versa; and it is better to orient the axes in the *computational* plane so that the greater number of grid spaces lies in the i-direction (Figure 3). In all the STREMR examples, the i-direction is the streamwise direction with respect to the inflow (west boundary), and the general direction of flow is from west to east (left to right) in both the Cartesian and computational planes. In all cases, the inflow velocity is uniform and constant through the west end of the grid (FLUX boundary), but the outflow velocity changes in response to the flow just upstream of the east end (OPEN boundary).

[1] Unpublished grid-generation code provided by M. L. Schneider, Research Hydraulic Engineer, August 1989, US Army Engineer Waterways Experiment Station, Vicksburg, MS.

[2] Unpublished plot code provided by S. E. Howington, Research Hydraulic Engineer, August 1989, US Army Engineer Waterways Experiment Station, Vicksburg, MS.

In principle, numerical modelers should try sucessively finer grids until there is no further change in predictions from one grid to the next. In practice, however, this needs to be repeated only until the grid-associated changes fall to a level that is acceptable for the application under consideration. Given the uncertainties associated with bottom friction, turbulence, secondary flow, and depth-averaged modeling in general, there is little point in further grid refinement when reduction of the grid spacing (by a factor of two) changes the computed flow by less than 5 percent.

The first set of examples (Examples 1A-1J) uses uniform rectangular grids to demonstrate the computed influence of submerged and unsubmerged channel features, but it does not show how the results change with grid refinement. The second set (Examples 2A and 2B) employs nonuniform rectangular grids, and demonstrates the relative effects of grid refinement, bottom friction, and turbulence adjustment on flow predictions for backsteps (channel expansions). The third set (Examples 3A and 3B) does likewise for unsubmerged spur dikes. The fourth set (Example 4) shows the effect of grid refinement on 2-D flow predictions for a gently curved surface (2-D hill), and the fifth set (Examples 5A-5C) does the same for a more sharply curved surface (2-D circular cylinder). The final set (Examples 6A-6C) demonstrates the effect of grid refinement on depth-averaged velocity predictions for a double bendway with a trapezoidal cross section.

Comparisons of STREMR predictions and test data are included with example sets 2, 4, and 6. Except for instances where the relative influence of the turbulence parameter RECAP is demonstrated, only the default value *RECAP = 2.5* was used in the calculations. Moreover, in *all* the reported calculations, only default values were used for the following parameters:

TURBIN = 0.003
PECLET = 50.
DRAG = 1.
AVIS = 1.
ASEC = 5.0
DSEC = 0.5

In some cases, better agreement with test data might have been obtained by using values other than the default values for these quantities; but that would have been contrary to the purpose of this report, which is to show prospective users what they can expect to achieve *without* case-specific tuning.

For the most part, the namelists in the examples do not show the parameters and flow variables for which default values were used. This feature of namelist format (that variables with default values can be omitted) leaves the input conveniently uncluttered. Any variable *not* shown in namelists BEGIN or PARAM has the default value indicated by Tables 1-6. Any quantity *not* specified with the general values has the default value indicated by Table 8.

The turbulence model and the secondary flow correction are activated by default in all the STREMR examples, but there is *no* production of secondary flow without bottom friction. In case there is any confusion in recognizing plots for grids, streamlines, and velocity vectors, figures showing the computed flow always have the grid at the top, the streamlines in the middle, and the velocity vectors at the bottom. Velocity vectors are shown for every grid cell in the j-direction, but not in the i-direction. The computed flows are steady, except where stated otherwise.

Example 1A: Uniform 50 X 12 Grid for Straight Channel

Figure 9 shows a namelist sequence and its resulting map of cell types for a grid with no bottom friction or depth variation. The flow region is a straight channel, 50 ft long, 12 ft wide, and 1 ft deep, for which a uniform 50 X 12 grid has been generated (Figure 10). In this case, the grid cells are genuinely square, and the grid is identical in both the Cartesian and computational planes. The computed flow (Figure 10) is from west to east, with FLUX cells at the inflow, OPEN cells at the outflow, and NOSLIP cells elsewhere along the north and south sidewalls (by default). Since the general value for the x-velocity is unity, and since no other velocities are specified, the normal (inflow) velocity remains constant along the west end (FLUX boundary). The normal (outflow) velocity along the east end (OPEN boundary) changes in response to the developing flow just upstream.

The 50 X 12 grid is much too coarse to resolve accurately the effects of sidewall shear stress, but it can still capture the qualitative influence of bathymetry, bottom friction, and sharp-cornered obstacles. Subsequent examples (1B-1J) demonstrate the effects of varying these channel features. The variations are achieved through namelist input alone, with input for cell types used to modify the 50 X 12 grid shown in Figure 9.

Example 1B: Uniform 50 X 12 Grid with Backstep

Figure 11 shows a namelist sequence and map of cell types for a backstep (channel expansion) with no bottom friction or depth variation. Input for cell types is used to form the expansion by creating a block of NOSLIP cells with a smaller block of OUT cells inside. Since previous cell types (except OPEN) can be changed to other types (except FIELD) by subsequent input, the final configuration is a block of OUT cells with a row of NOSLIP cells to the north, and a column of NOSLIP cells to the east. The modified grid and the computed flow are shown in Figure 12.

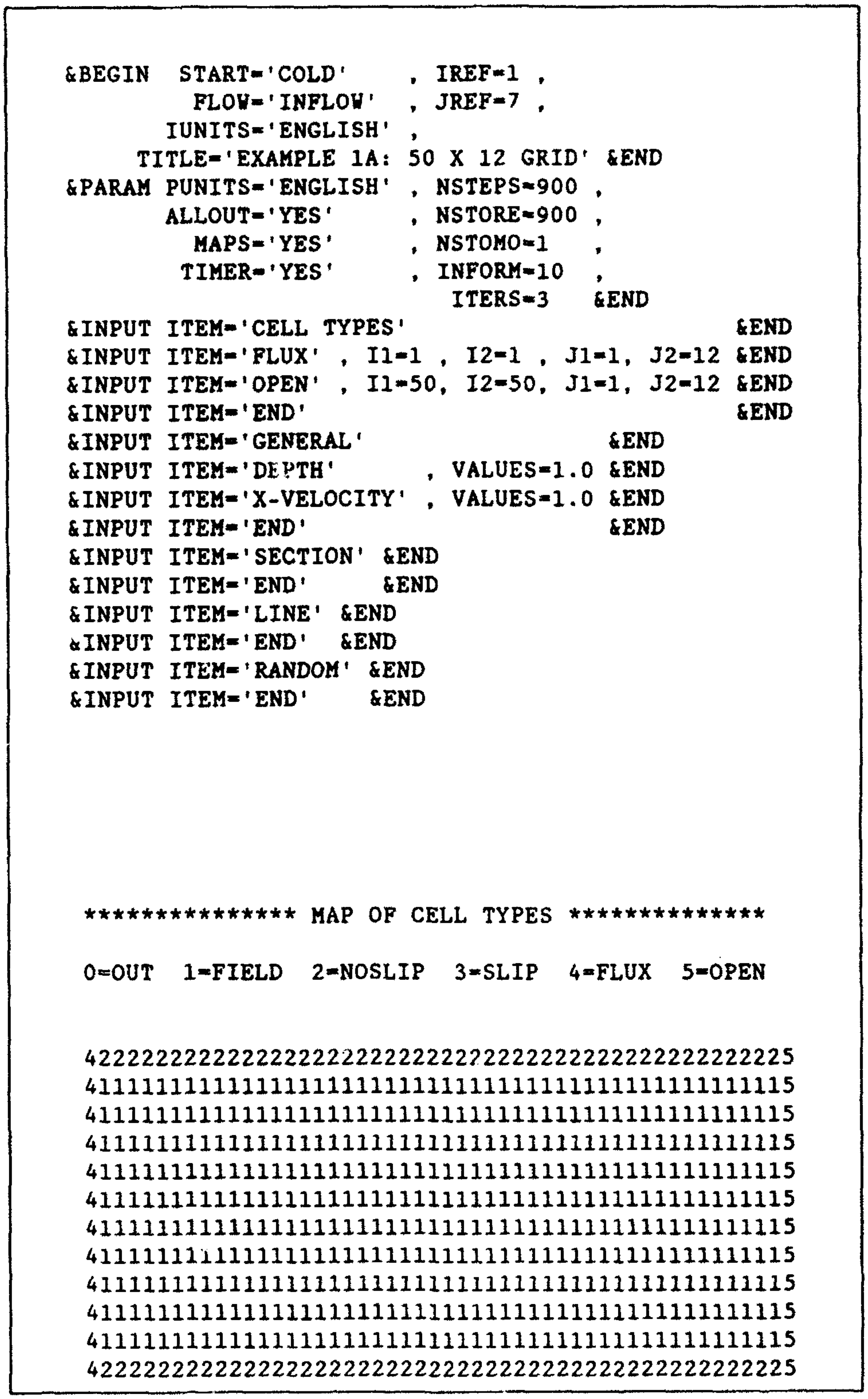

```
&BEGIN  START='COLD'     , IREF=1 ,
          FLOW='INFLOW'  , JREF=7 ,
        IUNITS='ENGLISH' ,
     TITLE='EXAMPLE 1A: 50 X 12 GRID' &END
&PARAM PUNITS='ENGLISH' , NSTEPS=900 ,
        ALLOUT='YES'     , NSTORE=900 ,
          MAPS='YES'     , NSTOMO=1   ,
         TIMER='YES'     , INFORM=10  ,
                            ITERS=3   &END
&INPUT ITEM='CELL TYPES'                         &END
&INPUT ITEM='FLUX' , I1=1 , I2=1 , J1=1, J2=12 &END
&INPUT ITEM='OPEN' , I1=50, I2=50, J1=1, J2=12 &END
&INPUT ITEM='END'                                &END
&INPUT ITEM='GENERAL'                    &END
&INPUT ITEM='DEPTH'       , VALUES=1.0 &END
&INPUT ITEM='X-VELOCITY' , VALUES=1.0 &END
&INPUT ITEM='END'                        &END
&INPUT ITEM='SECTION' &END
&INPUT ITEM='END'     &END
&INPUT ITEM='LINE' &END
&INPUT ITEM='END'  &END
&INPUT ITEM='RANDOM' &END
&INPUT ITEM='END'    &END
```

```
 *************** MAP OF CELL TYPES **************

 0=OUT  1=FIELD  2=NOSLIP  3=SLIP  4=FLUX  5=OPEN


 42222222222222222222222222222222222222222222222225
 41111111111111111111111111111111111111111111111115
 41111111111111111111111111111111111111111111111115
 41111111111111111111111111111111111111111111111115
 41111111111111111111111111111111111111111111111115
 41111111111111111111111111111111111111111111111115
 41111111111111111111111111111111111111111111111115
 41111111111111111111111111111111111111111111111115
 41111111111111111111111111111111111111111111111115
 41111111111111111111111111111111111111111111111115
 41111111111111111111111111111111111111111111111115
 42222222222222222222222222222222222222222222222225
```

Figure 9. STREMR input and resulting map of cell types for 50 × 12 grid (straight channel, no bottom friction, Example 1A)

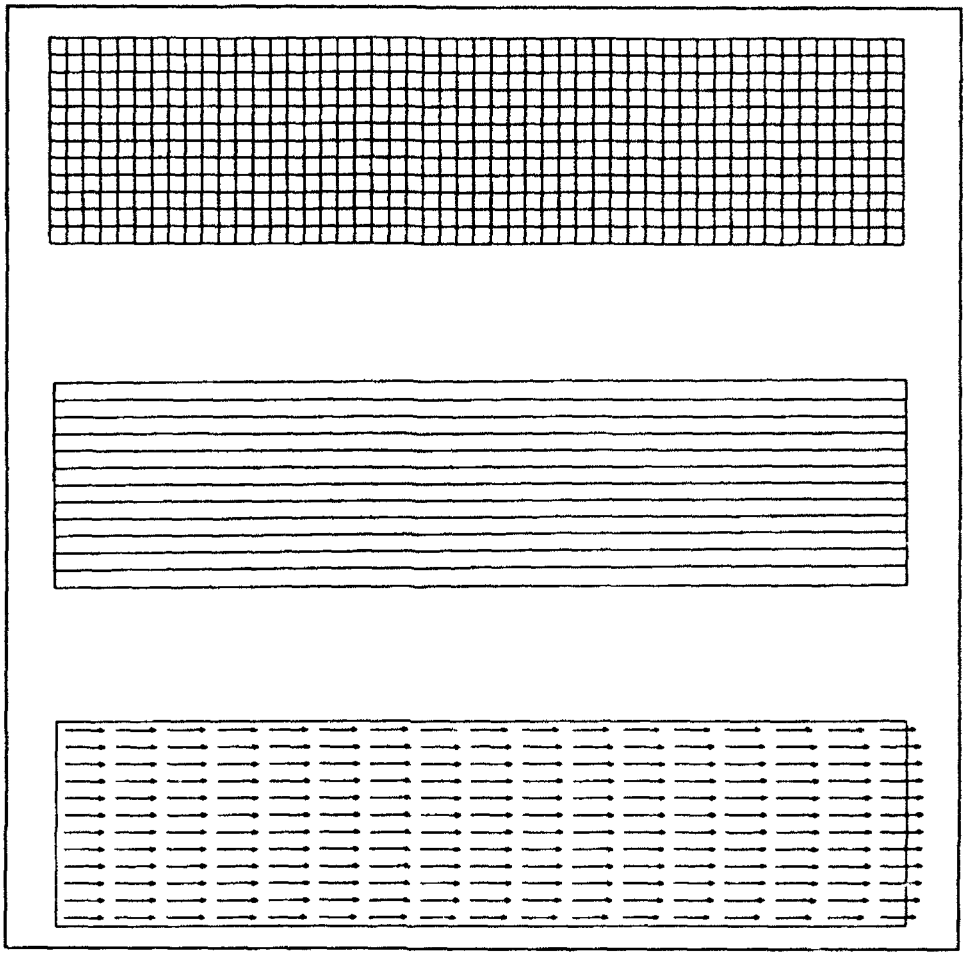

Figure 10. Uniform 50 × 12 grid with computed streamlines and velocity vectors for straight channel (Example 1A)

The flow separates from the step precisely at the expansion, and it reattaches to the wall 6.2 step widths downstream. The predicted reattachment point falls 20 percent short of the observed range for this 2-D configuration (Durst and Tropea 1981), because the grid is too coarse near the step.

This brings up an important point concerning STREMR calculations in particular, and numerical flow calculations in general. Wherever the flow encounters a sharp corner, there is some loss of streamwise momentum caused by false (numerical) diffusion normal to the flow. If the corner coincides with a channel expansion, this momentum loss is compounded by a rise in pressure (adverse pressure gradient) that further retards the flow. The inevitable result is that computed flows often separate at abrupt expansions, even when the grid is too coarse to resolve the downstream flow accurately.

```
&BEGIN  START='COLD'     , IREF=1 ,
         FLOW='INFLOW'   , JREF=7 ,
       IUNITS='ENGLISH'  ,
     TITLE='EXAMPLE 1B: 50 X 12 GRID WITH BACKSTEP' &END
&PARAM PUNITS='ENGLISH'  , NSTEPS=900 ,
       ALLOUT='YES'      , NSTORE=900 ,
         MAPS='YES'      , NSTOMO=1   ,
        TIMER='YES'      , INFORM=10  ,
                            ITERS=3   &END
&INPUT ITEM='CELL TYPES'                           &END
&INPUT ITEM='NOSLIP' , I1=1 , I2=6 , J1=1, J2=6    &END
&INPUT ITEM='OUT'    , I1=1 , I2=5 , J1=1, J2=5    &END
&INPUT ITEM='FLUX'   , I1=1 , I2=1 , J1=6, J2=12   &END
&INPUT ITEM='OPEN'   , I1=50, I2=50, J1=1, J2=12   &END
&INPUT ITEM='END'                                  &END
&INPUT ITEM='GENERAL'                   &END
&INPUT ITEM='DEPTH'      , VALUES=1.0   &END
&INPUT ITEM='X-VELOCITY' , VALUES=1.0   &END
&INPUT ITEM='END'                       &END
&INPUT ITEM='SECTION' &END
&INPUT ITEM='END'     &END
&INPUT ITEM='LINE' &END
&INPUT ITEM='END'  &END
&INPUT ITEM='RANDOM' &END
&INPUT ITEM='END'    &END




   *************** MAP OF CELL TYPES **************

   0=OUT  1=FIELD  2=NOSLIP  3=SLIP  4=FLUX  5=OPEN

   42222222222222222222222222222222222222222222222225
   41111111111111111111111111111111111111111111111115
   41111111111111111111111111111111111111111111111115
   41111111111111111111111111111111111111111111111115
   41111111111111111111111111111111111111111111111115
   41111111111111111111111111111111111111111111111115
   42222211111111111111111111111111111111111111111115
   00000211111111111111111111111111111111111111111115
   00000211111111111111111111111111111111111111111115
   00000211111111111111111111111111111111111111111115
   00000211111111111111111111111111111111111111111115
   00000222222222222222222222222222222222222222222225
```

Figure 11. STREMR input and resulting map of cell types for 50 × 12 grid with backstep (channel expansion, no bottom friction, Example 1B)

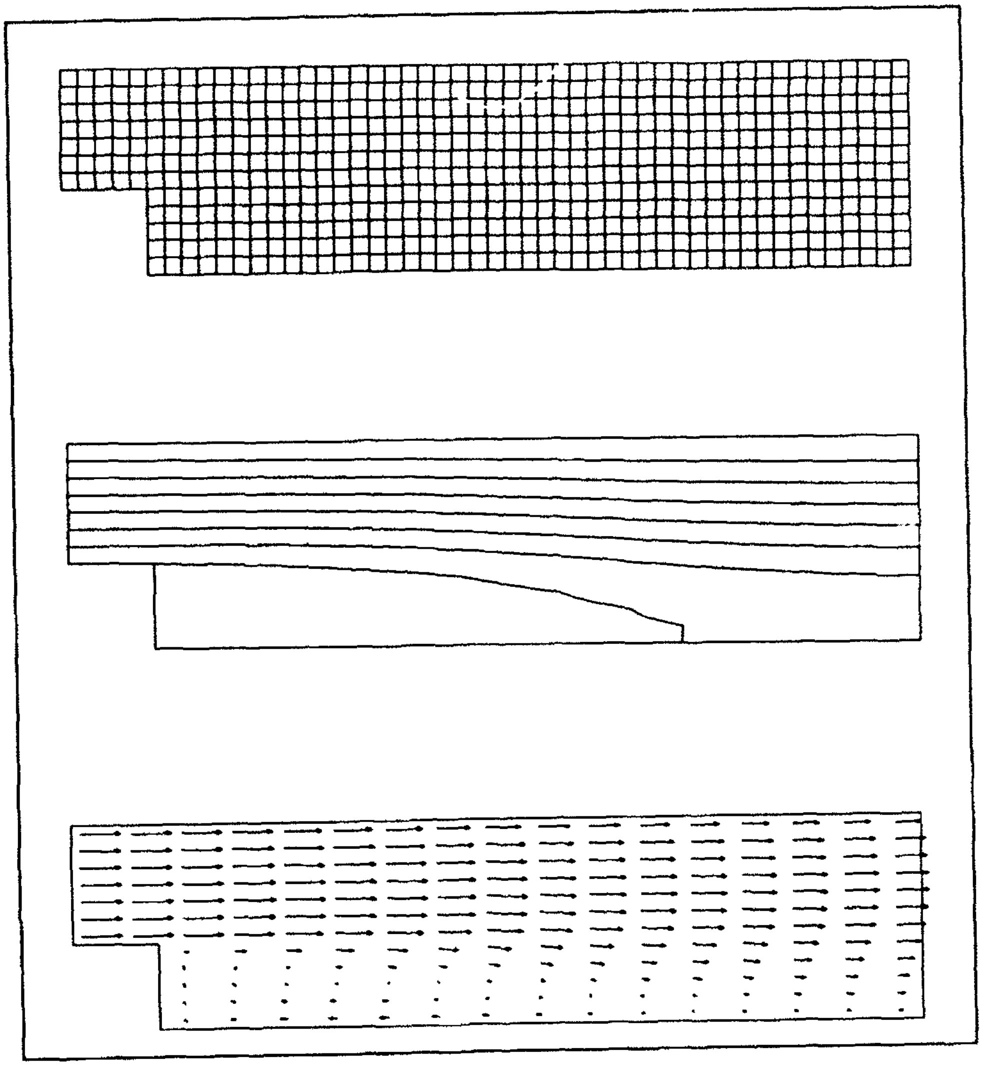

Figure 12. Uniform 50 × 12 grid with computed streamlines and velocity vectors for backstep (Example 1B)

Example 1C: Uniform 50 X 12 Grid with Forestep

Figure 13 shows a namelist sequence and map of cell types for a forestep (channel contraction) with no bottom friction or depth variation. As before, cell types have been manipulated to form the contraction by creating a block of NOSLIP cells with a smaller block of OUT cells inside. The final configuration is a block of OUT cells with a row of NOSLIP cells to the north, and a column of NOSLIP cells to the west. The modified grid and the computed flow are shown in Figure 14.

```
&BEGIN  START='COLD'     , IREF=1 ,
         FLOW='INFLOW'   , JREF=7 ,
       IUNITS='ENGLISH'  ,
     TITLE='EXAMPLE 1C: 50 X 12 GRID WITH FORESTEP' &END
&PARAM PUNITS='ENGLISH'  , NSTEPS=900 ,
       ALLOUT='YES'      , NSTORE=900 ,
         MAPS='YES'      , NSTOMO=1   ,
        TIMER='YES'      , INFORM=10  ,
                           ITERS=3    &END
&INPUT ITEM='CELL TYPES'                         &END
&INPUT ITEM='NOSLIP' , I1=16, I2=50, J1=1, J2=6  &END
&INPUT ITEM='OUT'    , I1=17, I2=50, J1=1, J2=5  &END
&INPUT ITEM='FLUX'   , I1=1 , I2=1 , J1=1, J2=12 &END
&INPUT ITEM='OPEN'   , I1=50, I2=50, J1=6, J2=12 &END
&INPUT ITEM='END'                                &END
&INPUT ITEM='GENERAL'                    &END
&INPUT ITEM='DEPTH'      , VALUES=1.0 &END
&INPUT ITEM='X-VELOCITY' , VALUES=1.0 &END
&INPUT ITEM='END'                     &END
&INPUT ITEM='SECTION' &END
&INPUT ITEM='END'     &END
&INPUT ITEM='LINE' &END
&INPUT ITEM='END'  &END
&INPUT ITEM='RANDOM' &END
&INPUT ITEM='END'    &END
```

```
   *************** MAP OF CELL TYPES **************

   0=OUT  1=FIELD  2=NOSLIP  3=SLIP  4=FLUX  5=OPEN


   42222222222222222222222222222222222222222222222225
   41111111111111111111111111111111111111111111111115
   41111111111111111111111111111111111111111111111115
   41111111111111111111111111111111111111111111111115
   41111111111111111111111111111111111111111111111115
   41111111111111111111111111111111111111111111111115
   41111111111111122222222222222222222222222222222225
   41111111111111120000000000000000000000000000000000
   41111111111111120000000000000000000000000000000000
   41111111111111120000000000000000000000000000000000
   41111111111111120000000000000000000000000000000000
   42222222222222220000000000000000000000000000000000
```

Figure 13. STREMR input and resulting map of cell types for 50 × 12 grid with forestep (channel contraction, no bottom friction, Example 1C)

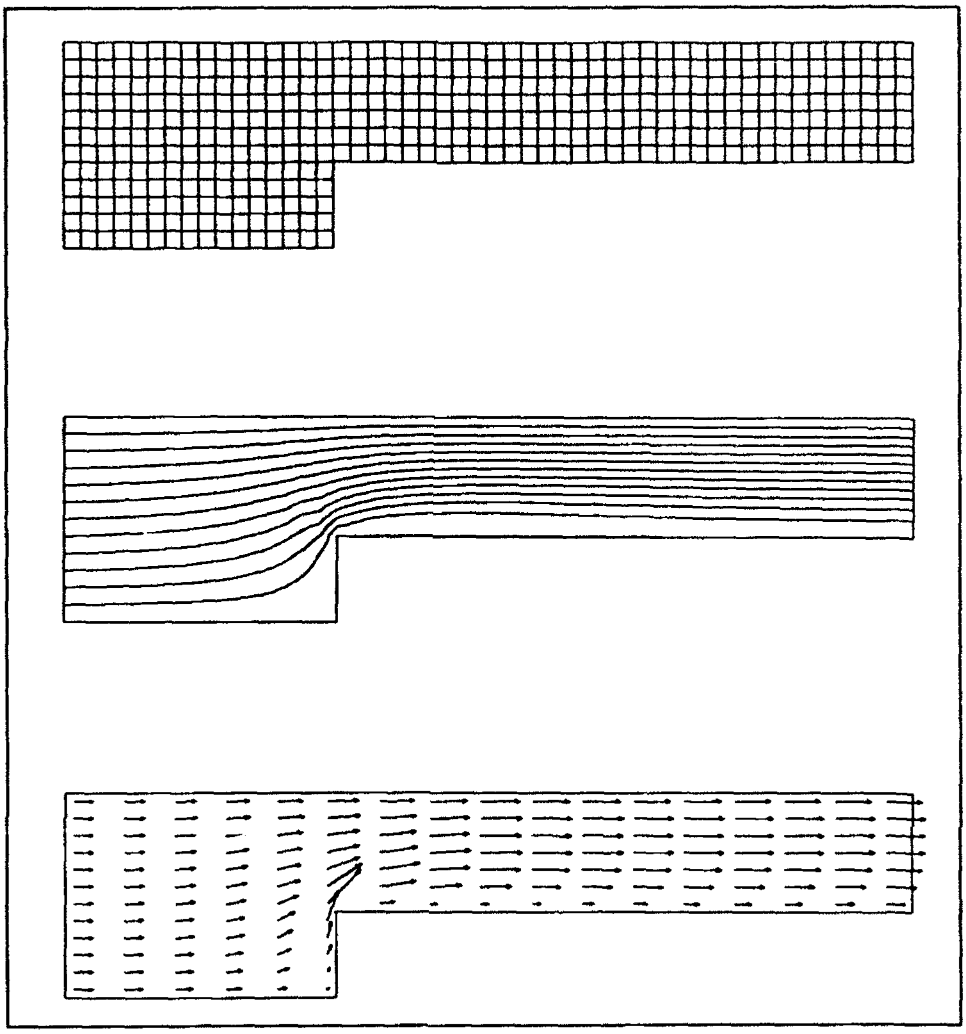

Figure 14. Uniform 50 x 12 grid with computed streamlines and velocity vectors for forestep (Example 1C)

The flow makes a sharp turn at the contraction, and the streamlines are pushed away from the wall downstream. No recirculation occurs, however, contrary to experimental observations made for similar 2-D configurations by Moss and Baker (1980). Although there is a loss of streamwise momentum via numerical diffusion as the flow turns the corner, this is countered by a decline in pressure (favorable pressure gradient) that accelerates the flow. The result in general is that the computed flow may *not* separate for an abrupt contraction if the grid is too coarse, as it is in this case.

Example 1D: Uniform 50 X 12 Grid with Square Dike

Figure 15 shows a namelist sequence and map of cell types for an unsubmerged square dike (contraction/expansion) with no bottom friction or depth variation. Input for cell types is used to form the dike by creating a block of NOSLIP cells with a smaller block of OUT cells inside. The final configuration is a block of OUT cells with a row of NOSLIP cells to the north, and columns of NOSLIP cells to the east and west. The modified grid and the computed flow are shown in Figure 16.

The grid is too coarse to resolve either the flow separation at the contraction or the recirculation observed along the north side of the dike (Moss and Baker 1980), but it does produce a recirculating flow downstream of the expansion. Previous comments about numerical diffusion and pressure gradients (Examples 1B and 1C) apply for this example as well.

Example 1E: Uniform 50 X 12 Grid with Square Pier

Examples 1A-1D all produce steady flow. In contrast, consider Figure 17, which shows a namelist sequence and map of cell types for a square pier in a channel with no bottom friction or depth variation. For this case, the cell-type input has been manipulated to form the pier by creating a block of NOSLIP cells with a smaller block of OUT cells inside. The final configuration is a block of OUT cells with rows of NOSLIP cells to the north and south, and columns of NOSLIP cells to the east and west. The modified grid and the computed flow are shown (for time-step 900) in Figure 18. At the time shown, the wake has become unsteady, and a vortex street has developed because of the periodic shedding of eddies from opposite sides of the pier.

As long as the damping effects of sidewall and bottom friction are not great enough to prevent it, unsteady wakes will arise spontaneously (even with coarse grids) in STREMR calculations for isolated obstacles with sharp corners. For curved obstacles *without* sharp corners, however, the grids employed must be fine enough to resolve adequately the points of flow separation. Otherwise, separation may occur so far aft (if at all) that only a steady wake (if any) is generated.

Example 1F: Uniform 50 X 12 Grid with L-Shaped Pier

Figure 19 shows a namelist sequence and map of cell types for a pier shaped like an inverted letter L (or Greek letter Γ) in a channel with no bottom

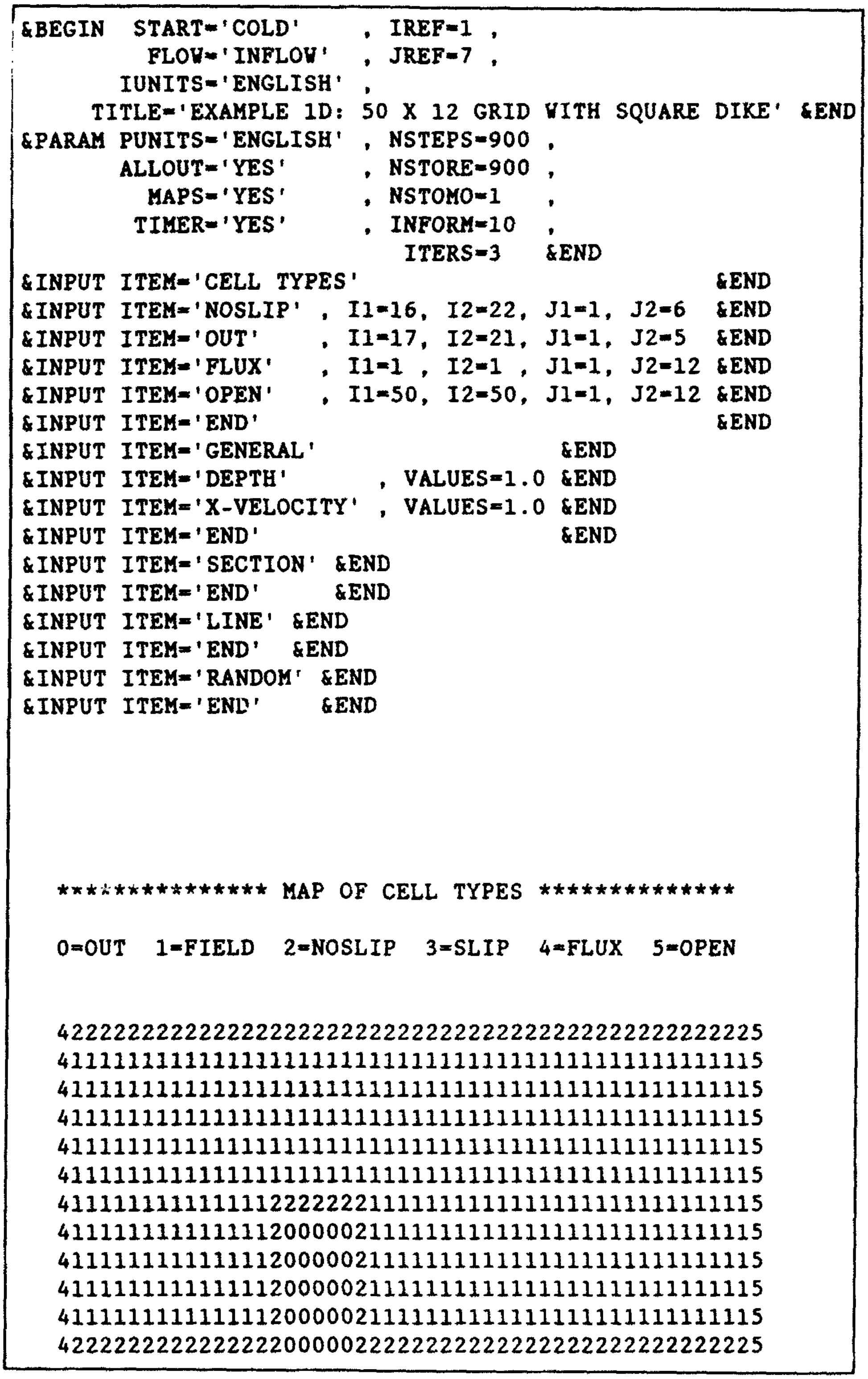

```
&BEGIN  START='COLD'     , IREF=1 ,
          FLOW='INFLOW'  , JREF=7 ,
        IUNITS='ENGLISH' ,
      TITLE='EXAMPLE 1D: 50 X 12 GRID WITH SQUARE DIKE' &END
&PARAM PUNITS='ENGLISH' , NSTEPS=900 ,
       ALLOUT='YES'     , NSTORE=900 ,
         MAPS='YES'     , NSTOMO=1   ,
        TIMER='YES'     , INFORM=10  ,
                          ITERS=3   &END
&INPUT ITEM='CELL TYPES'                         &END
&INPUT ITEM='NOSLIP' , I1=16, I2=22, J1=1, J2=6  &END
&INPUT ITEM='OUT'    , I1=17, I2=21, J1=1, J2=5  &END
&INPUT ITEM='FLUX'   , I1=1 , I2=1 , J1=1, J2=12 &END
&INPUT ITEM='OPEN'   , I1=50, I2=50, J1=1, J2=12 &END
&INPUT ITEM='END'                                &END
&INPUT ITEM='GENERAL'                 &END
&INPUT ITEM='DEPTH'      , VALUES=1.0 &END
&INPUT ITEM='X-VELOCITY' , VALUES=1.0 &END
&INPUT ITEM='END'                     &END
&INPUT ITEM='SECTION' &END
&INPUT ITEM='END'     &END
&INPUT ITEM='LINE' &END
&INPUT ITEM='END'  &END
&INPUT ITEM='RANDOM' &END
&INPUT ITEM='END'    &END




  *************** MAP OF CELL TYPES **************

  0=OUT  1=FIELD  2=NOSLIP  3=SLIP  4=FLUX  5=OPEN


  42222222222222222222222222222222222222222222222225
  41111111111111111111111111111111111111111111111115
  41111111111111111111111111111111111111111111111115
  41111111111111111111111111111111111111111111111115
  41111111111111111111111111111111111111111111111115
  41111111111111111111111111111111111111111111111115
  41111111111111122222221111111111111111111111111115
  41111111111111120000021111111111111111111111111115
  41111111111111120000021111111111111111111111111115
  41111111111111120000021111111111111111111111111115
  41111111111111120000021111111111111111111111111115
  42222222222222220000022222222222222222222222222225
```

Figure 15. STREMR input and resulting map of cell types for 50 × 12 grid with square dike (contraction/expansion, no bottom friction, Example 1D)

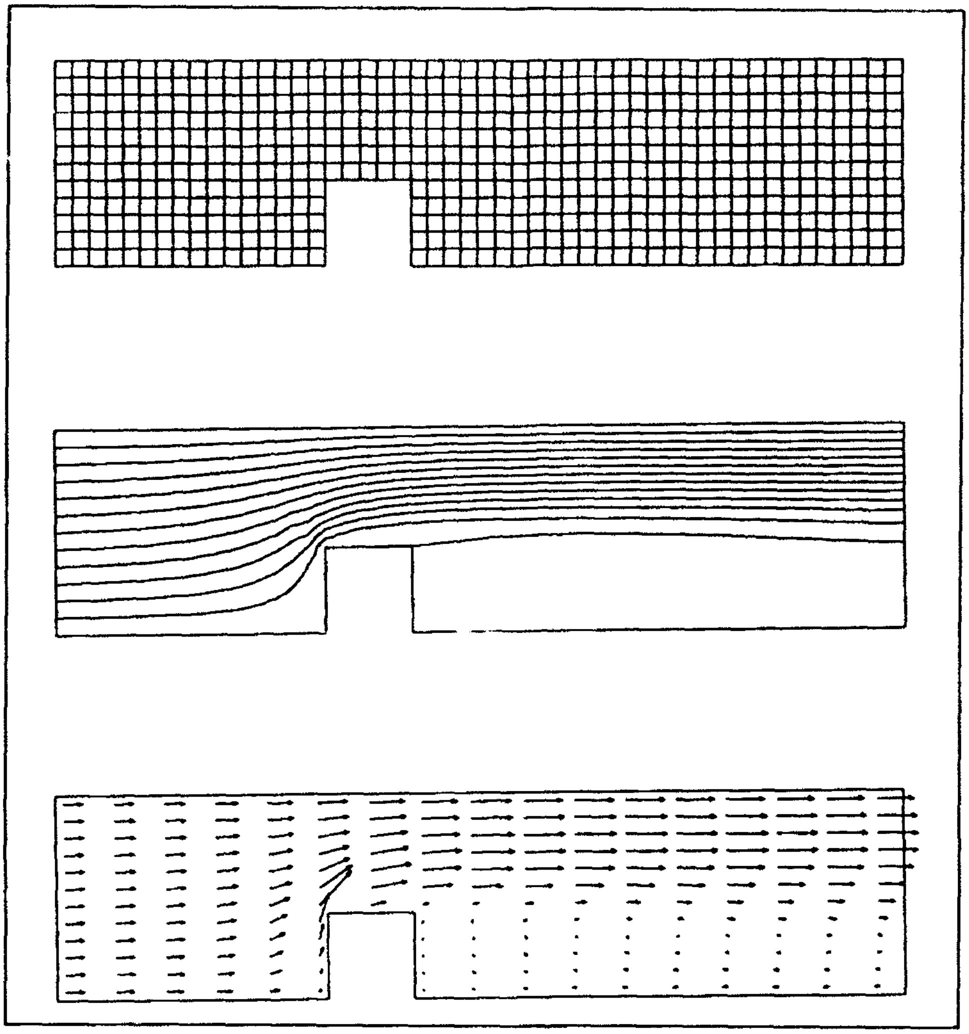

Figure 16. Uniform 50 × 12 grid with computed streamlines and velocity vectors for square dike (Example 1D)

friction or depth variation. Once again, input for cell types is used to form the pier, this time with 3 X 6 and 6 X 3 sections of NOSLIP cells, followed by a 4 X 1 row and a 1 X 4 column of OUT cells. Like the previous case, this example also develops an unsteady wake with a vortex street. The modified grid and computed flow are shown (for time-step 900) in Figure 20.

Example 1G: Uniform 50 X 12 Grid with V-Shaped Bottom

Examples 1A-1F do not include the effects of bottom friction and variable bathymetry. Figure 21 shows a namelist sequence and map of computed depths for a straight channel with a V-shaped cross section. An exaggerated

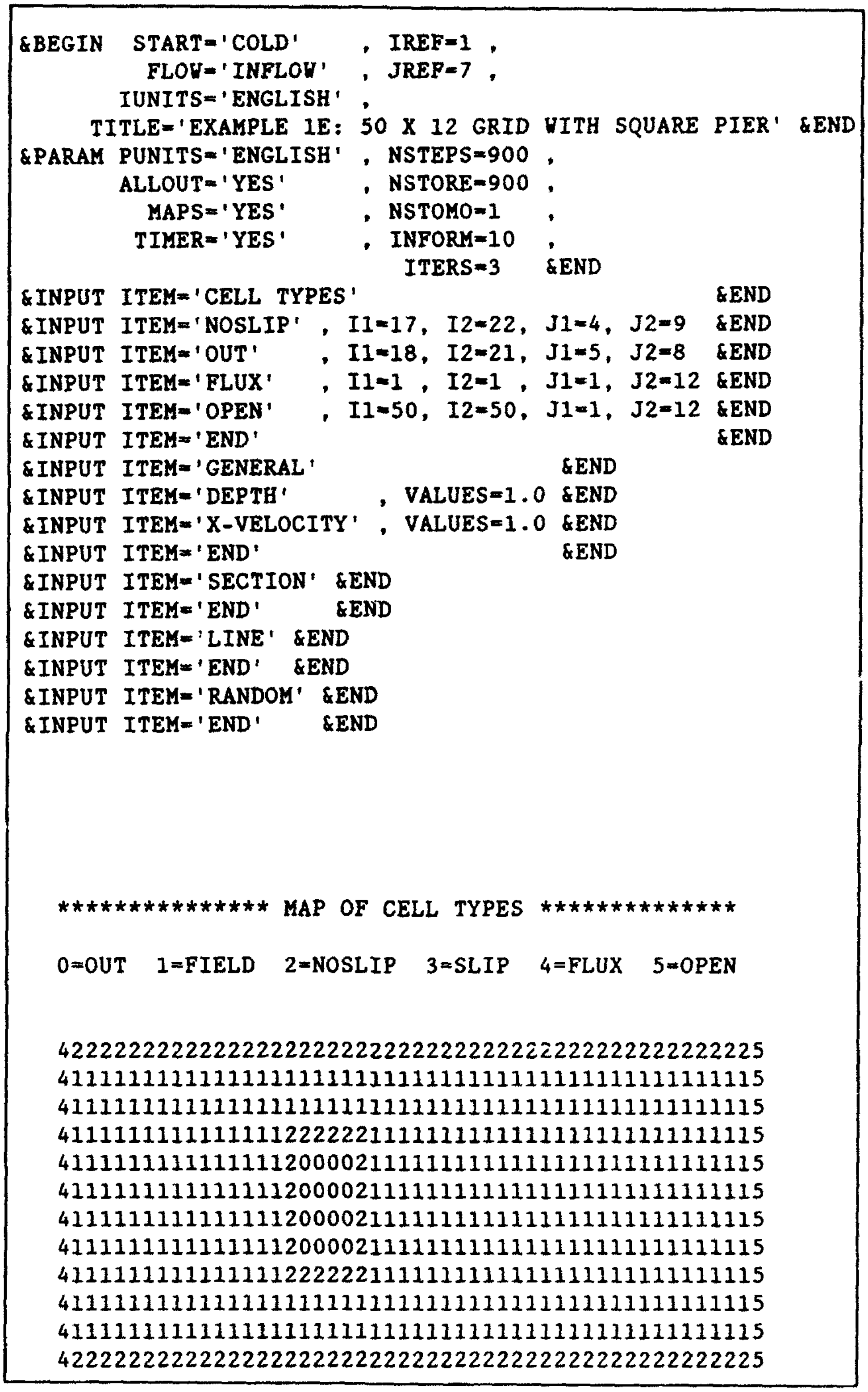

```
&BEGIN  START='COLD'     , IREF=1 ,
         FLOW='INFLOW'   , JREF=7 ,
       IUNITS='ENGLISH'  ,
     TITLE='EXAMPLE 1E: 50 X 12 GRID WITH SQUARE PIER' &END
&PARAM PUNITS='ENGLISH'  , NSTEPS=900 ,
       ALLOUT='YES'      , NSTORE=900 ,
         MAPS='YES'      , NSTOMO=1   ,
        TIMER='YES'      , INFORM=10  ,
                           ITERS=3   &END
&INPUT ITEM='CELL TYPES'                        &END
&INPUT ITEM='NOSLIP' , I1=17, I2=22, J1=4, J2=9  &END
&INPUT ITEM='OUT'    , I1=18, I2=21, J1=5, J2=8  &END
&INPUT ITEM='FLUX'   , I1=1 , I2=1 , J1=1, J2=12 &END
&INPUT ITEM='OPEN'   , I1=50, I2=50, J1=1, J2=12 &END
&INPUT ITEM='END'                               &END
&INPUT ITEM='GENERAL'                 &END
&INPUT ITEM='DEPTH'      , VALUES=1.0 &END
&INPUT ITEM='X-VELOCITY' , VALUES=1.0 &END
&INPUT ITEM='END'                     &END
&INPUT ITEM='SECTION' &END
&INPUT ITEM='END'     &END
&INPUT ITEM='LINE' &END
&INPUT ITEM='END'  &END
&INPUT ITEM='RANDOM' &END
&INPUT ITEM='END'    &END




   *************** MAP OF CELL TYPES **************

   0=OUT  1=FIELD  2=NOSLIP  3=SLIP  4=FLUX  5=OPEN


   42222222222222222222222222222222222222222222222225
   41111111111111111111111111111111111111111111111115
   41111111111111111111111111111111111111111111111115
   41111111111111112222221111111111111111111111111115
   41111111111111112000021111111111111111111111111115
   41111111111111112000021111111111111111111111111115
   41111111111111112000021111111111111111111111111115
   41111111111111112000021111111111111111111111111115
   41111111111111112222221111111111111111111111111115
   41111111111111111111111111111111111111111111111115
   41111111111111111111111111111111111111111111111115
   42222222222222222222222222222222222222222222222225
```

Figure 17. STREMR input and resulting map of cell types for 50 × 12 grid with square pier (no bottom friction, Example 1E)

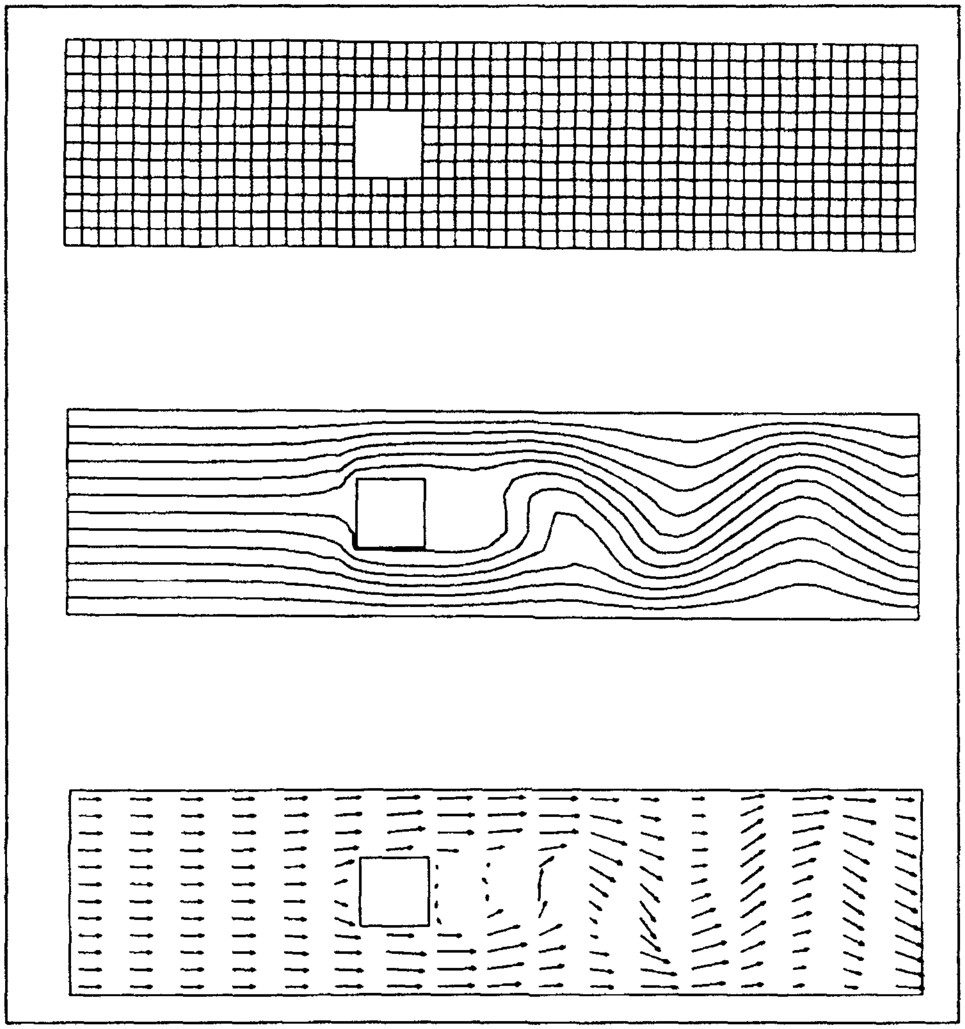

Figure 18. Uniform 50 × 12 grid with computed streamlines and velocity vectors for square pier (Example 1E, unsteady, time-step 900)

view of the bottom bathymetry (looking upstream) is given in Figure 22, which shows only the *bottom* of the channel.

Note the manner in which the V-shaped bottom is created with the line input for depth. After the INPUT namelist with ITEM = 'LINE', there are two INPUT namelists with ITEM = 'DEPTH'. These set the depth at 0.2 ft along the north and south sides (J = 1 and J = 12). Next come two similar namelists for the west and east ends of the channel (I = 1 and I = 50), which interpolate the depth from 0.2 ft at J = 1 to 1.0 ft at J = 6. Then come two namelists that fix the depth at 1.0 ft in the two rows of cells (J = 6 and J = 7) adjacent to the centerline. Finally come two more namelists for the ends of the channel (I = 1 and I = 50), which interpolate the depth from 1.0 ft at J = 7 to 0.2 ft at J = 12. The automatic interpolation scheme fills in the remaining depths for the grid. The Manning coefficient is uniformly set at 0.03 to produce a strong

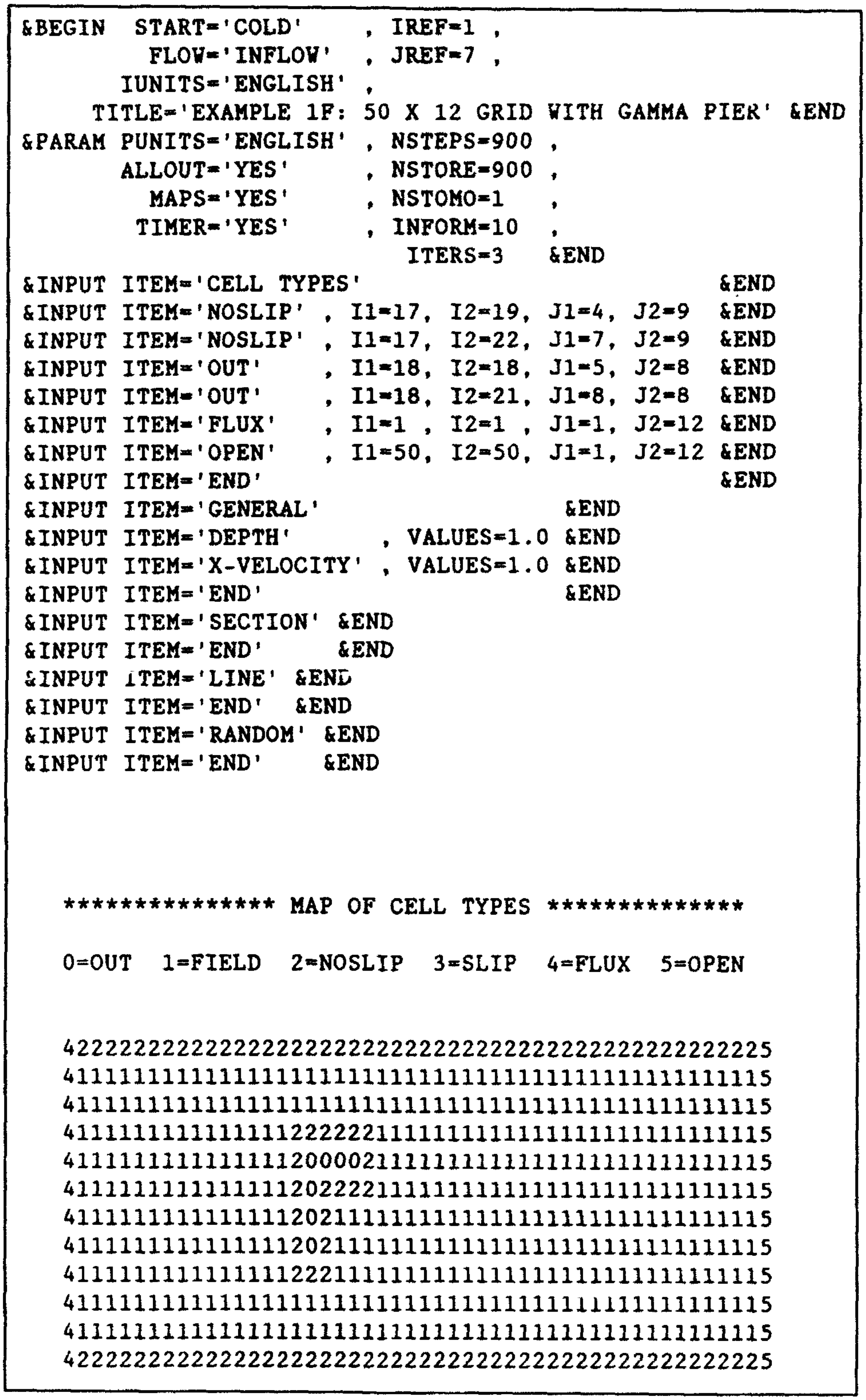

```
&BEGIN  START='COLD'     , IREF=1 ,
         FLOW='INFLOW'   , JREF=7 ,
       IUNITS='ENGLISH'  ,
     TITLE='EXAMPLE 1F: 50 X 12 GRID WITH GAMMA PIER' &END
&PARAM PUNITS='ENGLISH'  , NSTEPS=900 ,
       ALLOUT='YES'      , NSTORE=900 ,
         MAPS='YES'      , NSTOMO=1   ,
        TIMER='YES'      , INFORM=10  ,
                           ITERS=3   &END
&INPUT ITEM='CELL TYPES'                        &END
&INPUT ITEM='NOSLIP' , I1=17, I2=19, J1=4, J2=9  &END
&INPUT ITEM='NOSLIP' , I1=17, I2=22, J1=7, J2=9  &END
&INPUT ITEM='OUT'    , I1=18, I2=18, J1=5, J2=8  &END
&INPUT ITEM='OUT'    , I1=18, I2=21, J1=8, J2=8  &END
&INPUT ITEM='FLUX'   , I1=1 , I2=1 , J1=1, J2=12 &END
&INPUT ITEM='OPEN'   , I1=50, I2=50, J1=1, J2=12 &END
&INPUT ITEM='END'                               &END
&INPUT ITEM='GENERAL'                &END
&INPUT ITEM='DEPTH'      , VALUES=1.0 &END
&INPUT ITEM='X-VELOCITY' , VALUES=1.0 &END
&INPUT ITEM='END'                    &END
&INPUT ITEM='SECTION' &END
&INPUT ITEM='END'     &END
&INPUT ITEM='LINE' &END
&INPUT ITEM='END'  &END
&INPUT ITEM='RANDOM' &END
&INPUT ITEM='END'    &END




   *************** MAP OF CELL TYPES **************

   0=OUT  1=FIELD  2=NOSLIP  3=SLIP  4=FLUX  5=OPEN


   42222222222222222222222222222222222222222222222225
   41111111111111111111111111111111111111111111111115
   41111111111111111111111111111111111111111111111115
   41111111111111112222221111111111111111111111111115
   41111111111111112000021111111111111111111111111115
   41111111111111112022221111111111111111111111111115
   41111111111111112021111111111111111111111111111115
   41111111111111112021111111111111111111111111111115
   41111111111111112221111111111111111111111111111115
   41111111111111111111111111111111111111111111111115
   41111111111111111111111111111111111111111111111115
   42222222222222222222222222222222222222222222222225
```

Figure 19. STREMR input and resulting map of cell types for 50 × 12 grid with L-shaped pier (no bottom friction, Example 1F)

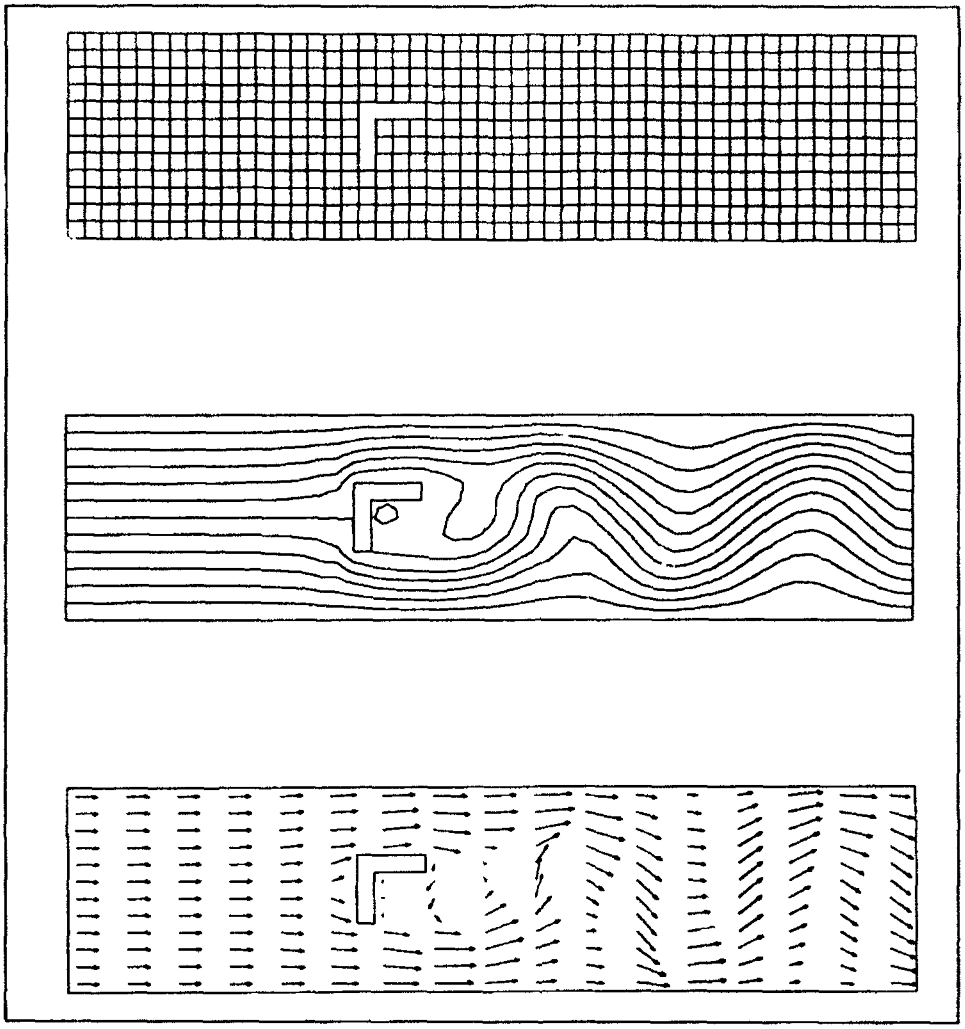

Figure 20. Uniform 50 × 12 grid computed streamlines and velocity vectors for L-shaped pier (Example 1F, unsteady, time-step 900)

bottom-friction influence, and the computed flow is shown with the unmodified grid in Figure 23.

Although the lateral distribution of velocity undergoes a gradual transition from uniform to parabolic, the streamlines are consistently more widely spaced next to the sides of the channel than in the middle. In this example, the variation in streamline spacing arises more from nonuniform depth than from nonuniform velocity. Recall that STREMR must integrate Equations 4 and 5 to obtain the stream function ψ. In these equations, the derivatives of ψ are proportional to the local depth h. As a result, for a channel with nonuniform depth, the streamlines may be unevenly spaced even when the velocity is uniform.

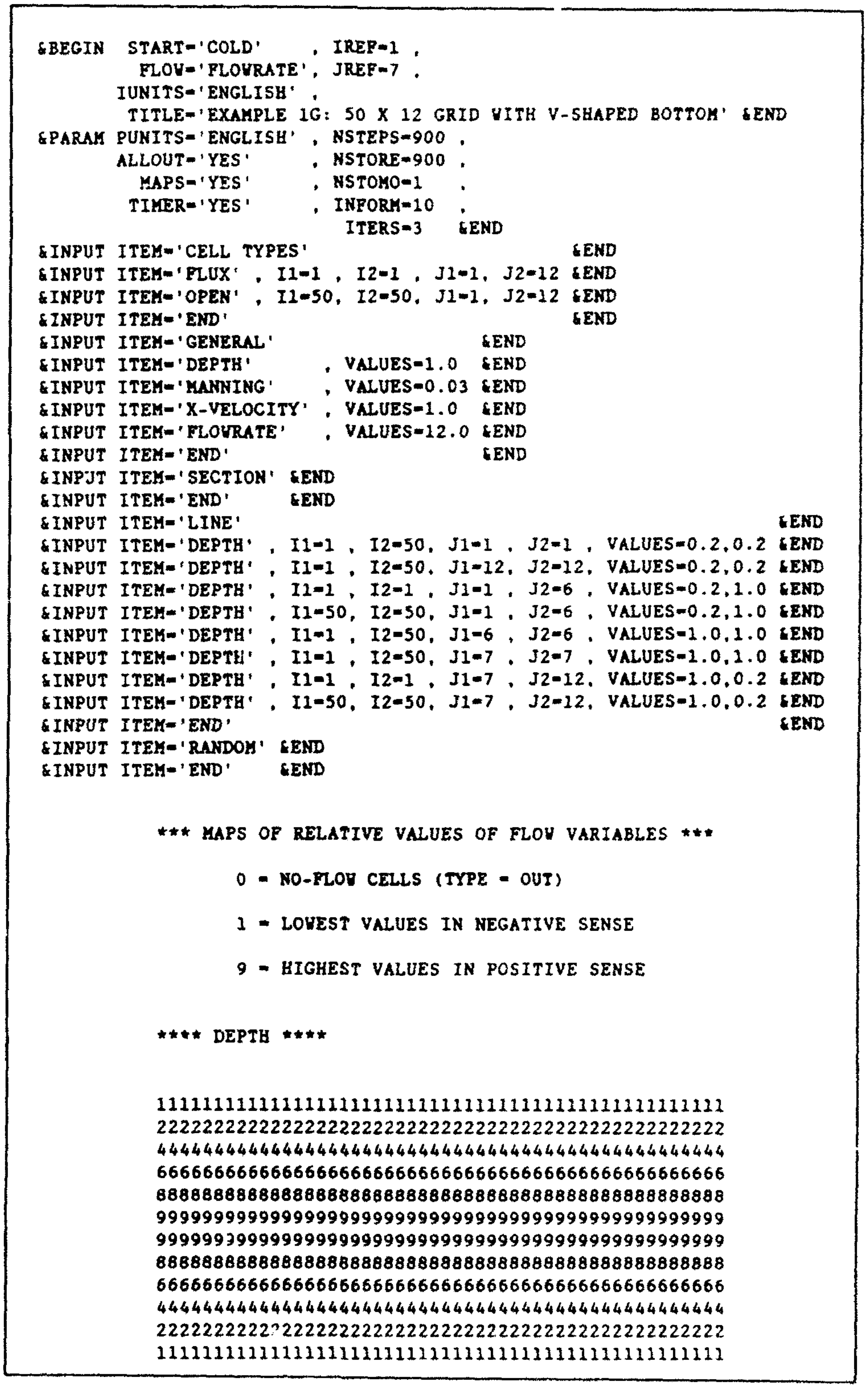

```
&BEGIN  START='COLD'     , IREF=1 ,
          FLOW='FLOWRATE', JREF=7 ,
        IUNITS='ENGLISH' ,
         TITLE='EXAMPLE 1G: 50 X 12 GRID WITH V-SHAPED BOTTOM' &END
&PARAM  PUNITS='ENGLISH' , NSTEPS=900 ,
        ALLOUT='YES'     , NSTORE=900 ,
          MAPS='YES'     , NSTOMO=1   ,
         TIMER='YES'     , INFORM=10  ,
                            ITERS=3   &END
&INPUT ITEM='CELL TYPES'                          &END
&INPUT ITEM='FLUX' , I1=1 , I2=1 , J1=1, J2=12 &END
&INPUT ITEM='OPEN' , I1=50, I2=50, J1=1, J2=12 &END
&INPUT ITEM='END'                                 &END
&INPUT ITEM='GENERAL'                     &END
&INPUT ITEM='DEPTH'       , VALUES=1.0  &END
&INPUT ITEM='MANNING'     , VALUES=0.03 &END
&INPUT ITEM='X-VELOCITY'  , VALUES=1.0  &END
&INPUT ITEM='FLOWRATE'    , VALUES=12.0 &END
&INPUT ITEM='END'                       &END
&INPJT ITEM='SECTION' &END
&INPUT ITEM='END'     &END
&INPUT ITEM='LINE'                                                          &END
&INPUT ITEM='DEPTH' , I1=1 , I2=50, J1=1 , J2=1 , VALUES=0.2,0.2 &END
&INPUT ITEM='DEPTH' , I1=1 , I2=50, J1=12, J2=12, VALUES=0.2,0.2 &END
&INPUT ITEM='DEPTH' , I1=1 , I2=1 , J1=1 , J2=6 , VALUES=0.2,1.0 &END
&INPUT ITEM='DEPTH' , I1=50, I2=50, J1=1 , J2=6 , VALUES=0.2,1.0 &END
&INPUT ITEM='DEPTH' , I1=1 , I2=50, J1=6 , J2=6 , VALUES=1.0,1.0 &END
&INPUT ITEM='DEPTH' , I1=1 , I2=50, J1=7 , J2=7 , VALUES=1.0,1.0 &END
&INPUT ITEM='DEPTH' , I1=1 , I2=1 , J1=7 , J2=12, VALUES=1.0,0.2 &END
&INPUT ITEM='DEPTH' , I1=50, I2=50, J1=7 , J2=12, VALUES=1.0,0.2 &END
&INPUT ITEM='END'                                                           &END
&INPUT ITEM='RANDOM' &END
&INPUT ITEM='END'    &END


          *** MAPS OF RELATIVE VALUES OF FLOW VARIABLES ***

                 0 = NO-FLOW CELLS (TYPE = OUT)

                 1 = LOWEST VALUES IN NEGATIVE SENSE

                 9 = HIGHEST VALUES IN POSITIVE SENSE


          **** DEPTH ****


          11111111111111111111111111111111111111111111111111
          22222222222222222222222222222222222222222222222222
          44444444444444444444444444444444444444444444444444
          66666666666666666666666666666666666666666666666666
          88888888888888888888888888888888888888888888888888
          99999999999999999999999999999999999999999999999999
          99999939999999999999999999999999999999999999999999
          88888888888888888888888888888888888888888888888888
          66666666666666666666666666666666666666666666666666
          44444444444444444444444444444444444444444444444444
          22222222222222222222222222222222222222222222222222
          11111111111111111111111111111111111111111111111111
```

Figure 21. STREMR input and resulting map of depths for 50 × 12 grid with V-shaped bottom (friction included, Example 1G)

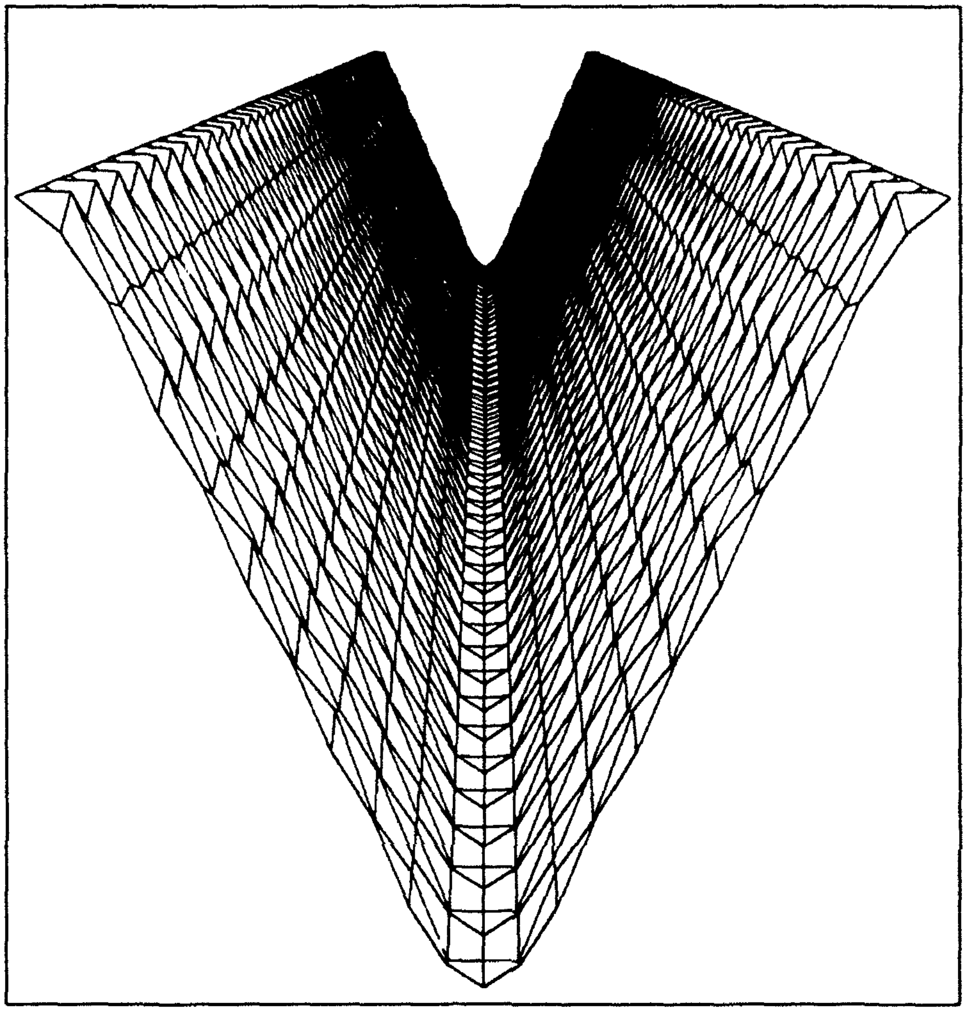

Figure 22. Exaggerated bathymetry (looking upstream) for straight channel with V-shaped bottom (Example 1G)

Example 1H: Uniform 50 X 12 Grid with Bottom Transition

In this example, both section input and line input are used to create a transition from V-shape to rectangular cross section. Figure 24 shows the namelist sequence and the resulting map of depths, and Figure 25 offers an exaggerated view of the bottom bathymetry (looking upstream). The section input creates a rectangular area of constant depth (flat bottom) next to the east end (outflow boundary), and the line input specifies depths along the entrance, sidewalls, and centerline, upstream of the flat bottom. Automatic interpolation for the remaining depths produces a V-shaped cross section at the entrance, followed by a gradual transition to the flat bottom. The Manning coefficient is

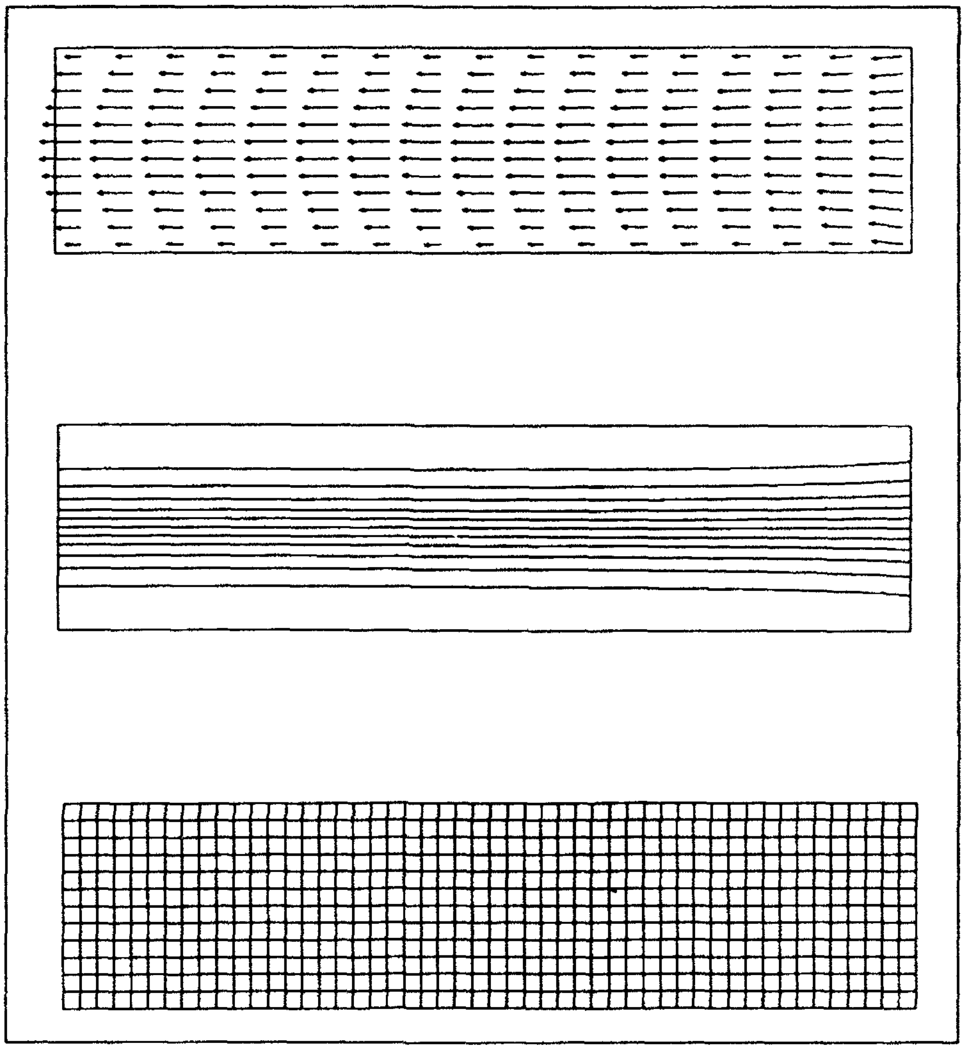

Figure 23. Uniform 50 × 12 grid with computed streamlines and velocity vectors for V-shaped bottom (Example 1G)

uniformly set at 0.03, and the computed flow is shown with the unmodified grid in Figure 26.

As in the previous example, the velocity distribution makes a gradual transition from uniform to parabolic. The lateral variation is greatest just upstream of the flat section, but it becomes somewhat less nonuniform by the time it reaches the outflow. The latter change occurs because the deceleration caused by bottom friction is less nonuniform with a flat bottom than with a V-shaped bottom.

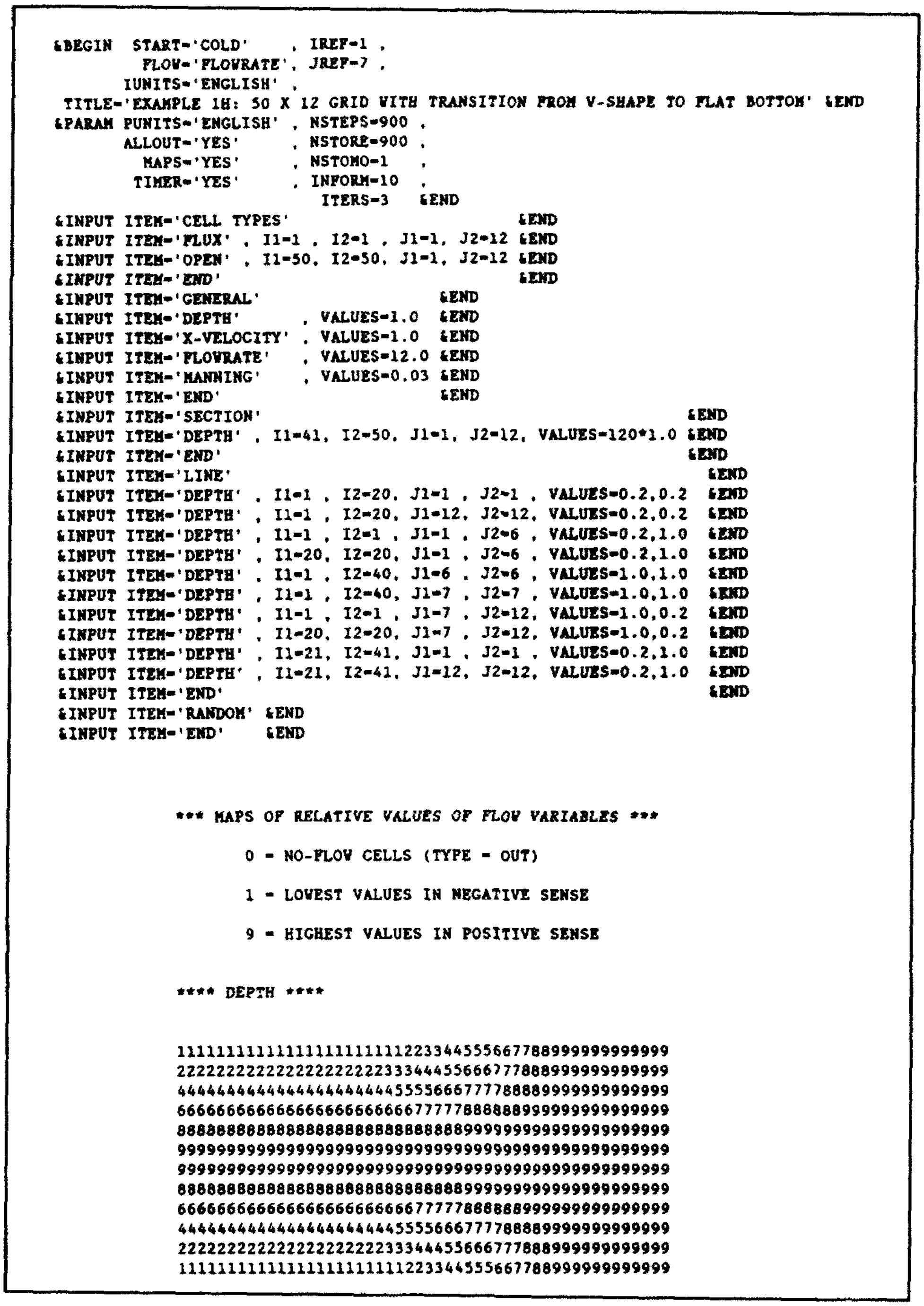

```
&BEGIN  START='COLD'     , IREF=1 ,
          FLOW='FLOWRATE', JREF=7 ,
        IUNITS='ENGLISH' ,
 TITLE='EXAMPLE 1H: 50 X 12 GRID WITH TRANSITION FROM V-SHAPE TO FLAT BOTTOM' &END
&PARAM PUNITS='ENGLISH' , NSTEPS=900 ,
       ALLOUT='YES'     , NSTORE=900 ,
         MAPS='YES'     , NSTOMO=1   ,
        TIMER='YES'     , INFORM=10  ,
                           ITERS=3   &END
&INPUT ITEM='CELL TYPES'                        &END
&INPUT ITEM='FLUX' , I1=1 , I2=1 , J1=1, J2=12 &END
&INPUT ITEM='OPEN' , I1=50, I2=50, J1=1, J2=12 &END
&INPUT ITEM='END'                               &END
&INPUT ITEM='GENERAL'                  &END
&INPUT ITEM='DEPTH'       , VALUES=1.0  &END
&INPUT ITEM='X-VELOCITY' , VALUES=1.0  &END
&INPUT ITEM='FLOWRATE'   , VALUES=12.0 &END
&INPUT ITEM='MANNING'    , VALUES=0.03 &END
&INPUT ITEM='END'                      &END
&INPUT ITEM='SECTION'                                                &END
&INPUT ITEM='DEPTH' , I1=41, I2=50, J1=1, J2=12, VALUES=120*1.0 &END
&INPUT ITEM='END'                                                    &END
&INPUT ITEM='LINE'                                                     &END
&INPUT ITEM='DEPTH' , I1=1 , I2=20, J1=1 , J2=1 , VALUES=0.2,0.2  &END
&INPUT ITEM='DEPTH' , I1=1 , I2=20, J1=12, J2=12, VALUES=0.2,0.2  &END
&INPUT ITEM='DEPTH' , I1=1 , I2=1 , J1=1 , J2=6 , VALUES=0.2,1.0  &END
&INPUT ITEM='DEPTH' , I1=20, I2=20, J1=1 , J2=6 , VALUES=0.2,1.0  &END
&INPUT ITEM='DEPTH' , I1=1 , I2=40, J1=6 , J2=6 , VALUES=1.0,1.0  &END
&INPUT ITEM='DEPTH' , I1=1 , I2=40, J1=7 , J2=7 , VALUES=1.0,1.0  &END
&INPUT ITEM='DEPTH' , I1=1 , I2=1 , J1=7 , J2=12, VALUES=1.0,0.2  &END
&INPUT ITEM='DEPTH' , I1=20, I2=20, J1=7 , J2=12, VALUES=1.0,0.2  &END
&INPUT ITEM='DEPTH' , I1=21, I2=41, J1=1 , J2=1 , VALUES=0.2,1.0  &END
&INPUT ITEM='DEPTH' , I1=21, I2=41, J1=12, J2=12, VALUES=0.2,1.0  &END
&INPUT ITEM='END'                                                      &END
&INPUT ITEM='RANDOM' &END
&INPUT ITEM='END'    &END


            *** MAPS OF RELATIVE VALUES OF FLOW VARIABLES ***

                   0 = NO-FLOW CELLS (TYPE = OUT)

                   1 = LOWEST VALUES IN NEGATIVE SENSE

                   9 = HIGHEST VALUES IN POSITIVE SENSE


            **** DEPTH ****

            11111111111111111111111223344555667788999999999999
            22222222222222222222233344455666777888999999999999
            44444444444444444444445555666777788889999999999999
            66666666666666666666666677777888888999999999999999
            88888888888888888888888888888999999999999999999999
            99999999999999999999999999999999999999999999999999
            99999999999999999999999999999999999999999999999999
            88888888888888888888888888888999999999999999999999
            66666666666666666666666677777888888999999999999999
            44444444444444444444445555666777788889999999999999
            22222222222222222222233344455666777888999999999999
            11111111111111111111111223344555667788999999999999
```

Figure 24. STREMR input and resulting map of depth for 50 × 12 grid with transition from V-shape to flat bottom (friction included, Example 1H)

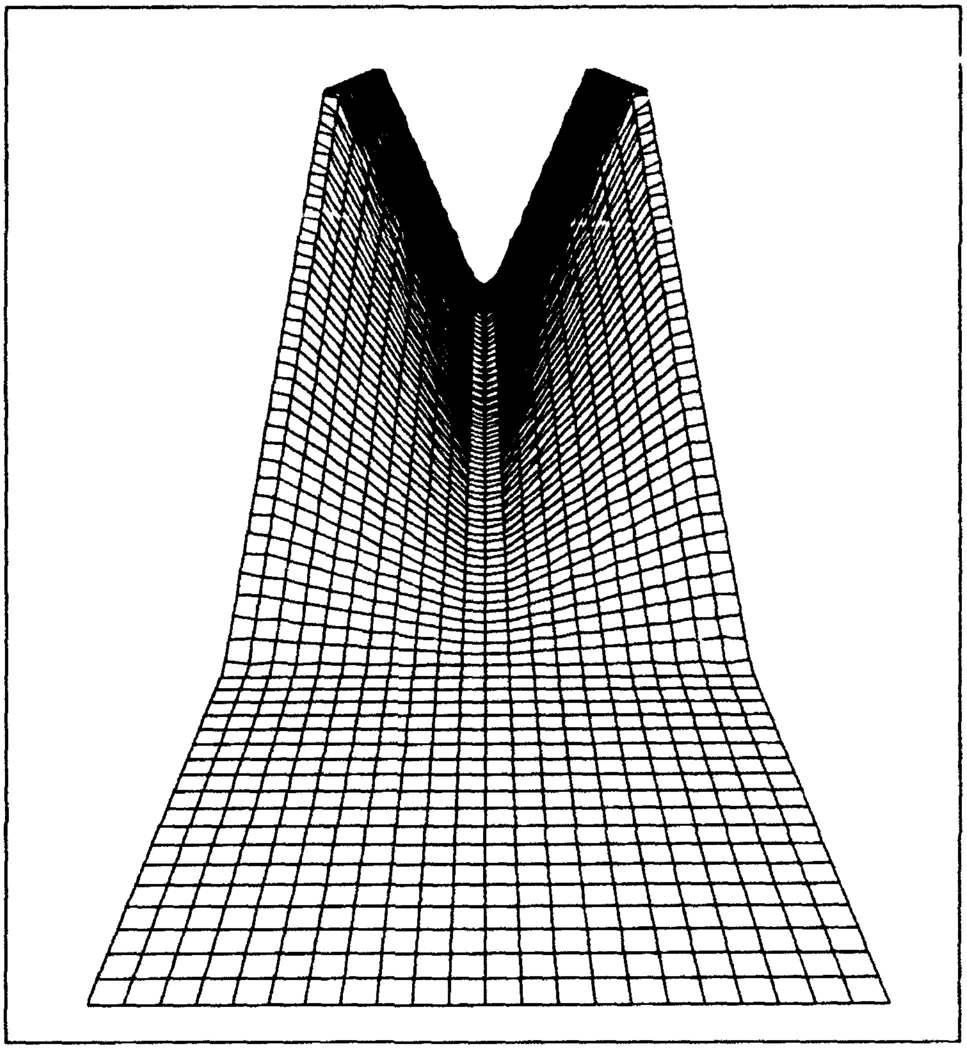

Figure 25. Exaggerated bathymetry (looking upstream) for straight channel with transition from V-shape to flat bottom (Example 1H)

Example 1I: Uniform 50 X 12 Grid with Uneven Bottom

Figure 27 shows the namelist sequence and resulting map of depths for a straight channel with an uneven bottom. Unlike Examples 1G and 1H, which used only the cell indices (I1,J1) and (I2,J2) to specify line input for depth, this example uses the Cartesian coordinates (X1,Y1) and (X2,Y2) as well, employing both line input and random input to create the uneven bottom. Figure 28 gives an exaggerated view of the bottom bathymetry (looking upstream). Automatic interpolation produc^s smooth transitions between the peaks, troughs, and ridges specified in the namelist input The Manning

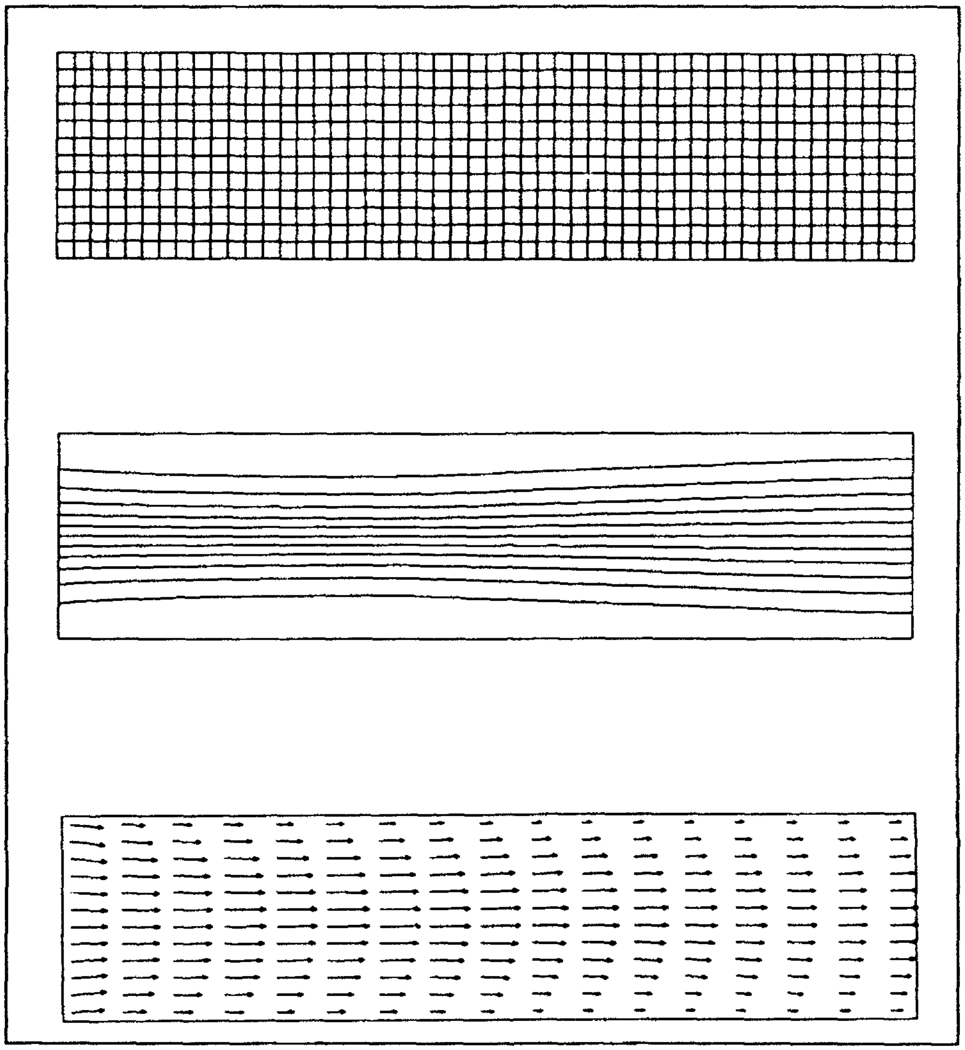

Figure 26. Uniform 50 × 12 grid with computed streamlines and velocity vectors for transition from V-shape to flat bottom (Example 1H)

coefficient is uniformly set at 0.03, and the computed flow is shown with the unmodified grid in Figure 29.

The uneven bottom has a very noticeable effect on the predicted flow. Most dramatic is the influence of the ridge near the upstream boundary (Figure 28), which diverts the flow toward either side (Figure 29) and changes the nearby velocities quite abruptly. It also creates a wake that persists for some distance downstream. The other submerged features, including the bumps near the downstream boundary (Figure 28), seem to have a lesser effect

```
&BEGIN  START='COLD'     , IREF=1 ,
         FLOW='FLOWRATE', JREF=7 ,
       IUNITS='ENGLISH' ,
        TITLE='EXAMPLE 1I: 50 X 12 GRID WITH UNEVEN BOTTOM' &END
&PARAM PUNITS='ENGLISH' , NSTEPS=900 ,
       ALLOUT='YES'     , NSTORE=900 ,
         MAPS='YES'     , NSTOMO=1   ,
        TIMER='YES'     , INFORM=10  ,
                            ITERS=3   &END
&INPUT ITEM='CELL TYPES'                            &END
&INPUT ITEM='FLUX' , I1=1 , I2=1 , J1=1, J2=12 &END
&INPUT ITEM='OPEN' , I1=50, I2=50, J1=1, J2=12 &END
&INPUT ITEM='END'                                   &END
&INPUT ITEM='GENERAL'                       &END
&INPUT ITEM='DEPTH'       , VALUES=0.5  &END
&INPUT ITEM='X-VELOCITY' , VALUES=1.0  &END
&INPUT ITEM='FLOWRATE'   , VALUES=12.0 &END
&INPUT ITEM='MANNING'    , VALUES=0.03 &END
&INPUT ITEM='END'                           &END
&INPUT ITEM='SECTION' &END
&INPUT ITEM='END'     &END
&INPUT ITEM='LINE'                                                             &END
&INPUT ITEM='DEPTH' , X1= 0.3, Y1=1.7, X2=11.9, Y2=8.4, VALUES=0.5,0.1 &END
&INPUT ITEM='DEPTH' , X1=12.6, Y1=7.8, X2=36.2, Y2=6.7, VALUES=0.1,1.0 &END
&INPUT ITEM='DEPTH' , X1=37.5, Y1=5.9, X2=48.4, Y2=9.1, VALUES=1.0,0.5 &END
&INPUT ITEM='END'                                                              &END
&INPUT ITEM='RANDOM'                                &END
&INPUT ITEM='DEPTH' , I1=30  , J1=8  , VALUES=0.1 &END
&INPUT ITEM='DEPTH' , I1=41  , J1=5  , VALUES=0.2 &END
&INPUT ITEM='DEPTH' , X1= 6.7, Y1=7.5, VALUES=0.9 &END
&INPUT ITEM='DEPTH' , X1=15.3, Y1=2.3, VALUES=0.7 &END
&INPUT ITEM='END'                                   &END
```

```
             *** MAPS OF RELATIVE VALUES OF FLOW VARIABLES ***

                    0 - NO-FLOW CELLS (TYPE - OUT)

                    1 - LOWEST VALUES IN NEGATIVE SENSE

                    9 - HIGHEST VALUES IN POSITIVE SENSE


             **** DEPTH ****


             44444444444444444444444444444444444444444444444444
             45555554444334444444444445554445555555555555555554
             45555554433223333344444455544455566666666666655544
             45555565322112223333444455554345677777777766665554
             44555685311111122233344555554156778888887777665554
             44444553222212223333444555667778889999998876665554
             44444322222222233333444455566677778889997666655554
             44443333333333344444444555566667777788751455555554
             44433333333334454444444455555666666777665445555554
             44444444444444565544444455555556666666655445555554
             44444444444444555544444455555555555555554555555554
             44444444444444444444444444444444444444444444444444
```

Figure 27. STREMR input and resulting map of depths for 50 × 12 grid with uneven bottom (friction included, Example 1I)

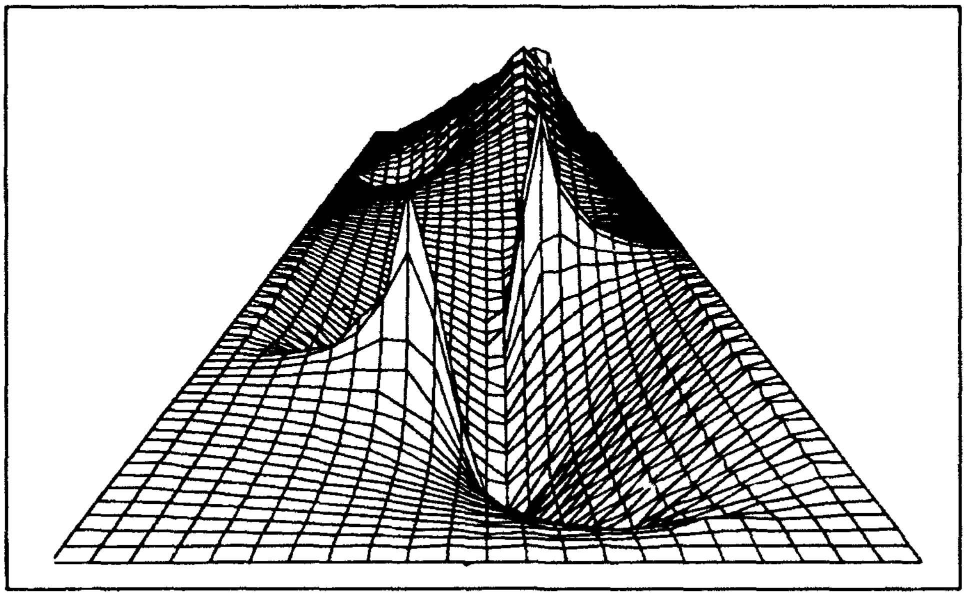

Figure 28. Exaggerated bathymetry (looking upstream) for straight channel with uneven bottom (Example 1I)

Example 1J: Uniform 50 X 12 Grid with Square Pier and Bottom Transition

This example combines namelist input for cell type and depth to create a transition from V-shape to flat bottom in a straight channel, with a square pier in the transition. Figure 30 gives the namelist sequence, and Figure 31 shows the resulting maps of cell types and depths. Figure 32 offers an exaggerated view of the bottom bathymetry (looking upstream), in which the dark rectangle represents the base of the pier. The Manning coefficient is uniformly set at 0.03, and the computed flow is shown with the modified grid in Figure 33.

Recall that in Example 1E, the square pier produced an unsteady wake (vortex street) in a straight channel with a flat bottom and no bottom friction (Figure 18). In the present case, however, the wake is only slightly unsteady (and slightly asymmetric), because the bottom friction imposes a damping influence strong enough here to prevent vortex shedding.

Example 2A: Nonuniform 60 X 30 Grid with Backstep

This example employs a nonuniform 60 X 30 grid for a channel 30 ft long and 0.2 ft deep. The grid (as originally generated) is rectangular, but cell-type designations are used in the STREMR input (Figure 34) to create a grid with a

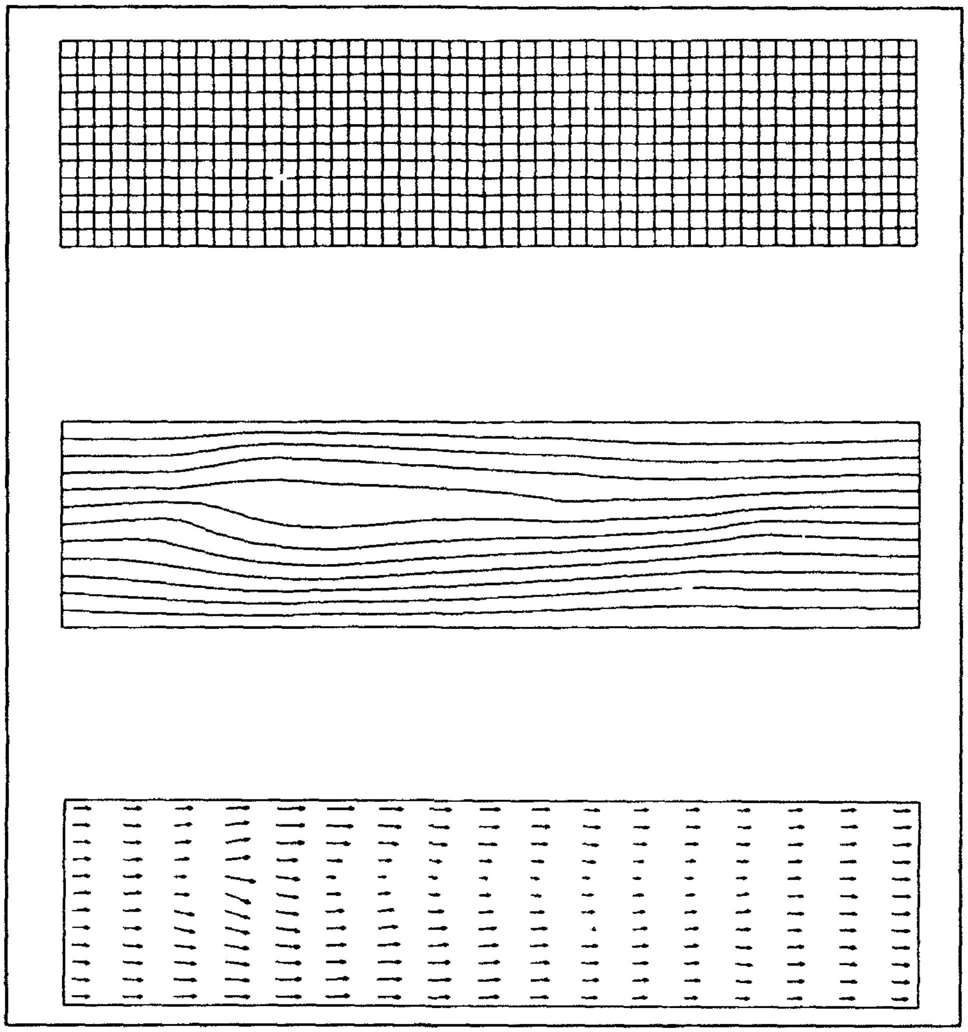

Figure 29. Uniform 50 × 12 grid with computed streamlines and velocity vectors for uneven bottom (Example 1I)

backstep (expansion) 10 ft from the west (inflow) boundary. The north side of the grid (Figure 35) is designated as a SLIP boundary (channel centerline) in the STREMR input. The resulting grid widths (channel half widths) are, respectively, H_1 = 10 ft and H_2 = 11 ft upstream and downstream of the step. The channel expansion ratio is H_2/H_1 = 1.1, and the step width is $H = H_2 - H_1$ = 1 ft.

Although the grid is nonuniform far from the step, the grid cells are perfectly square in the immediate vicinity of the step. The step width itself is divided into ten equal grid spaces (0.1 ft each), and the grid spacing gradually increases with distance from the step (in both directions). The resulting flow (no bottom friction) is shown with the modified 60 X 30 grid in Figure 35. The flow separates at the expansion, develops clockwise recirculation in the wake of the step, and reattaches to the wall about 5.5 step widths downstream.

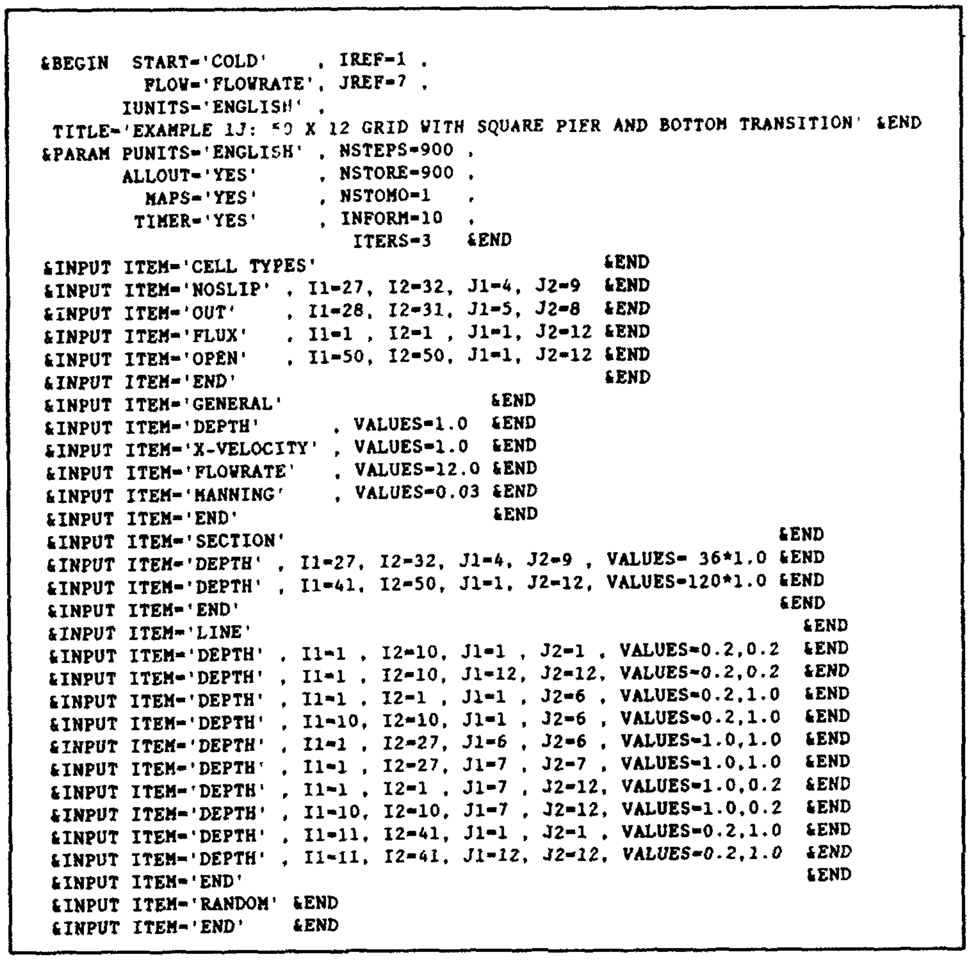

```
&BEGIN  START='COLD'     , IREF=1 ,
          FLOW='FLOWRATE', JREF=7 ,
        IUNITS='ENGLISH'  ,
 TITLE='EXAMPLE 1J: 50 X 12 GRID WITH SQUARE PIER AND BOTTOM TRANSITION' &END
&PARAM PUNITS='ENGLISH' , NSTEPS=900 ,
        ALLOUT='YES'     , NSTORE=900 ,
          MAPS='YES'     , NSTOMO=1   ,
         TIMER='YES'     , INFORM=10  ,
                            ITERS=3   &END
&INPUT ITEM='CELL TYPES'                              &END
&INPUT ITEM='NOSLIP' , I1=27, I2=32, J1=4, J2=9  &END
&INPUT ITEM='OUT'    , I1=28, I2=31, J1=5, J2=8  &END
&INPUT ITEM='FLUX'   , I1=1 , I2=1 , J1=1, J2=12 &END
&INPUT ITEM='OPEN'   , I1=50, I2=50, J1=1, J2=12 &END
&INPUT ITEM='END'                                &END
&INPUT ITEM='GENERAL'                 &END
&INPUT ITEM='DEPTH'       , VALUES=1.0  &END
&INPUT ITEM='X-VELOCITY'  , VALUES=1.0  &END
&INPUT ITEM='FLOWRATE'    , VALUES=12.0 &END
&INPUT ITEM='MANNING'     , VALUES=0.03 &END
&INPUT ITEM='END'                       &END
&INPUT ITEM='SECTION'                                                 &END
&INPUT ITEM='DEPTH' , I1=27, I2=32, J1=4, J2=9 , VALUES= 36*1.0 &END
&INPUT ITEM='DEPTH' , I1=41, I2=50, J1=1, J2=12, VALUES=120*1.0 &END
&INPUT ITEM='END'                                                 &END
&INPUT ITEM='LINE'                                                    &END
&INPUT ITEM='DEPTH' , I1=1 , I2=10, J1=1 , J2=1 , VALUES=0.2,0.2  &END
&INPUT ITEM='DEPTH' , I1=1 , I2=10, J1=12, J2=12, VALUES=0.2,0.2  &END
&INPUT ITEM='DEPTH' , I1=1 , I2=1 , J1=1 , J2=6 , VALUES=0.2,1.0  &END
&INPUT ITEM='DEPTH' , I1=10, I2=10, J1=1 , J2=6 , VALUES=0.2,1.0  &END
&INPUT ITEM='DEPTH' , I1=1 , I2=27, J1=6 , J2=6 , VALUES=1.0,1.0  &END
&INPUT ITEM='DEPTH' , I1=1 , I2=27, J1=7 , J2=7 , VALUES=1.0,1.0  &END
&INPUT ITEM='DEPTH' , I1=1 , I2=1 , J1=7 , J2=12, VALUES=1.0,0.2  &END
&INPUT ITEM='DEPTH' , I1=10, I2=10, J1=7 , J2=12, VALUES=1.0,0.2  &END
&INPUT ITEM='DEPTH' , I1=11, I2=41, J1=1 , J2=1 , VALUES=0.2,1.0  &END
&INPUT ITEM='DEPTH' , I1=11, I2=41, J1=12, J2=12, VALUES=0.2,1.0  &END
&INPUT ITEM='END'                                                 &END
&INPUT ITEM='RANDOM' &END
&INPUT ITEM='END'    &END
```

Figure 30. STREMR input for 50 × 12 grid with square pier and transition from V-shape to flat bottom (friction included, Example 1J)

Example 2B: Nonuniform 120 X 60 Grid with Backstep

This example employs a nonuniform 120 X 60 grid for the channel described in Example 2A. The STREMR input (Figure 36) is similar to Example 2A, but the input values for i and j now reflect the doubling of IMAX and JMAX . The grid spacing has been reduced by a factor of two, and the total number of time-steps (NSTEPS) has been increased because the allowable time-step size is proportional to the grid spacing.

Like the previous example, the grid cells are perfectly square in the immediate vicinity of the step, and the grid spacing gradually increases with distance from the step. In this case, however, the step width is divided into twenty equal grid spaces (0.05 ft each) instead of ten. The resulting flow (no bottom friction) is shown with the modified 120 X 60 grid in Figure 37.

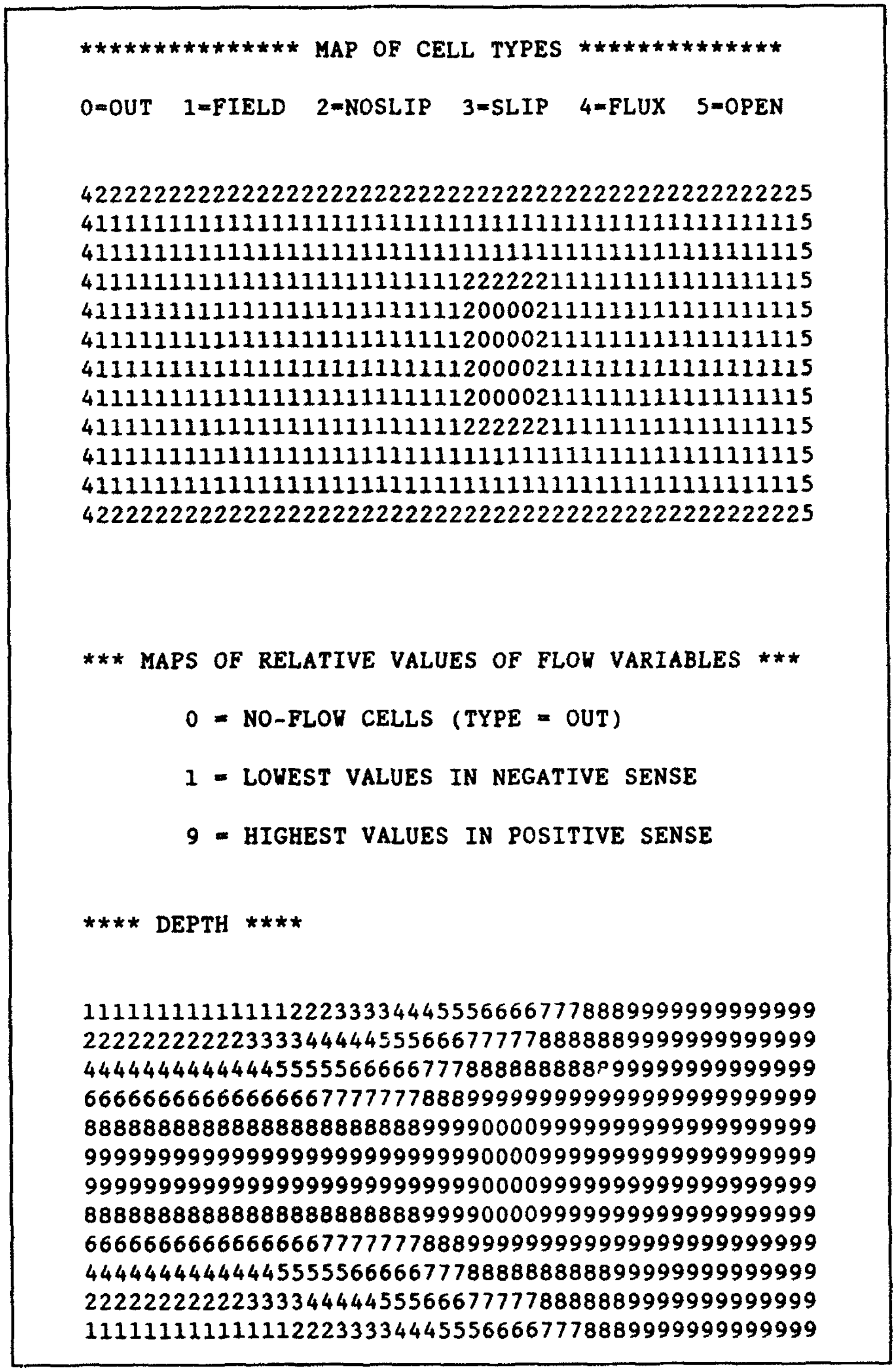

```
*************** MAP OF CELL TYPES **************

0=OUT  1=FIELD  2=NOSLIP  3=SLIP  4=FLUX  5=OPEN


42222222222222222222222222222222222222222222222225
41111111111111111111111111111111111111111111111115
41111111111111111111111111111111111111111111111115
41111111111111111111111111222222111111111111111115
41111111111111111111111111200002111111111111111115
41111111111111111111111111200002111111111111111115
41111111111111111111111111200002111111111111111115
41111111111111111111111111200002111111111111111115
41111111111111111111111111222222111111111111111115
41111111111111111111111111111111111111111111111115
41111111111111111111111111111111111111111111111115
42222222222222222222222222222222222222222222222225




*** MAPS OF RELATIVE VALUES OF FLOW VARIABLES ***

       0 = NO-FLOW CELLS (TYPE = OUT)

       1 = LOWEST VALUES IN NEGATIVE SENSE

       9 = HIGHEST VALUES IN POSITIVE SENSE


**** DEPTH ****


11111111111111222333344455566667778889999999999999
22222222222333344444555666777778888889999999999999
44444444444445555566666777888888888ᴾ99999999999999
66666666666666667777777888999999999999999999999999
88888888888888888888888999900099999999999999999999
99999999999999999999999999900099999999999999999999
99999999999999999999999999900099999999999999999999
88888888888888888888888999900099999999999999999999
66666666666666667777777888999999999999999999999999
44444444444445555566666777888888888899999999999999
22222222222333344444555666777778888889999999999999
11111111111111222333344455566667778889999999999999
```

Figure 31. Maps of cell types and depths for 50 × 12 grid with square pier and transition from V-shape to flat bottom (Example 1J)

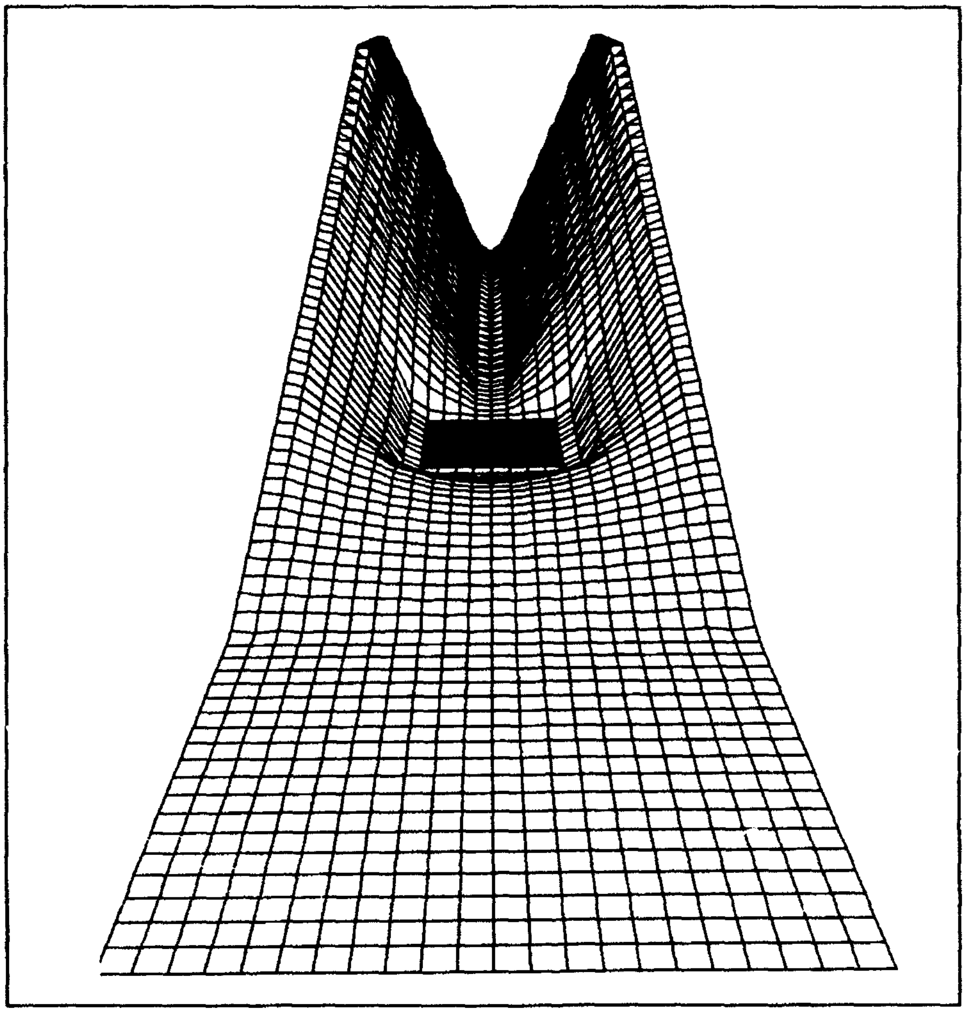

Figure 32. Exaggerated bathymetry (looking upstream) for straight channel with square pier and transition from V-shape to flat bottom (Example 1J)

The flow separates at the expansion, develops clockwise recirculation in the wake of the step (this time with a small zone of counter-clockwise recirculation at the base), and reattaches to the wall about 6.3 step widths downstream. This amounts to a 15 percent increase over the reattachment length predicted in Example 2A. Further refinement of the grid (by another factor of two) increases the reattachment length by less than 3 percent. To predict the largest eddies for a backstep, it appears that 20 grid spaces are enough for discretizing the step width (as far as grid error is concerned).

Comparison with Test Data for Backstep

The backstep is a standard problem for testing numerical methods and turbulence models for separated (recirculating) flow. The reattachment length, which is the horizontal distance x_R between flow separation and reattachment,

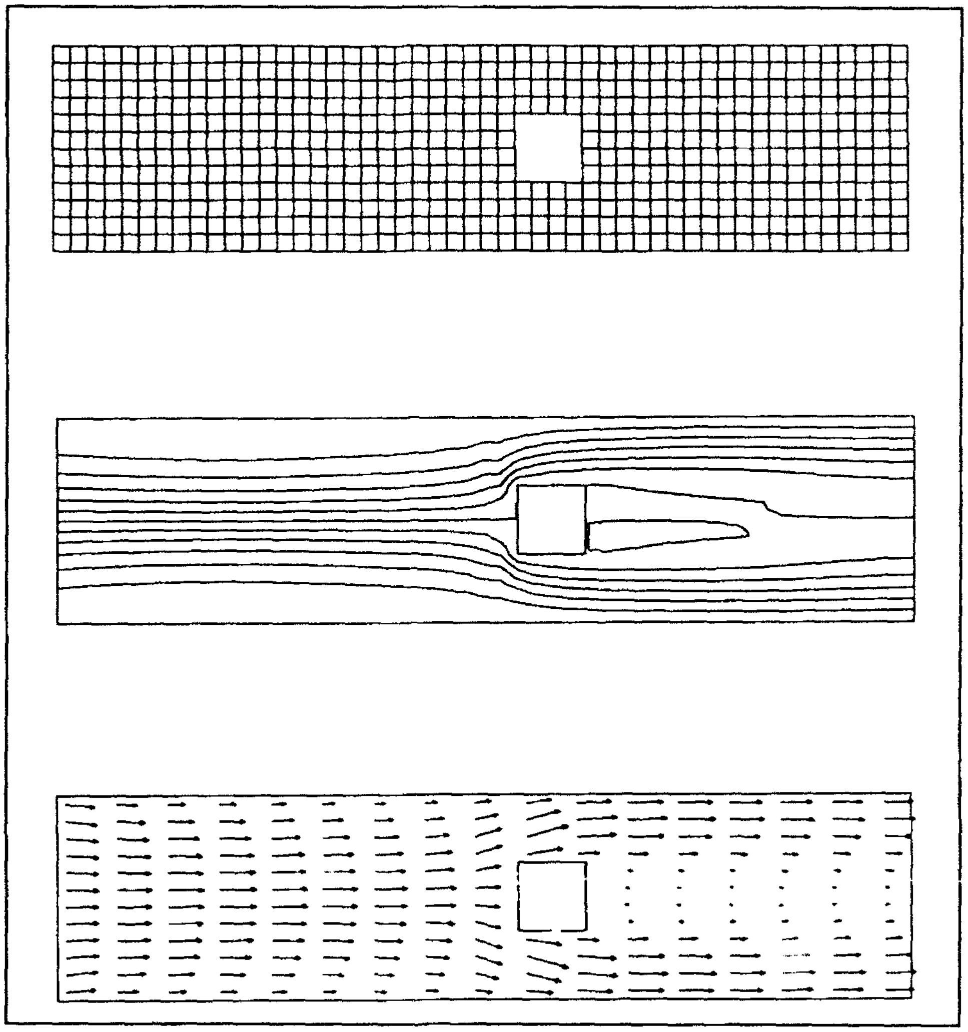

Figure 33. Uniform 50 × 12 grid with computed streamlines and velocity vectors for square pier and transition from V-shape to flat bottom (Example 1J)

is a measurement often used for comparison with predictions. Durst and Tropea (1981) have assembled reattachment data from diverse 2-D experiments (no bottom friction) for backsteps, and these show that x_R/H varies with the channel expansion ratio H_2/H_1.

To obtain STREMR predictions for the variation of x_R/H with H_2/H_1, input for cell types can be easily modified in Examples 2A and 2B to reduce the channel width and create expansion ratios greater than 1.1. First, a section of OUT cells has to be specified along the north side of the grid. This OUT section must be exactly IMAX cells long, but its width depends on the desired reduction in channel width. Next, the row of SLIP cells along the original north boundary (Figures 34 and 36) has to be moved southward to lie just inside the modified north boundary. Finally, the end columns of FLUX and OPEN cells have to be shortened to match the modified (narrower) grid.

```
&BEGIN  START='COLD'     , IREF=1  ,
          FLOW='INFLOW'  , JREF=15 ,
        IUNITS='ENGLISH' ,
      TITLE='EXAMPLE 2A: 60X30 GRID WITH BACKSTEP' &END
&PARAM PUNITS='ENGLISH' , NSTEPS=2500,
        ALLOUT='YES'     , NSTORE=2500,
          MAPS='YES'     , NSTOMO=1   ,
         TIMER='YES'     , INFORM=10  ,
                           ITERS=3    &END
&INPUT ITEM='CELL TYPES'                          &END
&INPUT ITEM='SLIP'    , I1=1 , I2=60, J1=30, J2=30 &END
&INPUT ITEM='NOSLIP'  , I1=1 , I2=16, J1=1 , J2=11 &END
&INPUT ITEM='OUT'     , I1=1 , I2=15, J1=1 , J2=10 &END
&INPUT ITEM='FLUX'    , I1=1 , I2=1 , J1=11, J2=30 &END
&INPUT ITEM='OPEN'    , I1=60, I2=60, J1=1 , J2=30 &END
&INPUT ITEM='END'                                  &END
&INPUT ITEM='GENERAL'                   &END
&INPUT ITEM='DEPTH'      , VALUES=0.2  &END
&INPUT ITEM='X-VELOCITY' , VALUES=1.0  &END
&INPUT ITEM='MANNING'    , VALUES=0.0  &END
&INPUT ITEM='END'                       &END
&INPUT ITEM='SECTION' &END
&INPUT ITEM='END'     &END
&INPUT ITEM='LINE' &END
&INPUT ITEM='END'  &END
&INPUT ITEM='RANDOM' &END
&INPUT ITEM='END'    &END
```

Figure 34. STREMR input for backstep on nonuniform 60 × 30 grid (Example 2A, no bottom friction; H_2/H_1 = 1.1)

In Figure 38, STREMR predictions for reattachment length (no bottom friction) are compared with the 2-D test data of Durst and Tropea (1981). The shape of the predicted curves is roughly the same as that suggested by the test data, which exhibit a spread of about 15 percent. Note that the 120 X 60 grid falls on the high side of the data with predictions that are 15 percent greater than those of the 60 X 30 grid. Further grid refinement (by a factor of two) yields an additional increase of less than 3 percent in x_R/H.

Parameter Variation for Backstep

The predictions in Figure 38 were all obtained with the default value for the turbulence parameter (RECAP = 2.5). It is apparent from these results that reattachment predictions may be slightly high if the grid is fine enough to eliminate most of the grid error. The default value for RECAP compensates somewhat for grid error on coarse grids; but it is higher than the correct value that should be used with fine grids. Figure 39 demonstrates the effect of RECAP for predictions in a channel with H_2/H_1 = 1.1.

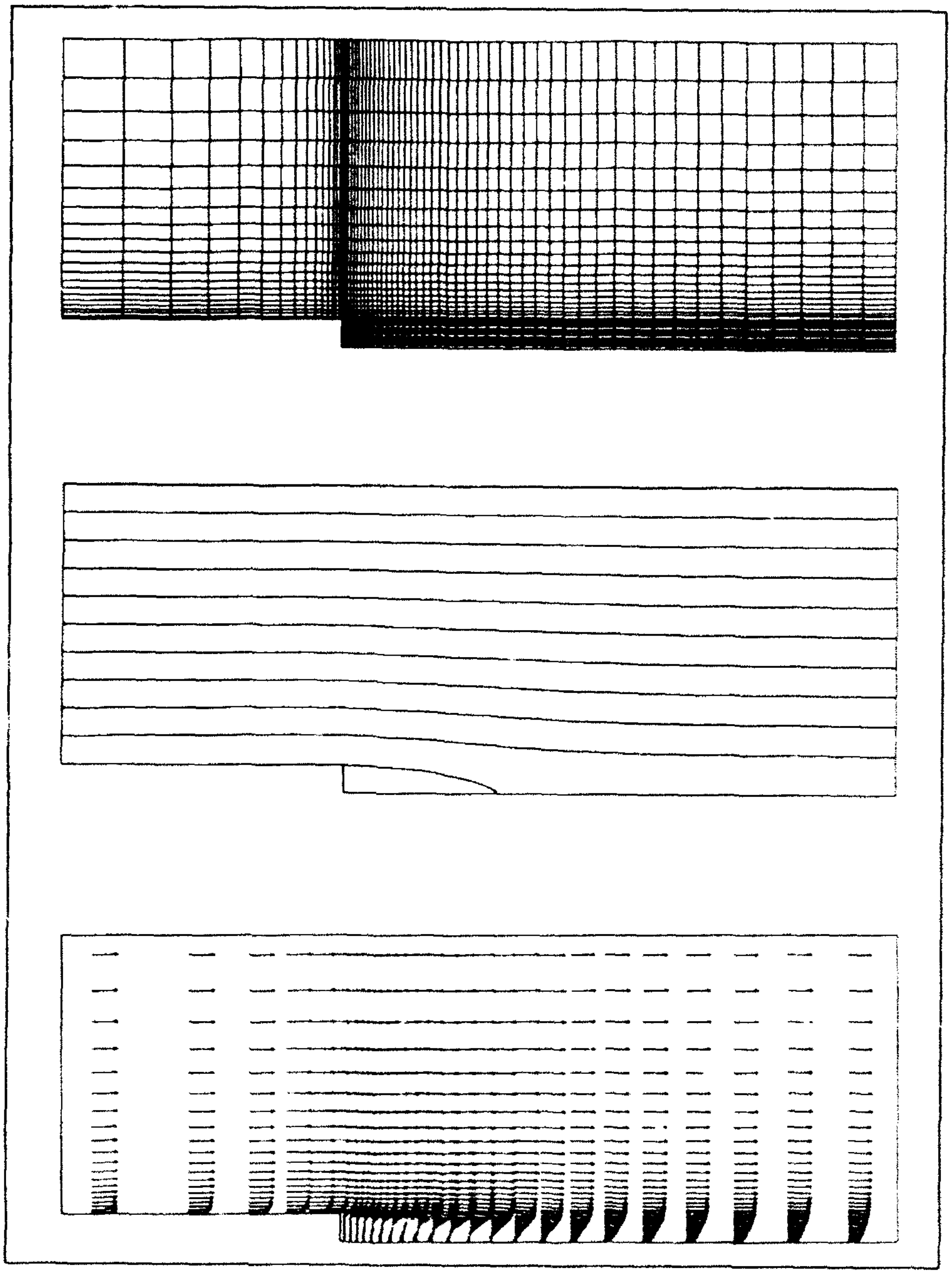

Figure 35. Nonuniform 60 × 30 grid with computed streamlines and velocity vectors for backstep (Example 2A, no bottom friction; H_2/H_1 = 1.1)

With this configuration, STREMR predictions for reattachment length are effectively grid independent with grids finer than the 120 X 60 grid in Figure 37. Since the test data (Figure 38) indicate that $5 < x_R/H < 6$ for H_2/H_1 = 1.1, one can infer (Figure 39) that the proper (grid-independent) value for RECAP lies between 1.5 and 2.0. Nevertheless, many STREMR users may be reluctant to employ grids as fine as the 120 X 60 grid, and the default value for RECAP has been set at 2.5 to compensate for anticipated grid error. This

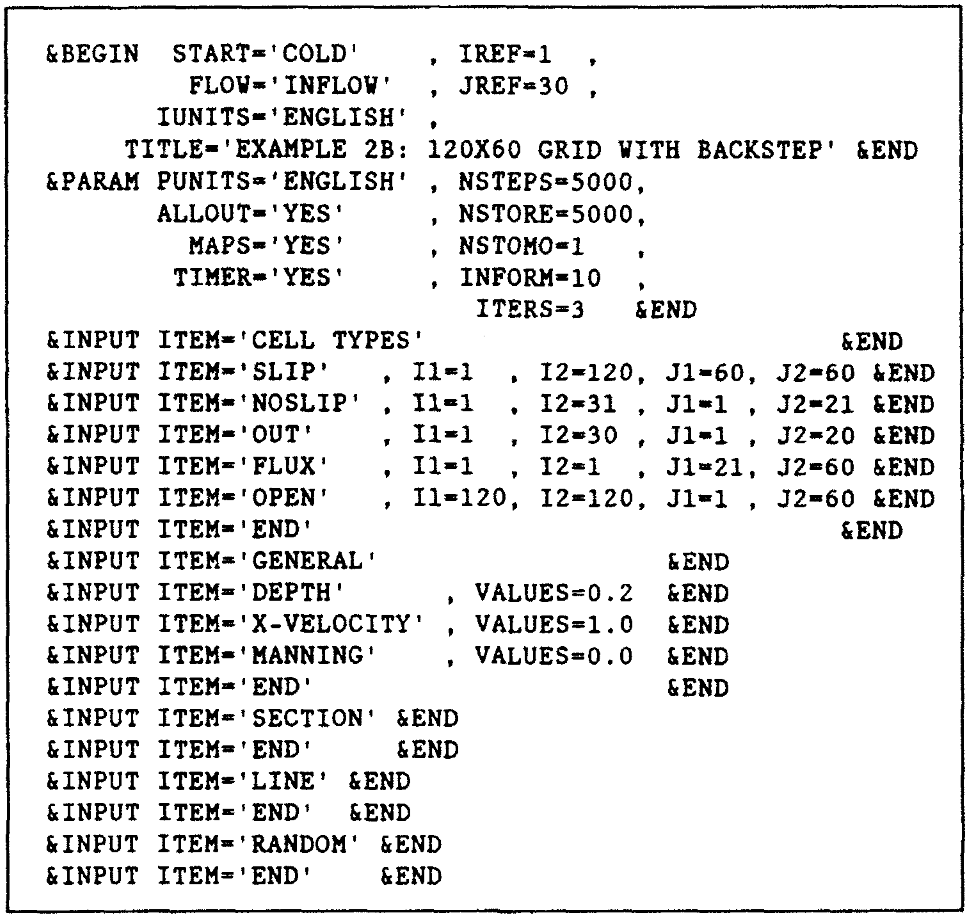

```
&BEGIN  START='COLD'     , IREF=1  ,
          FLOW='INFLOW'  , JREF=30 ,
        IUNITS='ENGLISH' ,
      TITLE='EXAMPLE 2B: 120X60 GRID WITH BACKSTEP' &END
&PARAM PUNITS='ENGLISH' , NSTEPS=5000,
       ALLOUT='YES'     , NSTORE=5000,
         MAPS='YES'     , NSTOMO=1   ,
        TIMER='YES'     , INFORM=10  ,
                           ITERS=3   &END
&INPUT ITEM='CELL TYPES'                            &END
&INPUT ITEM='SLIP'    , I1=1  , I2=120, J1=60, J2=60 &END
&INPUT ITEM='NOSLIP'  , I1=1  , I2=31 , J1=1 , J2=21 &END
&INPUT ITEM='OUT'     , I1=1  , I2=30 , J1=1 , J2=20 &END
&INPUT ITEM='FLUX'    , I1=1  , I2=1  , J1=21, J2=60 &END
&INPUT ITEM='OPEN'    , I1=120, I2=120, J1=1 , J2=60 &END
&INPUT ITEM='END'                                   &END
&INPUT ITEM='GENERAL'                  &END
&INPUT ITEM='DEPTH'       , VALUES=0.2  &END
&INPUT ITEM='X-VELOCITY' , VALUES=1.0  &END
&INPUT ITEM='MANNING'     , VALUES=0.0  &END
&INPUT ITEM='END'                      &END
&INPUT ITEM='SECTION' &END
&INPUT ITEM='END'     &END
&INPUT ITEM='LINE' &END
&INPUT ITEM='END'  &END
&INPUT ITEM='RANDOM' &END
&INPUT ITEM='END'    &END
```

Figure 36. STREMR input for backstep on nonuniform 120 × 60 grid (Example 2B, no bottom friction; H_2/H_1 = 1.1)

is a point to remember whenever fine grids are used to achieve accurate flow predictions *and* grid independence.

Bottom friction can also have a considerable effect on the predicted reattachment length for a backstep. Figure 40 presents STREMR results for Examples 2A and 2B with Manning coefficients from 0.0 to 0.02. The highest value n = 0.02 imposes a bottom friction factor C_f = 0.01 in the 0.2-ft-deep channel, which reduces x_R/H to 65 percent of its frictionless value.

Example 3A: Nonuniform 60 X 30 Grid with Spur Dike

This example again employs the nonuniform 60 X 30 grid of Example 2A for a channel 30 ft long and 0.2 ft deep. In this case, however, cell-type designations are used in the STREMR input (Figure 41) to create a grid with an unsubmerged spur dike (contraction/expansion) 10 ft from the west (inflow)

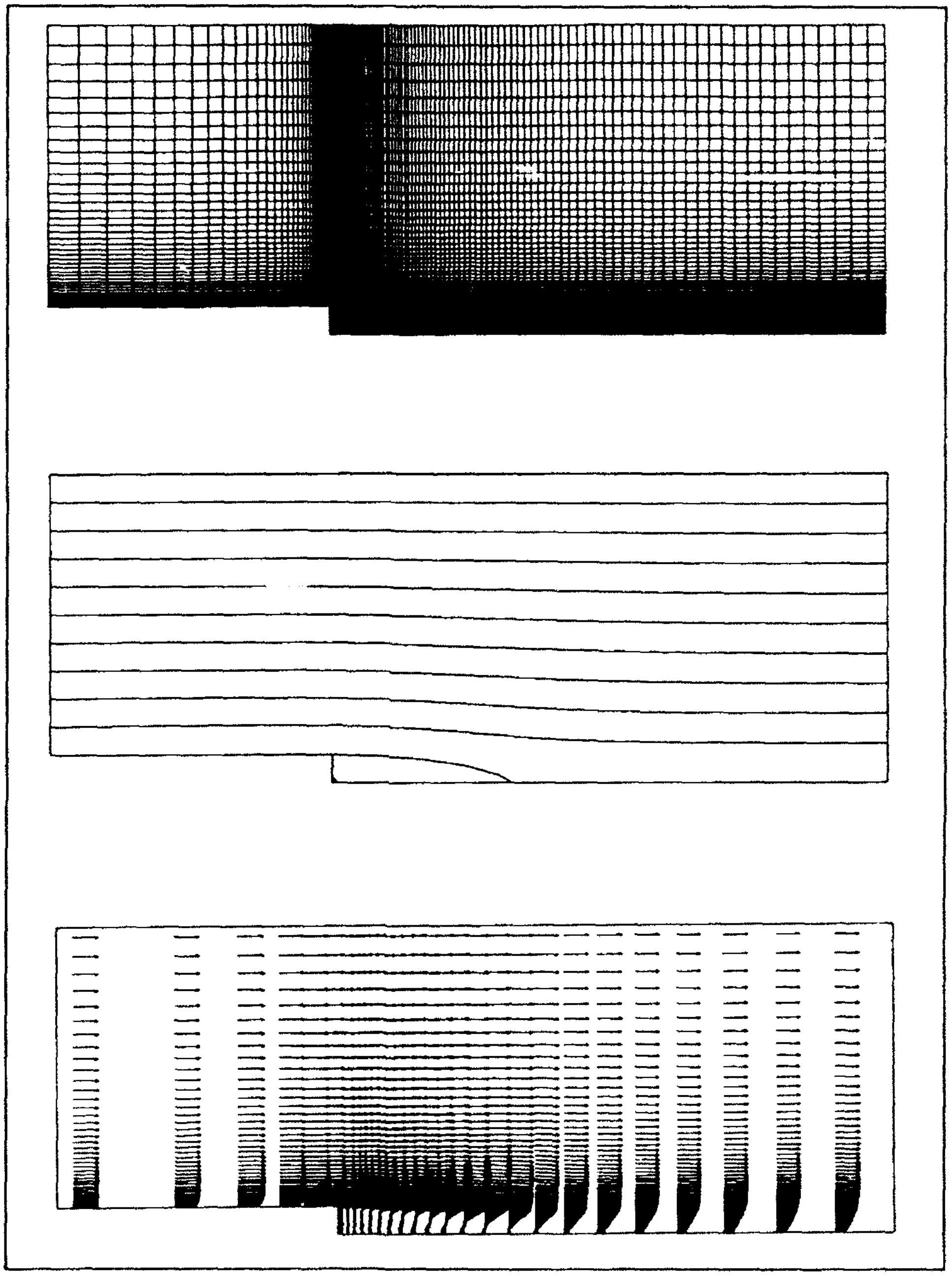

Figure 37. Nonuniform 120 × 60 grid with computed streamlines and velocity vectors for backstep (Example 2B, *no bottom friction*; $H_2/H_1 = 1.1$)

boundary. The north side of the grid (Figure 42) is designated as a SLIP boundary (channel centerline) in the STREMR input. The resulting grid widths (channel half widths) are $H_1 = 10$ ft at the contraction, and $H_2 = 11$ ft upstream and downstream. Thus, the channel expansion ratio is $H_2/H_1 = 1.1$, and the dike length is $H = H_2 - H_1 = 1$ ft. The thickness of the dike is 0.2 ft in the streamwise *x*-direction.

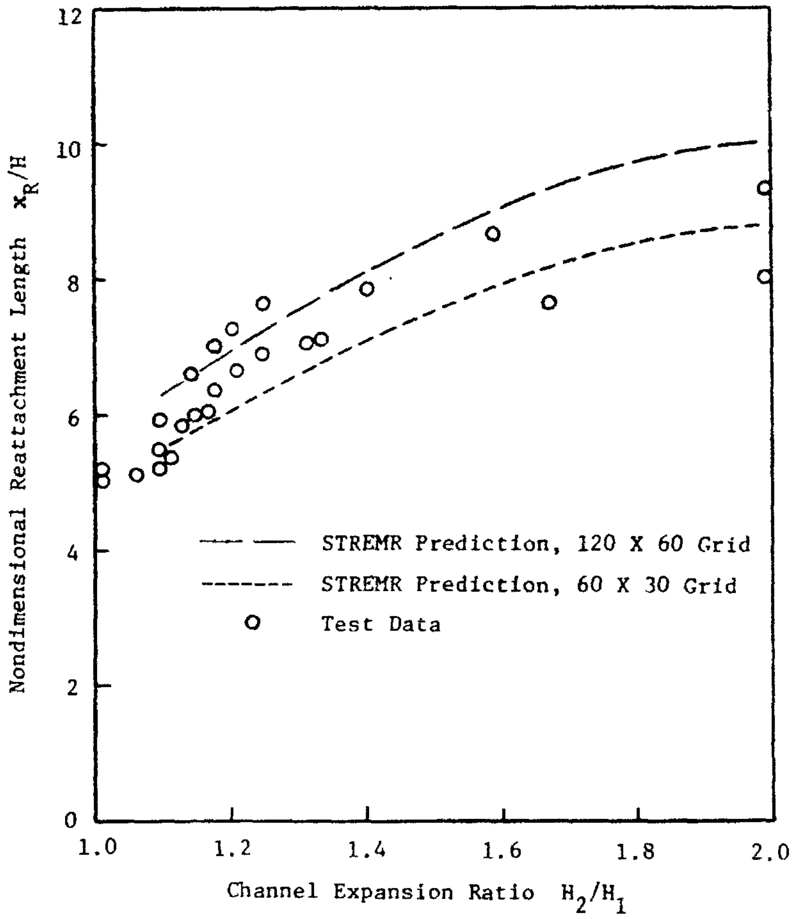

Figure 38. Comparison of STREMR predictions with test data for 2-D flow reattachment downstream of backstep (no bottom friction)

Although the grid is nonuniform far from the dike, the grid cells are perfectly square in its immediate vicinity. The dike length is divided into ten equal grid spaces (0.1 ft each), and the dike thickness is divided into two equal spaces (0.1 ft each). The grid spacing gradually increases with distance from the dike (in both directions). The resulting flow (no bottom friction) is shown with the modified 60 X 30 grid in Figure 42.

The flow separates near the base of the upstream side of the dike, and at the downstream corner of its north end. There are zones of clockwise recirculation on both sides of the dike, except at its downstream base, where there is a small zone of counter-clockwise recirculation. The flow reattaches to the wall about 15.7 dike lengths downstream.

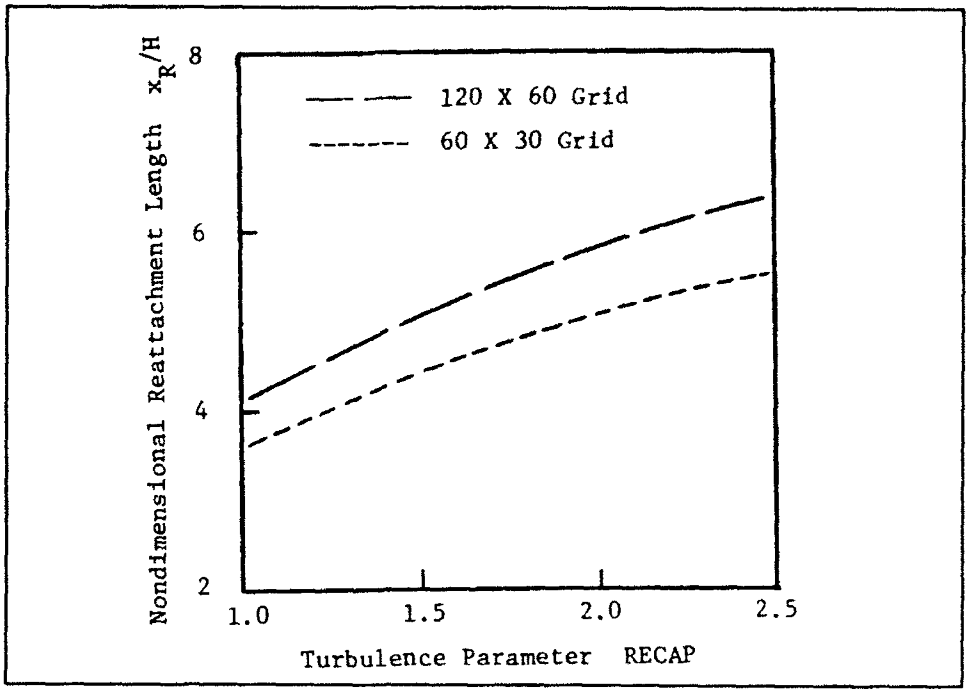

Figure 39. Effect of turbulence parameter RECAP on predicted 2-D flow reattachment for backstep (no bottom friction; H_2/H_1 = 1.1)

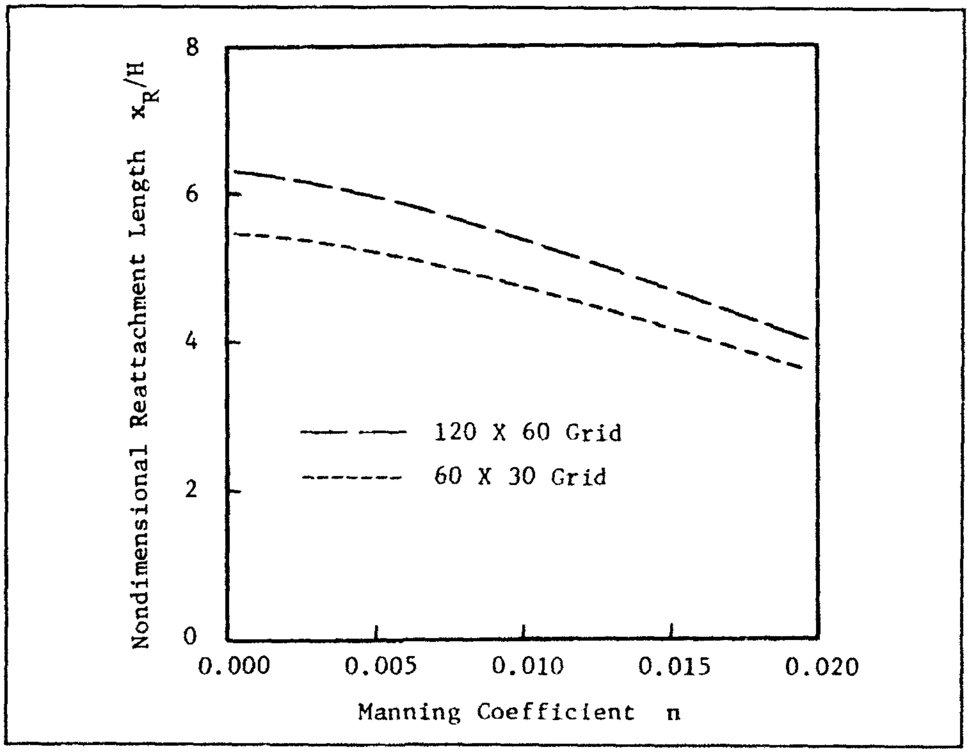

Figure 40. Effect of bottom friction on predicted flow reattachment for backstep with H_2/H_1 = 1.1 in 0.2-ft-deep channel

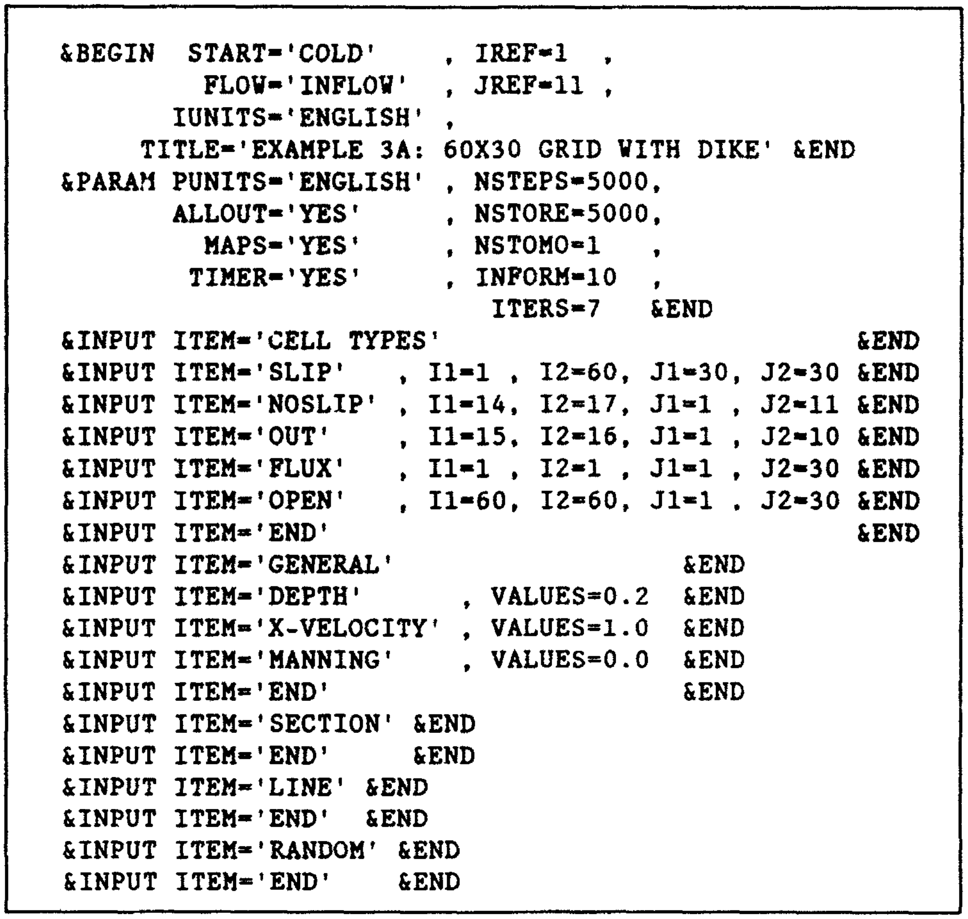

```
&BEGIN  START='COLD'     , IREF=1  ,
          FLOW='INFLOW'  , JREF=11 ,
       IUNITS='ENGLISH'  ,
     TITLE='EXAMPLE 3A: 60X30 GRID WITH DIKE' &END
&PARAM PUNITS='ENGLISH'  , NSTEPS=5000,
       ALLOUT='YES'      , NSTORE=5000,
         MAPS='YES'      , NSTOMO=1   ,
        TIMER='YES'      , INFORM=10  ,
                            ITERS=7   &END
&INPUT ITEM='CELL TYPES'                              &END
&INPUT ITEM='SLIP'    , I1=1 , I2=60, J1=30, J2=30 &END
&INPUT ITEM='NOSLIP'  , I1=14, I2=17, J1=1 , J2=11 &END
&INPUT ITEM='OUT'     , I1=15, I2=16, J1=1 , J2=10 &END
&INPUT ITEM='FLUX'    , I1=1 , I2=1 , J1=1 , J2=30 &END
&INPUT ITEM='OPEN'    , I1=60, I2=60, J1=1 , J2=30 &END
&INPUT ITEM='END'                                     &END
&INPUT ITEM='GENERAL'                   &END
&INPUT ITEM='DEPTH'      , VALUES=0.2  &END
&INPUT ITEM='X-VELOCITY' , VALUES=1.0  &END
&INPUT ITEM='MANNING'    , VALUES=0.0  &END
&INPUT ITEM='END'                       &END
&INPUT ITEM='SECTION' &END
&INPUT ITEM='END'     &END
&INPUT ITEM='LINE' &END
&INPUT ITEM='END'  &END
&INPUT ITEM='RANDOM' &END
&INPUT ITEM='END'    &END
```

Figure 41. STREMR input for spur dike on nonuniform 60 x 30 grid (Example 3A, no bottom friction; H_2/H_1 = 1.1)

Example 3B: Nonuniform 120 X 60 Grid with Spur Dike

This example employs the nonuniform 120 X 60 grid of Example 2B for the channel described in Example 3A. The STREMR input (Figure 43) is similar to Example 3A, but the input values for *i* and *j* now reflect the doubling of IMAX and JMAX. The grid spacing has been reduced by a factor of two, and the total number of time-steps (NSTEPS) has been increased because the allowable time-step size is proportional to the grid spacing.

Like the previous example, the grid cells are perfectly square in the immediate vicinity of the dike, and the grid spacing gradually increases with distance from the dike. In this case, however, the dike length is divided into twenty equal grid spaces (0.05 ft each) instead of ten. Likewise, the dike thickness is divided into four equal spaces (0.05 ft each) instead of two. The

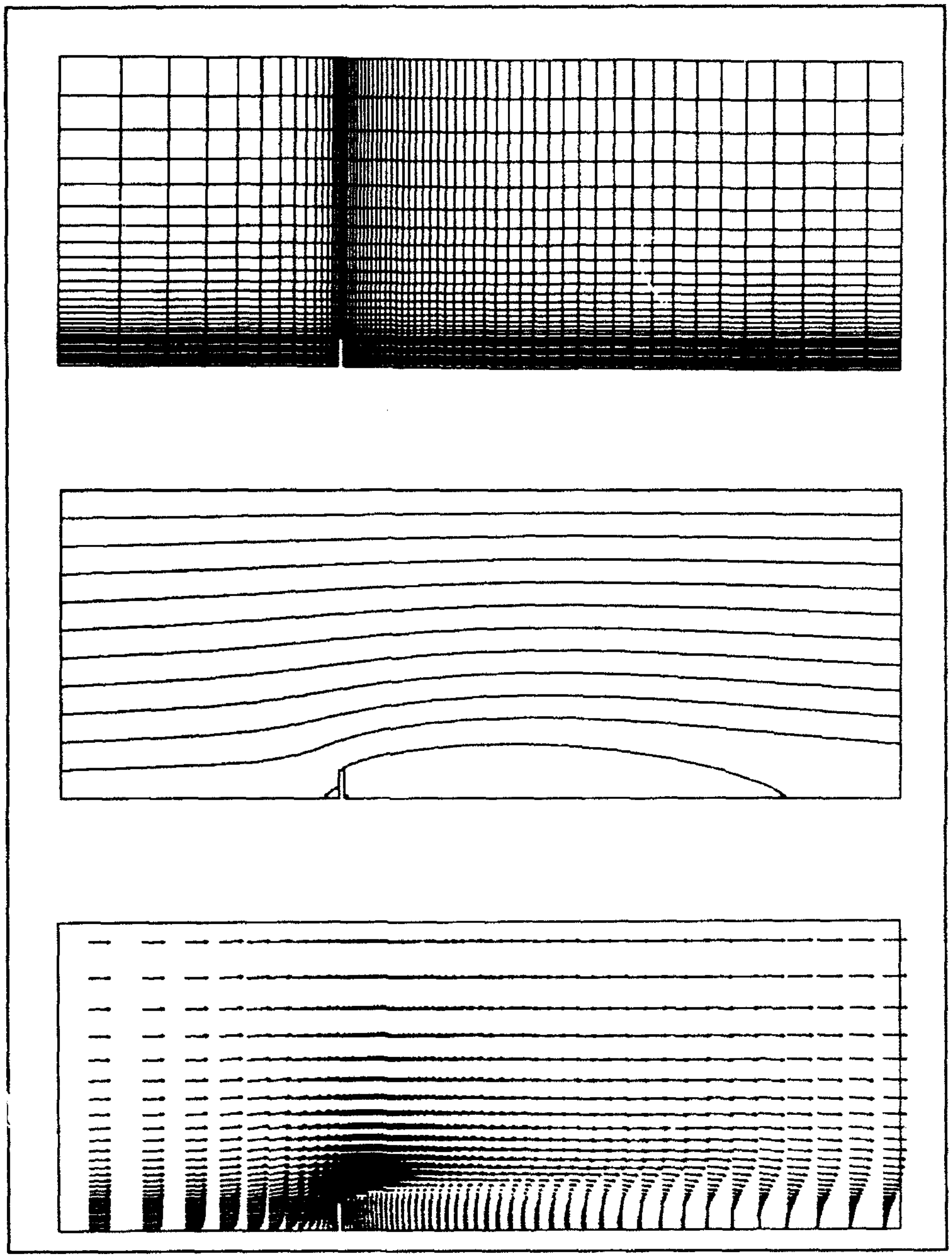

Figure 42. Nonuniform 60 × 30 grid with computed streamlines and velocity vectors for spur dike (Example 3A, no bottom friction; H_2/H_1 = 1.1)

resulting flow (no bottom friction) is shown with the modified 120 X 60 grid in Figure 44.

In this case, the flow separates near the base of the upstream side of the dike, and at the upstream corner of its north end. There are zones of clockwise recirculation on both sides of the dike, except at its downstream base, where there is a small zone of counter-clockwise recirculation. Note that all

```
&BEGIN  START='COLD'    , IREF=1  ,
         FLOW='INFLOW'  , JREF=21 ,
       IUNITS='ENGLISH' ,
     TITLE='EXAMPLE 3B: 120X60 GRID WITH DIKE' &END
&PARAM PUNITS='ENGLISH' , NSTEPS=15000,
       ALLOUT='YES'     , NSTORE=15000,
         MAPS='YES'     , NSTOMO=1    ,
        TIMER='YES'     , INFORM=10   ,
                           ITERS=7    &END
&INPUT ITEM='CELL TYPES'                           &END
&INPUT ITEM='SLIP'    , I1=1  , I2=120, J1=60, J2=60 &END
&INPUT ITEM='NOSLIP'  , I1=28 , I2=33 , J1=1 , J2=21 &END
&INPUT ITEM='OUT'     , I1=29 , I2=32 , J1=1 , J2=20 &END
&INPUT ITEM='FLUX'    , I1=1  , I2=1  , J1=1 , J2=60 &END
&INPUT ITEM='OPEN'    , I1=120, I2=120, J1=1 , J2=60 &END
&INPUT ITEM='END'                                  &END
&INPUT ITEM='GENERAL'                 &END
&INPUT ITEM='DEPTH'       , VALUES=0.2 &END
&INPUT ITEM='X-VELOCITY'  , VALUES=1.0 &END
&INPUT ITEM='MANNING'     , VALUES=0.0 &END
&INPUT ITEM='END'                     &END
&INPUT ITEM='SECTION' &END
&INPUT ITEM='END'     &END
&INPUT ITEM='LINE' &END
&INPUT ITEM='END'  &END
&INPUT ITEM='RANDOM' &END
&INPUT ITEM='END'    &END
```

Figure 43. STREMR input for spur dike on nonuniform 120 × 60 grid (Example 3B, no bottom friction; H_2/H_1 = 1.1)

the recirculation zones for the 120 X 60 grid are larger than those for the 60 X 30 grid.

The flow reattaches to the wall about 18 dike lengths downstream, and this amounts to a 15 percent increase over the reattachment length predicted in Example 3A. Further refinement of the grid (by another factor of two) increases the reattachment length by less than 3 percent. To predict the largest eddies for a spur dike, it appears that 20 grid spaces are enough for discretizing the dike length (as far as grid error is concerned).

The dike represents a more difficult problem than the backstep, because the dike is more sensitive to flow conditions immediately upstream. In particular, the flow on the upstream side determines the angle of flow separation at the end of the dike, which influences the reattachment length x_R downstream. As a result, the computed flow may change considerably with the distance of the dike from the inflow boundary. In Examples 3A and 3B, however, the dike has been placed far enough from the channel entrance that further (downstream) changes in position have no effect on the computed flow.

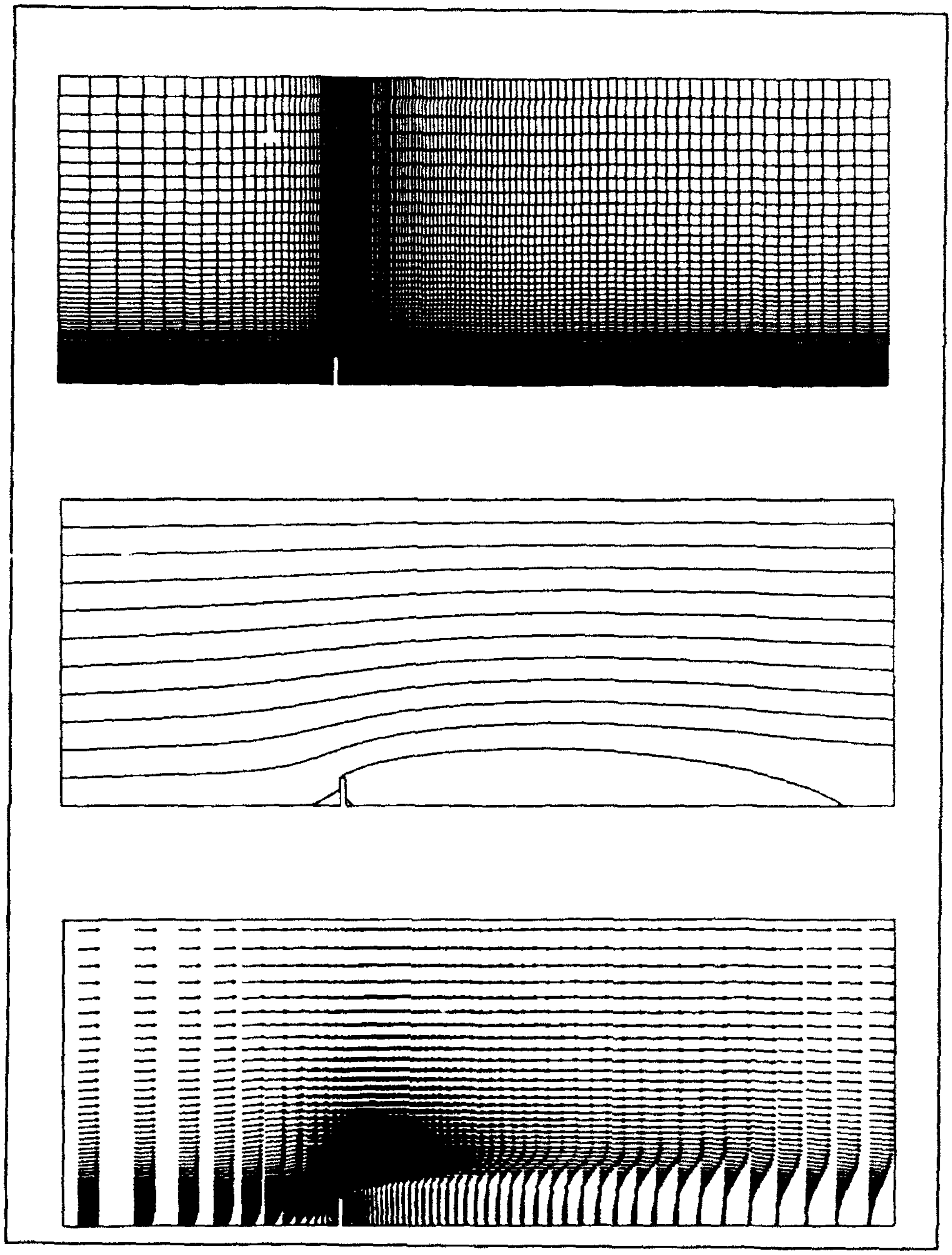

Figure 44. Nonuniform 120 × 60 grid with computed streamlines and velocity vectors for spur dike (Example 3B, no bottom friction; H_2/H_1 = 1.1)

Test Data for Dikes

Unfortunately, there seem to be fewer experimental data available for dikes than for backsteps. For a dike with (streamwise) thickness 2H, Moss and Baker (1980) report $x_R/H \approx 12$ in a wind tunnel with $H_2/H_1 = 1.1$. For thin dikes, Rajaratnum and Nwachukwu (1983) report $x_R/H \approx 12$ in smooth, shallow channels (0.5 to 0.84 ft deep) with $H_2/H_1 = 1.09$ to 1.2; however, Francis, Pattanick, and Wearne (1968) report $x_R/H \approx 13$ in smooth, shallow channels (0.21 ft deep) with $H_2/H_1 = 1.15$ to 1.21. These data are too few to indicate the general variation of reattachment length with channel expansion ratio, but they do suggest an approximate range for the correct value of x_R/H in Examples 3A and 3B.

Parameter Variation for Spur Dike

Figure 45 offers STREMR predictions (without verification) for the variation of x_R/H with H_2/H_1 (no bottom friction). These results were obtained by modifying the cell-type input in Examples 3A and 3B to reduce the channel width and create expansion ratios greater than 1.1. Note that x_R/H now *decreases* with increasing H_2/H_1. As the channel expansion ratio increases, the channel becomes narrower at the constriction imposed by the dike. This increased confinement reduces the angle of flow separation at the end of the dike, which shortens the reattachment length downstream.

The predictions in Figure 45 were all obtained with the default value for the turbulence parameter (RECAP = 2.5). Uncertainty in the bottom friction,

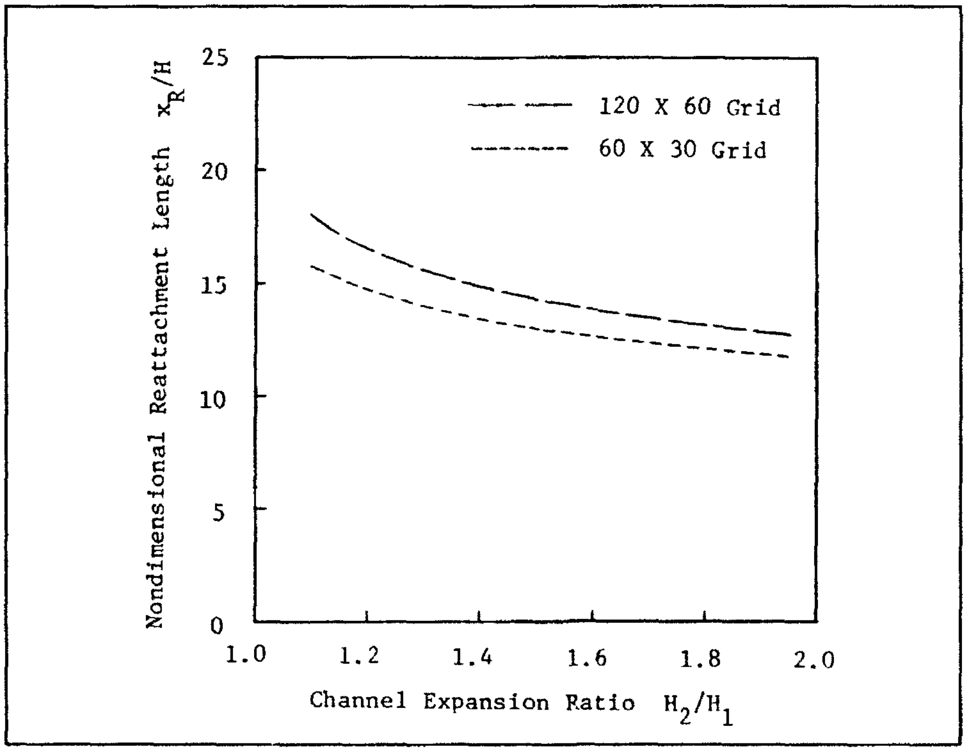

Figure 45. STREMR predictions for 2-D flow reattachment downstream of spur dike (no bottom friction)

however, compounds the difficulty of inferring the best value for RECAP from the scant experimental data cited above.

Figure 46 demonstrates the effect of RECAP on reattachment predictions made for H_2/H_1 = 1.1 with *no* bottom friction (*n* = 0.0). Here the 120 X 60 grid predicts x_R/H = 11.5 for RECAP = 1.0, x_R/H = 14.5 for RECAP = 1.5, and x_R/H = 17.3 for RECAP = 2.0.

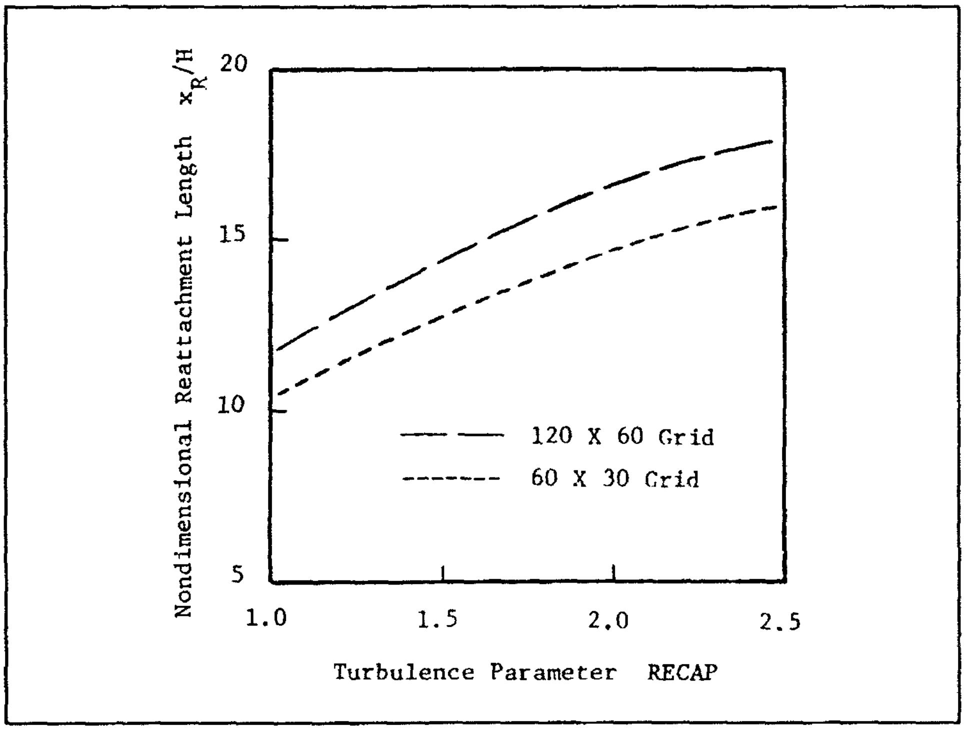

Figure 46. Effect of turbulence parameter RECAP on predicted 2-D flow reattachment for spur dike (no bottom friction; H_2/H_1 = 1.1)

Figure 47 presents reattachment predictions made for H_2/H_1 = 1.1 and RECAP = 2.5 with Manning coefficients from 0.0 to 0.02. The highest Manning coefficient n = 0.02 imposes a bottom friction factor C_f = 0.01 in the 0.2-ft-deep channel, for which the 120 X 60 grid predicts x_R/H = 12.5.

From Figures 46 and 47 together, one can infer that the 120 X 60 grid would predict $x_R/H \approx$ 11.7 with *n* = 0.01 and RECAP = 2.0, and likewise $x_R/H \approx$ 10.0 with *n* = 0.01 and RECAP = 1.5. Assuming that Manning's coefficient was somewhere between 0.0 and 0.01 in the cited experiments, the proper (grid-independent) value for RECAP then lies between 1.5 and 2.0. As stated earlier, however, many STREMR users may be reluctant to employ grids as fine as the 120 X 60 grid, and the default value for RECAP has been set at 2.5 to compensate for anticipated grid error.

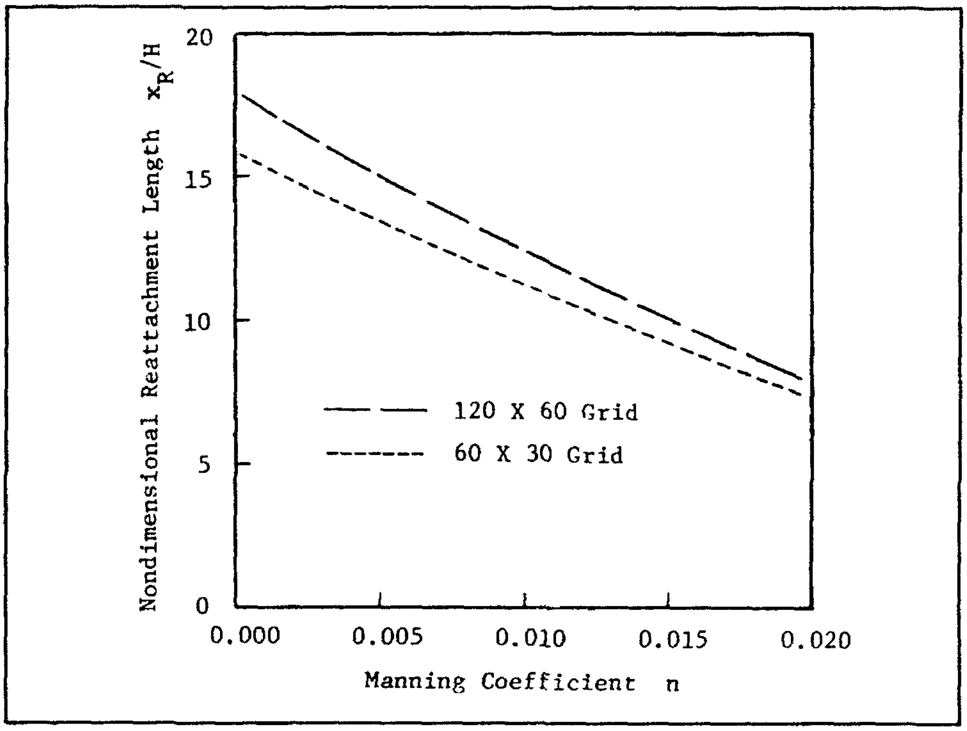

Figure 47. Effect of bottom friction on predicted flow reattachment for spur dike with H_2/H_1 = 1.1 in 0.2-ft-deep channel

Example 4: 83 X 25 Curvilinear Grid with 2-D Hill

In all the previous examples involving separated flow, the point of separation was invariably a sharp corner. It is a lucky accident, however, that real flows and computed flows both separate at sharp corners with adverse pressure gradients (except at very low Reynolds numbers). Real flows separate for physical reasons, but computed flows may separate (or fail to separate) for reasons that are partly nonphysical (Examples 1B-1F). With adverse pressure gradients, however, flow separation at a corner can occur even for SLIP boundaries, where there is supposed to be no tangential shear stress.

To predict flow separation on curved walls *without* sharp corners, numerical models must adequately approximate the gradient of pressure *and* the divergence (imbalance) of shear stress near the wall. The pressure poses no great problem, because it changes gradually with distance from the wall, and it is well approximated by STREMR calculations using fairly coarse grids. The shear stress, on the other hand, requires much finer grids that can better resolve the velocity and turbulence close to the wall.

To demonstrate the trial-and-error process of generating suitable grids for curved boundaries, the next set of STREMR calculations shows the effect of grid refinement on flow predictions for a gentle 2-D hill in elevation view.

The hill profile can also be regarded as a 2-D channel indentation in plan view, but the results are the same either way. There is no bottom friction, and the depth is arbitrary normal to the plane of flow.

Figure 48 shows the STREMR input for an 83 X 25 grid with arbitrary (default) depth. The grid (Figures 49-52) is 4.01 meters long, and 2.0 meters high at the east and west ends. The hill has a maximum height *H* of 0.208 meter, and it is centered 1.63 meters from the west (inflow) boundary. The surface of the hill is a circular arc of radius 1.08 meters, which is rounded off at its leading and trailing edges by arcs of radius 0.4 meter.

In Figures 49-52, the vertical grid spacing Δ*y* at the *lower* boundary is reduced by successive factors of two. This is accomplished simply by shifting gridlines toward the lower boundary, without changing the total number of grid spaces in the vertical. The STREMR input (Figure 48) is the same for each of these grids.

```
&BEGIN  START='COLD'   , IREF=1 ,
         FLOW='INFLOW  , JREF=15,
       IUNITS='METRIC' ,
        TITLE='EXAMPLE 4: 83 X 25 GRID WITH HILL' &END
&PARAM PUNITS='METRIC' , NSTEPS=1500,
       ALLOUT='NO'     , NSTORE=1500,
         MAPS='YES'    , NSTOMO=1  ,
        TIMER='YES'    , INFORM=10  ,
                          ITERS=3   ,
                          IPMIN=1   ,
                          IPMAX=83  ,
                          JPMIN=1   ,
                          JPMAX=10  ,
                          ISKIP=1   ,
                          JSKIP=1   &END
&INPUT ITEM='CELL TYPES'                           &END
&INPUT ITEM='SLIP' , I1=1 , I2=83, J1=25, J2=25 &END
&INPUT ITEM='FLUX'   I1=1 , I2=1 , J1=1 , J2=25 &END
&INPUT ITEM='OPEN' , I1=83, I2=83, J1=1 , J2=25 &END
&INPUT ITEM='END'                                  &END
&INPUT ITEM='GENERAL'                    &END
&INPUT ITEM='X-VELOCITY' , VALUES=20. &END
&INPUT ITEM='END'                        &END
&INPUT ITEM='SECTION' &END
&INPUT ITEM='END'     &END
&INPUT ITEM='LINE' &END
&INPUT ITEM='END'  &END
&INPUT ITEM='RANDOM' &END
&INPUT ITEM='END'    &END
```

Figure 48. STREMR input for curvilinear 83 × 25 grid with 2-D hill (Example 4)

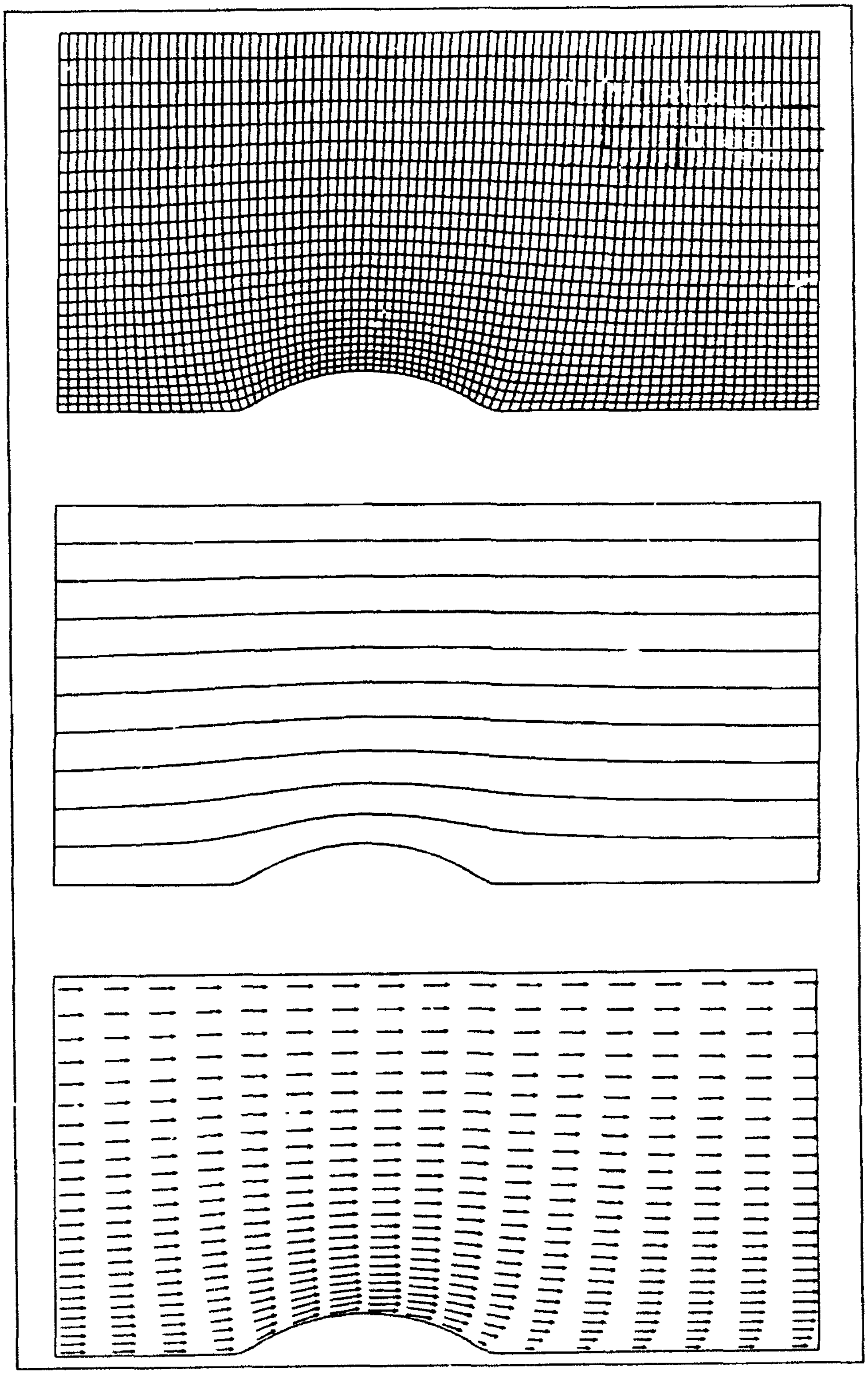

Figure 49. Coarse 83 × 25 grid ($\Delta y/H = 0.192$ along hillside) with computed streamlines and velocity vectors for 2-D hill

AD-A269 949 STREMR: NUMERICAL MODEL FOR DEPTH-AVERAGED INCOMPRESSIBLE FLOW(U) ARMY ENGINEER WATERWAYS EXPERIMENT STATION VICKSBURG MS HYDRAULICS LAB R BERNARD SEP 93 WES/TR/HL-REMR-HY-11 2/2

UNCLASSIFIED NL

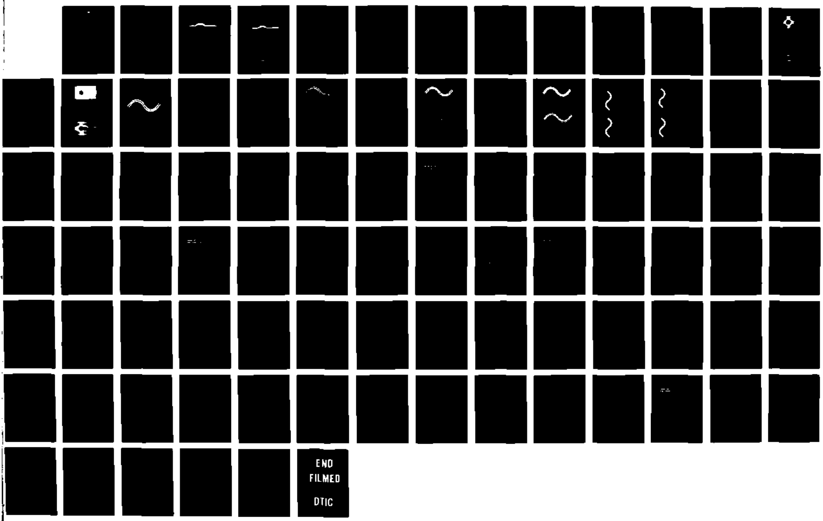

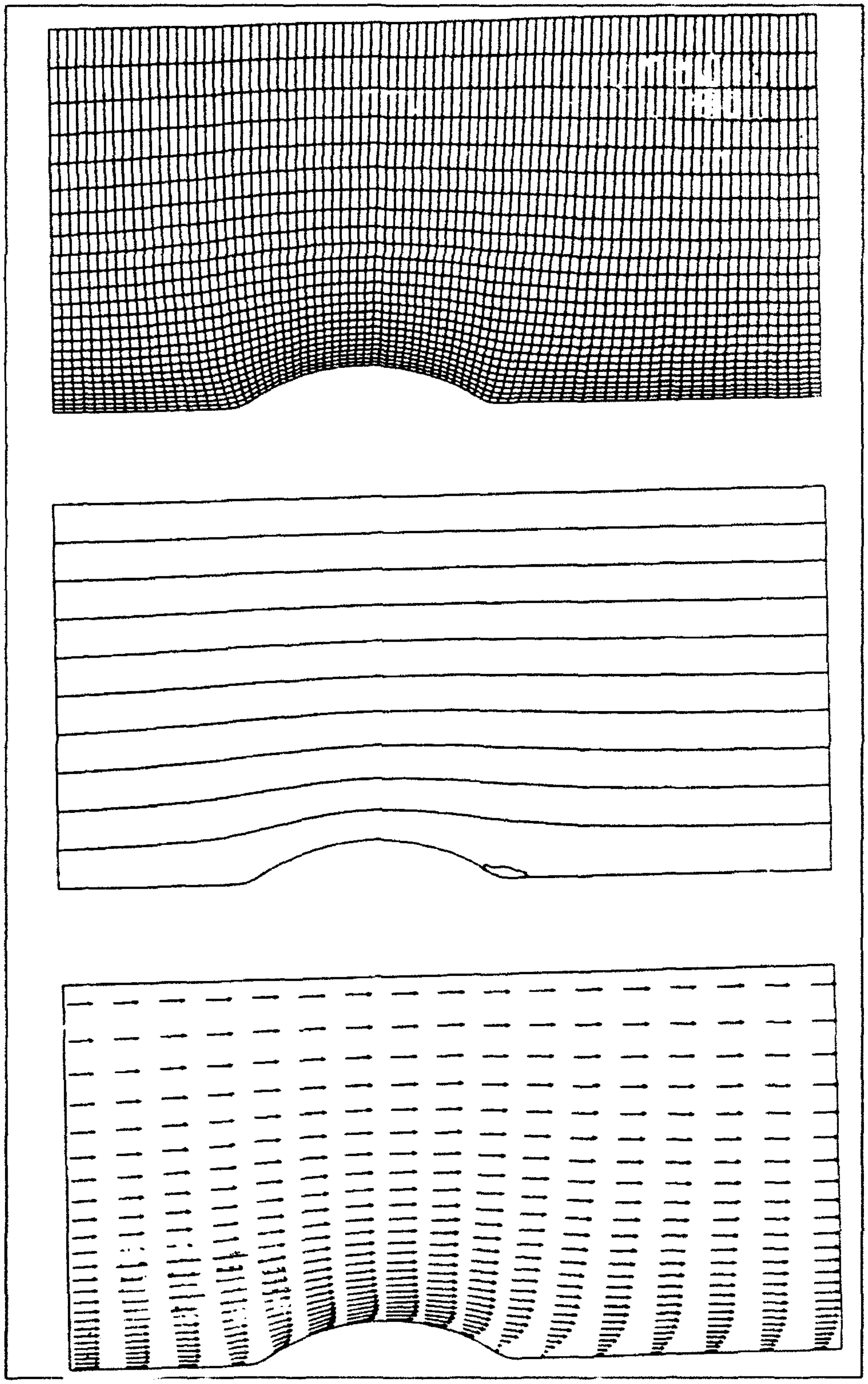

Figure 50. Medium 83 × 25 grid ($\Delta y/H$ = 0.096 along hillside) with computed streamlines and velocity vectors for 2-D hill

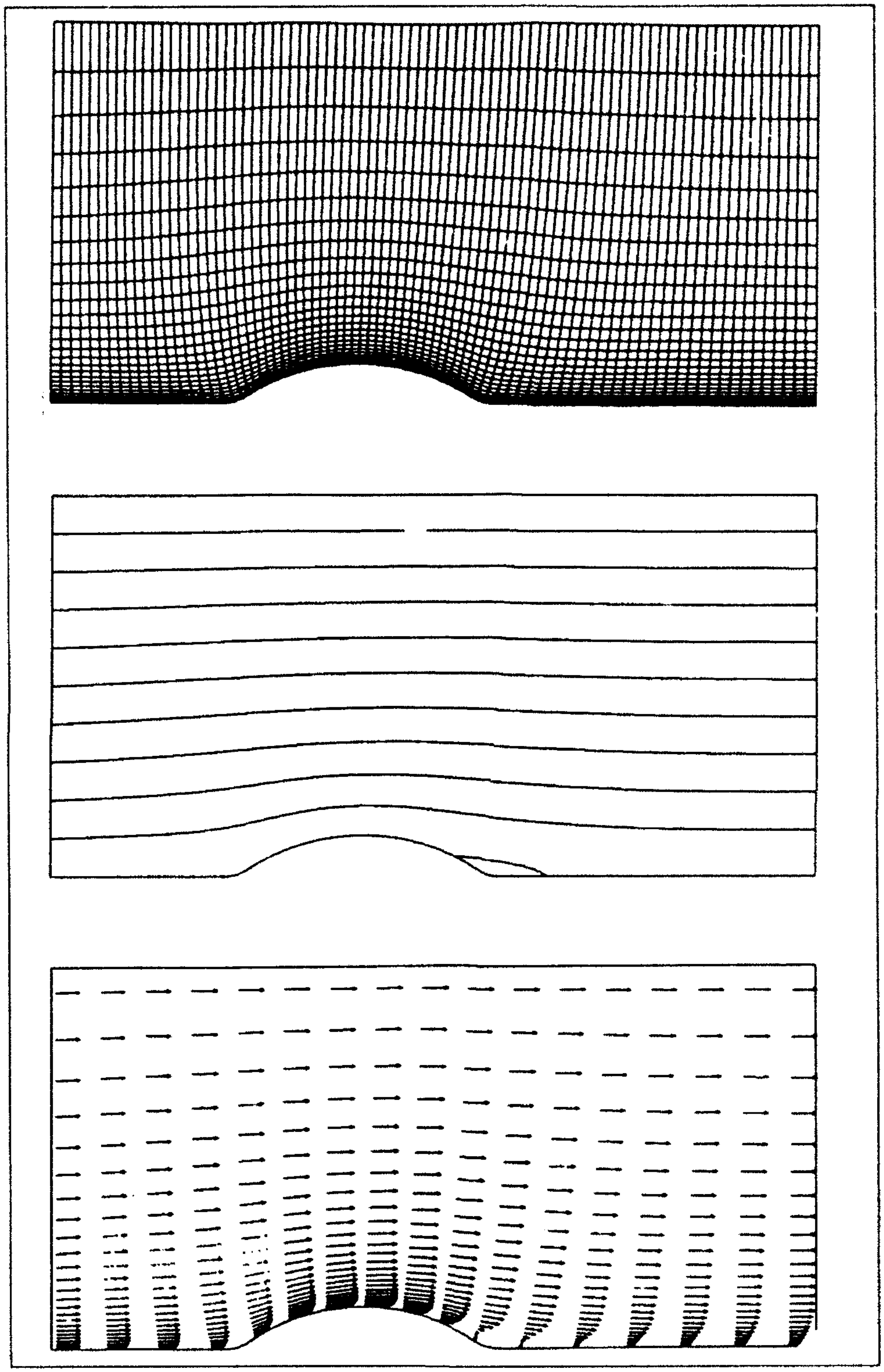

Figure 51. Fine 83 × 25 grid ($\Delta y/H = 0.048$ along hillside) with computed streamlines and velocity vectors for 2-D hill

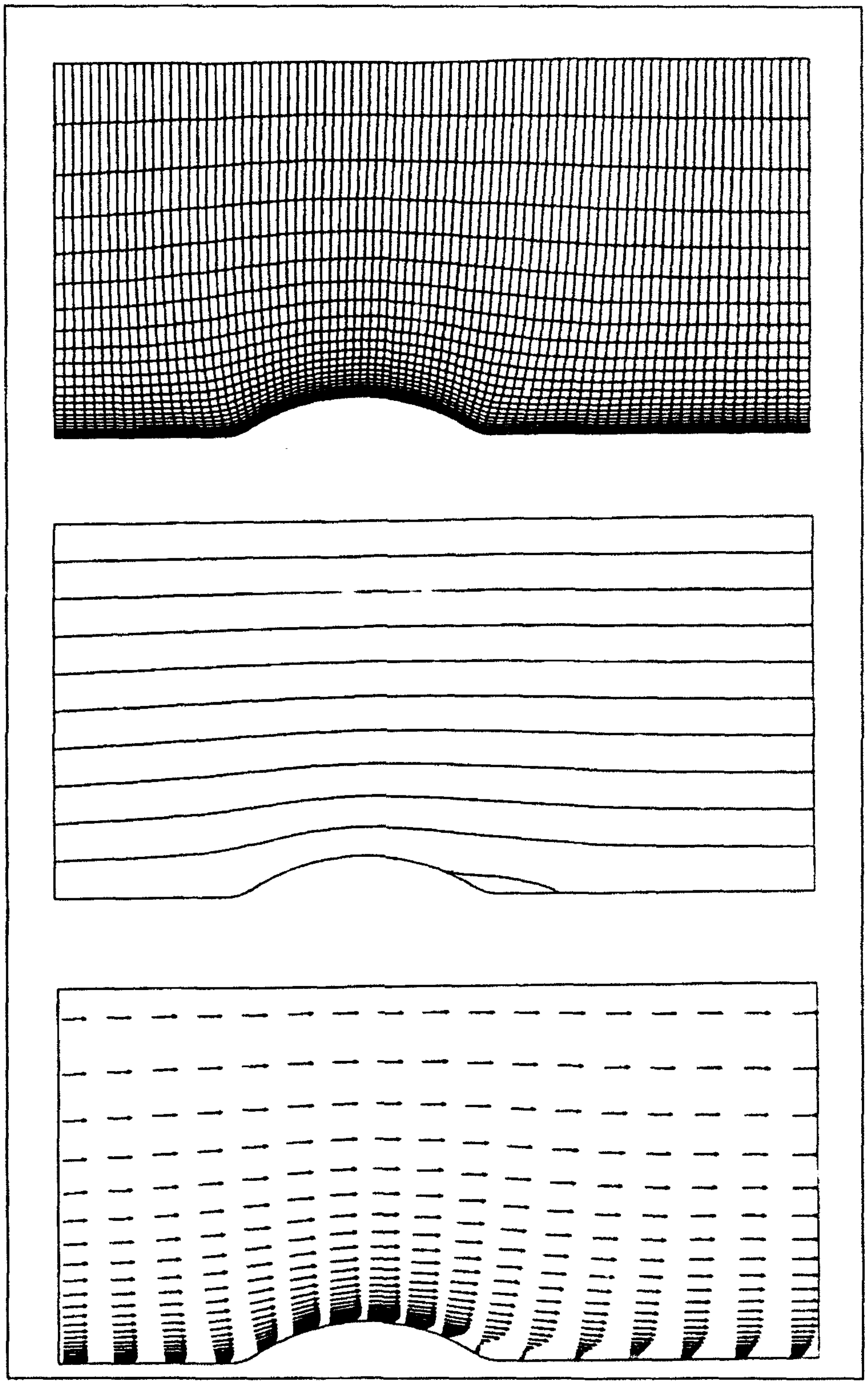

Figure 52. Ultrafine 83 × 25 grid ($\Delta y/H = 0.024$ along hillside) with computed streamlines and velocity vectors for 2-D hill

With $\Delta y/H = 0.192$, the coarse grid (Figure 49) approximates the shear stress so poorly that it produces no flow separation at all. With $\Delta y/H = 0.096$, the medium grid (Figure 50) yields a small recirculation zone; but this grid is still too coarse, and separation occurs too far downstream for even a qualitative simulation of a real flow. With $\Delta y/H = 0.048$, the fine grid (Figure 51) results in a longer recirculation zone; but this grid is not quite fine enough to achieve grid independence.

With $\Delta y/H = 0.024$, the ultrafine grid (Figure 52) produces flow separation 2.077 meters from the inflow (measured horizontally), followed by reattachment at 2.663 meters. Thus, the predicted reattachment length x_R is 0.586 meters, and x_R/H is 2.82. Further reduction of Δy (by another factor of two) increases x_R/H by less than 1 percent. On the other hand, reduction of the average *horizontal* spacing $\Delta x/H$ by a factor of two (from 0.232 to 0.116) increases x_R/H by 10 percent, with negligible increase thereafter. From this it appears that the reattachment predictions become effectively grid independent when $\Delta x/H = 0.116$ and $\Delta y/H = 0.024$.

Comparison with Test Data for 2-D Hill

Baskaran, Smits, and Joubert (1987) have studied the 2-D hill in wind-tunnel experiments, for which the Reynolds number was 277,000 based on the inflow velocity, the height of the hill, and the molecular viscosity. In these experiments, a trip wire was placed 0.153 meter (measured horizontally) from the inflow to induce transition to turbulence. Separation occurred at 2.095 meters, followed by reattachment at 2.720 meters. Thus, the observed reattachment length x_R was 0.625 meter, and x_R/H was 3.00. Figure 53 compares this datum to a plot of STREMR predictions made with $\Delta x/H = 0.232$ and variable $\Delta y/H$.

Note that the STREMR input (Figure 48) sets ALLOUT = 'NO', with nonzero values for the print indices (IPMIN, IPMAX, JPMIN, and JPMAX) in namelist PARAM. This produces a cell-by-cell listing of the flow variables for the specified range of *i* and *j*, followed by a similar listing of C_f and C_p for the included SLIP and NOSLIP cell faces. The latter two quantitites are the sidewall friction coefficient and pressure coefficient, respectively, defined by Equations 2 and 3 in Part IV.

Figure 54 compares the wind-tunnel test data for C_f and C_p against STREMR predictions made with the ultrafine grid (Figure 52). The values in Figure 54 were computed from the shear stress and the pressure *on* the lower boundary. For reference, the hill profile is drawn to scale at the top of the figure, and the distance along the abscissa is the corresponding horizontal position.

The predicted C_f is high near the entrance because of the high shear stress imposed by the fixed velocity at the inflow (FLUX) boundary. Downstream,

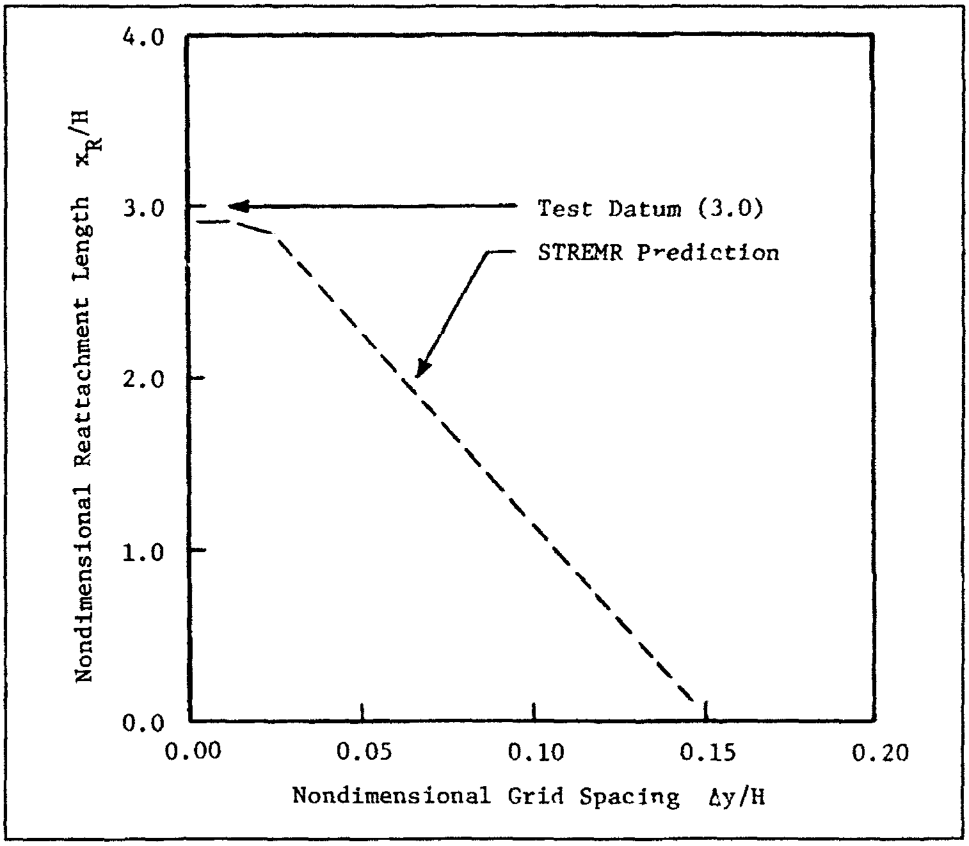

Figure 53. Effect of vertical grid spacing Δ along hillside on predicted flow reattachment for 2-D hill

the friction coefficient falls as the velocity near the lower boundary falls, reaching a minimum at the leading edge of the hill. It then climbs until it reaches a peak halfway up the hill, from which it falls until the point of flow separation ($C_f = 0$) at $x = 2.077$ meters.

Parameter Variation for 2-D Hill

At worst, the predicted values for C_f are in error by a factor of two. Reduction of TURBIN from 0.003 (default) to 0.001 in namelist BEGIN reduces the peak value of C_f by 20 percent, and it increases x_R/H by 10 percent. Reduction of $\Delta y/H$ from 0.024 to 0.0024 reduces the peak C_f by a factor of two, flattens the curve for C_f near the entrance, and increases x_R/H by less than 1 percent. Further reduction of $\Delta y/H$ flattens the predicted curve for C_f in general, and agreement with the measured C_f deteriorates thereafter. Apparently the empirical procedure for calculating turbulent shear stress is *not* applicable very close to the wall (i.e., inside a boundary layer). Fortunately, however, the predictions for x_R/H are not affected by the deterioration of C_f.

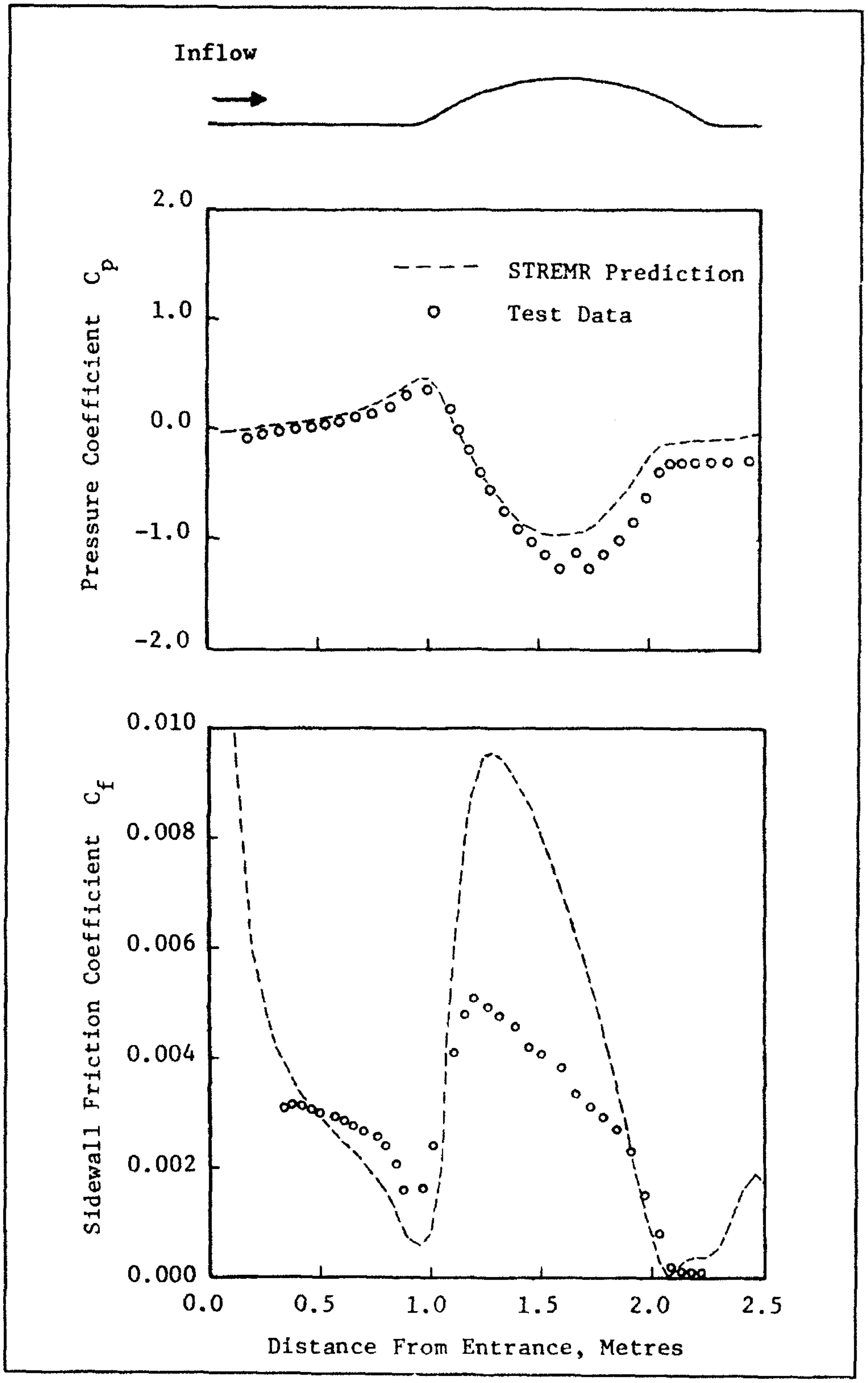

Figure 54. Comparison of STREMR 2-D hill predictions (ultrafine 83 × 25 grid) with test data for friction and pressure coefficients along hillside

Agreement between the measured and predicted values of C_p is fairly good, except that the predicted minimum is off by about 20 percent. Neither refinement of the grid nor adjustment of the empirical STREMR parameters has any significant effect on this discrepancy.

All the STREMR predictions for the 2-D hill (Figures 49-54) were made with RECAP = 2.5. With this (default) value, the ultrafine grid (Figure 52) yields x_R/H = 2.82, which is 6 percent less than the observed value. With RECAP = 2.0, the same grid gives x_R/H = 2.51 (16 percent low); and with RECAP = 1.5, it gives x_R/H = 2.21 (26 percent low). Assuming that these results include a 20 percent underprediction from the combined effects of grid error and uncertainty in TURBIN, it appears (once again) that the proper (grid-independent) value for RECAP lies between 1.5 to 2.0.

Example 5A: Curvilinear 40 X 34 Grid with 2-D Circular Cylinder

Figure 55 shows a curvilinear 40 X 34 grid as it appears in the Cartesian (x,y) and computational (i,j) planes. This grid represents a 2-D channel, 10 ft long and 6 ft wide in plan view, which contains a 2-ft-diameter cylinder centered 3 ft from the west (inflow) boundary. The cylinder is circular in the Cartesian plane, but it is square in the computational plane, with 10 grid spaces on each of its four sides. There is no bottom friction, and the depth is arbitrary normal to the plane of flow.

Figure 56 shows the STREMR input for the 40 X 34 grid. Since this flow configuration should develop an unsteady wake (vortex street), the input sets TIMER = 'NO' and specifies a fixed time-step DTIME = 0.02. The fixed time-step allows direct comparison of time-dependent results for this grid with those for other grids.

Figure 57 shows the 40 X 34 grid and the computed flow after 2500 time-steps (50 seconds). Although the flow does separate on the lee side of the cylinder, this occurs too far aft for vortex shedding to occur, and the predicted wake is only slightly unsteady and slightly asymmetric. In this case, the grid is too coarse to predict even the approximate location of the separation points, and the resulting flow is qualitatively incorrect. Refinement of the grid, however, changes the predictions considerably.

Example 5B: Curvilinear 80 X 60 Grid with 2-D Circular Cylinder

Figure 58 shows the STREMR input for the same channel (Example 5A) with an 80 X 60 grid. As before, the cylinder is circular in the Cartesian plane, but it is now divided into 20 grid spaces per side in the computational

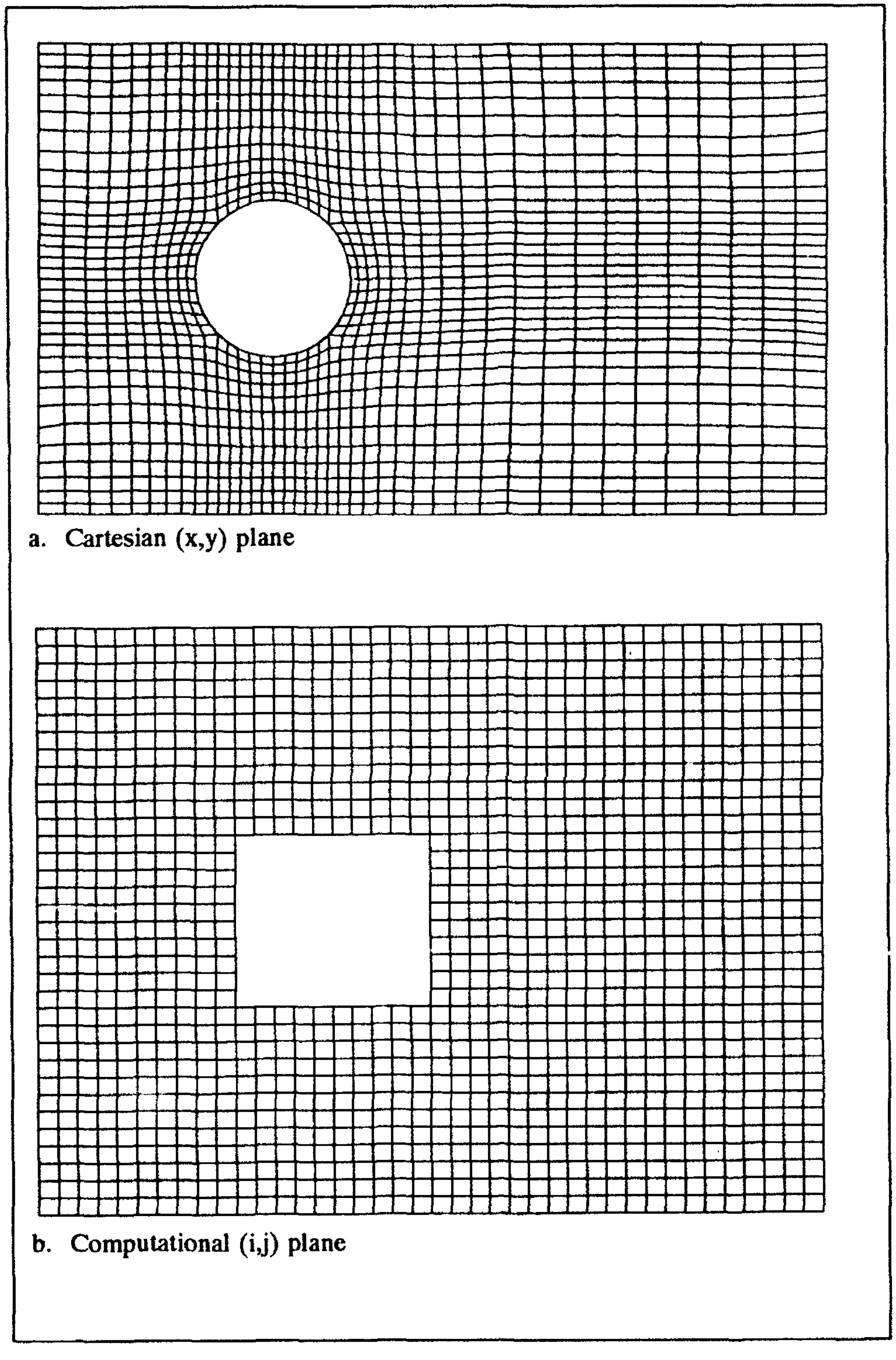

a. Cartesian (x,y) plane

b. Computational (i,j) plane

Figure 55. Curvilinear 40 × 34 grid with 2-D circular cylinder

```
&BEGIN  START='COLD'      , IREF=1  ,
         FLOW='INFLOW'    , JREF=17 ,
       IUNITS='ENGLISH'   ,
       TITLE='EXAMPLE 5A: 40 X 34 GRID WITH CYLINDER' &END
&PARAM PUNITS='ENGLISH' , NSTEPS=2500 , DTIME=0.02 ,
       ALLOUT='YES'     , NSTORE=2500 ,
         MAPS='YES'     , NSTOMO=1    ,
        TIMER='NO'      , INFORM=10   ,
                           ITERS=3    &END
&INPUT ITEM='CELL TYPES'                        &END
&INPUT ITEM='FLUX' , I1=1 , I2=1 , J1=1 , J2=34 &END
&INPUT ITEM='OPEN' , I1=40, I2=40, J1=1 , J2=34 &END
&INPUT ITEM='END'                               &END
&INPUT ITEM='GENERAL'                 &END
&INPUT ITEM='X-VELOCITY' , VALUES=1.0 &END
&INPUT ITEM='END'                     &END
&INPUT ITEM='SECTION' &END
&INPUT ITEM='END'     &END
&INPUT ITEM='LINE' &END
&INPUT ITEM='END'  &END
&INPUT ITEM='RANDOM' &END
&INPUT ITEM='END'    &END
```

Figure 56. STREMR input for curvilinear 40 × 34 grid with 2-D circular cylinder (no bottom friction, Example 5A)

plane. Figure 59 shows the 80 X 60 grid and the predicted flow after 2500 time-steps (50 seconds).

The computed flow shown in Figure 59 is radically different from that in Figure 57. With the 80 X 60 grid, separation occurs much further forward than with the 40 X 34 grid. This allows an unsteady wake to develop spontaneously behind the cylinder, with vortices being shed from opposite sides of the cylinder at regular time-intervals. Further refinement of the grid has little effect on the gross features of the vortex street.

Example 5C: Curvilinear 120 X 90 Grid with 2-D Circular Cylinder

Figure 60 shows the STREMR input for the same channel (Examples 5A and 5B) with a 120 X 90 grid. As before, the cylinder is circular in the Cartesian plane, but it is now divided into 30 grid spaces per side in the computational plane. Figure 61 shows the 120 X 90 grid and the predicted flow after 2500 time-steps (50 seconds).

There is little difference between the streamlines in Figure 59 and those in Figure 61. The two wakes are slightly out of phase with each other, but this is

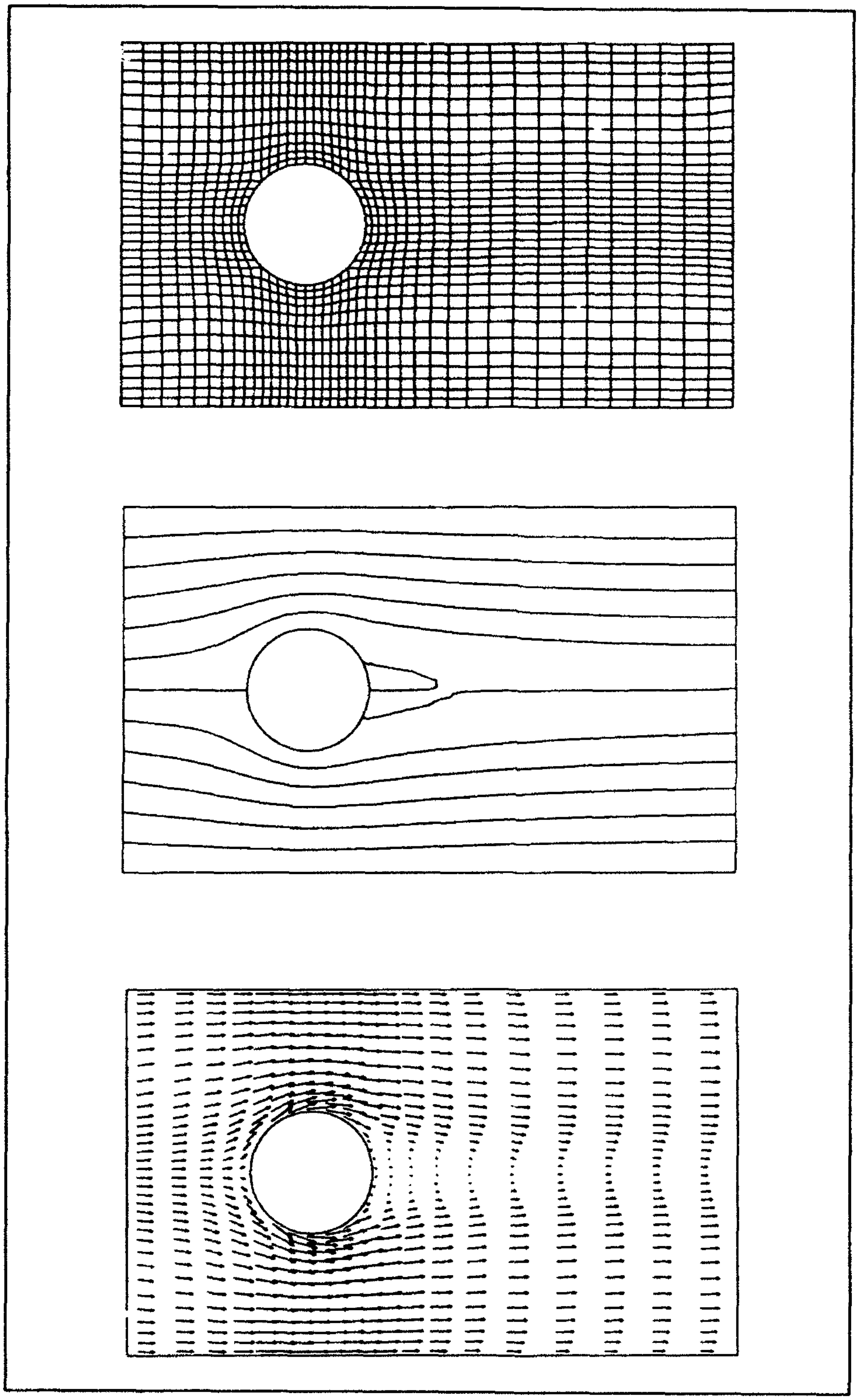

Figure 57. Curvilinear 40 × 34 grid with computed streamlines and velocity vectors for 2-D circular cylinder (Example 5A, time-step 2500)

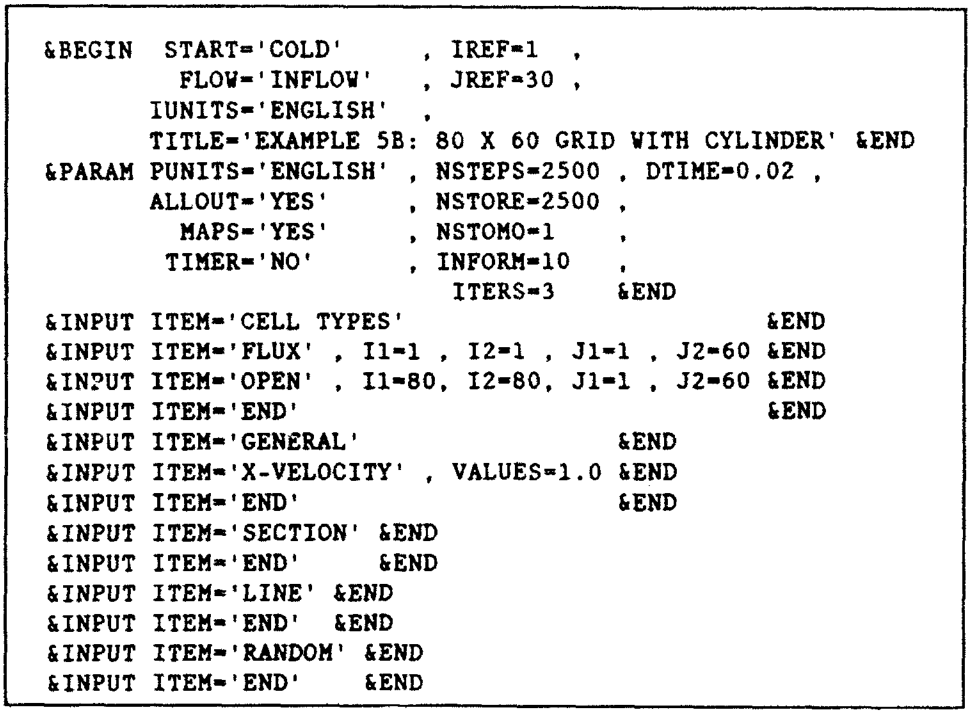

```
&BEGIN  START='COLD'      , IREF=1  ,
          FLOW='INFLOW'   , JREF=30 ,
       IUNITS='ENGLISH'   ,
       TITLE='EXAMPLE 5B: 80 X 60 GRID WITH CYLINDER' &END
&PARAM PUNITS='ENGLISH'  , NSTEPS=2500 , DTIME=0.02 ,
       ALLOUT='YES'      , NSTORE=2500 ,
         MAPS='YES'      , NSTOMO=1    ,
        TIMER='NO'       , INFORM=10   ,
                            ITERS=3    &END
&INPUT ITEM='CELL TYPES'                        &END
&INPUT ITEM='FLUX' , I1=1 , I2=1 , J1=1 , J2=60 &END
&INPUT ITEM='OPEN' , I1=80, I2=80, J1=1 , J2=60 &END
&INPUT ITEM='END'                               &END
&INPUT ITEM='GENERAL'                 &END
&INPUT ITEM='X-VELOCITY' , VALUES=1.0 &END
&INPUT ITEM='END'                     &END
&INPUT ITEM='SECTION' &END
&INPUT ITEM='END'     &END
&INPUT ITEM='LINE' &END
&INPUT ITEM='END'  &END
&INPUT ITEM='RANDOM' &END
&INPUT ITEM='END'    &END
```

Figure 58. STREMR input for curvilinear 80 × 60 grid with 2-D circular cylinder (no bottom friction, Example 5B)

not surprising in view of the large number of elapsed time-steps. As far as simulating the gross flow behavior is concerned, there is little reason to use the 120 X 90 grid instead of the 80 X 60 grid. Both grids yield essentially the same information downstream of the cylinder.

Physical Specifications for Double Bendway

The final set of examples concerns an S-shaped flume called the Channel Bend Facility, which has been investigated in experiments conducted by Maynord.[1] This channel has a trapezoidal cross section and consists of two 100-deg bends with a reversal in curvature. The pertinent linear dimensions are given in *feet* in the Figure 62, which shows the wetted cross section and the water surface (as represented by a 121 X 24 grid). Computed results for this channel demonstrate the influence of grid refinement *and* slope discretization on the STREMR velocity predictions.

Figure 63 shows the actual side slope along with its stair-stepped discretization for each of three different grids. The discrete depth for each grid cell is

[1] Unpublished test data and channel specifications provided by S. T. Maynord, Research Hydraulic Engineer, August 1987, US Army Engineer Waterways Experiment Station, Vicksburg, MS.

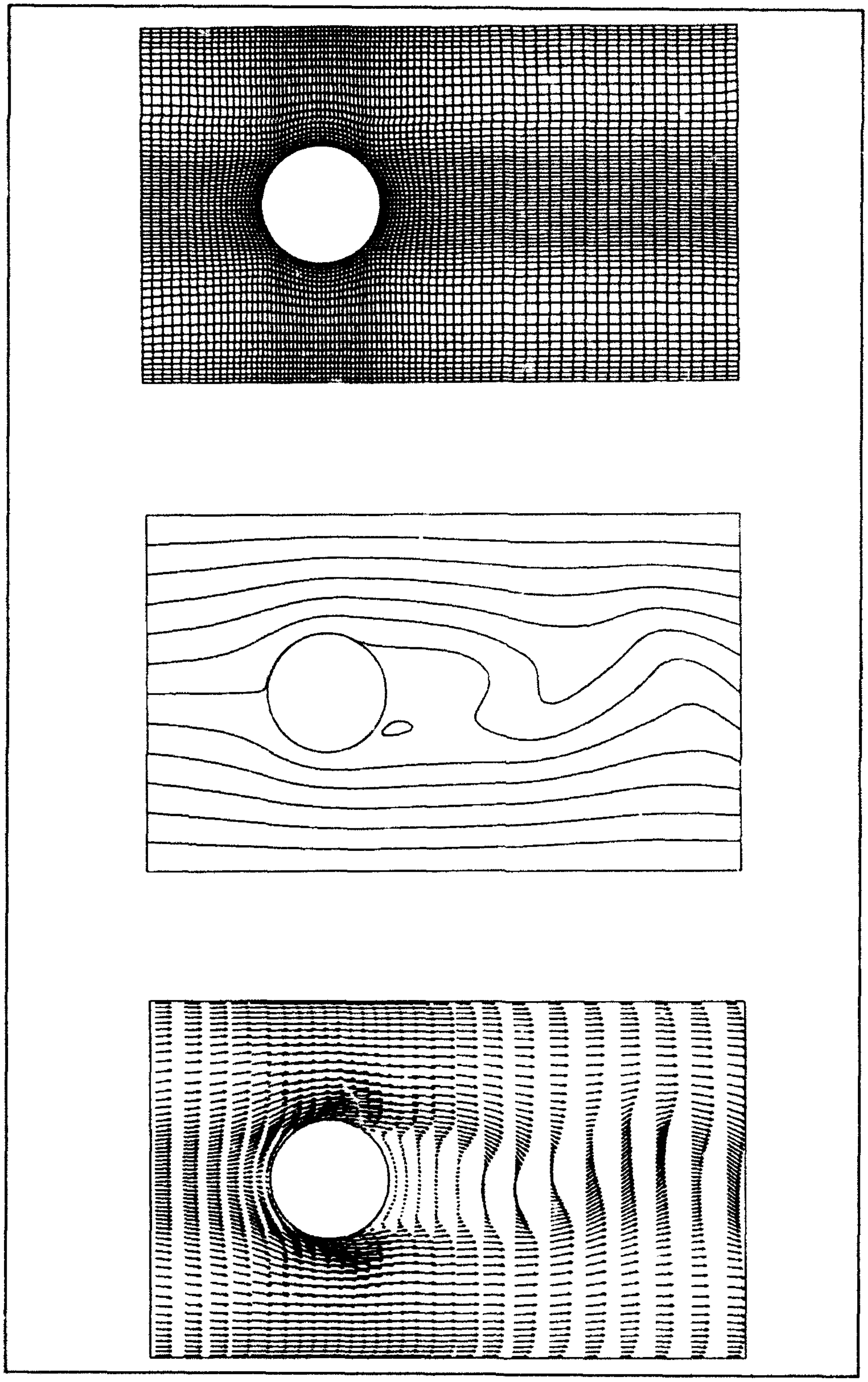

Figure 59. Curvilinear 80 × 60 grid with computed streamlines and velocity vectors for 2-D circular cylinder (Example 5B, unsteady, time-step 2500)

```
&BEGIN  START='COLD'      , IREF=1  ,
         FLOW='INFLOW'    , JREF=45 ,
       IUNITS='ENGLISH'   ,
       TITLE='EXAMPLE 5C: 120 X 90 GRID WITH CYLINDER' &END
&PARAM PUNITS='ENGLISH' , NSTEPS=2500 , DTIME=0.02 ,
       ALLOUT='YES'     , NSTORE=2500 ,
         MAPS='YES'     , NSTOMO=1    ,
        TIMER='NO'      , INFORM=10   ,
                           ITERS=3    &END
&INPUT ITEM='CELL TYPES'                           &END
&INPUT ITEM='FLUX' , I1=1   , I2=1   , J1=1 , J2=90 &END
&INPUT ITEM='OPEN' , I1=120, I2=120, J1=1 , J2=90 &END
&INPUT ITEM='END'                                  &END
&INPUT ITEM='GENERAL'                 &END
&INPUT ITEM='X-VELOCITY' , VALUES=1.0 &END
&INPUT ITEM='END'                     &END
&INPUT ITEM='SECTION' &END
&INPUT ITEM='END'     &END
&INPUT ITEM='LINE' &END
&INPUT ITEM='END'  &END
&INPUT ITEM='RANDOM' &END
&INPUT ITEM='END'    &END
```

Figure 60. STREMR input for curvilinear 120 × 90 grid with 2-D circular cylinder (no bottom friction, Example 5C)

the true depth measured at the center of the cell. The Manning coefficient is uniformly 0.02, which gives a bottom friction coefficient of 0.00754 at the maximum channel depth of 0.455 ft.

The actual flowrate in the experiments was 6.75 cfs, but the STREMR calculations impose a flowrate of 3.55 cfs. This does *not* change the physics of the flow as far as STREMR is concerned, but it does make the average velocity unity for any cross section. The computed velocities then represent *normalized* velocities (depth-averaged velocity divided by section-averaged velocity) which are convenient for comparison with Maynord's test data. This particular normalization suppresses errors in the average velocity magnitude, but it spotlights errors in the local velocity distribution.

Example 6A: Curvilinear 121 X 14 Grid with Double Bendway

Figure 64 displays the STREMR input for a curvilinear 121 X 14 grid, which is shown with the predicted streamlines and velocity vectors in Figure 65. On the side slopes of the channel, the grid has a uniform lateral spacing of 0.4 ft. Beyond the toe of the slope, however, this spacing gradually increases with distance from the toe.

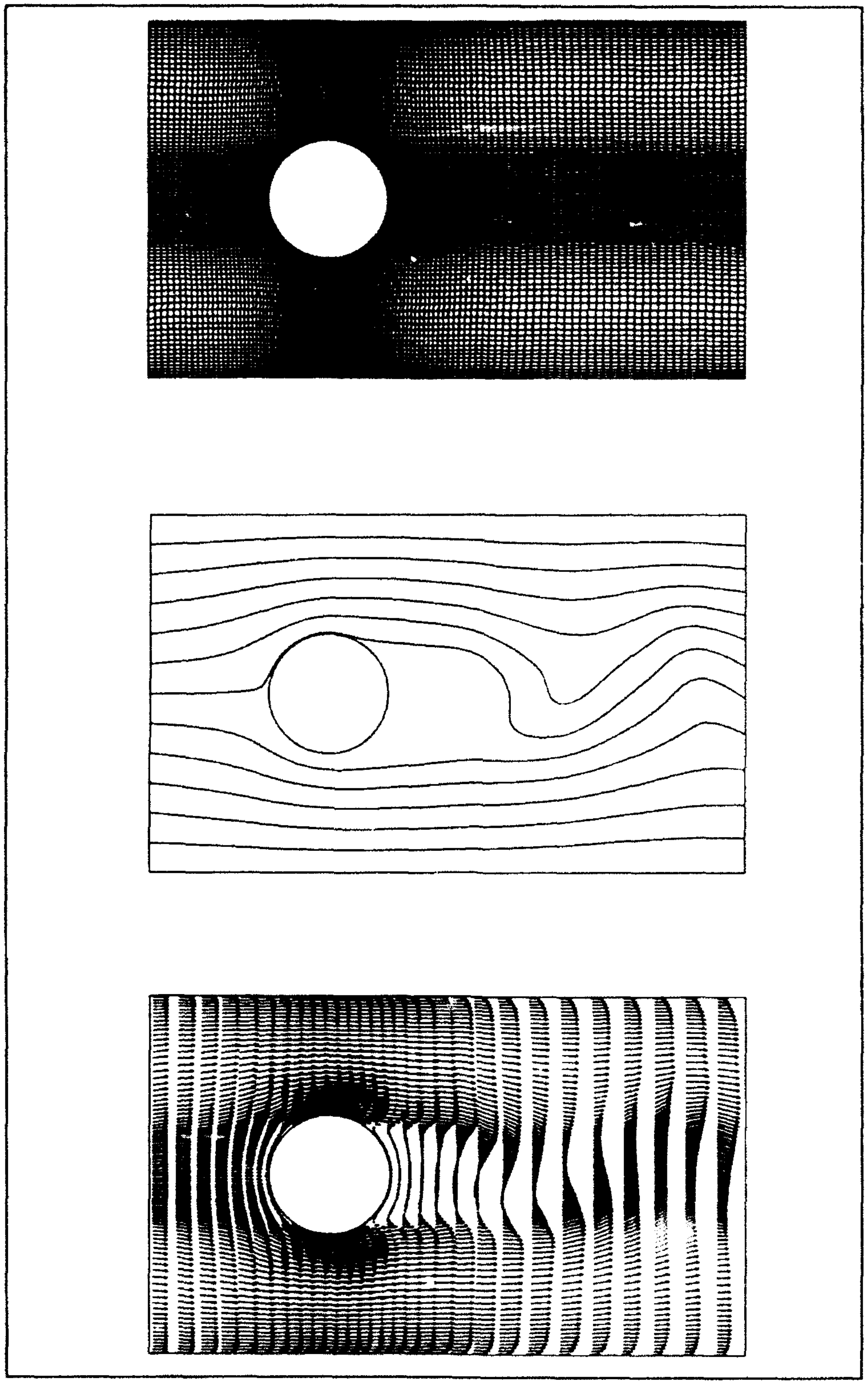

Figure 61. Curvilinear 120 × 90 grid with computed streamlines and velocity vectors for 2-D circular cylinder (Example 5C, unsteady, time-step 2500)

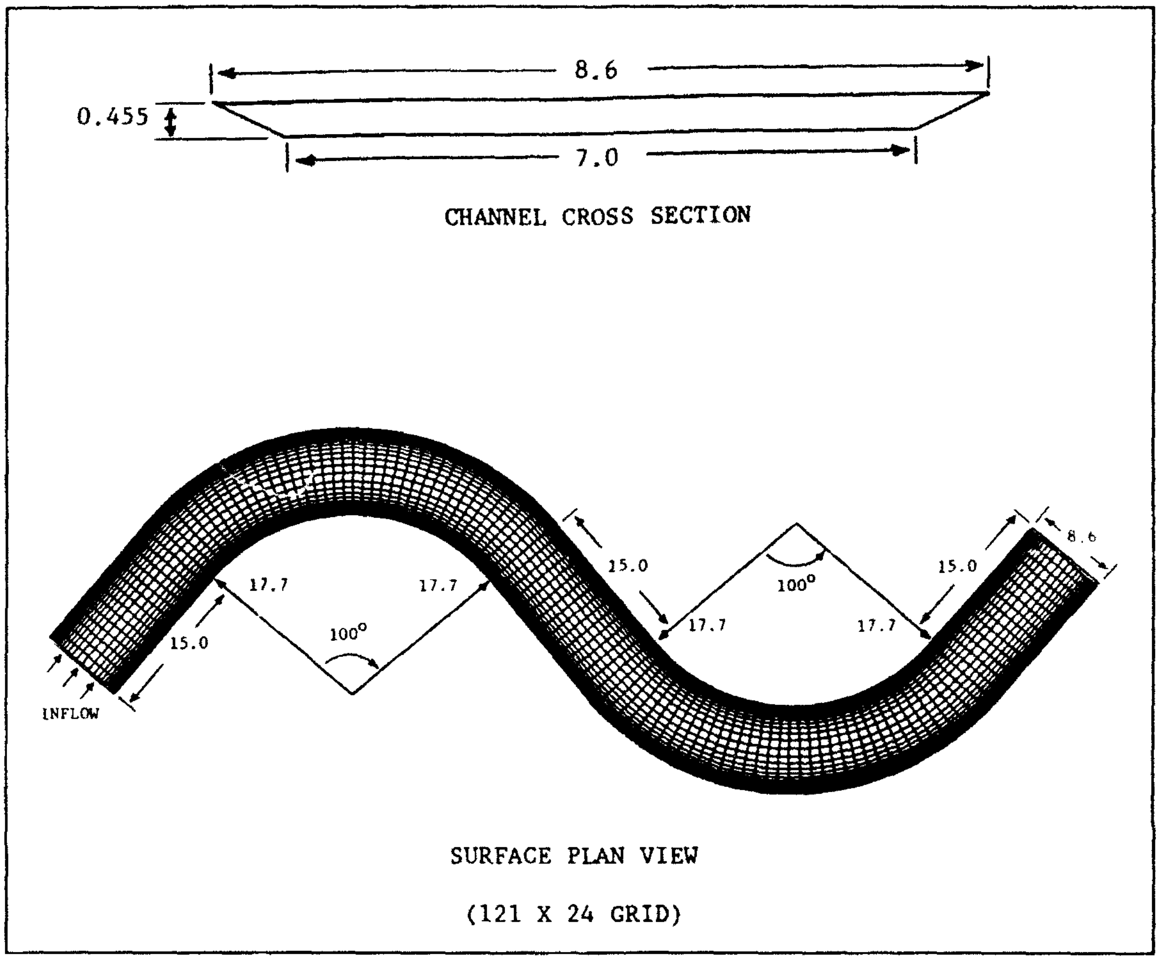

Figure 62. Channel cross section and grid (water surface) plan view for double bendway (Examples 6A-6C)

The streamlines indicate very little about the flow development, but the velocity vectors make it easy to trace the gradual migration of high velocity toward the outside of each bend. This behavior is typical for natural and artificial channels in which the ratio of depth to radius of curvature is small.

Example 6B: Curvilinear 121 X 24 Grid with Double Bendway

Figure 66 displays the STREMR input for a curvilinear 121 X 24 grid, which is shown with predicted streamlines and velocity vectors in Figure 67. On the side slopes of the channel, the grid has a uniform lateral spacing of 0.2 ft. Beyond the toe of the slope, this spacing gradually increases with distance from the toe.

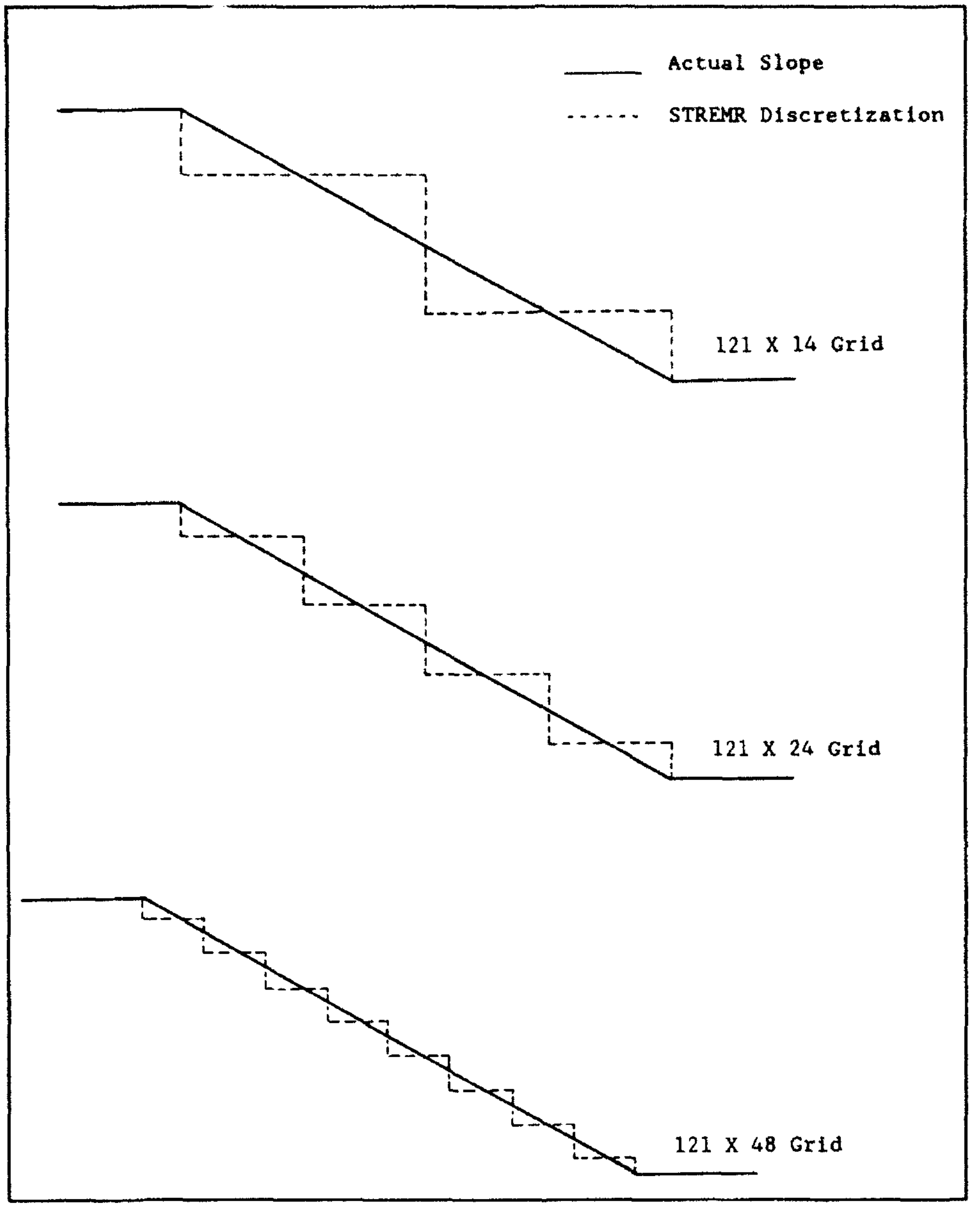

Figure 63. STREMR discretization of channel side slope for double bendway with successively refined grids (Examples 6A-6C)

Like those for Example 6A, the streamlines in Figure 67 indicate very little about the flow development, but the velocity vectors again make it easy to trace the gradual migration of high velocity toward the outside of each bend. Except for a greater density of plotted vectors in Figure 67, it is difficult to discern any difference in results obtained with the 121 X 14 grid and the 121 X 24 grid.

```
&BEGIN  START='COLD'      , IREF=1 ,
          FLOW='FLOWRATE' , JREF=7 ,
        IUNITS='ENGLISH'  ,
         TITLE='EXAMPLE 6A: 121 X 14 GRID WITH DOUBLE BENDWAY' &END
&PARAM PUNITS='ENGLISH' , NSTEPS=2500,
       ALLOUT='YES'     , NSTORE=2500,
         MAPS='YES'     , NSTOMO=1   ,
        TIMER='YES'     , INFORM=10  ,
                           ITERS=3   &END
&INPUT ITEM='CELL TYPES'                          &END
&INPUT ITEM='FLUX' , I1=1  , I2=1  , J1=1, J2=14  &END
&INPUT ITEM='OPEN' , I1=121, I2=121, J1=1, J2=14  &END
&INPUT ITEM='END'                                 &END
&INPUT ITEM='GENERAL'                    &END
&INPUT ITEM='FLOWRATE'   , VALUES=3.55   &END
&INPUT ITEM='DEPTH'      , VALUES=0.455  &END
&INPUT ITEM='MANNING'    , VALUES=0.020  &END
&INPUT ITEM='I-VELOCITY' , VALUES=1.0    &END
&INPUT ITEM='END'                        &END
&INPUT ITEM='SECTION'                                                 &END
&INPUT ITEM='DEPTH' , I1=1, I2=121, J1=3, J2=12, VALUES=1210*0.455    &END
&INPUT ITEM='END'                                                     &END
&INPUT ITEM='LINE'                                                        &END
&INPUT ITEM='DEPTH' , I1=1  , I2=121, J1=1 , J2=1 , VALUES=0.114,0.114    &END
&INPUT ITEM='DEPTH' , I1=1  , I2=121, J1=14, J2=14, VALUES=0.114,0.114    &END
&INPUT ITEM='DEPTH' , I1=1  , I2=1  , J1=1 , J2=2 , VALUES=0.114,0.341    &END
&INPUT ITEM='DEPTH' , I1=121, I2=121, J1=1 , J2=2 , VALUES=0.114,0.341    &END
&INPUT ITEM='DEPTH' , I1=1  , I2=1  , J1=13, J2=14, VALUES=0.341,0.114    &END
&INPUT ITEM='DEPTH' , I1=121, I2=121, J1=13, J2=14, VALUES=0.341,0.114    &END
&INPUT ITEM='END'                                                         &END
&INPUT ITEM='RANDOM' &END
&INPUT ITEM='END'    &END
```

Figure 64. STREMR input for curvilinear 121 × 14 grid with double bendway (bottom friction included, Example 6A)

Example 6C: Curvilinear 121 X 48 Grid with Double Bendway

Figure 68 displays the STREMR input for a curvilinear 121 X 48 grid, which is shown with predicted streamlines and velocity vectors in Figure 69. On the side slopes of the channel, the grid has a uniform lateral spacing of 0.1 ft. Beyond the toe of the slope, this spacing gradually increases with distance from the toe.

Like those for Examples 6A and 6B, the streamlines in Figure 69 indicate very little about the flow development, but the velocity vectors still make it easy to trace the gradual migration of high velocity toward the outside of each bend. Except for an even greater density of plotted vectors in Figure 69, it is difficult to discern any difference in results obtained with the 121 X 14 grid, the 121 X 24 grid, and the 121 X 48 grid.

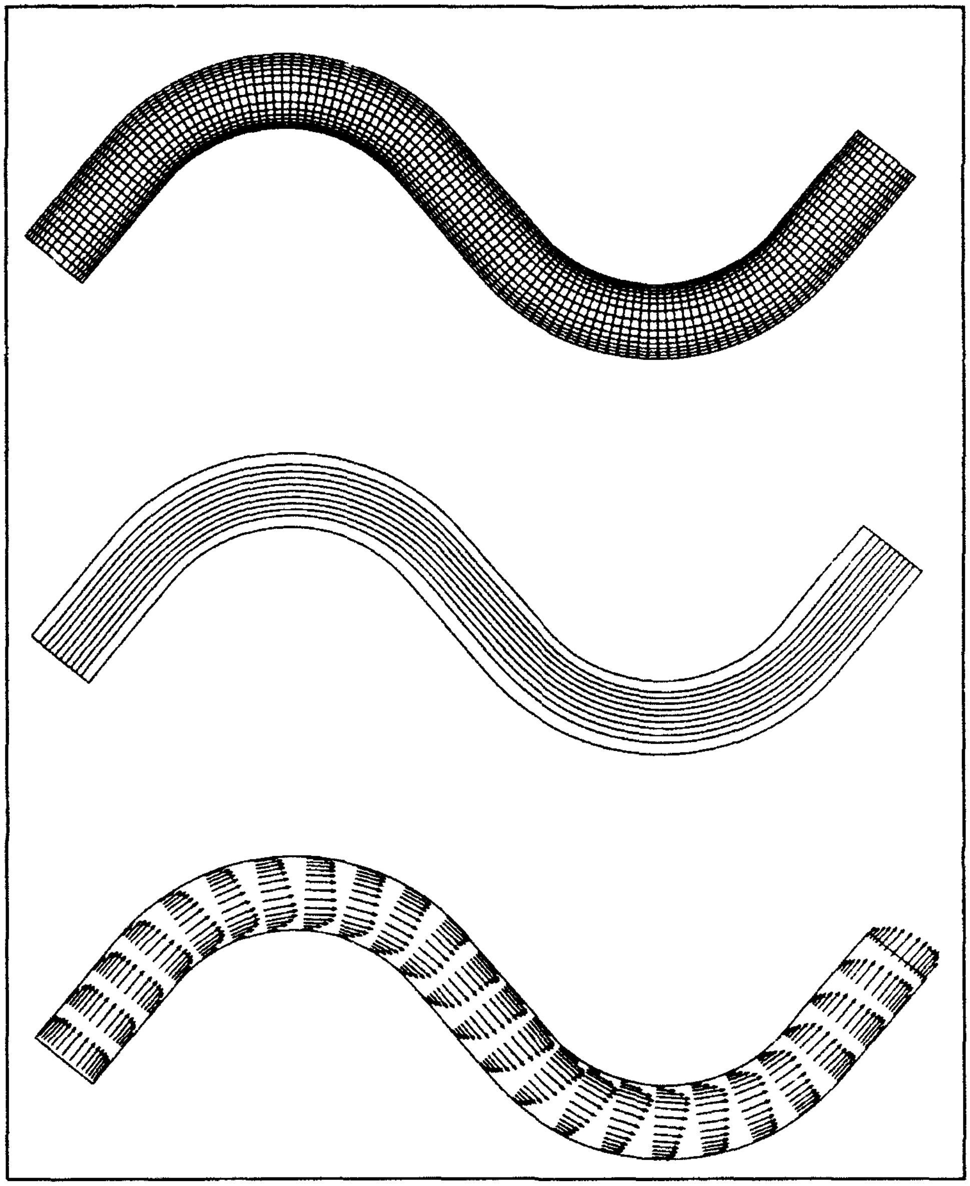

Figure 65. Curvilinear 121 × 14 grid with computed streamlines and velocity vectors for double bendway (Example 6A)

Comparison with Test Data for Double Bendway

Figures 70-73 compare normalized STREMR velocity predictions with normalized test data at four different stations in the channel. Each figure includes a plan view of the channel with an arrow showing the position and orientation of the observer. Normalized lateral position is the distance from the water's edge (indicated by the arrow), divided by the width of the water surface. The predictions reproduce the observed distributions within 7 percent for Stations 2-4 (Figures 71-73). Errors of 15 percent are evident for Station 1, however, near the toe of the inner slope (Figure 70).

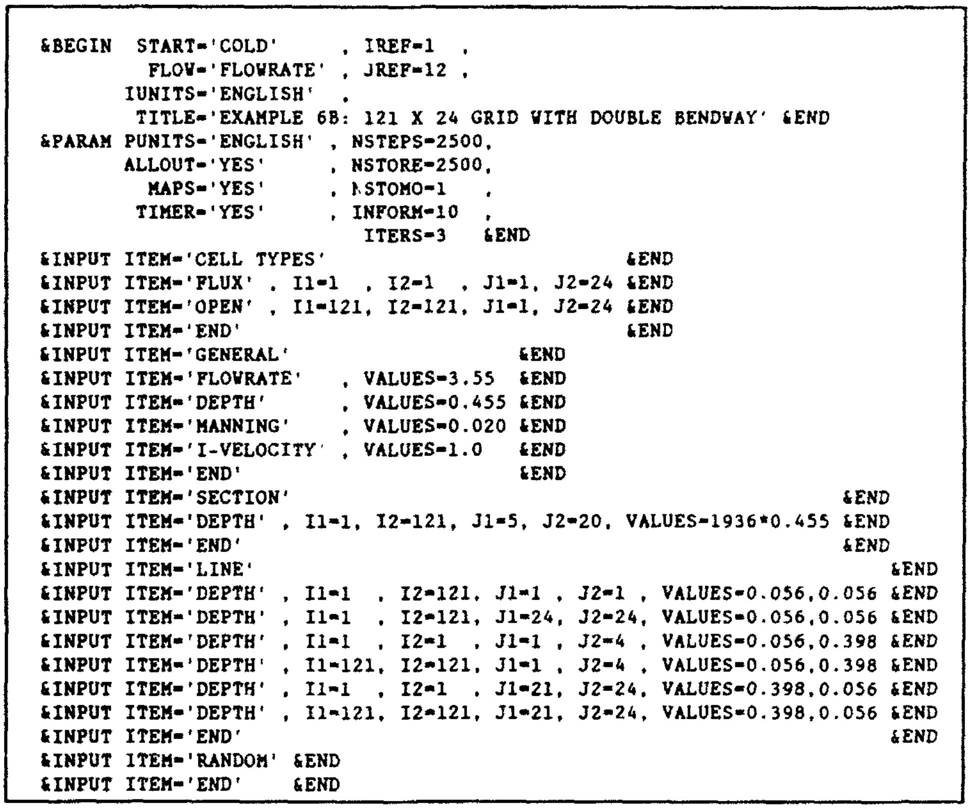

```
&BEGIN  START='COLD'      , IREF=1  ,
         FLOW='FLOWRATE' , JREF=12 ,
       IUNITS='ENGLISH'  ,
        TITLE='EXAMPLE 6B: 121 X 24 GRID WITH DOUBLE BENDWAY' &END
&PARAM PUNITS='ENGLISH' , NSTEPS=2500,
       ALLOUT='YES'     , NSTORE=2500,
         MAPS='YES'     , NSTOMO=1   ,
        TIMER='YES'     , INFORM=10  ,
                           ITERS=3   &END
&INPUT ITEM='CELL TYPES'                            &END
&INPUT ITEM='FLUX' , I1=1  , I2=1  , J1=1, J2=24 &END
&INPUT ITEM='OPEN' , I1=121, I2=121, J1=1, J2=24 &END
&INPUT ITEM='END'                                   &END
&INPUT ITEM='GENERAL'                    &END
&INPUT ITEM='FLOWRATE'   , VALUES=3.55  &END
&INPUT ITEM='DEPTH'      , VALUES=0.455 &END
&INPUT ITEM='MANNING'    , VALUES=0.020 &END
&INPUT ITEM='I-VELOCITY' , VALUES=1.0   &END
&INPUT ITEM='END'                        &END
&INPUT ITEM='SECTION'                                                  &END
&INPUT ITEM='DEPTH' , I1=1, I2=121, J1=5, J2=20, VALUES=1936*0.455 &END
&INPUT ITEM='END'                                                      &END
&INPUT ITEM='LINE'                                                          &END
&INPUT ITEM='DEPTH' , I1=1  , I2=121, J1=1 , J2=1 , VALUES=0.056,0.056 &END
&INPUT ITEM='DEPTH' , I1=1  , I2=121, J1=24, J2=24, VALUES=0.056,0.056 &END
&INPUT ITEM='DEPTH' , I1=1  , I2=1  , J1=1 , J2=4 , VALUES=0.056,0.398 &END
&INPUT ITEM='DEPTH' , I1=121, I2=121, J1=1 , J2=4 , VALUES=0.056,0.398 &END
&INPUT ITEM='DEPTH' , I1=1  , I2=1  , J1=21, J2=24, VALUES=0.398,0.056 &END
&INPUT ITEM='DEPTH' , I1=121, I2=121, J1=21, J2=24, VALUES=0.398,0.056 &END
&INPUT ITEM='END'                                                           &END
&INPUT ITEM='RANDOM' &END
&INPUT ITEM='END'    &END
```

Figure 66. STREMR input for curvilinear 121 × 24 grid with double bendway (bottom friction included, Example 6B)

It is puzzling that the worst errors occur in the short straight reach upstream of the first bend. Moreover, they occur on or near the side slopes, and they seem not to be related to channel curvature. Errors of the same kind and magnitude are typical even for long straight reaches with sloped sides (Bernard and Schneider 1992). They may come from the relatively simple approximation used for bottom friction (Appendix A), which depends on depth but not slope.

From a practical standpoint, grid refinement has little effect on the predictions shown in Figures 70-73. Computed results for the 121 X 24 grid and the 121 X 48 grid are almost indistinguishable. These two grids resolve the maximum velocity better than the 121 X 14 grid, but the slight improvement hardly justifies the additional computer time needed for the STREMR calculations with the finer grids.

This points up another reason for trying different grids at the beginning of a modeling effort. The grid should be no finer than is actually needed for the application at hand. Over-refinement of the grid may yield no useful information, but it always increases the execution time for STREMR.

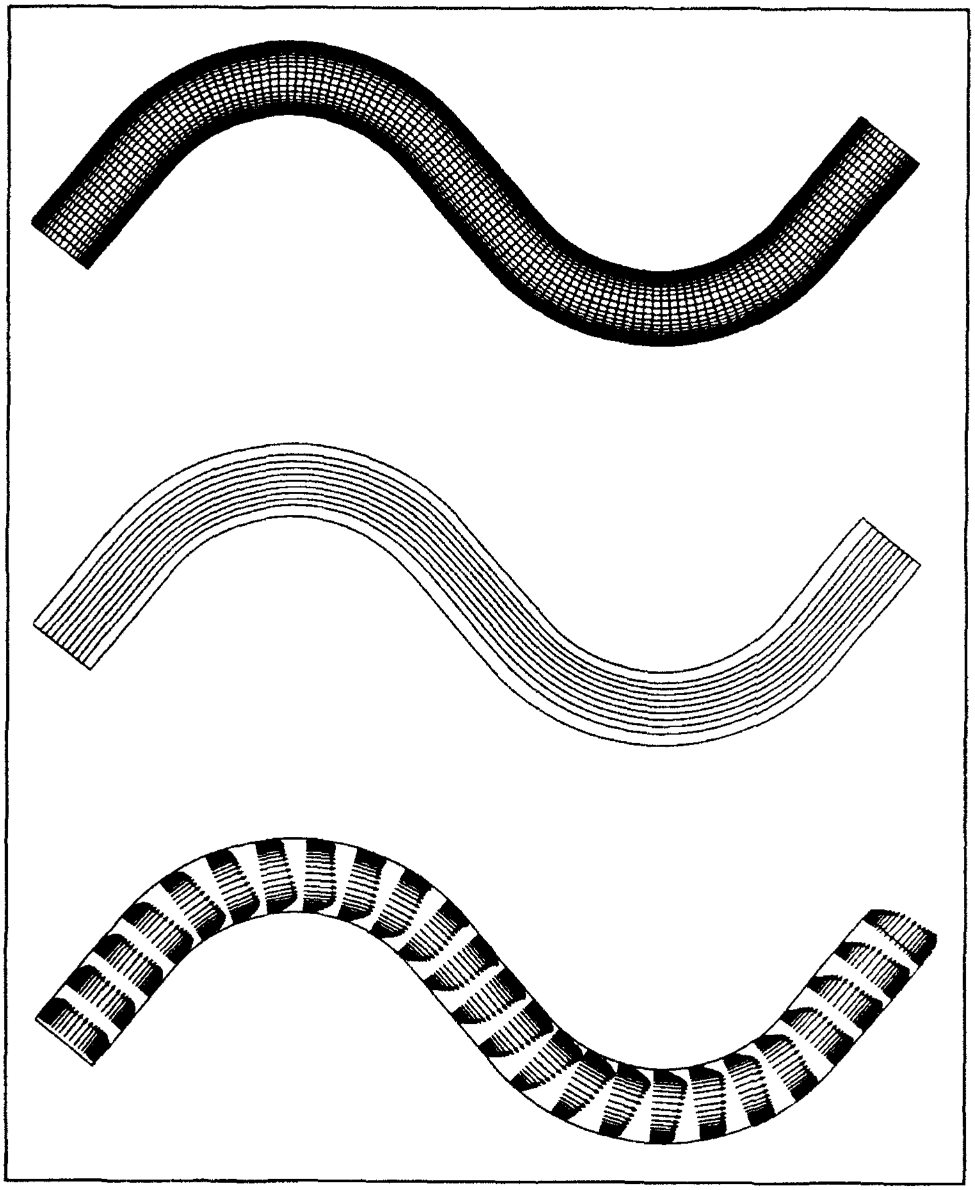

Figure 67. Curvilinear 121 x 24 grid with computed streamlines and velocity vectors for double bendway (Example 6B)

```
&BEGIN  START='COLD'     , IREF=1  ,
          FLOW='FLOWRATE' , JREF=24 ,
       IUNITS='ENGLISH'   ,
        TITLE='EXAMPLE 6C: 121 X 48 GRID WITH DOUBLE BENDWAY' &END
&PARAM PUNITS='ENGLISH' , NSTEPS=2500,
       ALLOUT='YES'     , NSTORE=2500,
         MAPS='YES'     , NSTOMO=1   ,
        TIMER='YES'     , INFORM=10  ,
                          ITERS=3   &END
&INPUT ITEM='CELL TYPES'                          &END
&INPUT ITEM='FLUX' , I1=1  , I2=1  , J1=1, J2=48 &END
&INPUT ITEM='OPEN' , I1=121, I2=121, J1=1, J2=48 &END
&INPUT ITEM='END'                                 &END
&INPUT ITEM='GENERAL'                    &END
&INPUT ITEM='FLOWRATE'   , VALUES=3.55  &END
&INPUT ITEM='DEPTH'      , VALUES=0.455 &END
&INPUT ITEM='MANNING'    , VALUES=0.020 &END
&INPUT ITEM='I-VELOCITY' , VALUES=1.0   &END
&INPUT ITEM='END'                        &END
&INPUT ITEM='SECTION'                                                  &END
&INPUT ITEM='DEPTH' , I1=1, I2=121, J1=9, J2=40, VALUES=3872*0.455 &END
&INPUT ITEM='END'                                                      &END
&INPUT ITEM='LINE'                                                         &END
&INPUT ITEM='DEPTH' , I1=1  , I2=121, J1=1 , J2=1 , VALUES=0.028,0.028 &END
&INPUT ITEM='DEPTH' , I1=1  , I2=121, J1=48, J2=48, VALUES=0.028,0.028 &END
&INPUT ITEM='DEPTH' , I1=1  , I2=1  , J1=1 , J2=8 , VALUES=0.028,0.426 &END
&INPUT ITEM='DEPTH' , I1=121, I2=121, J1=1 , J2=8 , VALUES=0.028,0.426 &END
&INPUT ITEM='DEPTH' , I1=1  , I2=1  , J1=41, J2=48, VALUES=0.426,0.028 &END
&INPUT ITEM='DEPTH' , I1=121, I2=121, J1=41, J2=48, VALUES=0.426,0.028 &END
&INPUT ITEM='END'                                                          &END
&INPUT ITEM='RANDOM' &END
&INPUT ITEM='END'    &END
```

Figure 68. STREMR input for curvilinear 121 × 48 grid with double bendway (bottom friction included, Example 6C)

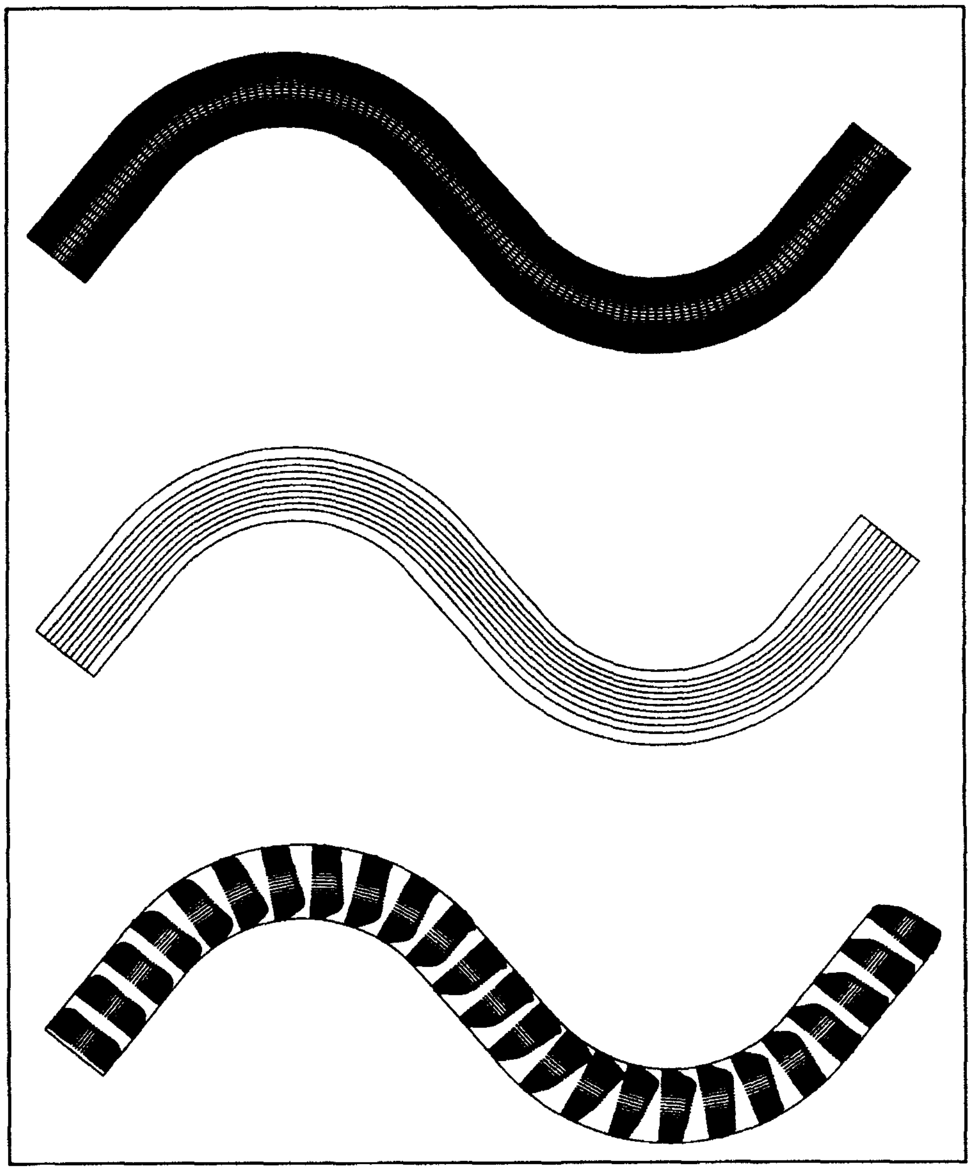

Figure 69. Curvilinear 121 × 48 grid with computed streamlines and velocity vectors for double bendway (Example 6C)

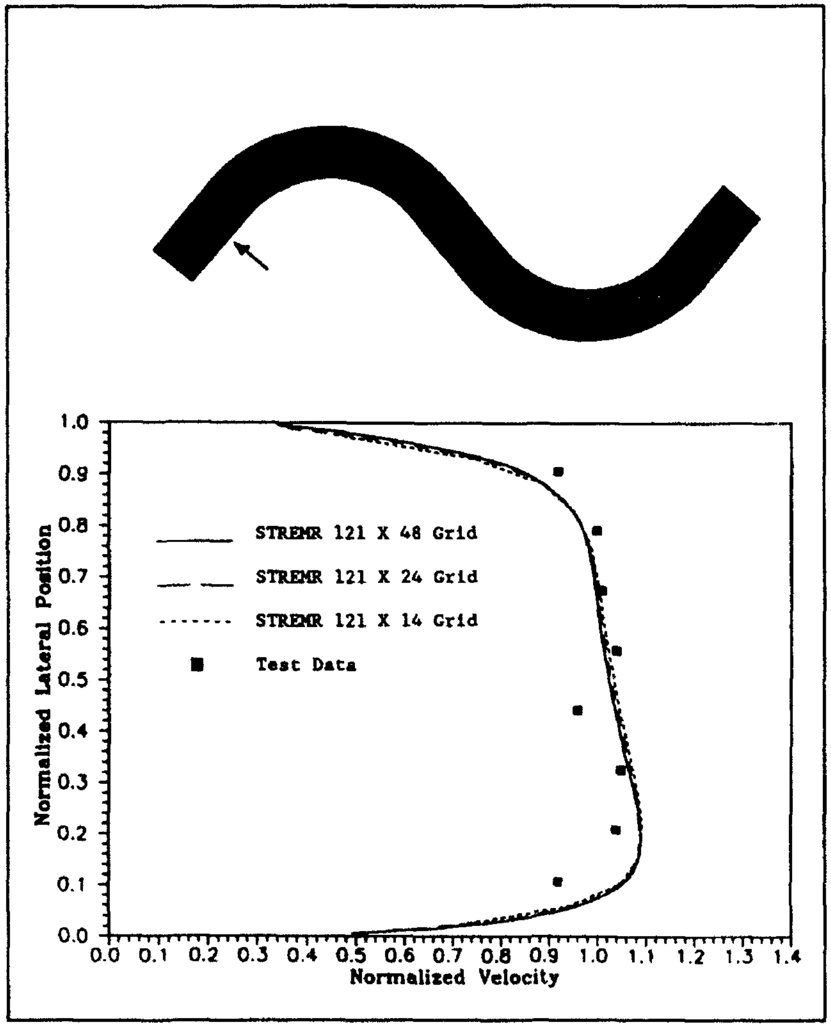

Figure 70. Comparison of STREMR predictions with test data for station 1 of double bendway (arrow shows position and orientation of observer)

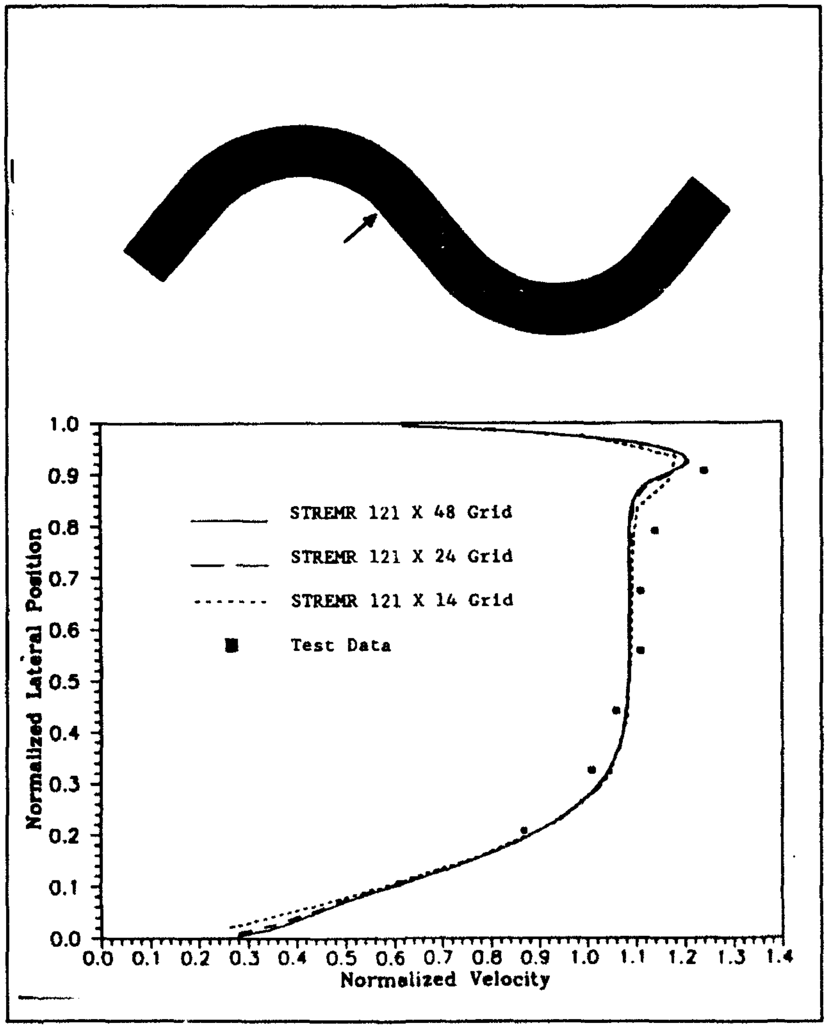

Figure 71. Comparison of STREMR predictions with test data for station 2 of double bendway (arrow shows position and orientation of observer)

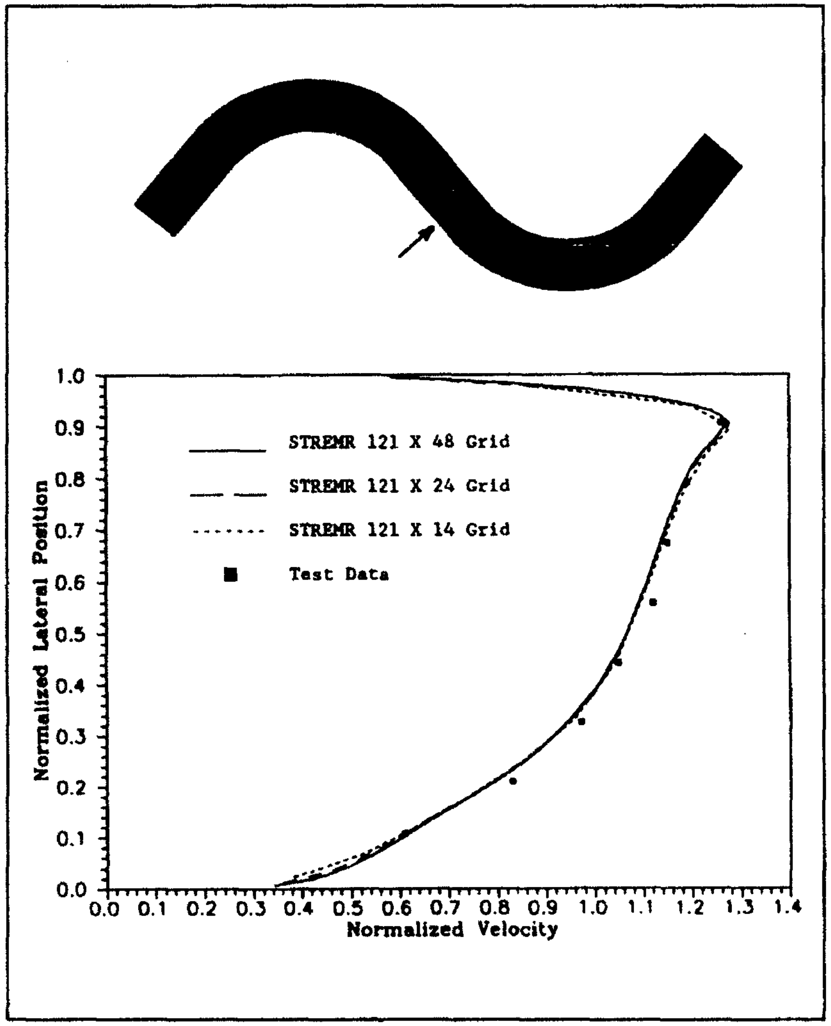

Figure 72. Comparison of STREMR predictions with test data for station 3 of double bendway (arrow shows position and orientation of observer)

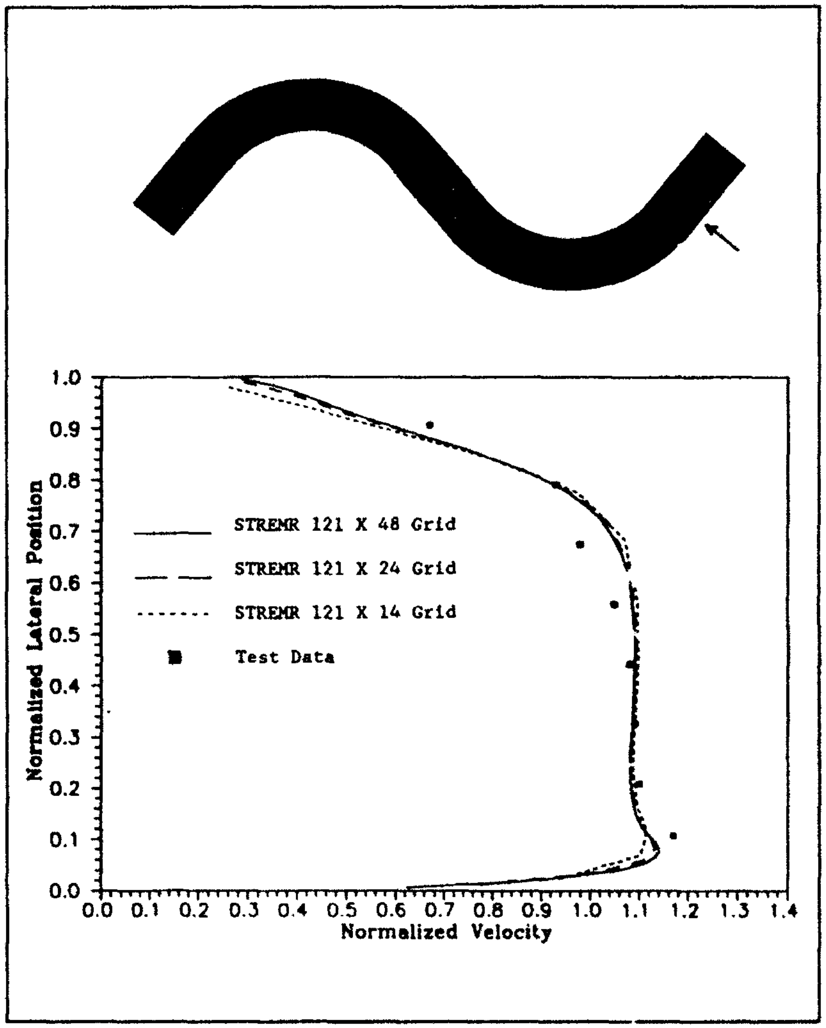

Figure 73. Comparison of STREMR predictions with test data for station 4 of double bendway (arrow shows position and orientation of observer)

6 Conclusion

The STREMR code is now ready for routine implementation by field engineers and others with an interest in depth-averaged flow modeling. It can be executed by almost anyone with access to a suitable computer, but the interpretation of its output requires some understanding of fluid mechanics. The deeper the understanding, the better the physical interpretation will be.

Concerning misinterpretation, perhaps the greatest danger is that some users may accept first-cut predictions at face value, with no attempt at grid refinement. Grid refinement may not actually be necessary, but the only way to find out is to try two or more grids for the same flow configuration.

In any case, to resolve separated (recirculating) flow, smooth boundaries require finer *local* grid spacing than do boundaries with sharp corners; but the latter may require a greater *total* number of grid cells to reproduce the full extent of the recirculation zone. Since bottom friction impedes lateral flow separation and reduces the lengths of computed eddies, however, the required number of grid cells may decrease with increasing bottom friction.

Unseparated (nonrecirculating) flow requires considerably less grid resolution than does separated flow, at least for depth-averaged calculations in which bottom friction is the most important resisting force. An exception to this would be any attempt to compute the flow in a boundary layer, which STREMR is not designed to do anyway. The STREMR procedure for computing sidewall shear stress seeks only to model (roughly) the influence of boundary layers without actually resolving them.

The k-ε turbulence model eliminates the need for guessing an eddy viscosity, and the secondary flow correction accounts for the 3-D influence of streamline curvature. Although the STREMR input includes several adjustable (empirical) parameters that influence the turbulence and secondary flow, these do *not* have to be changed for each new flow configuration or modeling effort. They are intended to be universal constants, independent of the physical setting.

In particular, the STREMR version of the k-ε turbulence model includes an adjustable parameter (RECAP) that reduces the eddy viscosity in regions of low velocity and high turbulence. This has little effect on unidirectional shear flow, but it increases the lengths of eddies created by obstacles and sidewall features. The default value (2.5) is slightly high to compensate for anticipated grid error in recirculating flow predictions made with coarse grids. With grids fine enough to achieve grid-independent predictions, however, RECAP should be given a value between 1.5 and 2.0. Setting RECAP = 1.0 imposes the *standard* k-ε model, which overpredicts eddy viscosity (and underpredicts eddy size) for recirculating flow.

The secondary flow correction enables STREMR to make credible flow predictions for curved channels with nonuniform bathymetry, and it reproduces quantitatively the observed migration of high velocity toward the outsides of channel bends. On the other hand, the Manning equation for bottom friction could stand some improvement in its prediction of the flow resistance on side slopes. Errors in excess of 15 percent are not uncommon for 30-deg slopes (with respect to the horizontal).

The technical development of STREMR is now complete. Future versions of the code may have internal improvements that speed up execution, but the input and output variables are not likely to change. The present version runs on any computer with a FORTRAN 77 compiler that supports namelist input. The required memory depends on the STREMR array dimensions IDIM and JDIM , but none of the examples in Part V exceeded two megawords. Execution times may vary from 3 milliseconds per grid cell per time-step on a 20-MHz personal computer, to 0.03 milliseconds per grid cell per time-step on a CRAY Y-MP supercomputer. Re-programming STREMR for automatic vectorization could speed up execution by another factor of 5 to 10 on the CRAY.

For applications involving large amounts of input, even the namelist format can be cumbersome. Pre-processors are now under development that will allow users to input flow parameters and bathymetry data with point-and-click operations on screen, but these will not remove the option of using namelists. Interactive pre- and post-processors will simply be components of an automated STREMR user's package. Thus, they will facilitate the manipulation of input and output, but they will not affect the STREMR code itself.

References

Anderson, D. A., Tannehill, J. C. , and Pletcher, R. H. 1984. *Computational Fluid Mechanics and Heat Transfer,* Hemisphere Publishing, McGraw-Hill, New York.

Baskaran, V., Smits, A. J., and Joubert, P. N. 1987. "A Turbulent Flow over a Curved Hill, Part 1: Growth of an Internal Boundary Layer," *Journal of Fluid Mechanics,* Vol 182, pp 47-83.

Bernard, R. S. 1986 (Sep). "Discrete Solution of the Anelastic Equations for Mesoscale Modelling," Report GKSS 86/E/51, GKSS-Forschungszentrum, Postfach 1160, 2054 Geesthacht, Germany.

__________. 1989 (Mar). "Explicit Numerical Algorithm for Modeling Incompressible Approach Flow," Technical Report REMR-HY-5, US Army Engineer Waterways Experiment Station, Vicksburg, MS.

__________. 1991 (Sep). "A Turbulence Model for Recirculating Flow," Technical Report HL-91-14, US Army Engineer Waterways Experiment Station, Vicksburg, MS.

Bernard, R. S., and Kapitza H. 1992. "How to Discretize the Pressure Gradient for Curvilinear MAC Grids," *Journal of Computational Physics,* Vol 99, No. 2, pp 288-298.

Bernard, R. S., and Schneider, M. L. 1992. "Depth-Averaged Numerical Modeling for Curved Channels," Technical Report HL-92-9, US Army Engineer Waterways Experiment Station, Vicksburg, MS.

Boussinesq, J. 1877. "Essai Sur La Theorie Des Eaux Courantes," *Mem. Presentes Acad. Sci.,* Paris, Vol 23, p 46.

Durst, F., and Tropea, C. 1981. "Turbulent, Backward-Facing Step Flows in Two-Dimensional Ducts and Channels," *Proceedings of the Third Symposium on Turbulent Shear Flows,* 9-11 September 1981, University of California, Davis, CA.

Francis, J. R., Pattanick, A., and Wearne, S. 1968 (Dec). "Observations of Flow Patterns Around Some Simplified Groyne Structures in Channels," Technical Note No. 8, *Proceedings*, Institute of Civil Engineers, London, England, pp 829-846.

Johannesson, H., and Parker, G. 1989. "Velocity Redistribution in Meandering Rivers," accepted and scheduled for publication in ASCE *Journal of Hydraulic Engineering.*

Kapitza, H. 1987 (May). "User's Guide for Conjugate-Gradient Poisson Solvers," letter report on file, prepared by Mississippi State University for the US Army Engineer Waterways Experiment Station, Vicksburg, MS.

Kapitza, H., and Eppel, D. 1987. "A 3-D Poisson Solver Based on Conjugate Gradients Compared to Standard Iterative Methods and Its Performance on Vector Computers," *Journal of Computational Physics*, Vol 68, pp 474-484.

Launder, B. E., and Spalding, D. B. 1974. "The Numerical Calculation of Turbulent Flows," *Computer Methods in Appplied Mechanics and Engineering*, Vol 3, pp 269-289.

MacCormack, R. W. 1969. "The Effect of Viscosity in Hypervelocity Impact Cratering," AIAA Paper 69-354, American Institute of Aeronautics and Astronautics, Cincinnati, OH.

Moss, W. D., and Baker, S. 1980. "Recirculating Flows Associated with Two-Dimensional Steps," *The Aeronautical Quarterly*, Vol 31, Part 3, pp 151-172.

Orlanski, I. 1976. "A Simple Boundary Condition for Unbounded Hyperbolic Flows," *Journal of Computational Physics*, Vol 21, pp 251-269.

Patel, V. C., Rodi, W., and Scheurer, G. 1985. "Turbulence Models for Near-Wall and Low Reynolds Number Flows: A Review," *AIAA Journal*, Vol 23, No. 9, pp 1308-1319.

Rajaratnam, N., and Nwachukwu, B. 1983. "Flow Near Groyne-Like Structures," *Journal of Hydraulic Engineering*, Vol 109(HY3), pp 463-480.

Thompson, J. F. 1983 (Mar). "A Boundary-Fitted Coordinate Code for General Two-Dimensional Regions with Obstacles and Intrusions," Technical Report E-83-8, US Army Engineer Waterways Experiment Station, Vicksburg, MS.

Thompson, J. F., Warsi, Z. U. A., and Mastin, C. W. 1985. *Numerical Grid Generation: Foundations and Applications*, North-Holland, Elsevier, New York.

Appendix A
Primary Flow

Notation

Standard fluid-mechanical notation is used throughout Appendices A-F. Quantities defined in one appendix retain the same definitions in subsequent appendixes, except where indicated otherwise. All symbols with an underbar represent vectors, and the subscripts x, y, t, ξ, and η indicate partial derivatives. Other subscripts and superscripts convey individual meanings that are defined when they are first used. All references cited in this appendix and subsequent appendixes are included in the list of references at the end of the main text.

Equations of Motion

Depth-averaged incompressible flow (with a rigid lid) obeys the equations for conservation of momentum and mass, given respectively by

$$\frac{d\underline{u}}{dt} = \underline{F} - \rho^{-1}\nabla p \tag{A1}$$

$$\nabla \cdot (h\underline{u}) = 0 \tag{A2}$$

where

$\underline{u}$ = velocity vector (u,v)
∇ = gradient operator $(\partial/\partial x, \partial/\partial y)$
ρ = density
p = pressure
t = time
h = depth

and

$$\frac{d}{dt} = \frac{\partial}{\partial t} + \underline{u} \cdot \nabla \tag{A3}$$

The operator *d/dt* is the total derivative with respect to time. The vector *F* includes the forces per unit mass (accelerations) due to viscosity, bottom friction, and secondary flow

$$\underline{F} = \underline{T} - \underline{X} + \underline{S} \tag{A4}$$

where
$\underline{T}$ = viscous force
$\underline{X}$ = friction force
$\underline{S}$ = secondary force

Upon multiplying Equation A1 by depth and taking the divergence thereof, one obtains a Poisson equation for the pressure

$$\nabla \cdot (h \nabla p) = \rho \nabla \cdot \left[h \left(\underline{F} - \frac{d\underline{u}}{dt} \right) \right] \tag{A5}$$

The solution of Equation A5, subject to the constraint of Equation A2, yields the spatial distribution of pressure needed to conserve mass.

Viscous Force

The viscous force $\underline{T}$ has Cartesian *x*- and *y*-components T_1 and T_2, respectively. These arise from the divergence of the depth-averaged shear stress

$$T_1 = \rho^{-1} h^{-1} \left[(h\tau_{11})_x + (h\tau_{12})_y \right] \tag{A6}$$

$$T_2 = \rho^{-1} h^{-1} \left[(h\tau_{12})_x + (h\tau_{22})_y \right] \qquad \text{(A7)}$$

The subscripts x and y indicate partial x- and y-derivatives, and

$$\tau_{11} = 2\nu\rho u_x \qquad \text{(A8)}$$

$$\tau_{22} = 2\nu\rho v_y \qquad \text{(A9)}$$

$$\tau_{12} = \nu\rho(u_y + v_x) \qquad \text{(A10)}$$

where ν is the kinematic eddy viscosity, and τ_{11}, τ_{22}, and τ_{12} are depth-averaged components of the turbulent shear stress.

Assuming that Equation A2 is satisfied, and that derivatives of depth are insignificant in the viscous terms, then

$$T_1 \approx h^{-1}\nu\nabla\cdot(h\nabla u) + 2\nu_x u_x + \nu_y(u_y + v_x) \qquad \text{(A11)}$$

$$T_2 \approx h^{-1}\nu\nabla\cdot(h\nabla v) + 2\nu_y v_y + \nu_x(v_x + u_y) \qquad \text{(A12)}$$

The second derivatives in Equations A11 and A12 now have the same form as those on the left-hand side of Equation A5, which is convenient for discretization.

Friction Force

Flow deceleration caused by frictional resistance on the bottom is represented in STREMR by

$$\underline{X} = C_f \, h^{-1} \, \underline{u}|\underline{u}| \tag{A13}$$

where C_f is the bottom friction factor. The simplest, and perhaps the most widely used, approximation for C_f is given by Manning's equation

$$C_f = 9.81 \, n^2 \, h^{-1/3} \tag{A14}$$

where n is the Manning coefficient. Depth has replaced the usual hydraulic radius in Equation A14, and the coefficient 9.81 applies only when h is given in meters. Otherwise, if depth is given in feet, the coefficient becomes 14.5 instead of 9.81.

Secondary Force

Curved channels often develop a helical secondary flow which creates a shear stress in excess of that produced by viscosity. This can result in velocity distributions that are noticeably different from those for purely two-dimensional flow.

In general, secondary flow is to be expected wherever the depth-averaged streamlines are curved. This produces a streamwise acceleration of the depth-averaged flow, given approximately by

$$\underline{S} \approx \rho^{-1} \frac{\underline{u}}{|\underline{u}|} \left[h^{-1} \underline{n} \cdot \nabla(h\tau_s) + 2r^{-1}\tau_s \right] \tag{A15}$$

where

τ_s = secondary shear stress
$\underline{n}$ = unit vector normal to $\underline{u}$
r = local radius of curvature

The scalar product $\underline{n} \cdot \nabla(h\tau_s)$ is the normal derivative of the depth-integrated secondary shear stress

$$\underline{n} \cdot \nabla(h\tau_s) = \frac{v(h\tau_s)_x - u(h\tau_s)_y}{|\underline{u}|} \tag{A16}$$

and the radius of curvature is related to the velocity derivatives by

$$r = \frac{|\underline{u}|^3}{uv(v_y - u_x) + u^2 v_x - v^2 u_y} \tag{A17}$$

The secondary stress is positive in the direction of motion, and the normal derivative and radius of curvature can be either positive or negative. The sign of r (as given by Equation A17) is positive for counterclockwise motion and negative for clockwise motion. The normal derivative (as given by Equation A16) is positive when $h\tau_s$ increases in the positive radial direction.

Appendix B Turbulence

Background

Turbulence occurs whenever there is too little viscosity to prevent small disturbances from growing and disrupting a laminar flow. The resulting eddies take on so many different sizes that it is impossible to represent them all on a computational grid of reasonable dimensions. Nevertheless, if the influence of the smaller eddies can be approximated with a turbulence model, then the larger eddies can still be captured by discretization. The turbulence, by definition, then comprises only the eddies that are too small to be resolved directly on the grid.

When the Navier-Stokes equations are averaged over a time-interval that is short compared with the periods of the large eddies, but long compared with those of the turbulence, stresses arise that are proportional to the time-averaged products of the fluctuating velocity components. These are called Reynolds stresses, and the process of time-averaging is called Reynolds averaging.

Strictly speaking, the complete turbulent velocity distribution must be known in order to calculate the Reynolds stresses exactly, but engineers generally make do with empirical approximations based on mean-flow (Reynolds-averaged) velocities. The simplest of these, suggested by Boussinesq (1877), consists of replacing the molecular viscosity with an eddy viscosity in the Newtonian expression for shear stress (Equations A8-A10). Turbulence models that use the Boussinesq approach are called eddy viscosity models, and they are classified according to the manner in which they obtain the eddy viscosity from the properties of the local mean flow. Hereafter, any reference to the flow will imply the mean flow, unless stated otherwise.

Since kinematic viscosity has units of length squared divided by time, eddy viscosity can be made proportional to any combination of turbulence quantities that yields these same units. Algebraic models obtain the eddy viscosity by calculating turbulence quantities directly from the local flow, without accounting for transport by the flow itself. Since they involve no equations for turbulence transport, these models are also called zero-equation models. In contrast, one-equation models include a transport equation for one of the turbulence quantities, with local algebraic approximations for the rest. Two-equation models add a transport equation for a second quantity, and so on.

Depth-Averaged Turbulence Modeling

In STREMR, the friction force on the bottom is presumed to account for the vertical transport of momentum by the turbulence. This is a crude representation for a phenomenon so complex as turbulence, but it is adequate for depth-averaged calculations as long as the lateral variation of depth is very gentle. Thus, the turbulence model used in STREMR must approximate only the lateral transport of depth-averaged momentum. Two-equation models are well suited for general 2-D applications, because they allow distinct turbulence quantities to be created in one place and transported to another, where their influence is felt through the eddy viscosity.

Standard *k*-ε Turbulence Model

The *k*-ε turbulence model (Launder and Spalding 1974) is one of the most widely used of the two-equation models. Here the symbol *k* represents the turbulence energy (per unit mass), and ε is the dissipation rate for *k*. Taking these as the primary turbulence quantities, each of which is governed by a transport equation, the eddy viscosity is then related to *k* and ε by

$$\nu = C_\nu \frac{k^2}{\varepsilon} \tag{B1}$$

where C_ν is a dimensionless empirical coefficient.

The governing equations for *k* and ε consist of two semi-empirical transport equations, each of which has the form

Advection = Production - Dissipation + Diffusion

Advection means transport by the mean flow; production means creation from the large eddies; dissipation means frictional loss through the small eddies; and diffusion means the spreading that occurs because of eddy viscosity. In the standard *k*-ε model, the depth-averaged equations are

$$\frac{dk}{dt} = \nu\Gamma - \varepsilon + \sigma_k^{-1}[h^{-1}\nu\nabla\cdot(h\nabla k) + \nabla\nu\cdot\nabla k] \tag{B2}$$

$$\frac{d\varepsilon}{dt} = C_1 \nu \Gamma \frac{\varepsilon}{k} - C_2 \frac{\varepsilon^2}{k} + \sigma_\varepsilon^{-1} [h^{-1} \nu \nabla \cdot (h \nabla \varepsilon) + \nabla \nu \cdot \nabla \varepsilon] \qquad \text{(B3)}$$

The first term on the right of Equations B2 and B3 is the production term, which is proportional to

$$\Gamma = 2(u_x{}^2 + v_y{}^2) + (u_y + v_x)^2 \qquad \text{(B4)}$$

The second term on the right of Equations B2 and B3 is the dissipation term, and the quantities inside the brackets make up the diffusion term. The standard set of (dimensionless) empirical coefficients is

$C_\nu = 0.09$
$C_1 = 1.44$
$C_2 = 1.92$
$\sigma_k = 1.0$
$\sigma_\varepsilon = 1.3$

The governing equations for the mean flow are the Reynolds-averaged, incompressible Navier-Stokes equations. Their counterparts in STREMR are the depth-averaged equations for conservation of momentum and mass (A1 and A2). By solving Equations B2 and B3 for k and ε, along with Equations A1 and A5 for $\underline{u}$ and p, one can obtain mean-flow approximations that are useful within certain limits. Specifically, when adequate approximations are imposed for the shear stress, turbulence energy, and dissipation rate along the sidewalls, then the standard k-ε model works fairly well for unidirectional flow. Some modification of the model is needed, however, for recirculating flow.

Model Adjustment for Recirculating Flow

The standard k-ε model sometimes overpredicts turbulence energy and eddy viscosity in regions of low velocity, and this is especially a problem for 2-D recirculating flow. In the latter case, the overprediction can be reduced by increasing the dissipation rate in response to low velocity and high vorticity. Previous work (Bernard 1991) has shown that considerable improvement can be achieved by reducing the value of C_2 to that of C_1 as the eddy Reynolds number

$$R_E = \frac{|\underline{u}|^2}{\nu\, |v_x - u_y|} \tag{B5}$$

falls toward zero. This enhances the dissipation rate for recirculating flow (where R_E becomes small), and it indirectly reduces the turbulence energy and eddy viscosity.

Since turbulence production rises also in response to the turbulence energy itself, the energy overprediction can likewise be controlled by defining an energy ratio

$$R_k = \frac{|\underline{u}|^2}{k} \tag{B6}$$

and then redefining the eddy viscosity as

$$\nu = C_\nu f(R_k) \frac{k^2}{\varepsilon} \tag{B7}$$

The present version of STREMR uses Equation B7 with

$$f(R_k) = \frac{1}{R_C} + \left(1 - \frac{1}{R_C}\right) \tanh\left(\frac{R_k^{\,2}}{R_0^{\,2}}\right) \tag{B8}$$

where R_C is the maximum reduction factor (RECAP in STREMR) for the eddy viscosity. Equation B8 dictates that $f(R_k) \approx 1/R_C$ when $R_k << R_0$, and that $f(R_k) \approx 1$ when $R_k \geq 1.7\, R_0$. Thus, $f(R_k)$ multiplies the standard eddy viscosity (Equation B1) by the factor $1/R_C$ whenever the kinetic energy of the turbulence is comparable with that of the mean flow. Note that if R_C is set equal to unity, then $f(R_k) = 1$ and Equation B7 reduces to the standard definition for eddy viscosity (Equation B1). Based on comparisons of STREMR predictions with test data for recirculating flow (Durst and Tropea 1981), it appears that R_C lies in the range

$$1.5 \leq R_C \leq 2.0 \qquad \text{(B9)}$$

with $R_0 \approx 65$. Unless grids are used that are fine enough to achieve grid-independent flow predictions, however, the lengths of the computed eddies will *still* be underpredicted. The default value in STREMR is set at $R_C = 2.5$ to compensate for anticipated grid error on coarse grids. For modeling efforts in which fine grids are employed to achieve accurate flow predictions *and* grid independence, R_C should always be given a value between 1.5 and 2.0.

Equation B8 is not unique in its ability to improve model predictions. Other functions can be used for $f(R_k)$ if they reduce ν dramatically when R_k falls well below R_0. Of course, the empirical parameters R_0 and R_C have to be adjusted initially to reconcile model predictions with experimental data, but their values are fixed thereafter and presumed to be universal constants.

Model Adjustment for Sidewalls

Further adjustment is needed for sidewalls, where gradients in both the turbulence and the mean flow are quite large. This complicates the problem of modeling turbulence close to a wall, especially for boundary layers with strong pressure gradients. Boundary-layer calculations in general demand grid resolution and turbulence modeling on a scale much finer than that needed otherwise. In particular, the grid must be fine enough to resolve the flow in the boundary layer before and after separation; and the model equations have to be altered considerably to approximate the velocity, shear stress, turbulence energy, and dissipation rate near the wall. The extensive modifications needed for turbulent boundary layers have been discussed in detail by Patel, Rodi, and Scheurer (1985) in an excellent paper on low-Reynolds-number (near-wall) k-ε models.

STREMR is not intended as a numerical model for boundary layers, but it must approximate their influence well enough to predict the flow at larger scales. The main requirement is that the combined effect of the computed shear stress and pressure gradient should render accurate predictions of flow separation. This calls for some adjustment of the model equations next to sidewalls, but not as much as would be needed for detailed calculations in boundary layers.

The appropriate sidewall adjustments are not known in advance, nor can they be deduced from scratch. Moreover, different combinations can produce similar results. One must simply make informed guesses for the sidewall coefficients and boundary conditions, and then test the entire prescription by comparing model predictions with physical measurements. The model adjustments described in the following paragraphs were developed in this way, using the separated-flow experiments of Baskaran, Smits, and Joubert (1987) as benchmarks for comparison.

To compute the shear stress on a sidewall, it is necessary first to assume a functional form for the velocity near the wall. Although logarithmic distributions have often been used for this purpose, they are generally applicable only for weak pressure gradients and for grids that are fine enough to resolve boundary layers. STREMR applications typically involve strong pressure gradients and grids that are too coarse for boundary layers, and it seems better to use a power-law velocity distribution of the form

$$\frac{u_B(\delta)}{\delta^{1/7}} = const \tag{B10}$$

where u_B is the tangential velocity component, δ is the distance normal to the wall, and the 1/7 exponent roughly approximates the velocity variation in a turbulent boundary layer. For small curvature, the tangential shear stress τ_B now becomes

$$\tau_B \approx \frac{\nu(\delta) u_B(\delta)}{7\delta} \tag{B11}$$

In STREMR calculations, δ is the distance from the wall to the *center* of the adjacent NOSLIP cell, and the shear stress τ_D at the wall is taken to be

$$\tau_D \approx \frac{C_D \nu(\delta) u_B(\delta)}{7\delta} \tag{B12}$$

where

$$C_D = 1 \tag{B13}$$

The coefficient C_D (DRAG in STREMR) allows some adjustment of τ_D for exceedingly coarse grids. Otherwise, however, if the computational grid is fine enough to resolve the flow outside the boundary layer and downstream of separation, then Equation B12 should suffice with C_D equal to unity.

The normal derivative $\partial k/\partial\delta$ is needed to compute the gradient flux of turbulence energy through a sidewall. Although k may vary only slightly with δ throughout much of a boundary layer *($\partial k/\partial\delta \approx 0$)*, there is a thin sublayer next to the wall where k falls rapidly to zero *($\partial k/\partial\delta >> 0$)*. The sublayer then gives an average value of $\partial k/\partial\delta$ that is slightly positive well beyond the sublayer, and this warrants the use of a small positive exponent for the dependence of k upon δ. Assuming that k varies with the 1/7 power of δ near the wall, then

$$\frac{k(\delta)}{\delta^{1/7}} \approx const \tag{B14}$$

and the normal derivative of k becomes

$$\frac{\partial k}{\partial \delta} \approx \frac{k(\delta)}{7\delta} \tag{B15}$$

Using the derivative given by Equation B15, STREMR approximates the gradient flux of k through the wall with

$$\nu\frac{\partial k}{\partial \delta} \approx \frac{\nu(\delta)k(\delta)}{7\delta} \tag{B16}$$

Similarly, the normal derivative $\partial\varepsilon/\partial\delta$ is needed to compute the gradient flux of the dissipation rate through a sidewall. In STREMR calculations, this is taken to be zero near the wall, so the gradient flux of ε through the wall is

$$\nu\frac{\partial \varepsilon}{\partial \delta} \approx 0 \tag{B17}$$

Although ε is known experimentally to decrease sharply with increasing δ in a boundary layer $(\partial\varepsilon/\partial\delta << 0)$, there is an inflection point $(\partial\varepsilon/\partial\delta = 0)$ near the wall where $\partial\varepsilon/\partial\delta$ changes sign. Whenever Equation B17 is used as the boundary condition for ε, the presumption is that $\partial\varepsilon/\partial\delta$ is negligible from the cell center to the wall (instead of at a single inflection point).

Equations B16 and B17 are poor approximations for the gradient fluxes of k and ε near a sidewall, but their respective errors offset each other somewhat in practice. In particular, Equation B17 may underestimate the rise in ε near the wall, making the dissipation rate too small to balance the energy production; but Equation B16 imposes an additional loss of energy at the wall that partially compensates for the underpredicted rise in ε. STREMR carries this compensation a step further by setting $C_2 = C_1 = 1.44$ in all NOSLIP cells, which reduces the near-wall decay rate for ε.

The last item needed in the list of sidewall adjustments is an approximation for the turbulence energy production $\nu(\delta)\Gamma(\delta)$ in NOSLIP cells. This quantity is especially difficult to calculate, because it requires accurate approximations for eddy viscosity and the velocity derivatives near the wall. After much trial and error, the best approach seems to be to compute the near-wall *difference* between production and dissipation with the approximation

$$\nu(\delta)\,\Gamma(\delta) - \varepsilon(\delta) \approx \nu(2\delta)\,\Gamma(2\delta) - \varepsilon(2\delta) \tag{B18}$$

where

$$\nu(2\delta) = \frac{1}{2}\left[\nu(\delta) + \nu(3\delta)\right] \tag{B19}$$

and

$$\varepsilon(2\delta) = \frac{1}{2}\left[\varepsilon(\delta) + \varepsilon(3\delta)\right] \tag{B20}$$

Note that the *center* of the NOSLIP cell lies at a distance δ from the wall, and that of the adjacent FIELD cell lies at a distance 3δ. The velocity derivatives needed for $\Gamma(2\delta)$ are computed with central-difference approximations at a distance 2δ from the wall.

Model Adjustment for Other Boundaries

The normal derivatives of k and ε are assumed to be zero on SLIP boundaries and OPEN boundaries. Along FLUX boundaries, small fixed values, $k = k_0$ and $\varepsilon = \varepsilon_0$, are assigned in OUT cells adjacent to FLUX cells. These are used in the discrete advective terms in Equations B2 and B3, where they help prevent the computed values just inside the grid from drifting. In the diffusion terms, however, the normal derivatives are set to zero on FLUX boundaries. Furthermore, because of uncertainties in production and dissipation next to these boundaries, the constraint $\nu\Gamma - \varepsilon = 0$ is imposed in all FLUX cells.

The values $k = k_0$ and $\varepsilon = \varepsilon_0$ are assigned initially to the entire flow field, but these quantities change as the flow develops. If the flow reaches a steady state, then k and ε likewise reach a steady state. The initial energy k_0 is taken to be a small fraction (TURBIN) of the initial velocity squared $(u_0^2+v_0^2)$ in the reference cell (IREF,JREF):

$$TURBIN = \frac{k_0}{u_0^2 + v_0^2} \tag{B21}$$

where u_0 and v_0 are the reference velocity components. The default value in STREMR is TURBIN = 0.003.

The initial dissipation rate ε_0 is computed from k_0 and the initial eddy viscosity ν_0 as follows:

$$\varepsilon_0 = \frac{C_\nu k_0^2}{\nu_0} \tag{B22}$$

The viscosity ν_0 is computed by STREMR to produce a specified value for the initial Peclet number (PECLET) in the reference cell; i.e.

$$PECLET = \frac{u_0 \Delta x_0 + v_0 \Delta y_0}{\nu_0} \tag{B23}$$

where Δx_0 and Δy_0 are the local x- and y-components of the grid spacing. The default value in STREMR is $PECLET = 50$.

Turbulence Model Applicability

With the proposed adjustments, the k-ε turbulence model yields sidewall shear stresses that are accurate within a factor of two, as long as δ is roughly 1 to 10 times greater than the nominal thickness of the turbulent boundary layer. If δ lies much above this range, then the grid is too coarse to resolve either the shear stress or the flow. When δ lies far below the acceptable range, the predicted shear stress may be unacceptably low. Fortunately, however, predictions of flow separation seem to be adversely affected only when the grid is too coarse.

Flow calculations in general require that the local grid spacing be sufficiently fine to resolve the direction of flow at corners and other abrupt changes in the boundaries. Just upstream of an obstacle or contraction, the computed flow is quite sensitive to the spacing and orientation of the grid. Under these conditions, it is necessary to try successively refined grids until the same results are obtained on two different grids. Otherwise, there is no guarantee that the computed flow is grid independent.

Above all, one should keep in mind that the purpose of STREMR is not to reproduce the details of the turbulence, but rather to capture the large-scale features of the 2-D mean flow. In pursuit of that end, the k-ε turbulence model allows STREMR users to concern themselves with bathymetry, lateral geometry, and inflow/outflow distribution, without having to estimate local or global values for eddy viscosity.

Appendix C
Secondary Flow

Depth-Averaging

Genuine two-dimensional (2-D) flows are uncommon in hydraulics, but quasi-2-D flows are common enough to warrant the implementation of 2-D depth-averaged models like STREMR. Depth-averaging cannot account directly for vertical motion, but it can account indirectly (albeit empirically) for vertical inhomogeneity. Thus, meaningful calculations for shallow water must include adjustments for effects that have their origins in three dimensions.

Bottom friction and turbulence are universally important, but there is a third mechanism that depends on geometry. When the depth-averaged streamlines are curved, centrifugal forces create a streamwise torque that generates helicity in the flow. This is like a screw advancing or retreating in the streamwise direction, which makes fluid particles follow spiral paths. The shear stress produced by the out-of-plane motion may noticeably affect the depth-averaged flow.

Helical secondary flow is well known for slender meandering channels, where it alters the depth-averaged flow (and ultimately the bed itself). It has often been simulated with algebraic and numerical models for slender channels (for which a *uniform* curvature can be specified), but these channels encompass only a few of the planview geometries that STREMR seeks to represent. For depth-averaged calculations in general, one needs a secondary flow model that responds to dynamic changes in streamline curvature.

Absence of detail is acceptable for the secondary flow as long as the depth-averaged velocities are adequately predicted. Thus, the model should include just enough detail to approximate the depth-averaged shear stress τ_s. That is the guiding principle for the idealized picture adopted in STREMR.

Secondary Shear Stress

Let z be the vertical direction, and let $\underline{u}'(z)$ be a z-dependent perturbation of the depth-averaged velocity vector $\underline{u}$. With the water surface (rigid lid) at $z = h/2$ and the bottom at $z = -h/2$, the perturbation must satisfy the constraint

$$\int_{-h/2}^{h/2} \underline{u}' \, dz = 0 \tag{C1}$$

If one substitutes $\underline{u} + \underline{u}'$ for $\underline{u}$ when deriving the depth-averaged momentum equation, there arises a perturbation $h\tau'$ of the depth-integrated shear stress $h\tau_{12}'$

$$h\tau' = -\rho \int_{-h/2}^{h/2} u'v' \, dz \tag{C2}$$

where

u' = x-component of $\underline{u}'$
v' = y-component of $\underline{u}'$

Even though the depth integrals $\int u'dz$ and $\int v'dz$ are both identically zero, the perturbation stress τ' is not necessarily zero. The simplest functions that satisfy Equation C1 but leave τ' nonzero are

$$u' = \omega_2 z \tag{C3}$$

$$v' = -\omega_1 z \tag{C4}$$

where

ω_1 = x-component of depth-averaged vorticity
ω_2 = y-component of depth-averaged vorticity

If the primary flow is in the x-direction, so that $v = 0$ but $u \neq 0$, then ω_1 is the streamwise vorticity associated with out-of-plane (spiral) motion of the fluid particles. The other vorticity component ω_2 is perpendicular to ω_1 and characterizes the skewness (z-dependence) of the streamwise velocity in the vertical plane of flow. Upon substitution of Equations C3 and C4 into C2, there results

$$\tau' = \frac{\rho h^2 \omega_1 \omega_2}{12} \qquad \text{(C5)}$$

Following Johannesson and Parker (1989), let ω_2 be roughly proportional to $\sqrt{C_f}$ such that

$$\omega_2 \sim C_2 \frac{u\sqrt{C_f}}{h} \qquad \text{(C6)}$$

where C_2 is the constant of proportionality. Equations C5 and C6 then yield

$$\tau' = \rho h u \frac{C_2 \omega_1}{12} \sqrt{C_f} \qquad \text{(C7)}$$

Assuming that Equations C6 and C7 are valid regardless of the direction of the velocity (i.e., with u replaced by $/\underline{u}/$), one can then approximate the depth-averaged secondary shear stress with the relation

$$\tau_s = \rho h \Omega \sqrt{C_f}\ |\underline{u}| \qquad \text{(C8)}$$

where

$$\Omega = \frac{C_2 \omega_s}{12} \qquad \text{(C9)}$$

and ω_s is the streamwise vorticity. This leaves only Ω to be determined in order to calculate τ_s.

Streamwise Vorticity

Consider a vertical column of water in a flow that has radius of curvature r in planview. Let the streamwise velocity $u_s(z)$ be given by

$$u_s = |\underline{u}|\left[1 + C_2\frac{z}{h}\sqrt{C_f}\right] \qquad \text{(C10)}$$

with the outward radial velocity $u_r(z)$ given by

$$u_r = \omega_s z \qquad \text{(C11)}$$

At any elevation z, there is a centrifugal (outward radial) acceleration, u_s^2/r, due to the curvature. This creates a torque per unit mass, zu_s^2/r, along the column. Assuming that the no-slip condition holds, and that there is a vertical eddy viscosity proportional to $C_f^{1/2}$, then there is a radial shear stress, roughly proportional to $\rho h\omega_s C_f^{1/2}/\underline{u}/$, at the bottom of the column. Subject to these forces, conservation of angular momentum for the column requires that

$$\rho\frac{d}{dt}\int_{-h/2}^{h/2}\omega_s\, z^2 dz = -\frac{1}{2}C_1 h^2\sqrt{C_f}\,\rho\omega_s|\underline{u}| + \rho\int_{-h/2}^{h/2}\frac{u_s^2}{r}\, zdz \qquad \text{(C12)}$$

where C_1 is a constant of proportionality. When Equations C10 and C12 are combined and integrated, there follows

$$\frac{d\omega_s}{dt} = 2C_2\sqrt{C_f}\,\frac{|\underline{u}|^2}{rh} - 6C_1\sqrt{C_f}\,\omega_s\,\frac{|\underline{u}|}{h} \qquad \text{(C13)}$$

Substitution of Equation C9 into C13 then results in

$$\frac{d\Omega}{dt} = \frac{1}{6}C_2^2\sqrt{C_f}\,\frac{|\underline{u}|^2}{rh} - 6C_1\sqrt{C_f}\,\Omega\,\frac{|\underline{u}|}{h} \qquad \text{(C14)}$$

Equation C14 shows the dependence of $d\Omega/dt$ on the streamwise velocity, the radius of curvature, the depth, the friction factor, and Ω itself. Its functional form comes from the assumed z-dependence of the streamwise and out-of-plane velocities, and from the imposition of centrifugal and frictional forces on a vertical column of water. The constants C_1 and C_2 are arbitrary, and they have to be inferred from experimental data, without which Equation C14 is only of qualitative value.

The right-hand side of Equation C14 contains empirically derived terms for production and dissipation (damping) of Ω. If one regards Ω as being truly proportional to streamwise vorticity, then the governing equation should include terms for diffusion and vortex-stretching as well. The vortex-stretching term, proportional to $\underline{\Omega}\cdot\nabla\underline{u}$, will be insignificant compared to the advection term $\underline{u}\cdot\nabla\underline{\Omega}$ as long as $/h\Omega/$ is small compared to $/\underline{u}/$. With its empirical coefficients rearranged and turbulent diffusion added, Equation C14 gives way to the following depth-averaged equation for Ω:

$$\frac{d\Omega}{dt} = A_s\sqrt{C_f}\,\frac{|\underline{u}|^2}{rh} - D_s\sqrt{C_f}\,\Omega\,\frac{|\underline{u}|}{h} + \frac{\nu}{h}\,\nabla\cdot(h\nabla\Omega) + \nabla\nu\cdot\nabla\Omega \qquad \text{(C15)}$$

where

A_s = empirical coefficient (ASEC in STREMR)
D_s = empirical coefficient (DSEC in STREMR)

From experience gained to date (Bernard and Schneider 1992), it appears that suitable values for A_s and D_s are

$$A_s \approx 5.0 \qquad \text{(C16)}$$

$$D_s \approx 0.5 \qquad \text{(C17)}$$

Equation C15 is valid only when $h << r$. Otherwise, the depth is comparable to the radius of curvature, and the source term (i.e., the first term) on the right-hand side of Equation C15 may become much larger than is physically reasonable. To avoid this problem, the source term can be multiplied by a self-limiting function such that Equation C15 gives way to

$$\frac{d\Omega}{dt} = \frac{A_s\sqrt{C_f}\,|\underline{u}|^2}{rh(1 + 9h^2/r^2)} - D_s\sqrt{C_f}\,\Omega\,\frac{|\underline{u}|}{h} + \frac{\nu}{h}\,\nabla\cdot(h\nabla\Omega) + \nabla\nu\cdot\nabla\Omega \qquad \text{(C18)}$$

This leaves Equation C15 essentially unaltered for $h << r$, but it reduces the source term by a factor of 10 when $h = r$.

Equations C8 and C18 are the equations used for secondary flow in STREMR. In order to complete the empirical model, however, it is necessary to specify boundary conditions for Ω.

Boundary Conditions

In the implementation of Equation C18, one assumes that the secondary flow is created entirely within the computed flow field, and that no streamwise vorticity is brought in from upstream. Thus, Ω is fixed at zero for the inflow boundaries, and extrapolated from the interior for all other boundaries.

Production of Ω should approach zero on the sidewalls, where the streamwise velocity decreases rapidly. In order roughly to account for this, STREMR reduces A_s by one-half in all boundary-adjacent cells, which results in smaller values of Ω near the sidewalls.

While Equation C18 is important for the creation and propagation of Ω, it is the sidewall boundaries and the depth variations that induce the largest gradients in $h\tau_s$ normal to the streamwise direction. The importance of the sidewalls has been clarified by Johannesson and Parker (1989) who demonstrated that the sidewall-induced normal derivatives are necessary for the gradual migration of higher velocities toward the outside of a channel bend.

Model Applicability

From the development of Equations C8 and C18, it should be evident that the proposed secondary-flow model is certainly no substitute for computation in three dimensions. Nevertheless, the balance of advection, diffusion, production, and dissipation yields the same pattern of development and decay that is commonly observed for shallow flows. Helicity arises wherever the streamlines are curved, and this is followed by a gradual redistribution of the depth-averaged velocities. Downstream of the curved region, the secondary flow dies off but continues to influence the depth-averaged flow for some distance. Eventually the effects of upstream curvature are lost through bottom friction and diffusion.

Appendix D Curvilinear Coordinates

Boundary-Conforming Grids

Irregular boundaries are common in hydraulics, and these can make finite-difference discretization cumbersome for Cartesian grids with rectangular cells. These grids require that smooth curves and line segments be replaced with staircases that poorly represent the physical shapes, and they make it difficult to maintain tangency of the velocity and to impose Neumann conditions along boundaries so represented.

With numerically generated curvilinear grids, however, it is possible to fit the gridlines to the boundaries, and to avoid stair-stepping altogether (Thompson et al. 1985). The only catch is that one must transform the governing equations from Cartesian coordinates to general curvilinear coordinates. Thus, for the equations in Appendices A-C, transformations have to be found for the gradient, divergence, and Laplacian operators.

Transformation of the Gradient

Let the two-dimensional curvilinear coordinates (ξ,η) be arbitrary functions of the Cartesian coordinates

$$\xi = \xi(x,y) \tag{D1}$$

$$\eta = \eta(x,y) \tag{D2}$$

Transformation of the gradient for these coordinates is contingent upon the chain rule, which states that

$$\psi_\xi = x_\xi \psi_x + y_\xi \psi_y \tag{D3}$$

and

$$\psi_\eta = x_\eta \psi_x + y_\eta \psi_y \tag{D4}$$

where ψ is an arbitrary scalar function, and the subscripts ξ and η indicate ξ- and η-derivatives. Upon solving Equations D3 and D4 for the x- and y-derivatives of ψ, one obtains the x- and y-components of the gradient,

$$\psi_x = J^{-1}(y_\eta \psi_\xi - y_\xi \psi_\eta) \tag{D5}$$

$$\psi_y = J^{-1}(x_\xi \psi_\eta - x_\eta \psi_\xi) \tag{D6}$$

The quantity J is the Jacobian of the transformation, given by

$$J = x_\xi y_\eta - x_\eta y_\xi \tag{D7}$$

When Equations D5 and D6 are inserted into the Cartesian expression for $\underline{u}\cdot\nabla\psi$, they yield the transformed operation for depth-averaged advection

$$\underline{u}\cdot\nabla\psi = h^{-1}J^{-1}(U\psi_\xi + V\psi_\eta) \tag{D8}$$

where U and V are components of volumetric flux in the ξ- and η-directions, respectively,

$$U = h(y_\eta u - x_\eta v) \tag{D9}$$

$$V = h(x_\xi v - y_\xi u) \tag{D10}$$

Transformation of the Divergence

The divergence of a vector (e.g., $\nabla \cdot [h\underline{u}]$) is defined by the Gauss Theorem, which says that for an arbitrary volume V_c with total surface area S_c

$$\iiint_{V_c} \nabla \cdot [h\underline{u}] \, dV_c = \iint_{S_c} \underline{n} \cdot [h\underline{u}] \, dS_c \tag{D11}$$

where

dV_c = differential volume
dS_c = differential surface area
$\underline{n}$ = unit vector (outward) normal to dS_c

Consider an infinitesimal cube in a three-dimensional curvilinear (ξ,η,z) space in which z is an independent coordinate direction, normal to both the Cartesian (x,y) and curvilinear (ξ,η) planes. Cube faces of constant ξ and constant η then have surface areas given, respectively, by

$$dS_c^{(\xi)} = dz d\eta \sqrt{x_\eta^2 + y_\eta^2} \tag{D12}$$

$$dS_c^{(\eta)} = dz d\xi \sqrt{x_\xi^2 + y_\xi^2} \tag{D13}$$

The unit vectors normal to these faces are, respectively, given by

$$\underline{n}^{(\xi)} = \frac{\nabla \xi}{|\nabla \xi|} \tag{D14}$$

$$\underline{n}^{(\eta)} = \frac{\nabla \eta}{|\nabla \eta|} \tag{D15}$$

To evaluate the gradients in D14 and D15, one substitutes ξ and η for ψ in Equations D5 and D6. Since ξ and η are independent of each other, it follows immediately that

$$\xi_x = J^{-1} y_\eta \tag{D16}$$

$$\xi_y = -J^{-1} x_\eta \tag{D17}$$

and

$$\eta_x = -J^{-1} y_\xi \tag{D18}$$

$$\eta_y = J^{-1} x_\xi \tag{D19}$$

Then after substituting *hu* and *hv* for ψ in Equations D5 and D6, and using the results with Equations D12-D19, it is easy to obtain the scalar product $\underline{n}\cdot[h\underline{u}]dS_c$ for the constant-ξ and constant-η faces of the cube, respectively

$$\underline{n}^{(\xi)}\cdot[h\underline{u}]dS_c^{(\xi)} = U\ dzd\eta \tag{D20}$$

$$\underline{n}^{(\eta)}\cdot[h\underline{u}]dS_c^{(\eta)} = V\ dzd\xi \tag{D21}$$

where *U* and *V* are given by Equations D9 and D10, respectively. Assuming no variation of *h* or $\underline{u}$ in the *z*-direction for the infinitesimal cube, the right-hand side of Equation D11 is

$$\begin{aligned}\iint_{S_c} \underline{n}\cdot[h\underline{u}]dS_c &= dzd\eta\left[(U)_{\xi=\xi^+} - (U)_{\xi=\xi^-}\right] \\ &+ dzd\xi\left[(V)_{\eta=\eta^+} - (V)_{\eta=\eta^-}\right]\end{aligned} \tag{D22}$$

where

$$\xi^{\pm} = \xi \pm \frac{d\xi}{2}$$)

$$\eta^{\pm} = \eta \pm \frac{d\eta}{2} \tag{D24}$$

To evaluate the left-hand side of Equation D11, it is necessary to obtain an expression for the infinitesimal volume dV_c. Let $\underline{i}$, $\underline{j}$, and $\underline{k}$ be unit vectors in the x-, y-, and z-directions, respectively. Infinitesimal displacements $d\xi$, $d\eta$, and dz in the curvilinear (ξ,η,z) space produce infinitesimal vector displacements in the Cartesian (x,y,z) space ; i.e.

$$d\underline{x}^{(\eta,z)} = (\underline{i}\, x_{\xi} + \underline{j}\, y_{\xi})\, d\xi \tag{D25}$$

$$d\underline{x}^{(\xi,z)} = (\underline{i}\, x_{\eta} + \underline{j}\, y_{\eta})\, d\eta \tag{D26}$$

$$d\underline{x}^{(\xi,\eta)} = \underline{k}\, dz \tag{D27}$$

where

$d\underline{x}^{(\eta,z)}$ = displacement with constant η and z
$d\underline{x}^{(\xi,z)}$ = displacement with constant ξ and z
$d\underline{x}^{(\xi,\eta)}$ = displacement with constant ξ and η

In curvilinear (ξ,η,z) space the displacements $d\xi$, $d\eta$, and dz coincide with three intersecting edges of the infinitesimal cube; but the corresponding vector displacements in Cartesian (x,y,z) space (Equations D25-D27) coincide with three intersecting edges of an infinitesimal parallelipiped. The volume of the latter is given by the triple scalar product

$$dV_c = [d\underline{x}^{(\eta,z)} \times d\underline{x}^{(\xi,z)}] \cdot d\underline{x}^{(\xi,\eta)} \tag{D28}$$

Combining Equations D25-D28 then produces

$$dV_c = J\, d\xi d\eta dz \tag{D29}$$

After substituting the right-hand side of Equation D29 for dV_c in Equation D11, and equating the result with the right-hand side of Equation D22, the limit as $d\xi$, $d\eta$, and dz approach zero gives

$$\nabla \cdot [h\underline{u}] = J^{-1}[U_\xi + V_\eta] \tag{D30}$$

where U and V are the ξ- and η-components of volumetric flux given by Equations D9 and D10, respectively.

Lest there be confusion about the z-coordinate and the depth h in this appendix, note that z is used only to establish a coordinate direction for the displacement dz, which is needed for defining infinitesimal volumes and surface areas. In the limit, dz divides out of Equation D11, and the final result (Equation D30) collapses into two dimensions. The depth h and velocity $\underline{u}$ play the respective roles of arbitrary scalar and vector in the derivation, but their product $h\underline{u}$ is convenient for demonstration because it appears in the continuity equation (A2).

Transformation of the Laplacian

With curvilinear expressions in hand for the gradient and the divergence, it is straightforward to transform the generalized Laplacian, $\nabla \cdot (h\nabla\psi)$, in which ψ_x and ψ_y play the same roles as u and v, respectively, in the left-hand side of Equation D30. Thus, it follows that

$$\nabla \cdot (h\nabla\psi) = J^{-1}\left[\frac{\partial}{\partial\xi}(y_\eta\psi_x - x_\eta\psi_y) + \frac{\partial}{\partial\eta}(x_\xi\psi_y - y_\xi\psi_x)\right] \tag{D31}$$

where ψ_x and ψ_y are given by Equations D5 and D6. There is little point in further reducing Equation D31, however, without first discussing how it is to be discretized.

Appendix E Discretization

Computational Coordinates

STREMR uses a marker-and-cell (MAC) grid (Figure 2) for discretizing the equations in Appendices A-C, assuming that they have been converted from Cartesian coordinates (x,y) to curvilinear coordinates (ξ,η) with the transformations given in Appendix D. The computational counterparts of the curvilinear coordinates (ξ,η) are the integer computational coordinates (i,j). The grid cells may have any shape in the Cartesian (x,y) plane, but they are rectangular in the computational (i,j) plane. All discrete calculations are done in the computational plane, in which the grid cells are uniformly square with sides of unit length

$$\Delta\xi = \Delta\eta = 1 \tag{E1}$$

The lengths of the cell sides in the Cartesian plane can be found from Equations D12 and D13. The computational coordinates define the locations of the grid nodes (Figures 2 and 3) as well as the integer values ot the curvilinear coordinates:

$$\xi = i \tag{E2}$$

$$\eta = j \tag{E3}$$

The curvilinear coordinates of the cell centers (ξ_{cc},η_{cc}) are then given by

$$\xi_{cc} = i - \frac{1}{2} \tag{E4}$$

$$\eta_{cc} = j - \frac{1}{2} \tag{E5}$$

Thus, the computational (i,j) plane and the curvilinear (ξ,η) plane are identical. As discussed in Part II, the indices (i,j) also serve as labels for cell (i,j) whose northeast corner lies at node (i,j) in the computational plane.

Marker-and-Cell Grid

Each cell has distinct quantities defined for the cell center and for the midpoints of the cell faces. The cell-centered (cell-averaged) quantities are the pressure p, the Cartesian velocity components (u,v), the viscosity ν, the depth h, the turbulence energy k, the turbulence-energy dissipation rate ε, and the streamwise vorticity Ω. The face-centered (face-averaged) quantities are the volumetric flux components (U,V), with U defined on the east and west faces, and V defined on the north and south faces.

Coordinate Derivatives

The nodal coordinates $x(i,j)$ and $y(i,j)$ coincide with the northeast corner of cell (i,j); but on the east face as a whole, the central-difference approximation for x_ξ requires cell-centered coordinates:

$$x_\xi^e = x_{cc}(i+l,j) - x_{cc}(i,j) \tag{E6}$$

The subscript cc denotes cell-centered (cell-averaged) quantities, where

$$x_{cc}(i,j) = \frac{1}{4}\left[x(i,j) + x(i-1,j) + x(i,j-1) + x(i-1,j-1)\right] \tag{E7}$$

Either nodal or cell-centered coordinates can be used for central-difference approximations of x_η on the east face; i.e.,

$$x_\eta^e = \frac{1}{4}\Big[x_{cc}(i,j+1) + x_{cc}(i+1,j+1) - x_{cc}(i,j-1) \\ - x_{cc}(i+1\ j-1)\Big] \tag{E8}$$

$$x_{\eta}^{E} = x(i,j) - x(i,j-1) \qquad \text{(E9)}$$

The superscripts *e* and *E* both indicate the east face; but the lower-case *e* refers to the derivative computed with cell-centered coordinates, while the upper-case *E* refers to the derivative computed with nodal coordinates. The same convention applies for superscripts referring to derivatives of *x* and *y* on the north (*n*,*N*), south (*s*,*S*), and west (*w*,*W*) faces. For example, on the north face

$$x_{\eta}^{n} = x_{cc}(i,j+1) - x_{cc}(i,j) \qquad \text{(E10)}$$

$$x_{\xi}^{n} = \frac{1}{4}\Big[x_{cc}(i+1,j) + x_{cc}(i+1,j+1) - x_{cc}(i-1,j) - x_{cc}(i-1,j+1)\Big] \qquad \text{(E11)}$$

$$x_{\xi}^{N} = x(i,j) - x(i-1,j) \qquad \text{(E12)}$$

Coordinate derivatives are also needed at the cell centers. These are indicated by the superscript *c* (lower case) and computed from nodal coordinates by using central-difference approximations:

$$x_{\xi}^{c} = \frac{1}{2}\big[x(i,j) + x(i,j-1) - x(i-1,j) - x(i-1,j-1)\big] \qquad \text{(E13)}$$

$$x_{\eta}^{c} = \frac{1}{2}\big[x(i,j) + x(i-1,j) - x(i,j-1) - x(i-1,j-1)\big] \qquad \text{(E14)}$$

Henceforth, the upper- and lower-case conventions for *superscripts* will also apply for *subscripts*.

Generalized Laplacian

Coordinate derivatives using *nodal* coordinates are needed for computing fluxes *through* the cell faces, and coordinate derivatives using *cell-centered* coordinates are needed for computing other derivatives *on* the cell faces. For example, the components of $\nabla\psi$ on the east face are

$$\psi_x^e = J_e^{-1}\left[y_\eta^e\ \psi_\xi^e - y_\xi^e\ \psi_\eta^e\right] \tag{E15}$$

$$\psi_y^e = J_e^{-1}\left[x_\xi^e\ \psi_\eta^e - x_\eta^e\ \psi_\xi^e\right] \tag{E16}$$

where

$$J_e = x_\xi^e\ y_\eta^e - x_\eta^e\ y_\xi^e \tag{E17}$$

$$\psi_\xi^e = \psi(i+1,j) - \psi(i,j) \tag{E18}$$

$$\psi_\eta^e = \frac{1}{4}\left[\psi(i,j+1) + \psi(i+1,j+1) - \psi(i,j-1) - \psi(i+1,j-1)\right] \tag{E19}$$

For $\Delta z = 1$, however, the flux of $\nabla\psi$ through the east face is

$$\iint (\underline{n}\cdot\nabla\psi)_e\ dS_E = y_\eta^E\ \psi_x^e - x_\eta^E\ \psi_y^e \tag{E20}$$

Likewise, the flux of $\nabla\psi$ through the north face is

$$\iint (\underline{n}\cdot\nabla\psi)_n\ dS_N = x_\xi^N\ \psi_y^n - y_\xi^N\ \psi_x^n \tag{E21}$$

where

$$\psi_x^n = J_n^{-1}\left[y_\eta^n\ \psi_\xi^n - y_\xi^n\ \psi_\eta^n\right] \tag{E22}$$

$$\psi_y^n = J_n^{-1}\left[x_\xi^n \, \psi_\eta^n - x_\eta^n \, \psi_\xi^n\right] \tag{E23}$$

$$J_n = x_\xi^n \, y_\eta^n - x_\eta^n \, y_\xi^n \tag{E24}$$

$$\psi_\eta^n = \psi(i,j+1) - \psi(i,j) \tag{E25}$$

$$\psi_\xi^n = \frac{1}{4}\left[\psi(i+1,j) + \psi(i+1,j+1) - \psi(i-1,j) - \psi(i-1,j+1)\right] \tag{E26}$$

Similar arguments apply for the south and west faces. Substitution of these relations into Equation D31 yields a discretized Laplacian that is the sum of four gradient fluxes

$$J_c \, \nabla\cdot(h\nabla\psi) = h_e(y_\eta^E \, \psi_x^e - x_\eta^E \, \psi_y^e) - h_w(y_\eta^W \, \psi_x^w - x_\eta^W \, \psi_y^w) + h_n(x_\xi^N \, \psi_y^n - y_\xi^N \, \psi_x^n) - h_s(x_\xi^S \, \psi_y^s - y_\xi^S \, \psi_x^s) \tag{E27}$$

where

$$J_c = x_\xi^c \, y_\eta^c - x_\eta^c \, y_\xi^c \tag{E28}$$

Cell-centered depths are averaged for adjacent cells to get depths on their common faces; e.g.

$$h_e = \frac{1}{2}\left[h(i,j) + h(i+1,j)\right] \tag{E29}$$

$$h_n = \frac{1}{2}\left[h(i,j) + h(i,j+1)\right] \tag{E30}$$

After all the terms and coefficients have been expanded for Equation E27, the discretized Laplacian takes the final form

$$\begin{aligned} J_c\ \nabla\cdot(h\nabla\psi) &= A_{cc}\psi(i,j) + A_{ee}\psi(i+1,j) + A_{ww}\psi(i-1,j) \\ &+ A_{nn}\psi(i,j+1) + A_{ss}\psi(i,j-1) + A_{ne}\psi(i+1,j+1) \\ &+ A_{nw}\psi(i-1,j+1) + A_{se}\psi(i+1,j-1) + A_{sw}\psi(i-1,j-1) \end{aligned} \tag{E31}$$

For cells *not* adjacent to boundaries, the A-coefficients are

$$A_{cc} = -\alpha_e - \alpha_w - \beta_n - \beta_s \tag{E32}$$

$$A_{ee} = \alpha_e - \gamma_n + \gamma_s \tag{E33}$$

$$A_{ww} = \alpha_w + \gamma_n - \gamma_s \tag{E34}$$

$$A_{nn} = \beta_n - \gamma_e + \gamma_w \tag{E35}$$

$$A_{ss} = \beta_s + \gamma_e - \gamma_w \tag{E36}$$

$$A_{ne} = -\gamma_n - \gamma_e \tag{E37}$$

$$A_{nw} = \gamma_n + \gamma_w \tag{E38}$$

$$A_{sw} = -\gamma_s - \gamma_w \tag{E39}$$

$$A_{se} = \gamma_s + \gamma_e \tag{E40}$$

and the α-, β-, and γ-coefficients for *all* cells are

$$\alpha_e = \frac{h_e}{J_e}\left[x_\eta^E\ x_\eta^e + y_\eta^E\ y_\eta^e\right] \tag{E41}$$

$$\beta_n = \frac{h_n}{J_n}\left[x_\xi^{\ N} x_\xi^{\ n} + y_\xi^{\ N} y_\xi^{\ n}\right] \tag{E42}$$

$$\gamma_e = \frac{h_e}{4J_e}\left[x_\eta^{\ E} x_\xi^{\ e} + y_\eta^{\ E} y_\xi^{\ e}\right] \tag{E43}$$

$$\gamma_n = \frac{h_n}{4J_n}\left[x_\xi^{\ N} x_\eta^{\ n} + y_\xi^{\ N} y_\eta^{\ n}\right] \tag{E44}$$

The corresponding formulas for the west and south faces are identical to Equations E41-E44, except that (w,W) and (s,S) replace (e,E) and (n,N), respectively, as the subscripts and superscripts.

Equation E31 represents the discretized Laplacian for any cell-centered quantity, and the same A-coefficients (given by Equations E32-E40) can be used for the momentum equation (A1), the Poisson equation for pressure (A5), the turbulence equations (B2 and B3), and the secondary flow equation (C18). Moreover, since the A-coefficients are constants, they have to be calculated only once for a given flow geometry.

Laplacian for Boundary Cells

Equation E31 requires cell-centered values for coordinates (x_{cc}, y_{cc}) and dependent variables in OUT cells. Suppose, for example, that cell (i,j) is a boundary cell, and that the cells to the right are OUT cells. Two apparent dilemmas then arise. First, Equation E27 demands that the gradient flux through the east face be uniquely specified (as defined by Equation E20). Second, Equations E22 and E23 demand that ξ-derivatives be computed for x, y, and ψ on the north and south faces. According to Equations E11 and E26, these derivatives would need cell-centered quantities for cells $(i+1,j)$, $(i+1,j+1)$, and $(i+1,j-1)$, all of which are OUT cells.

The resolution of the first dilemma is straightforward. One simply replaces the east flux in Equation E27 with a known value (given in advance), and then expands the three remaining fluxes to obtain expressions for the A-coefficients that appear in Equation E31. In STREMR the boundary value for the gradient flux is always set equal to zero so that the A-coefficients will be the same for *all* cell-centered variables. Nonzero boundary values are subsequently added (as needed) to the explicit Laplacian for each dependent variable.

The A-coefficients cannot be calculated, however, until the second dilemma is resolved. The problem is that Equations E11 and E26 include values that lie in OUT cells, and it appears that one must either extrapolate known values across the grid boundary, or use difference equations other than E11 and E26. The two alternatives are equivalent, and previous work (Bernard and Kapitza 1992) has demonstrated that when the east face of a cell coincides with a boundary, Equations E11 and E26 should be replaced with

$$x_\xi^n = \frac{1}{2}\Big[x_{cc}(i,j) + x_{cc}(i,j+1) - x_{cc}(i-1,j) - x_{cc}(i-1,j+1)\Big] \tag{E45}$$

$$\psi_\xi^n = \frac{1}{2}\big[\psi(i,j) + \psi(i,j+1) - \psi(i-1,j) - \psi(i-1,j+1)\big] \tag{E46}$$

These are one-sided difference approximations, but the same effect can be achieved by using the following extrapolations in Equations E11 and E26:

$$x_{cc}(i+1,j) = 2x_{cc}(i,j) - x_{cc}(i-1,j) \tag{E47}$$

$$\psi(i+1,j) = 2\psi(i,j) - \psi(i-1,j) \tag{E48}$$

Either way, the nonzero A-coefficients turn out to be

$$A_{cc} = -\alpha_w - \beta_n - \beta_s - 2\gamma_n + 2\gamma_s \tag{E49}$$

$$A_{nn} = \beta_n + \gamma_w - 2\gamma_n \tag{E50}$$

$$A_{ss} = \beta_s - \gamma_w + 2\gamma_s \tag{E51}$$

$$A_{ww} = \alpha_w + 2\gamma_n - 2\gamma_s \tag{E52}$$

$$A_{nw} = 2\gamma_n + \gamma_w \tag{E53}$$

$$A_{sw} = -2\gamma_s - \gamma_w \tag{E54}$$

and three of the coefficients are identically zero; i.e.,

$$A_{ee} = A_{ne} = A_{se} = 0 \tag{E55}$$

This is only one example of the special treatment needed in deriving the A-coefficients for a boundary-adjacent cell, but the same principles apply for any cell that has at least one entire *face* on a boundary.

A different situation that requires special treatment is one where a cell has only one *corner* touching a boundary. Consider a cell *(i,j)* for which only the northeast corner lies on a boundary. Among the immediate neighbors of cell *(i,j)*, only cell *(i+1,j+1)* is an OUT cell. In this case, none of the gradient fluxes is identically zero in Equation E27, but Equations E8, E11, E19, and E26 still require cell-centered quantities in cell *(i+1,J+1)*. One way out of the ambiguity is to use Equations E45 and E46 in place of E11 and E26, and to replace Equations E8 and E19, respectively, by

$$\begin{aligned} x_\eta^e = \frac{1}{2}\Big[& x_{cc}(i,j) + x_{cc}(i+1,j) - x_{cc}(i,j-1) \\ & - x_{cc}(i+1,j-1)\Big] \end{aligned} \tag{E56}$$

$$\begin{aligned} \psi_\eta^e = \frac{1}{2}\Big[& \psi(i,j) + \psi(i+1,j) - \psi(i,j-1) \\ & - \psi(i+1,j-1)\Big] \end{aligned} \tag{E57}$$

With these modifications, the A-coefficients now become

$$A_{cc} = -\alpha_e - \alpha_w - \beta_n - \beta_s - 2\gamma_n - 2\gamma_e \tag{E58}$$

$$A_{nn} = \beta_n - 2\gamma_n + \gamma_w \tag{E59}$$

$$A_{ss} = \beta_s + 2\gamma_e - \gamma_w \tag{E60}$$

$$A_{ee} = \alpha_e - 2\gamma_e + \gamma_s \tag{E61}$$

$$A_{ww} = \alpha_w + 2\gamma_e - \gamma_s \tag{E62}$$

$$A_{ne} = 0 \tag{E63}$$

$$A_{nw} = 2\gamma_n + \gamma_w \qquad \text{(E64)}$$

$$A_{se} = 2\gamma_e + \gamma_s \qquad \text{(E65)}$$

$$A_{sw} = -\gamma_s - \gamma_w \qquad \text{(E66)}$$

Conservation of Mass

It is easy to see from Equations A2 and D30 that in the $\xi\eta$-plane, the continuity equation (for conservation of mass) gives way to the simple constraint

$$U_\xi + V_\eta = 0 \qquad \text{(E67)}$$

In discrete form, this reduces to a balance of the fluxes through the four faces of each grid cell; i.e.

$$U_E - U_W + V_N - V_S = 0 \qquad \text{(E68)}$$

where

$$U_E = h_e\left[y_\eta^E\, u_E - x_\eta^E\, v_E\right] \qquad \text{(E69)}$$

$$V_N = h_n\left[x_\xi^N\, v_N - y_\xi^N\, u_N\right] \qquad \text{(E70)}$$

with similar expressions for the west and south faces. The upper-case subscripts for *u* and *v* indicate that the face-centered velocity components are *not* to be calculated simply by averaging cell-centered values, but are to be obtained by some other means.

Suppose there exists a flux distribution (U', V') that does not satisfy Equation E68; i.e.

$$U_E' - U_W' + V_N' - V_S' \neq 0 \qquad \text{(E71)}$$

The distribution (U',V') can be made to conserve mass by adding the gradient of a scalar function ϕ, such that

$$U_E = U_E' - h_e\left[y_\eta^E \, \phi_x^e - x_\eta^E \, \phi_y^e\right] \tag{E72}$$

$$V_N = V_N' - h_n\left[x_\xi^N \, \phi_y^n - y_\xi^N \, \phi_x^n\right] \tag{E73}$$

Substitution of Equations E72 and E73 (with similar expressions for the west and south faces) into Equation E68 produces a discretized Poisson equation

$$J_c \, \nabla\cdot(h\nabla\phi) = U_E' - U_W' + V_N' - V_S' \tag{E74}$$

If no changes are demanded for the fluxes through the boundaries (i.e., if the boundary fluxes are given correctly in advance), then the function ϕ is subject to the same constraints as the function ψ (Equations E27 and E31), and their discretized Laplacians are identical.

Now suppose that at some time t the flow conserves mass. Let U' and V' be the fluxes that would exist if the flow were allowed to evolve from t to t + Δt without a pressure gradient. The pressure needed to achieve conservation of mass at the end of this interval is then related to the solution of Equation E74 by

$$p = \frac{\rho\phi}{\Delta t} \tag{E75}$$

Even if the flow did not conserve mass at time t, the pressure given by Equation E75 would make it do so at time $t + \Delta t$. Thus, by solving Equation E74 iteratively in each discrete time-step through which the flow evolves, one is able to maintain approximate conservation of mass *and* remove errors that might be left over from previous time-steps. The latter advantage is important because it prevents accumulation of error caused by incomplete convergence in the iterative solution of Equation E74.

Advection

Each of the governing equations in Appendices A-C contains an advection term (i.e., $\underline{u}\cdot\nabla\psi$), which is perhaps the most troublesome of all the terms to be discretized. It is this term that shapes the algorithms in STREMR, and its influence is best understood with reference to the equation for pure advection

$$\psi_t + \underline{u}\cdot\nabla\psi = 0 \tag{E76}$$

In general curvilinear coordinates, Equation E76 becomes

$$hJ_c\psi_t + U\psi_\xi + V\psi_\eta = 0 \tag{E77}$$

The advection equation has long been an object of computational research, and the prescriptions for its discretization are varied and many (Anderson et al. 1984). Two of the simplest are the Euler upwind scheme (Anderson et al.) and the MacCormack predictor-corrector scheme (MacCormack 1969). STREMR uses the MacCormack scheme for the primary-flow momentum equation and the upwind scheme for the turbulence and secondary flow equations.

The Euler upwind scheme favors propagation in the directions of positive U and V. Thus, with forward differencing in time and upwinding in space, the advection equation takes the discrete form

$$\begin{aligned} hJ_c\frac{\Delta\psi}{\Delta t} &= U^{(+)}\left[\psi(i,j) - \psi(i+1,j)\right] + U^{(-)}\left[\psi(i-1,j) - \psi(i,j)\right] \\ &+ V^{(+)}\left[\psi(i,j) - \psi(i,j+1)\right] + V^{(-)}\left[\psi(i,j-1) - \psi(i,j)\right] \end{aligned} \tag{E78}$$

where

$$U^{(+)} = \frac{1}{2}\left[U_E - |U_E|\right] \tag{E79}$$

$$U^{(-)} = \frac{1}{2}\left[U_W + |U_W|\right] \tag{E80}$$

$$V^{(+)} = \frac{1}{2}\left[V_N - |V_N|\right] \tag{E81}$$

$$V^{(-)} = \frac{1}{2}\left[V_S + |V_S|\right] \tag{E82}$$

The quantities on the right-hand side of Equation E78 are those existing at time t, and the new value of ψ at time $t + \Delta t$ is

$$\psi \doteq \psi + \Delta\psi \tag{E83}$$

where the symbol $\doteq$ means that the sum on the right replaces the previous value of the quantity on the left. Close inspection of Equations E78-E82 reveals that E78 uses one-sided differencing, because $U^{(+)}$ and $U^{(-)}$ cannot be simultaneously nonzero, nor can $V^{(+)}$ and $V^{(-)}$.

The MacCormack scheme also uses one-sided differencing, but this is taken in *opposite* spatial directions during the predictor phase and the corrector phase. The predictor phase begins with

$$\begin{aligned} hJ_c \frac{\Delta\psi}{\Delta t} &= U_E(i-1+r,j)\left[\psi(i-1+r,j) - \psi(i+r,j)\right] \\ &+ V_N(i,j-1+s)\left[\psi(i,j-1+s) - \psi(i,j+s)\right] \end{aligned} \tag{E84}$$

The integer shift indices (r,s) control the direction of the differencing. Values of 1 and 0 produce forward and backward differencing, respectively, and the initial pair (r,s) is chosen from four combinations: (0,0), (1,0), (0,1), and (1,1). The predictor phase concludes with the provisional value of ψ

$$\psi^* = \psi + \Delta\psi \tag{E85}$$

The corrector phase begins by reversing the difference directions that were used in the predictor; i.e.

$$r^* = 1 - r \tag{E86}$$

$$s^* = 1 - s \tag{E87}$$

The difference equation for the corrector then becomes

$$\begin{aligned} hJ_c \frac{\Delta\psi^*}{\Delta t} &= U_E^*(i-1+r^*,j)\left[\psi^*(i-1+r^*,j) - \psi^*(i+r^*,j)\right] \\ &+ V_N^*(i,j-1+s^*)\left[\psi^*(i,j-1+s^*) - \psi^*(i,j+s^*)\right] \end{aligned} \tag{E88}$$

Equation E88 is used to obtain a second provisional value of ψ

$$\psi^{**} = \psi^{*} + \Delta\psi^{*} \tag{E89}$$

Finally, the corrector phase concludes with the value of ψ at time $t + \Delta t$

$$\psi = \frac{1}{2}\left[\psi + \psi^{**}\right] \tag{E90}$$

To avoid the accumulation of directional bias caused by repeated use of the same shift indices, each of the four possible (r,s) combinations is used (in the predictor phase) once in every four time-steps.

Close inspection of Equations E67 and E77 reveals that if E67 is satisfied, then E77 can be replaced by its conservative form

$$hJ_c\psi_t + (U\psi)_\xi + (V\psi)_\eta = 0 \tag{E91}$$

That is, the advection operator can be expressed in either of two equivalent forms

$$U\psi_\xi + V\psi_\eta = (U\psi)_\xi + (V\psi)_\eta \tag{E92}$$

When the discrete continuity equation (E68) is satisfied (on a MAC grid), the Euler upwind and MacCormack schemes preserve the equivalency demonstrated in Equation E92 and achieve a true finite-volume discretization.

Cell-Centered Velocities

Prior to the first time-step in a cold start, STREMR calculates initial mass-conserving fluxes (U,V) from the gradient of a scalar potential. These fluxes then evolve as the flow evolves, and they are updated and adjusted for mass conservation in each phase of the MacCormack predictor-corrector scheme. In other words, the volumetric fluxes (U,V) are regarded as the true dependent variables of the flow, and the Cartesian velocity components (u,v) are dummy variables that are retained only temporarily. Nevertheless, the momentum equation and the transport equations for turbulence and secondary flow still require velocities at the cell centers.

In the Euler upwind scheme used for the turbulence and secondary flow, the cell-centered velocities can be obtained simply by averaging the face-centered fluxes; i.e.

$$u = h^{-1} J_c^{-1}\left[x_\xi^{\,c}\, U_{cc} + x_\eta^{\,c}\, V_{cc}\right] \tag{E93}$$

$$v = h^{-1} J_c^{-1}\left[y_\xi^{\,c}\, U_{cc} + y_\eta^{\,c}\, V_{cc}\right] \tag{E94}$$

where

$$U_{cc} = \frac{1}{2}(U_E + U_W) \tag{E95}$$

$$V_{cc} = \frac{1}{2}(V_N + V_S) \tag{E96}$$

Equations E93-E96 suffice for defining the velocities and the derivatives thereof needed in the right-hand sides of Equations B2, B3, and C18.

The cell-centered velocities play a different role in the momentum equation, where they appear temporarily as the *dependent* variables of the flow. At first inspection, there is no obvious way of relating cell-centered velocities to face-centered fluxes except by averaging (as in Equations E93-E96). With the forward-backward logic of the MacCormack scheme, however, there is an admissible alternative.

Let the shift indices (r,s) determine not only the difference dirrctions for advection, but also the cell faces and fluxes that will be used for defining the cell-centered velocities. Thus, let

$$U_E(r) = U_E(i-r,j) \tag{E97}$$

$$V_N(s) = V_N(i,j-s) \tag{E98}$$

$$h_e(r) = \frac{1}{2}\left[h(i+1-r,j) + h(i-r,j)\right] \tag{E99}$$

$$h_n(s) = \frac{1}{2}\left[h(i,j+1-s) + h(i,j-s)\right] \tag{E100}$$

$$x_\xi^{\,N}(s) = x_\xi^{\,N}(i,j-s) \tag{E101}$$

$$x_{\eta}^{E}(r) = x_{\eta}^{E}(i-r,j) \qquad \text{(E102)}$$

with similar definitions for $y_{\xi}^{N}(s)$ and $y_{\eta}^{E}(r)$. If $u(r,s)$ and $v(r,s)$ are the cell-centered velocities defined by (r,s), and if these velocities are used instead of u_E, v_E, u_N, and v_N in Equations E69 and E70, then

$$U_E(r) = h_e(r)\left[y_{\eta}^{E}(r)\ u(r,s) - x_{\eta}^{E}(r)\ v(r,s)\right] \qquad \text{(E103)}$$

$$V_N(s) = h_n(s)\left[x_{\xi}^{N}(s)\ v(r,s) - y_{\xi}^{N}(s)\ u(r,s)\right] \qquad \text{(E104)}$$

Solving Equations E103 and E104 for $u(r,s)$ and $v(r,s)$, one obtains

$$u(r,s) = \frac{1}{J(r,s)}\left[\frac{x_{\xi}^{N}(s)\ U_E(r)}{h_e(r)} + \frac{x_{\eta}^{E}(r)\ V_N(s)}{h_n(s)}\right] \qquad \text{(E105)}$$

$$v(r,s) = \frac{1}{J(r,s)}\left[\frac{y_{\xi}^{N}(s)\ U_E(r)}{h_e(r)} + \frac{y_{\eta}^{E}(r)\ V_N(s)}{h_n(s)}\right] \qquad \text{(E106)}$$

where

$$J(r,s) = x_{\xi}^{N}(s)\ y_{\eta}^{E}(r) - x_{\eta}^{E}(r)\ y_{\xi}^{N}(s) \qquad \text{(E107)}$$

Equations E105 and E106 define the velocity components to be used in the MacCormack solution of the discretized momentum equation.

Face-Centered Flux Increments

The increments of velocity calculated during a predictor or corrector phase have to be converted into flux increments and transferred back to the cell faces from which the fluxes were taken. To accomplish this, one uses Equations E103 and E104, with velocity increments $(\Delta u,\Delta v)$ in place of velocities (u,v), and flux increments $(\Delta U,\Delta V)$ in place of fluxes (U,V); i.e.

$$\Delta U_E(r) = h_e(r)\left[y_\eta^{\ E}(r)\ \Delta u(r,s) - x_\eta^{\ E}(r)\ \Delta v(r,s)\right] \tag{E108}$$

$$\Delta V_N(s) = h_n(s)\left[x_\xi^{\ N}(s)\ \Delta v(r,s) - y_\xi^{\ N}(s)\ \Delta u(r,s)\right] \tag{E109}$$

Once the flux increments have been calculated, the velocities and velocity increments can be discarded. STREMR computes the cell-centered velocity increments with the pressure gradient omitted from the momentum equation, so the flux increments given by Equations E108 and E109 do not conserve mass. These flux increments are added to the existing fluxes to obtain

$$U_E^{'}(r) = U_E(r) + \Delta U_E(r) \tag{E110}$$

$$V_N^{'}(s) = V_N(s) + \Delta V_N(s) \tag{E111}$$

The nonconservative fluxes given by Equations E110 and E111 are used in the right-hand side of the Poisson equation (E74), which STREMR solves iteratively with a conjugate-gradient scheme developed by Kapitza and Eppel (1987). The resulting scalar potential ϕ is then used in Equations E72 and E73 to correct U' and V' for conservation of mass.

This procedure is carried out in both the predictor and corrector phases, but in the corrector phase the nonconservative fluxes are calculated using

$$U_E^{'}(r^*) = \frac{1}{2}\left[U_E(r^*) + U_E^*(r^*) + \Delta U_E^*(r^*)\right] \tag{E112}$$

$$V_N^{'}(s^*) = \frac{1}{2}\left[V_N(s^*) + V_N^*(s^*) + \Delta V_N^*(s^*)\right] \tag{E113}$$

where

U_E^* = conservative U-flux at end of predictor phase
V_N^* = conservative V-flux at end of predictor phase

and

ΔU_E^* = nonconservative U-increment for corrector
ΔV_N^* = nonconservative V-increment for corrector

If ϕ and p are the scalar potential and pressure, respectively, for the predictor phase, then p is related to ϕ by Equation E75. For the corrector phase, however, p^* is related to ϕ^* by

$$p^* = \frac{2\rho\phi^*}{\Delta t} \tag{E114}$$

The factor 2 appears because the flux increments for the corrector phase are multiplied by 1/2 in Equations E112 and E113. The significance here is that p and p^* each act for *half* a time-step.

Cell-Centered Gradients

The momentum equation and the transport equations for turbulence and secondary flow all contain products of first-order spatial derivatives; e.g.

$$\frac{d\psi}{dt} = \nabla v \cdot \nabla \psi + \textit{other terms} \tag{E115}$$

The right-hand side includes ξ- and η-derivatives that have to be evaluated at the cell centers. When the Euler upwind scheme is used for advection of the turbulence and secondary flow, these derivatives are approximated with central differences:

$$\psi_\xi = \frac{1}{2}\left[\psi(i+1,j) - \psi(i-1,j)\right] \tag{E116}$$

$$\psi_\eta = \frac{1}{2}\left[\psi(i,j+1) - \psi(i,j-1)\right] \tag{E117}$$

On the other hand, when the MacCormack predictor-corrector scheme is used for advection of the primary flow, the derivatives are represented with alternate one-sided differencı:g controlled by the shift indices:

$$\psi_\xi = \psi(i+r,j) - \psi(i+r-1,j) \tag{E118}$$

$$\psi_\eta = \psi(i,j+s) - \psi(i,j+s-1) \tag{E119}$$

When Equations E116-E119 call for external values of the depth h or the transport variable ψ outside the grid, these are equated with values inside the grid. Thus, when the east face coincides with a boundary

$$\psi(i+1,j) = \psi(i,j) \tag{E120}$$

The only exception is when cell (i,j) is a FLUX cell, in which case the external values for k and ε are $k(i+1,j) = k_0$ and $\varepsilon(i+1,j) = \varepsilon_0$, as explained in Appendix B. External values of quantities *other* than the transport variables (such as viscosity) are provided by extrapolation; e.g.

$$\nu(i+1,j) = 2\nu(i,j) - \nu(i-1,j) \tag{E121}$$

The discretization schemes used for the advection terms and for the cell-centered first-derivatives do not affect the diffusion term $\nu\nabla\cdot(h\nabla\psi)$, which is always discretized in the manner indicated by Equations E27-E66.

Radiation Boundary Condition

STREMR recognizes two distinct types of inflow/outflow boundaries (FLUX and OPEN), both of which allow fluid to enter or leave the grid. The volumetric flux components (U,V) are fixed and unchanging for the boundary faces of a FLUX cell. This is not the case for an OPEN cell, whose boundary fluxes are free to change in response to the flow inside the grid.

OPEN boundaries are not physical boundaries. They are frontiers beyond which the flow is unknown and through which the flow passes as if no boundary were present at all. In principle, their only property is transparency, and they should absorb outward-moving disturbances without producing any reflections. Orlanski (1976) has proposed a discrete version of the Sommerfeld radiation condition that makes computational boundaries effectively transparent.

STREMR uses the radiation condition only for the velocity components $(\tilde{u},\tilde{v})$ *normal* to OPEN boundary faces. The equation for the radiation of $\tilde{u}$ through an east or west face is

$$\tilde{u}_t + c_1\tilde{u}_\xi = 0 \tag{E122}$$

and for the radiation of $\tilde{v}$ through a north or south face

$$\tilde{v}_t + c_2\tilde{v}_\eta = 0 \tag{E123}$$

where

c_1 = propagation velocity for discrete changes in $\tilde{u}$
c_2 = propagation velocity for discrete changes in $\tilde{v}$

The propagation velocities have to be obtained from the computed flow in the FIELD cells next to the OPEN cell. For example, let cell (*i,j*) be an OPEN cell whose east face is a boundary face, and let the superscript *m* denote the elapsed number of discrete time-steps (Δt) at the beginning of the MacCormack predictor phase. The propagation velocity for $\tilde{u}$ is then taken to be

$$c_1 = - \left[\frac{\tilde{u}_t}{\tilde{u}_\xi} \right]_{i-1}^{m-1/2} \qquad \text{(E124)}$$

The superscript *m-1/2* means that the quantity in brackets is evaluated halfway between time-steps *m* and *m-1*, and the subscript *i-1* means that it is evaluated at the center of cell (*i-1,j*). Using central-difference approximations in space and time, the discrete equation for c_1 in the predictor phase is

$$\frac{c_1 \Delta t}{\Delta \xi} = \frac{\tilde{u}_E^m(i-1,j) - \tilde{u}_E^{m-1}(i-1,j) + \tilde{u}_E^m(i-2,j) - \tilde{u}_E^{m-1}(i-2,j)}{\tilde{u}_E^m(i-2,j) + \tilde{u}_E^{m-1}(i-2,j) - \tilde{u}_E^m(i-1,j) - \tilde{u}_E^{m-1}(i-1,j)} \qquad \text{(E125)}$$

Equation E125 defines the radiation Courant number

$$C = \frac{c_1 \Delta t}{\Delta \xi} \qquad \text{(E126)}$$

Since the object is for the east face of cell (*i,j*) to transmit information only to the right, *C* is set equal to zero if the right-hand side (RHS) of Equation E125 is negative; i.e.

$$C = Max\left[0 , RHS(E125) \right] \qquad \text{(E127)}$$

To avoid numerical instability that might be caused by $C > 1$, STREMR supplements Equation E127 with a second constraint,

$$C = Min\left[1 , RHS(E127) \right] \qquad \text{(E128)}$$

Equations E127 and E128 keep the radiation Courant number between zero and unity, and the value for $\tilde{u}$ at the end of the predictor phase becomes

$$\tilde{u}_E^*(i,j) = (1 - C)\, \tilde{u}_E^m(i,j) + C\, \tilde{u}_E^m(i-1,j) \qquad \text{(E129)}$$

For the corrector phase, the definition of C^* is

$$C^* = \frac{\tilde{u}^*_E(i-1,j) - \tilde{u}^m_E(i-1,j) + \tilde{u}^*_E(i-2,j) - \tilde{u}^m_E(i-2,j)}{\tilde{u}^*_E(i-2,j) + \tilde{u}^m_E(i-2,j) - \tilde{u}^*_E(i-1,j) - \tilde{u}^m_E(i-1,j)} \qquad \text{(E130)}$$

and C^* is likewise constrained to lie between zero and unity. In keeping with the logic of the MacCormack scheme, the value for $\tilde{u}$ at the end of the corrector phase is given by

$$\tilde{u}^{m+1}_E(i,j) = \frac{1}{2}\left[\tilde{u}^m_E(i,j) + (1 - C^*)\,\tilde{u}^*_E(i,j) + C^*\,\tilde{u}^*_E(i-1,j)\right] \qquad \text{(E131)}$$

In both the predictor and corrector phases, the individual fluxes have to be adjusted so that the total volumetric flux is constant through each continuous segment of OPEN faces. This adjustment is necessary for maintaining a constant flow rate through the grid.

Sidewall Shear Stress

STREMR assigns a NOSLIP designation by default to all non-OUT cells that touch the boundaries of the grid, except for those cells specified otherwise by the user. The shear stress for NOSLIP boundary faces is calculated either from the near-wall vorticity (turbulent flow) or from a true no-slip condition (laminar flow). This reinstates the force that was omitted from the viscous diffusion term $\nu\nabla\{h\nabla\underline{u}]$ by the assumption that $\underline{n}\cdot\nabla\underline{u} = 0$ (Equations E45-E55). It is this force that distinguishes a NOSLIP boundary face from a SLIP boundary face, for which the condition $\underline{n}\cdot\nabla\underline{u} = 0$ means there is no shear stress unless there is curvature.

In the case of turbulent flow, the near-wall vorticity is calculated from the tangential velocity at the center of the NOSLIP cell adjacent to the wall. Suppose cell (i,j) is a NOSLIP cell, and cell $(i,j-1)$ is an OUT cell. The south face of cell (i,j) is then a NOSLIP boundary face, onto which the tangential velocity $\underline{u}_B$ has to be projected from the cell-centered velocity $\underline{u}$. The unit vector $\underline{t}$ tangent to the (constant-η) boundary is

$$\underline{t} = \frac{\underline{i}\,x_\xi + \underline{j}\,y_\xi}{\sqrt{x_\xi^2 + y_\xi^2}} \qquad \text{(E132)}$$

with the coordinate derivatives evaluated on the south face; i.e.

$$x_\xi = x(i,j-1) - x(i-1,j-1) \tag{E133}$$

$$y_\xi = y(i,j-1) - y(i-1,j-1) \tag{E134}$$

The tangential velocity (vector) is

$$\underline{u}_B = (\underline{u}\cdot\underline{t})\,\underline{t} \tag{E135}$$

Thus, the *x*- and *y*-components of the tangential velocity (u_B, v_B) become

$$u_B = \frac{x_\xi\left[x_\xi u + y_\xi v\right]}{x_\xi^2 + y_\xi^2} \tag{E136}$$

$$v_B = \frac{y_\xi\left[x_\xi u + y_\xi v\right]}{x_\xi^2 + y_\xi^2} \tag{E137}$$

Where *u* and *v* are the cell-centered velocity components *u(r,s)* and *v(r,s)* given by Equations E105 and E106.

Assuming that the tangential velocity is proportional to the 1/7 power of the normal distance δ from the wall, then the absolute value of the near-wall vorticity ω is

$$|\omega| = \frac{1}{7\delta}\sqrt{u_B^2 + v_B^2} \tag{E138}$$

STREMR approximates the resisting shear stress τ_D with

$$\tau_D = \rho C_D \nu \frac{\sqrt{u_B^2 + v_B^2}}{7\delta} \tag{E139}$$

where, for this case,

$$\delta = \frac{J_c}{\sqrt{(x_\xi^c)^2 + (y_\xi^c)^2}} \tag{E140}$$

The resultant shear force has a direction opposite that of the tangential velocity vector $\underline{u}_B$, and the coefficient C_D (DRAG in STREMR) has a default value of unity. The user can raise or lower C_D to increase or decrease τ_D if necessary.

Laminar No-Slip Condition

STREMR uses Equation E139 to calculate the sidewall shear stress only if the turbulence model is activated (KETURB = 'YES'). Otherwise (KETURB = 'NO'), the code imposes a viscous no-slip condition in the following manner for laminar flow.

Suppose cell *(i,j)* is a NOSLIP cell, and cell *(i,j-1)* is an OUT cell. The south face of cell *(i,j)* is then a NOSLIP boundary face, on which the velocity is to be identically zero. A Taylor-series expansion of the velocity for cell *(i,j-1)* gives the velocity (u_s, v_s) on the south face of cell *(i,j)*:

$$u_s(i,j) = u(i,j-1) + u_\eta \frac{\Delta\eta}{2} + u_{\eta\eta} \frac{\Delta\eta^2}{8} + \cdots = 0 \qquad \text{(E141)}$$

with a similar expansion for v_s. Note that the south face of NOSLIP cell *(i,j)* is also the north face of OUT cell *(i,j-1)*. After introducing finite-difference approximations in Equation E141 for u_η and $u_{\eta\eta}$

$$u_\eta \approx \frac{-3u(i,j-1) + 4u(i,j) - u(i,j+1)}{2\Delta\eta} \qquad \text{(E142)}$$

$$u_{\eta\eta} \approx \frac{u(i,j-1) - 2u(i,j) + u(i,j+1)}{\Delta\eta^2} \qquad \text{(E143)}$$

one then obtains an extrapolated approximation for *u(i,j-1)*; i.e.

$$u(i,j-1) \approx \frac{1}{3}u(i,j+1) - 2u(i,j) \qquad \text{(E144)}$$

with a similar extrapolation for *v(i,j-1)*. On the south face of cell *(i,j)*, the ξ- and η-derivatives of *u* now become

$$u_\xi^{\,s} = 0 \qquad \text{(E145)}$$

$$u_{\eta}^{s} = 3u(i,j) - \frac{1}{3}u(i,j+1) \qquad \text{(E146)}$$

with similar expressions for the ξ- and η-derivatives of v. The ξ-derivative is zero because the velocity is identically zero on the boundary, which is tangent to the ξ-direction.

Equations E145 and E146 are now used to calculate the viscous flux of u through the south face of cell (i,j):

$$\iint \nu_s h_s (\underline{n}\cdot\nabla u)_s \, dS_s = \nu_c h_c \left[x_{\xi}^{c} \, u_{y}^{s} - y_{\xi}^{c} \, u_{x}^{s} \right] \qquad \text{(E147)}$$

where the x- and y-derivatives are given by

$$u_{x}^{s} = J_{c}^{-1} \left[y_{\eta}^{c} \, u_{\xi}^{s} - y_{\xi}^{c} \, u_{\eta}^{s} \right] \qquad \text{(E148)}$$

$$u_{y}^{s} = J_{c}^{-1} \left[x_{\xi}^{c} \, u_{\eta}^{s} - x_{\eta}^{c} \, u_{\xi}^{s} \right] \qquad \text{(E149)}$$

with similar equations for the viscous flux of v.

Appendix F Algorithms

Interpolation of Input Variables

If INTERP = 'YES' in namelist BEGIN, STREMR uses interpolation to create smooth distributions of depth (or elevation) and Manning's coefficient. Since the interpolation procedure is the same in all cases, let the generic function ψ represent the variable to be interpolated.

In boundary cells, the default value (specified in the general input) is used for ψ, except where changed by subsequent (section, line, or random) namelist input. In FIELD cells, however, *the default value is ignored*; *i.e.*, *if no* ψ-value is assigned to FIELD cell (i,j) by the namelists for section, line, or random input, then $\psi(i,j)$ will be interpolated from values in neighboring cells. Otherwise, if a value for ψ *has* been assigned to FIELD cell (i,j), that value will be held fixed.

In FIELD cells for which ψ has not been specified by namelist input, the interpolated values of ψ must satisfy the Laplace equation

$$J\nabla^2\psi = 0 \tag{F1}$$

whose discretized left-hand side is given by Equation E31. Note that for interpolation, the A-coefficients are those defined by Equations E32-E40, with h equal to unity.

Initial Flow

STREMR uses input velocities to calculate volumetric fluxes (Equations D9 and D10) through the boundary faces of all OPEN cells and FLUX cells. These fluxes are then adjusted so that the net inflow and outflow are equal. If VGUESS = 'YES' in namelist BEGIN, the input velocities are also used to calculate tentative nonzero values for the remaining fluxes (U',V'). Otherwise, if VGUESS = 'NO' (default), the remaining fluxes (U',V') are tentatively set to zero. In either case, this may violate the continuity equation for one or more of the grid cells; i.e.

$$U'_\xi + V'_\eta \neq 0 \qquad \text{(F2)}$$

STREMR converts the tentative fluxes to mass-conserving fluxes by adding to them the gradient of a scalar potential (ϕ_x, ϕ_y) so that

$$U = U' - h\left[y_\eta \phi_x - x_\eta \phi_y\right] \qquad \text{(F3)}$$

$$V = V' - h\left[x_\xi \phi_y - y_\xi \phi_x\right] \qquad \text{(F4)}$$

for which ϕ must satisfy a Poisson equation

$$J \, \nabla \cdot (h \nabla \phi) = U'_\xi + V'_\eta \qquad \text{(F5)}$$

Equations F3 and F4 define the initial flow, from which the later flow must evolve.

If VGUESS = 'NO', the flow is initially irrotational, which means that it is free of vorticity (circulation). At later times it may have changed considerably, however, due to the combined effects of friction, inflow, turbulence, secondary flow, and possibly truncation error. The flow may approach a steady state for some boundary configurations and initial conditions; but it may remain (or become) quite unsteady for others, perhaps exhibiting periodic behavior (as with vortex shedding).

Turbulence and Secondary Flow

Appendix B presents the Cartesian form of the governing equations (B2 and B3) for the k-ε turbulence model. With the advection terms expressed in curvilinear form. the semi-discrete equations for k and ε are

$$\frac{\Delta k}{\Delta t} + \frac{\left[U k_\xi + V k_\eta\right]}{h J} = \nu \Gamma - \varepsilon + \sigma_k^{-1} h^{-1} \nabla \cdot (\nu h \nabla k) \qquad \text{(F6)}$$

$$\frac{\Delta\varepsilon}{\Delta t} + \frac{\left[U\varepsilon_\xi + V\varepsilon_\eta\right]}{hJ} = \frac{\varepsilon}{k}\left[C_1\nu\Gamma - C_2\varepsilon\right] + \sigma_\varepsilon^{-1} h^{-1}\nabla\cdot(\nu h\nabla\varepsilon) \qquad \text{(F7)}$$

Appendix C likewise presents the Cartesian form of the governing equation (C18) for the secondary flow. With the advection term expressed in curvilinear form, the semi-discrete equation for Ω is

$$h\frac{\Delta\Omega}{\Delta t} + J^{-1}\left[U\Omega_\xi + V\Omega_\eta\right] = \frac{A_s\sqrt{C_f}\,(u^2+v^2)}{r(1+9h^2/r^2)} - D_s\Omega\sqrt{C_f(u^2+v^2)} \qquad \text{(F8)}$$
$$+\nabla\cdot(h\nu\nabla\Omega)$$

Each of Equations F6-F8 can be expressed as a generic advection-diffusion equation with terms added for production and dissipation (damping):

$$\frac{\Delta\psi}{\Delta t} + \frac{\left[U\psi_\xi + V\psi_\eta\right]}{hJ} = P - D + \frac{\nu}{h}\nabla\cdot(h\nabla\psi) + \nabla\nu\cdot\nabla\psi \qquad \text{(F9)}$$

where *P* is the production term and *D* is the damping term.

To calculate Δψ, STREMR uses the Euler upwind scheme for advection (Equations E78-E82), with cell-centered discretization for the diffusion term (Equation E31) and for the gradient terms (Equations E116 and E117). The increment Δψ is then given explicitly by

$$\Delta\psi = \Delta t\left[P - D - h^{-1}J^{-1}\left(U\psi_\xi + V\psi_\eta\right) + \frac{\nu}{h}\nabla\cdot(h\nabla\psi) + \nabla\nu\cdot\nabla\psi\right] \qquad \text{(F10)}$$

The right-hand side of Equation F10 consists entirely of old information at time *t*. The new value of ψ at time $t + \Delta t$ is

$$\psi \doteq \psi + \Delta\psi \qquad \text{(F11)}$$

and the symboi $\doteq$ means that the sum on the right replaces the previous value of the quantity on the left. This is the manner in which *k*, ε, and Ω are advanced from one time-step to the next.

Primary Flow

With the advection term expressed in curvilinear form, but with all forces except the pressure gradient still represented by the vector $\underline{F}$, the depth-averaged momentum equation (A1) is

$$\frac{\partial \underline{u}}{\partial t} + h^{-1}J^{-1}\left[U\frac{\partial \underline{u}}{\partial \xi} + V\frac{\partial \underline{u}}{\partial \eta}\right] = \underline{F} - \rho^{-1}\nabla p \tag{F12}$$

Let $\underline{u}(r,s)$ be a velocity vector whose components are defined in terms of the shift indices (r,s) by Equations E105 and E106; and let $U(r)$ and $V(s)$ be flux components similarly defined by Equations E97 and E98. With these substitutions, and with the pressure gradient omitted, the momentum equation takes the semi-discrete form

$$\begin{aligned}\Delta\underline{u}(r,s) = \Delta t\Bigg[\underline{F}(r,s) - h^{-1}J^{-1}\Bigg(&U(r)\frac{\partial \underline{u}(r,s)}{\partial \xi}\\ &+ V(s)\frac{\partial \underline{u}(r,s)}{\partial \eta}\Bigg)\Bigg]\end{aligned} \tag{F13}$$

STREMR begins the predictor phase of the MacCormack scheme at time t with the fluxes U and V, and with the index pair (r,s) chosen from one of four possible combinations: (0,0), (1,0), (0,1), or (1,1). These regulate not only the difference direction for advection (Equation E84), but also the cell faces from which the fluxes are taken to define the cell-centered velocities (Equations E105 and E106). The increment $\Delta\underline{u}(r,s)$ subsequently determines the flux increments $\Delta U(r)$ and $\Delta V(s)$ through Equations E108 and E109, which are added to the existing fluxes to obtain

$$U'(r) = U(r) + \Delta U(r) \tag{F14}$$

$$V'(s) = V(s) + \Delta V(s) \tag{F15}$$

These fluxes do not conserve mass, because the pressure gradient was omitted from Equation F13. Thus, the next step is to add the gradient of a scalar potential $\nabla\phi$ (Fquations F3 and F4), which must satisfy Equation F5, and which is related to the pressure by

$$\phi = \frac{p\Delta t}{\rho} \tag{F16}$$

This final step produces the mass-conserving fluxes U^* and V^*, and it marks the end of the MacCormack predictor phase.

The corrector phase begins with the fluxes U^* and V^*, and it repeats the steps of the predictor phase with $r^* = 1 - r$ and $s^* = 1 - s$, which reverses the difference directions for advection. In this phase, however, the nonconservative fluxes (analogous to Equations F14 and F15) are defined by

$$U'(r^*) = \frac{1}{2}\left[U(r^*) + U^*(r^*) + \Delta U^*(r^*)\right] \qquad \text{(F17)}$$

$$V'(s^*) = \frac{1}{2}\left[V(s^*) + V^*(s^*) + \Delta V^*(s^*)\right] \qquad \text{(F18)}$$

In the final step of the corrector phase, the gradient of a scalar potential $\nabla\phi^*$ is added (in the manner of Equations F3 and F4) to the nonconservative fluxes given by Equations F17 and F18. This produces the mass-conserving fluxes at time $t + \Delta t$.

The potential ϕ^* must also satisfy Equation F5, but it is related to the pressure p^* for the corrector phase by

$$\phi^* = \frac{p^*\Delta t}{2\rho} \qquad \text{(F19)}$$

Close inspection of Equations F17 and F18 reveals that the pressure gradient needed to correct $U'(r^*)$ and $V'(s^*)$ acts for only half a time-step.

The shift indices influence the forces concealed in the vector $\underline{F}(r,s)$ only insofar as they control the values of the cell-centered velocity components (Equations E105 and E106) and the difference directions for cell-centered gradients (Equations E118 and E119). Otherwise, they have no effect on second derivatives.

Variable Time-Step

The MacCormack scheme and the Euler upwind scheme are both explicit algorithms. They use only the existing values to calculate new values of the flow variables, and this can lead to trouble if the increments are too big. Consider, for example, the differential equation

$$\psi_t + \lambda\psi = 0 \qquad \text{(F20)}$$

The exact solution to Equation F20 is

$$\psi(t) = \psi(0)\, e^{-\lambda t} \qquad \text{(F21)}$$

where $\psi(0)$ is the initial value of ψ and λ is a positive constant. Note that if the initial value $\psi(0)$ is positive, then $\psi(t)$ remains positive forever. Now consider the discrete version of Equation F21,

$$\Delta\psi = -\lambda\Delta t\ \psi(t) \qquad \text{(F22)}$$

Suppose that the following two statements are true at time t:

$$\psi(t) > 0 \qquad \text{(F23)}$$

$$\lambda\Delta t > 1 \qquad \text{(F24)}$$

Then it follows immediately from Equation F22 that

$$\Delta\psi < 0 \qquad \text{(F25)}$$

and

$$|\Delta\psi| > \psi(t) \qquad \text{(F26)}$$

which means that

$$\psi(t+\Delta t) = \psi(t) + \Delta\psi < 0 \qquad \text{(F27)}$$

Thus, the function ψ, which should have remained positive forever, has become negative in a single time-step. If one proceeds in the same fashion through another time-step, then it turns out that

$$\psi(t+2\Delta t) > 0 \qquad \text{(F28)}$$

which means that the discrete solution for ψ is oscillating about zero. The amplitude of this numerical oscillation depends on the magnitude of $\lambda\Delta t$, and it leads to numerical instability, in which $/\psi/$ grows without bound.

A similar problem can arise with the explicit algorithms in STREMR. This is evident if one writes the discretized governing equation for any flow variable (except pressure) in the form

$$\frac{\Delta\psi(i,j)}{\Delta t} = -\lambda(i,j)\ \psi(i,j) + \textit{other terms} \tag{F29}$$

where $\lambda(i,j)$ is the sum of the absolute values of coefficients that multiply $\psi(i,j)$. Disregarding the effects of the other terms in Equation F29, the time-step must satisfy the following criterion if oscillation and instability are to be avoided:

$$\Delta t < \frac{1}{\lambda(i,j)} \tag{F30}$$

Inequality F30 gives an estimate of the maximum allowable time-step for a given cell (i,j). The cell with the largest value of $\lambda(i,j)$ then determines the maximum allowable time step for the whole grid:

$$\Delta t_{\text{max}} = \frac{1}{\lambda(i,j)_{\text{max}}} \tag{F31}$$

If TIMER = 'YES' in namelist BEGIN, STREMR uses Equation F31, with $\lambda(i,j)$ obtained from the momentum equation, to set the time-step size for the MacCormack scheme and the Euler upwind scheme.

REPORT DOCUMENTATION PAGE

Form Approved
OMB No. 0704-0188

1. AGENCY USE ONLY ***(Leave blank)***

2. REPORT DATE
September 1993

3. REPORT TYPE AND DATES COVERED
Final report

4. TITLE AND SUBTITLE
STREMR: Numerical Model for Depth-Averaged
Incompressible Flow

5. FUNDING NUMBERS
Work Units 32319
and 32656

6. AUTHOR(S)
Bernard, Robert S.

7. PERFORMING ORGANIZATION NAME(S) AND ADDRESS(ES)
USAEWES
Hydraulics Laboratory
3909 Halls Ferry Road
Vicksburg, MS 39180-6199

8. PERFORMING ORGANIZATION REPORT NUMBER
Technical Report
REMR-HY-11

9. SPONSORING/MONITORING AGENCY NAME(S) AND ADDRESS(ES)
US Army Corps of Engineers
Washington, DC 20314-1000

10. SPONSORING/MONITORING AGENCY REPORT NUMBER

11. SUPPLEMENTARY NOTES
A report of the Hydraulics Problem Area of the Repair, Evaluation, Maintenance, and Rehabilitation (REMR) Research Program. Available from National Technical Information Service, 5285 Port Royal Road, Springfield, VA 22161.

12a. DISTRIBUTION/AVAILABILITY STATEMENT
Approved for public release; distribution is unlimited.

12b. DISTRIBUTION CODE

13. ABSTRACT ***(Maximum 200 words)***

The STREMR computer code is a two-dimensional numerical model for depth-averaged incompressible flow. It accommodates irregular boundaries and nonuniform bathymetry, and it includes empirical corrections for turbulence and secondary flow. Although STREMR uses a rigid-lid surface approximation, the resulting pressure is equivalent to the displacement of a free surface. Thus, the code can be used to model free-surface flow wherever the local Froude number is 0.5 or less. STREMR uses a finite-volume scheme to discretize and solve the governing equations for primary flow, secondary flow, and turbulence energy and dissipation rate. The turbulence equations are taken from the standard k-ε turbulence model, and the equation for secondary flow is developed herein. Appendices to this report summarize the principal equations, as well as the procedures used for their discrete solution.

14. SUBJECT TERMS

Depth-averaged models	Secondary flow
Incompressible flow	Subcritical flow
Mathematical models	Turbulence models

15. NUMBER OF PAGES
181

16. PRICE CODE

17. SECURITY CLASSIFICATION OF REPORT
UNCLASSIFIED

18. SECURITY CLASSIFICATION OF THIS PAGE
UNCLASSIFIED

19. SECURITY CLASSIFICATION OF ABSTRACT

20. LIMITATION OF ABSTRACT